

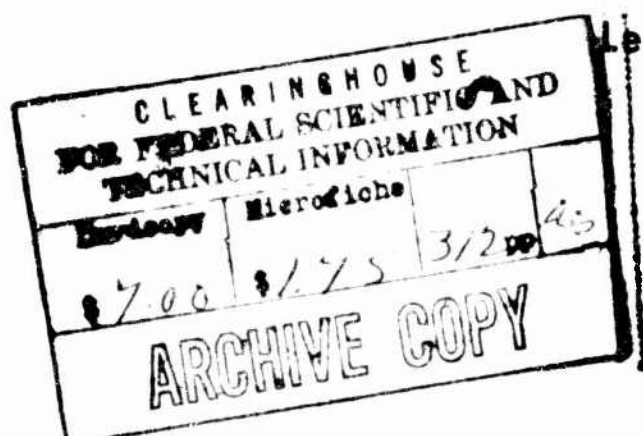
AD

USAAVLABS TECHNICAL REPORT 65-40

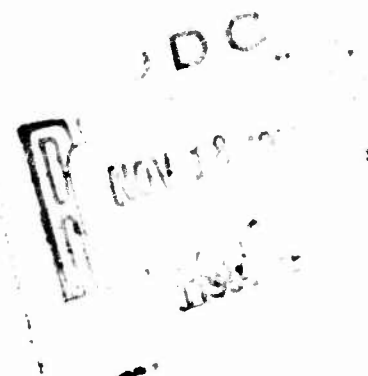
**POWER TRANSMISSION STUDIES
FOR
SHAFT-DRIVEN HEAVY-LIFT HELICOPTERS**

By

Lester R. Burroughs



October 1965



**U. S. ARMY AVIATION MATERIEL LABORATORIES
FORT EUSTIS, VIRGINIA**

CONTRACT DA 44-177-AMC-240(T)

**SIKORSKY AIRCRAFT
DIVISION OF UNITED AIRCRAFT CORPORATION**



DDC Availability Notices

Qualified requesters may obtain copies of this report from DDC.

This report has been furnished to the Department of Commerce for sale to the public.

Disclaimer

The findings in this report are not to be construed as an official Department of the Army position, unless so designated by other authorized documents.

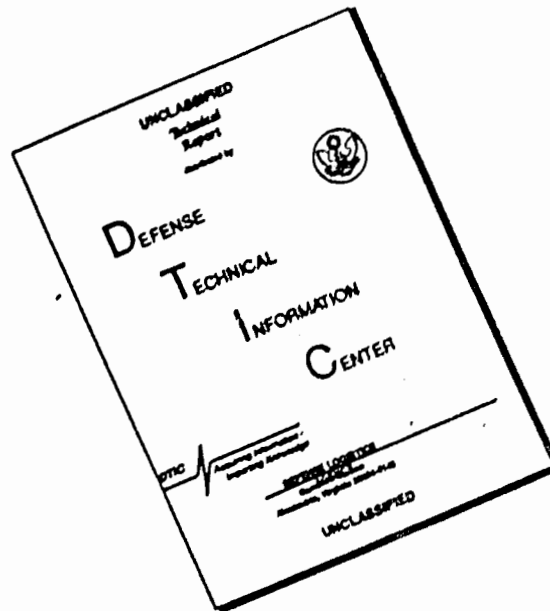
When Government drawings, specifications, or other data are used for any purpose other than in connection with a definitely related Government procurement operation, the United States Government thereby incurs no responsibility nor any obligation whatsoever; and the fact that the Government may have formulated, furnished, or in any way supplied the said drawings, specifications, or other data is not to be regarded by implication or otherwise as in any manner licensing the holder or any other person or corporation, or conveying any rights or permission, to manufacture, use, or sell any patented invention that may in any way be related thereto.

Trade names cited in this report do not constitute an official indorsement or approval of the use of such commercial hardware or software.

Disposition Instructions

Destroy this report when it is no longer needed. Do not return it to the originator.

DISCLAIMER NOTICE



THIS DOCUMENT IS BEST
QUALITY AVAILABLE. THE COPY
FURNISHED TO DTIC CONTAINED
A SIGNIFICANT NUMBER OF
PAGES WHICH DO NOT
REPRODUCE LEGIBLY.

**BLANK PAGES
IN THIS
DOCUMENT
WERE NOT
FILMED**



DEPARTMENT OF THE ARMY
U. S. ARMY AVIATION MATERIEL LABORATORIES
FORT EUSTIS VIRGINIA 23604

This report represents a part of the U. S. Army Aviation Materiel Laboratories' program to investigate mechanical transmission system concepts for a shaft-driven heavy-lift helicopter of the 75,000- to 95,000-pound-gross-weight class. The purpose of the investigation was to determine the high-risk or problem areas that could be expected in the development of a drive train for a mechanically driven heavy-lift helicopter.

This report presents a comparative analysis of several power train concepts for use in a single-rotor shaft-driven heavy-lift helicopter.

This command concurs with the contractor's recommendations and conclusions reported herein.

Task 1M121401D14414
Contract DA 44-177-AMC-240(T)
USAAVLABS Technical Report 65-40
October 1965

POWER TRANSMISSION STUDIES
FOR
SHAFT-DRIVEN HEAVY-LIFT HELICOPTERS

Sikorsky Engineering Report 50401

By

Lester R. Burroughs

Prepared by

Sikorsky Aircraft
Division of United Aircraft Corporation
Stratford, Connecticut

For

U. S. ARMY AVIATION MATERIEL LABORATORIES
FORT EUSTIS, VIRGINIA

SUMMARY

This report covers a 6-month design investigation of transmission system concepts capable of operation in a single-rotor heavy-lift helicopter of 75,000 to 95,000 pounds gross weight.

The study has covered the selection of engines, considering engine installations utilizing models of four different engines. An evaluation of each engine installation and effect on overall performance has been included herein. Two separate installations, the first incorporating front-drive turbines and the second incorporating rear-drive turbines, have been utilized for the layout design of conventional and alternate transmission system concepts.

Specific areas considered in the design have included the study of high-speed bevel gears and bearings utilized in the initial reduction stages, high-torque lightweight planetary gearing and bearings, and the design of hypercritical shafting systems.

The results of this study indicate that the total power transmission system weight for a single rotor HLH is approximately 8,850 pounds. This weight, which includes all gearboxes, shafting, rotor brake, and lubrication systems, is approximately 7 percent less than the results of earlier studies. The mechanical efficiency of this transmission system is greater than 96.2 percent.

Studies of alternate drive concepts including the harmonic drive, the roller gear drive, and redundant power path gearing systems indicate the suitability of the roller drive for inclusion in the HLH transmission system, since this concept may afford a weight saving as high as 10 percent over conventional planetary drives.

A comparative reliability analysis of the HLH and a current model aircraft designed for similar mission operation (based on available service failure data for that aircraft) has been included as appendix IV.

PREFACE

This report covers the study of several power transmission concepts capable of satisfying the power requirements of a single-rotor heavy-lift helicopter (contract DA 44-177-AMC-240(T)). Sikorsky Aircraft, a Division of United Aircraft Corporation, was the contractor for this study. The Gleason Works, The Thompson Ramo Wooldridge Corporation, and the Curtiss-Wright Division provided pertinent data upon which portions of the study were based. Data on the growth versions of current production engines were provided by Allison Division of the General Motors Corporation, the General Electric Company, and the Lycoming Division of the Avco Corporation.

The principals for this investigation were L.R. Burroughs, Assistant Supervisor, Mechanical Design and Development Section, J.L. Lastine, Senior Design Analytical Engineer, and L. Webb, Design Engineer, Sikorsky Aircraft. The government representatives at U.S. Army Aviation Materiel Laboratories, Fort Eustis, Virginia, were Mr. E.M. Manning, Contracts Administrator, Mr. J. Nelson Daniel, Group Leader, Aeronautical Systems and Equipment Group, and Mr. W.A. Hudgins, Project Engineer.

CONTENTS

	<u>Page</u>
SUMMARY	iii
PREFACE	v
LIST OF ILLUSTRATIONS	x
LIST OF TABLES	xiv
LIST OF SYMBOLS	xvi
INTRODUCTION	1
CONCLUSIONS	2
RECOMMENDATIONS	3
BASIC DATA	4
DESIGN CHARACTERISTICS	4
MISSION REQUIREMENTS	4
VEHICLE DESCRIPTION	5
PRELIMINARY AIRCRAFT PERFORMANCE	6
MISSION ANALYSIS	7
POWER AND FLAPPING SPECTRA	9
DESIGN LOADS	14
DESIGN REQUIREMENTS	16
GENERAL TRANSMISSION SYSTEM DESIGN	20
BASIC TRANSMISSION SYSTEM	20
MAIN GEARBOX	23
Discussion	23
Stress Analysis	26
Bearing Analysis	39
Planetary Gear Reductions	45
Main Rotor Shaft	57
Overrunning Clutch	65
Lubrication and Efficiency Analysis	68
Weight Summary	71
ENGINE REDUCTION GEARBOX - TWO FORWARD ENGINES	72
Lubrication and Efficiency Analysis	75
Weight Summary	78

	<u>Page</u>
INPUT DRIVE SHAFT - MAIN GEARBOX	79
ACCESSORY DRIVE SHAFT	84
ACCESSORY GEARBOX	87
HYPERCRITICAL TAIL ROTOR DRIVE SYSTEM	92
Tail Drive Shafting	92
Intermediate Gearbox	103
Tail Rotor Gearbox	113
ROTOR BRAKE	141
OIL COOLER AND BLOWER SUMMARY	149
COMPONENT WEIGHT SUMMARY, BASIC TRANSMISSION SYSTEM	150
 ALTERNATE TRANSMISSION SYSTEM DESIGNS, MAIN ROTOR DRIVE TRAIN	 152
HARMONIC DRIVE	152
ROLLER GEAR DRIVE	162
REDUNDANT DRIVE MAIN GEARBOX	169
INFINITE INDEXING SPRING CLUTCH	175
WEIGHT AND EFFICIENCY COMPARISON, ENGINE TO MAIN ROTOR DRIVE SYSTEMS	 178
 ALTERNATE SUBCRITICAL TAIL ROTOR DRIVE SYSTEMS	 179
COMPARATIVE WEIGHTS, HYPERCRITICAL VERSUS SUBCRITICAL SPEED TAIL ROTOR DRIVE SYSTEMS	 188
EFFECT ON C.G. OF ALTERNATE TAIL ROTOR DRIVE SYSTEMS	189
 CONTROL SYSTEMS	 191
MODIFIED HAFNER SYSTEM	191
DOUBLE ECCENTRIC SYSTEM	197
CONVENTIONAL SYSTEM	204
COMPARATIVE DRAG ANALYSIS	211
SUMMARY, WEIGHTS COMPARISON, CONTROL SYSTEMS STUDY	213
 PERFORMANCE	 214
WEIGHT AND BALANCE ANALYSIS	214
WEIGHT SUMMARY, HEAVY-LIFT HELICOPTER	215
MISSION PERFORMANCE VERIFICATION	218
 METHODS OF MANUFACTURING	 219
 BIBLIOGRAPHY	 222
 DISTRIBUTION	 223

	<u>Page</u>
APPENDIXES	
I. TRANSMISSION SYSTEM DRAWINGS	225
II. ENGINE INSTALLATION STUDIES	261
III. SUMMARY OF GEAR DATA	281
IV. COMPARATIVE RELIABILITY ANALYSIS OF HLH AND S-61	287

ILLUSTRATIONS

<u>Figure</u>		<u>Page</u>
1	Transmission System Schematic, Front-Drive Engines	21
2	Transmission System Schematic, Rear-Drive Engines	22
3	High-Speed-Input Bevel	27
4	High-Speed-Driven Bevel	28
5	Quill Shaft (Input Bevel to Freewheel Shaft)	29
6	Freewheel Housing	30
7	Input Bevel Pinion	32
8	Outer Shaft	34
9	Tail Take off Bevel Gear Shaft	36
10	Tail Take off Spur Gear Shaft	37
11	Stress and Deflection Versus Planetary Plate Thickness, First Stage	55
12	Stress and Deflection Versus Planetary Plate Thickness, Second Stage	56
13	Main Rotor Shaft	58
14	S-N Curve, 4340 Steel, $F_{tu} = 200,000$ psi (Main Rotor Shaft)	64
15	Roller-type Freewheel Unit	66
16	Lubrication System, Main Gearbox	70
17	Pinion, Engine Reduction Gearbox	73
18	Output Gear Shaft, Engine Reduction Gearbox	74
19	Lubrication System, Engine Reduction Gearbox	77

<u>Figure</u>		<u>Page</u>
20	Typical Drive Shaft End Fitting	80
21	Accessory Drive Shaft	84
22	Lubrication System, Accessory Gearbox	90
23	Normalized Tail Drive Shaft Deflection (Fuselage - Tail Cone Shafting)	95
24	Intermediate Gearbox Shafting	104
25	Lubrication System, Intermediate Gearbox	111
26	Bevel Gear Shafts, Tail Gearbox	115
27	Tail Rotor Shaft Loading	120
28	Stress and Deflection Versus Planetary Plate Thickness, Tail Gearbox	126
29	Tail Rotor Shaft	135
30	S-N Curve, 9310 Carburized Steel (R_c 30-40 Core Hardness)	136
31	Lubrication System, Tail Rotor Gearbox	139
32	Main Rotor Decay Curve	143
33	Rotor Brake System	146
34	Rotor Brake Requirements	147
35	Transmission System Schematic With Harmonic Drive	153
36	Harmonic Drive Elements	154
37	Horsepower Versus Diameter, Harmonic Drive	155
38	Horsepower Versus Weight, Harmonic Drive	160
39	Roller and Roller Gear Elements	163
40	Roller Gear Drive Transmission System	166

<u>Figure</u>		<u>Page</u>
41	30:1 Roller Gear Drive Schematic	167
42	Redundant Drive Main Gearbox (HLH-10-22)	173
43	Spring Clutch Installation	176
44	Tail Rotor Drive System Schematic	188
45	Modified Hafner Internal Control System	192
46	Modified Goodman Diagram for 7075-T6 Aluminum	198
47	Double Eccentric Internal Control System	199
48	Conventional External Control System	205
49	Comparative Sizes, Main Transmissions	221
50	12- to 20-Ton Crane - Front-Drive Turbine Installation (HLH-10)	227
51	12- to 20-Ton Crane Transmission System Schematic, Front-Drive Turbine Installation (HLH-10-1)	229
52	12- to 20-Ton Crane - Rear-Drive Turbine Installation (HLH-20)	231
53	12- to 20-Ton Crane Transmission System Schematic, Rear-Drive Turbine Installation (HLH-20-1)	233
54	Main Gearbox (HLH-10-20, sheet 1)	235
54	Main Gearbox (HLH-10-20, sheet 2)	237
55	Engine Reduction Gearbox (HLH-10-10)	239
56	Intermediate Gearbox (HLH-10-40)	241
57	Tail Gearbox (HLH-10-60)	243
58	Accessory Gearbox (HLH-10-80)	245
59	Rotor Brake (HLH-10-21)	247

<u>Figure</u>		<u>Page</u>
60	Alternate Intermediate Gearbox (HLH-30-40)	249
61	Alternate Tail Gearbox (HLH-30-60)	251
62	Angular Input Drive, Main Gearbox, Rear-Drive Engines (HLH-20-22)	253
63	Hafner Internal Control System (HLH-15-20)	255
64	Double Eccentric Control System (HLH-15-21)	257
65	Conventional Control System (HLH-15-22)	259
66	Front-Drive Engine Installation, T64-S5A Turbines (Basic Transmission System)	268
67	"Fan" Engine Installation, 548-C2 Rear-Drive Turbines (Alternate Transmission System)	269
68	Four Rear-Drive Engines	270
69	Three-Engine Installation, Rear-Drive Turbines, Bifurcated Center Engine Exhaust	271
70	Three Rear-Drive Engines, Rear Engine Inlet Facing Aft	273
71	Five Front-Drive Engines	275
72	Semi-radial Configuration, Four Front-Drive Turbines	277
73	Semi-radial Configuration, Four Rear-Drive Turbines	278
74	Semi-radial Configuration, Four Front-Drive Turbines	279
75	Gearing Schematic, Transmission System	282

TABLES

<u>Table</u>	<u>Page</u>
1 Representative Power Spectra, 12-Ton Transport Mission	9
2 Representative Power Spectra, 20-Ton Heavy-Lift Mission	10
3 Representative Power Spectra, 1,500-Nautical-Mile Ferry Mission	11
4 Representative Spectra, Main Rotor Flapping Angle - β	12
5 Representative Spectra, Tail Rotor Flapping Angle - β	13
6 Bearing-Life Summary, Main Gearbox	44
7 Planetary Gear Data	50
8 Weight Summary, Main Gearbox	71
9 Weight Summary, Engine Reduction Gearbox	78
10 Itemized Weight of One Input Drive Shaft System	83
11 Itemized Weight of Accessory Drive Shaft	86
12 Weight Summary, Accessory Gearbox	91
13 Itemized Weight, Tail Drive Shafting	102
14 Weight Summary, Intermediate Gearbox	112
15 Planetary Gear Summary, Tail Rotor Gearbox	124
16 Weight Summary, Tail Rotor Gearbox	140
17 Oil Cooler Capacities and Weights	149
18 Component Weight Summary, Basic Transmission System	150
19 Comparison of Drive Train Efficiencies	159
20 Roller Gear Design Summary	165

<u>Table</u>		<u>Page</u>
21	Reduction Ratios, Redundant Drive Main Transmission	170
22	Weight Summary, Redundant Drive Main Transmission	172
23	Weight and Efficiency Comparison, Engine to Main Rotor Drive Systems	178
24	Itemized Weights of Subcritical Speed Tail Drive Shaft System, 5,922 RPM Fuselage - Tail Cone Shafting, 3,760 RPM Pylon Drive Shaft	182
25	Itemized Weights of Subcritical Speed Tail Drive Shaft System, 3,300 RPM Fuselage - Tail Cone Shafting, 2,095 RPM Pylon Drive Shaft	187
26	Comparative Weights, Hypercritical Versus Subcritical Speed Tail Rotor Drive Systems	188
27	Summary, Weights Comparison, Control Systems Study	213
28	Weight Summary, Heavy-Lift Helicopter	215
29	Comparison, Transmission System Weights, Front and Rear Drive Engines	217
30	Engine Data	262
31	Engine Installation Performance Summary	264
32	Engine Installation Performance Data	266
33	Spiral Bevel Gear Summary	283
34	Spur Gear Summary	285

SYMBOLS

A	Area, in. ²
b	Number of blades
BRR	Basic radial rating, lb.
c	Damping coefficient
C	Blade chord, ft.
C _b	Bearing load rating, lb.
C _e	Oil flow experience factor
C _{do}	Profile drag coefficient
C _p	Specific heat, BTU/lb./°F
d	Outside diameter - pinion bearing inner race, in.
D _c	Pitch diameter of circular spline, in.
D _p	Pitch diameter - pinion, in.
D _r	Pitch diameter - ring, in.
D _R	Root diameter, in.
D _s	Pitch diameter - sun, in.
e	Offset of hinge pin from center line of rotation, in.
E	Modulus of elasticity, psi
f _a	Axial stress, psi
f _b	Bending stress, psi

f_s	Shear stress, psi
f_v	Vibratory stress, psi
F_c	Centrifugal force, lb., or allowable compressive stress, psi
F_{en}	Endurance limit, psi
F_{HP}	Friction horsepower
F_{tu}	Ultimate tensile strength, psi
F_{stu}	Torsional modulus of rupture, psi
g	Distance between planetary plates, in.
G.W.	Gross weight, lb.
HP	Horsepower
i	Shaft inclination angle, degrees
I	Moment of inertia, in. ⁴
$\overline{I.D.}$	Inside diameter, in.
J	Rotor system inertia, ft.-lb. sec. ²
K	Ratio - basic radial rating to basic thrust rating
K_t	Stress concentration factor
L	Chordal distance between center lines of planet pinions, in.
M	Moment, in.-lb.
ΔM	Mass increment, slugs
M.S.	Margin of safety
n.m.	Nautical mile
N	Number of teeth

N_{ci}	Shaft critical speed (1...i...n), RPM
N_{pp}	Number of planet pinions
$\overline{O.D.}$	Outside diameter, in.
P	Axial force, lb.
P_d	Diametral pitch
P_h	Roller radial load, lb.
P_t	Roller tangential load, lb.
PLV	Pitch line velocity, fpm
Q	Profile drag torque, ft.-lb.
Q_G	Heat generated, BTU/HR.
$Q_{o.c.}$	Oil cooler heat rejection rate, BTU/HR.
Q_{case}	Heat conducted through case, BTU/HR.
RE	Radial equivalent, lb.
RR	Reduction ratio
t	Plate thickness, in.
t_b	Fed thickness, in.
Δt	Δ Time, seconds
ΔT	Δ Temperature, °F
ΔT_c	Δ Temperature, °C
T	Torque, in.-lb. or ft.-lb.
U	BTU/HR./in. ² /°C
V	Speed

W_o	Oil flow, gallons/minute
W_r	Separating force, lb.
W_t	Tangential force, lb.
W_x	Axial force, lb.
Z	Section modulus, in. ³
Z_B	Mass eccentricity
β	Flapping angle, degrees
γ, Γ	Pitch angle - bevel gears, degrees
δ	Deflection, in.
θ	Angular distance, radians
λ	Plate slope, in./in.
ρ	Mass density of air, lb./ft. ³
ρ_a	Mass density of aluminum, lb./ft. ³
ρ_o	Mass density of MIL-L-7808 oil, lb./ft. ³
ϕ	Pressure angle, degrees
ψ	Spiral angle, degrees
ψ_f	Full load nip angle, degrees
ω	Angular velocity, radians per second
ξ	Damping factor

INTRODUCTION

The parametric study of Sikorsky Engineering Report 50273, completed by the contractor in June 1962, depicts a single rotor crane configuration capable of carrying a 12- to 20-ton payload. Since this aircraft meets the basic mission requirements of the contract, it will be used as the airframe for the transmission study.

To determine the configuration, weight, and efficiency of the 20-ton heavy-lift helicopter drive train, a comparative evaluation of several power train concepts has been made and is presented herein. The initial power train arrangement is based on what is considered by the contractor to be a conventional design using current state of the art design procedures and parameters. Against this conventional or "basic" design, other power transmission concepts such as the harmonic drive, roller gear drive, and redundant power path arrangements have been evaluated.

All design evaluations have been made using allowable design stresses to assure operating intervals for dynamic components of at least 1,200 hours between overhauls and minimum service life of 3,600 hours.

CONCLUSIONS

As a result of this power transmission design study, it is concluded that:

1. Shaft-driven single-rotor helicopters can successfully fulfill all the contract mission requirements with growth versions of current production engines without the necessity of thrust augmentation or regenerative combustion cycles.
2. The engine selection is based on the 12-ton OGE, 6,000-foot, 95°F hot-day hover requirement and the fuel expended during the ferry mission. The engines best meeting the power and SFC levels required for minimum overall aircraft weight are the T64/S5A and the 548-C2. The "basic" transmission study has been made using the T64/S5A, and necessary modifications to accommodate the 548-C2 are presented as secondary evaluations.
3. A conventional geared transmission system can be designed and fabricated for power levels up to 18,000 HP at a reduction ratio of 97 to 1 and with a mechanical efficiency of greater than 96.2 percent for a weight of less than 0.49 pound per horsepower. No major problems or high-risk development items are anticipated.
4. The lightest tail rotor drive is that system incorporating hypercritical shafting (operating at 5,922 RPM) from the main transmission to the 1.575:1 ratio intermediate gearbox and supercritical (3,760 RPM) pylon shafting driving a tail rotor gearbox of 6.18:1 ratio. In comparison to a conventional subcritical system, a weight savings of 189 pounds is realized and the aft weight moment affecting the center of gravity of the aircraft is reduced by 7,800 foot-pounds.
5. The roller gear drive concept is practical for high ratio-high torque power transmission systems and appears, from preliminary investigations, to afford weight savings and increased efficiency over conventional geared systems.
6. The low efficiency and high weight of the harmonic drive make this concept impractical at this stage of its development when compared to the conventional and roller gear drive systems.
7. Integration of the rotating control system within the main rotor shaft of the main gearbox appears entirely feasible and affords some weight saving over an external system.

RECOMMENDATIONS

1. Re-evaluate the selection of engines made herein based on the results of the U. S. Army Aviation Materiel Laboratories (USAAML) HLH power plant studies, including the effect on the single rotor helicopter transmission system design. Amend the analyses presented herein to include the engine installation and transmission modifications determined from this reiteration, including effects of weight, efficiency, and system reliability.
2. The design investigation of the roller gear drive concept initiated herein should be continued. Conduct, in this extended study phase, an analytical evaluation of all design parameters affecting roller gear drive operation, including sun, planet, and ring gear stresses as well as stresses and deflections of the carrier. Develop an analytical solution for gear rollers and planet pinion bearings, journals, and gears for deflection and life similar to the contractor's planetary bearing program. Evaluate roller gear drive empirically and modify the proposed analytical methods to design a unit compatible with heavy-lift requirements.
3. Conduct a detail design program for the spring-type freewheel unit leading to a prototype component and associated hardware. Initiate a development test program to evaluate this concept in both driving and long duration freewheeling modes (i.e., ferry mission) against the empirical data currently available for cam roller units of the HLH size (i.e., CH-54A, CH-53A).
4. Continue design study of integrating rotating controls within the transmission system, expanding the scope of the evaluation to include hydraulics and nonrotating as well as rotating controls.
5. Conduct a study to determine the design, manufacturing, and installation practices necessary to increase the reliability of high malfunction-rate components (such as seals, bearings, "O" rings, etc., Reference Appendix IV). The goal of this follow-on study would be to achieve a reliability of these components approaching that of the structural components of the transmission system (i.e., gearing, shafting, couplings, housings, etc.).

BASIC DATA

DESIGN CHARACTERISTICS

Gross Weight: 75,000-95,000 pounds
Turbine Powered
Autorotation Capabilities at Design Gross Weight Under
Normal Disc Loading
Design Load Factor at Design Gross Weight: 2.5
Crew: one Pilot, one Copilot, and one Crew Chief
Component TBO: 1,200 hours
Minimum Service Life: 3,600 hours

MISSION REQUIREMENTS

For the power train design covered herein, it has been assumed that the frequency of occurrence of the transport and heavy-lift missions is approximately equal. The contractor's mission analysis indicates that this assumption results in higher design horsepower requirements over considering equal importance of all three missions.

Transport Mission

Payload: 12 tons (outbound)
Radius: 100 n.m.
Vcruise: 110 knots (12-ton payload)
Vcruise: 130 knots (no payload)
Hovering time: 3 min. at take off (with 12-ton payload)
2 min. at midpoint
Reserve Fuel: 10% of initial fuel
Hover Capability: 6,000 ft., 95°F (OGE) Take off Gross
Mission Altitude: Sea Level, Standard Atmosphere
Fuel Allowance for Start, Warm-up, and Take off:
MIL-C-5011A

Heavy-Lift Mission

Payload: 20 tons (outbound)
Radius: 20 n.m.
Vcruise: 95 knots (20-ton payload)
Vcruise: 130 knots (no payload)

Hovering Time: 5 min. at take off
10 min. at destination with payload
Reserve Fuel: 10% of initial fuel
Hover Capability: Sea Level, Standard Atmosphere
Fuel Allowance for Start, Warm-up, and Take off:
MIL-C-5011A

Ferry Mission

Ferry Range: 1,500 n. m. (no payload, STOL, take off)
Reserve Fuel: 10% of initial fuel
Fuel Allowance for Start, Warm-up, and Take off:
MIL-C-5011A
Minimum Design Load Factor of 2.0
Mission Altitude: Sea Level, Standard Atmosphere
Best Speed for Range

VEHICLE DESCRIPTION

As indicated in Reference 3, page 48, the selected aircraft has a single main rotor, 95 feet in diameter, and a single tail rotor, 22 feet in diameter, for torque balance and yaw control. The C.G. range selected is 50 inches, which is more than adequate for crane-type missions. A 12-foot ground clearance is provided. The fuselage and landing gear are so arranged that standard truck trailer containers, 35-feet long and 8 feet by 8 feet in cross section, can be trucked into position from the rear and secured at 4 points to the fuselage. Winching at these points allows subsequent lowering of the modules either after landing or during hovering. Other objects up to 12 feet in width can also be winched and secured to the fuselage. The general arrangement of this aircraft is shown in Appendix I, Figures 50 and 52.

PRELIMINARY AIRCRAFT PERFORMANCE

As recommended in Reference 3, all aircraft operation will be flown at a main rotor tip speed of 700 feet per second, excepting the 6,000 feet-95°F hover requirement of the 12-ton transport mission. For this design condition, hover performance has been based on a main rotor tip speed of 650 feet per second, in accordance with Reference 3, requiring a reduction in engine free turbine RPM.

Required Engine Power

To determine the installed engine power required for this aircraft, it was initially assumed that the 12-ton transport hover requirement was the critical design condition.

For hover at 6,000 feet-95°F at a rotor tip speed of 650 feet per second:

$$\begin{aligned} \text{SHP} &= \frac{.0437 (\text{GW})^{3/2}}{D} + \frac{.0275 (\text{GW})(D)}{D} \quad (\text{Reference 3, Equation 16, page 17.}) \\ &= \frac{.0437(74,000)^{3/2}}{95} + \frac{.0275(74,000)(95)}{95} \\ &= 11,300 \text{ horsepower at } 95^\circ\text{F.} \end{aligned}$$

Checking the required power to hover at sea level on a standard day (59°F) for the 20-ton heavy-lift mission, the above equation becomes:

$$\begin{aligned} \text{SHP} &= \frac{.03798(\text{GW})^{3/2}}{D} + \frac{.0335(\text{GW})(D)}{D} \\ &= 13,000 \text{ horsepower at } 59^\circ\text{F.} \end{aligned}$$

Engine Selection

As indicated in Appendix II to this report, four different manufacturers' engines were considered. Summarized below are the manufacturer's model, number of engines, and installed weights of engine and fuel required for the average (or prorated) power for the 12-ton transport mission.

The number of engines required is based on the hot-day (95°F) power requirement of 11,300 HP.

The prorated engine output power for the 12-ton mission, applying the equation of page 15 to the power spectrum of Table 9, is as follows:

$$\text{Prorated Power} = 6,800 \text{ HP}$$

$$\text{Prorated Power/Engine} = 6,800 \text{ HP/number of engines}$$

For this preliminary engine weight evaluation analysis, it has been assumed that all installed engines are operating continuously throughout the entire mission at prorated power. It is believed that shutting down one or more engines during the mission will result in approximately the same fuel saving regardless of the model engine selected.

Model	No. Eng. Reqd.	Total Engine Weight (lb.)	Fuel Weight (lb.)	Total Weight (lb.)
T64/S5A	4	3,060	7,760	10,820
JFTD-12A	3	3,075	10,500	13,575
LTC4B-11A	5	3,200	9,300	12,500
548-C2	4	*	*	10,790

*Reference Allison Report EDR 4010

Based on this simplified analysis, it appears that the most desirable engines for this aircraft on the basis of engine and fuel weight are the T64/S5A and the 548-C2. A detailed evaluation of engine installations and estimated installation losses is presented in Appendix II.

MISSION ANALYSIS

Representative power and flapping spectra have been derived for the single-rotor heavy-lift helicopter using estimated gross weights and the performance data from Reference 3 as well as flight test information developed from CH-54A (Sikorsky S-64A) flying crane experience as a guide. These spectra are based on the following estimated gross weights:

Transport Mission	=	74,000 pounds
Heavy-lift Mission	=	86,000 pounds
Ferry Mission	=	100,000 pounds

The anticipated frequency and breakdown of shaft horsepower to the major segments of the power train is presented in Tables 1, 2, and 3 .

The following charts, Tables 4 and 5, outline the anticipated main and tail rotor blade flapping angles and frequency of occurrence.

TABLE 1
REPRESENTATIVE POWER SPECTRA,
12-TON TRANSPORT MISSION

Flight Condition	% Time	Shaft Horse- Power	Main Rotor Horse- Power	Tail Rotor Horse- Power	Accessory Horse- Power
Warm-up, Take off, and Climb	.53 1.60	16,000 13,800	14,200 12,365	1,500 1,155	300 280
Hover at Take off	1.62	10,630	9,440	890	300
Left Turn	.58	11,470	9,440	1,860	170
Right Turn	.58	9,795	9,440	185	170
Cruise Out	.10	9,100	8,210	590	300
V _{AW} = 110 Knots	1.10 5.40 30.96 10.20 2.50 .20	5,420 5,650 5,800 6,400 6,500 13,800	4,830 5,080 5,345 5,840 5,900 12,960	290 270 275 280 320 560	300 300 180 280 280 280
Hover at Destination	1.05 .40 .40	10,140 10,930 9,345	9,000 9,000 9,000	840 1,760 175	300 170 170
Cruise Back	.05	4,400	3,900	300	200
V _{AW} = 130 Knots	1.00 12.62 18.20 8.33 2.33 .25	3,550 4,800 5,300 5,400 6,500 13,800	3,000 4,355 4,875 4,980 5,945 12,890	175 220 225 250 295 610	200 180 200 170 260 300

TABLE 2
REPRESENTATIVE POWER SPECTRA,
20-TON HEAVY-LIFT MISSION

Flight Condition	% Time	Shaft Horse- Power	Main Rotor Horse- Power	Tail Rotor Horse- Power	Accessory Horse- Power
Warm-up, Take off, and Climb					
	2.00	16,000	14,200	1,500	300
	3.51	13,800	12,365	1,155	280
Hover					
	6.42	13,000	11,560	1,140	300
	1.60	13,800	11,560	2,070	170
	3.20	12,160	11,560	430	170
	1.60	14,030	11,560	2,300	170
Cruise Out					
	.07	11,650	10,540	830	280
	.70	6,900	6,235	365	300
	11.00	6,400	5,838	282	280
	13.00	6,500	5,918	282	300
	6.20	6,650	6,087	283	280
	1.14	7,250	6,643	306	300
	.25	13,800	12,900	620	280
Hover at Destination					
	12.84	12,695	11,320	1,075	300
	6.40	13,280	11,320	1,790	170
	6.40	11,880	11,320	390	170
Cruise Back					
	.04	4,350	3,875	280	195
	.45	3,550	3,000	175	200
	8.00	4,800	4,355	220	180
	8.70	5,300	4,875	225	200
	4.70	5,400	4,950	250	200
	1.53	6,500	5,945	295	260
	.25	13,800	12,890	610	300

TABLE 3
REPRESENTATIVE POWER SPECTRA,
1,500-NAUTICAL-MILE FERRY MISSION

Flight Condition	% Time	Shaft Horse- Power	Main Rotor Horse- Power	Tail Rotor Horse- Power	Accessory Horse- Power
Warm-up, Take off, and Climb at Normal Rated Power	.025	16,000	14,200	1,500	300
Cruise	.215	9,700	8,830	660	210
V = Best Speed for Range	2.15	5,550	5,070	280	200
	29.85	6,150	5,710	280	160
	41.65	6,450	5,950	280	220
	20.35	6,600	6,110	290	200
	5.43	7,500	6,920	320	260
	.33	16,000	14,200	1,500	300

TABLE 4
REPRESENTATIVE SPECTRA,
MAIN ROTOR FLAPPING ANGLE - β

% Time	β Degrees	
	12-Ton Transport Mission	20-Ton Heavy-Lift Mission
.01	10.56	12.00
.54	10.12	11.50
.40	8.86	10.07
.80	6.79	7.72
3.88	5.30	6.02
2.95	4.58	5.21
2.80	4.31	4.90
20.43	3.90	4.43
13.85	3.34	3.80
2.14	3.17	3.60
6.06	2.80	3.18
23.46	2.56	2.91
14.51	2.38	2.70
1.17	2.19	2.49
3.00	2.06	2.34
2.00	1.52	1.73
2.00	.79	.90

Note: The anticipated main rotor flapping for the 1,500-n.m. ferry mission is less severe than either the 12-ton transport or the 20-ton heavy-lift mission spectra.

TABLE 5
 REPRESENTATIVE SPECTRA,
 TAIL ROTOR FLAPPING ANGLE - β

% Time	β Degrees
1.77	5.00
1.77	4.00
2.00	3.40
1.15	3.20
6.14	3.10
6.01	2.75
4.29	2.50
2.00	2.40
1.18	2.30
2.06	2.20
13.13	2.0
19.21	1.9
34.13	1.8
1.80	1.6
2.42	1.5
.12	1.15
.82	1.00

DESIGN LOADS

To determine the required design loads for each dynamic component (i.e., gears and shafting), the cumulative damage theory can be applied to the power spectra and representative S-N curves using 3,600 hours as the minimum design life for these components.

Gearing and Shafting

The spiral bevel gear S-N curve (Reference 6, page 30) modified for a reliability of 0.999 has been used for determination of the following design powers:

Component	Design Power (HP)
Engine Reduction Box	4,500
Main Gearbox	
Input Bevel Pinions	4,500
Driven Bevel Gear	4,500*
Planetary Stages	14,200
Tail Rotor Take off	2,300
Accessory Drive	300
Intermediate Gearbox	2,300
Tail Rotor Gearbox	2,300

*Note: Four pinions drive the driven bevel gear; therefore, each mesh was designed for 4,500 horsepower.

Bearings

For bearing selection, a prorated power is determined for each segment of the drive train for the power spectra considering equal occurrence of the 12-ton transport and 20-ton heavy-lift missions. Prorated (or time-weighted) power can be determined using the following equation:

$$T = \frac{(63,025)(HP)}{(RPM)}$$

$$\text{Prorated Torque } T @ RPM_1 = T_1 \left[t_1 + t_2 \left(\frac{T_2}{T_1} \right)^{3.33} \frac{RPM_2}{RPM_1} + \dots t_n \left(\frac{T_n}{T_1} \right)^{3.33} \frac{RPM_n}{RPM_1} \right]^{0.3}$$

The design prorated loads are as follows:

Component	Prorated Power (Horsepower)
Engine Reduction Gearbox	2,055
Main Gearbox	
Input Bevel Pinion	2,055
Driven Bevel Gear Shaft	8,070
Planetary Stages	7,030
Accessory Drives	150
Tail Rotor Take off	875
Intermediate Gearbox	875
Tail Rotor Gearbox	875

DESIGN REQUIREMENTS

Design Lives

The single-rotor heavy-lift helicopter transmission system components evaluated herein have been designed to achieve a minimum service interval of 3,600 hours at a reliability (R) of 0.999 or greater. All bearings have been designed to achieve a B-10 life of approximately 3,600 hours. Based on service experience obtained on large single-rotor helicopters of gross weights between 18,000 and 42,000 pounds, these design goals should assure a component time between overhaul (TBO) of 1,200 hours or more.

Critical components such as the main and tail rotor shafts and control systems have been designed for service intervals of at least 3,600 hours at an anticipated structural reliability (R) of 0.9999.

Materials

The selection of materials for the transmission and control system components evaluated in this study is based on Sikorsky Aircraft's extensive test and production aircraft experience. All materials considered for the HLH are currently used in similar applications on production aircraft.

The use of special alloys such as AMS 6265 vacuum processed alloy steel has been limited to critical bearing applications or components where its higher fatigue strength justifies its use.

It should be noted here, that while the fatigue strength of smooth vacuum processed hardened alloy steels has been reported to be higher than air processed steels, this difference in fatigue strength diminishes considerably when notches or stress concentrations are present.* Where stress concentration factors of 2.4 or greater are present, no significant differences in the fatigue strength of air and vacuum processed steels are apparent. Fatigue testing conducted at WADC** indicates that two heats of 4340 steel heat treated to $F_{tu} = 190,000$ psi revealed no significant difference between vacuum and air melt materials when using notched specimens with a concentration factor of 2.6.

Since the root radius concentration factor on the average gear is in the order of 2.0 to 2.4, vacuum processed steel is not warranted.

On highly polished (or ground) parts such as bearings there is considerable evidence to indicate that the vacuum melt steels are justified. The service life of 52100 bearings, for example, has been reportedly increased by a factor of 3 to 10 times by the use of vacuum processed steels. Therefore, vacuum processed steels will be used for highly loaded bearings where the calculated B-10 life is 5,000 hours or less.

The use of titanium alloys has been limited to such parts as planetary carrier plates and the tail rotor shaft. Titanium has been used in similar applications on several Sikorsky production aircraft. An investigation of the resulting weight saving by the use of this material for the main rotor shaft is also included in this report.

Allowable Design Stresses

Gearing

Material: AMS 6260 (SAE 9310) steel

Spiral Bevel Gears

Bending Stress,* $F_b = 25,800$ psi ($R = 0.999$)
Compressive Stress, $F_c = 200,000$ psi

*Note: The industry accepted design stress for
 $R = 0.95$ is 30,000 psi.

* P.E. Ruff and R.W. Steur, "Vacuum Melting Improves Properties of H-11 Steel," Metal Progress, Volume 80, December 1961, pp. 79-84.

** F. B. Stulen, WADC TR59-507, August 1959

Spur Gearing

Bending Stress, $F_b = (35,750 - .704 \text{ PLV}) \text{ psi}$

Compressive Stress, $F_c = 140,000 \text{ psi}$

Planetary Spur Gearing

Bending Stress, $F_b = (31,500 - 0.625 \text{ PLV}) \text{ psi}$

Compressive Stress, $F_c = 140,000 \text{ psi}$

Shafting

Material: AMS 6260 (SAE 9310) steel
 R_c 30-45 Core Hardness

Bending Stress, $F_b = 19,500 \text{ psi}$ ($R = 0.9999$)

Torsional Stress, $F_s = 30,000 \text{ psi}$

Material: AMS 5000 (SAE 4340) steel
 $F_{tu} = 200,000 \text{ psi}$

Bending Stress, $F_b = 21,800 \text{ psi}$ ($R = 0.9999$)

Torsional Stress, $F_s = 35,000 \text{ psi}$

Housings*

Material: AZ91C Magnesium Castings
ZK60A Magnesium Forgings

*Note: For design allowables see MIL-HDBK-5, August 1962

Control-System Push Rods

Material: 7075-T6 Aluminum

Bending Stress, $F_b = 13,100$ psi ($R = .9999$)

Planetary Carrier Plates

Material: AMS 5000 (SAE 4340) steel

$F_{tu} = 150,000$ psi

Steady Bending Stress, $F_b = 45,000$ psi

Plate Deflection = 0.0010 inch per inch

Material: 6Al-4V Titanium

$F_{tu} = 130,000$ psi

$F_b = 42,000$ psi

Plate Deflection = 0.0010 inch per inch

GENERAL TRANSMISSION SYSTEM DESIGN

BASIC TRANSMISSION SYSTEM

The basic and alternate transmission systems have been designed and evaluated assuming supercritical input shafting and hypercritical tail rotor drive shafting. A separate evaluation of hypercritical and subcritical shaft operation including stress and weight analyses is made in a separate section of this report.

Both front* (Figure 50, page 227) and rear** (Figure 52, page 231) drive turbine installations giving similar performance for this aircraft have been selected for the basic transmission study to determine what weight advantage, if any, is afforded by this mounting variable. In the more detailed study of Appendix II, several other engine arrangements are evaluated for estimated performance in comparison to the preferred engines.

A schematic of the basic transmission system incorporating front drive engines is presented in Figure 1, page 21. The gear ratios, maximum design torques (for take off power), and the shaft speeds are given.

A similar schematic for the basic rear-drive engine system is shown in Figure 2, page 22.

*T64/S5A
**548-C2

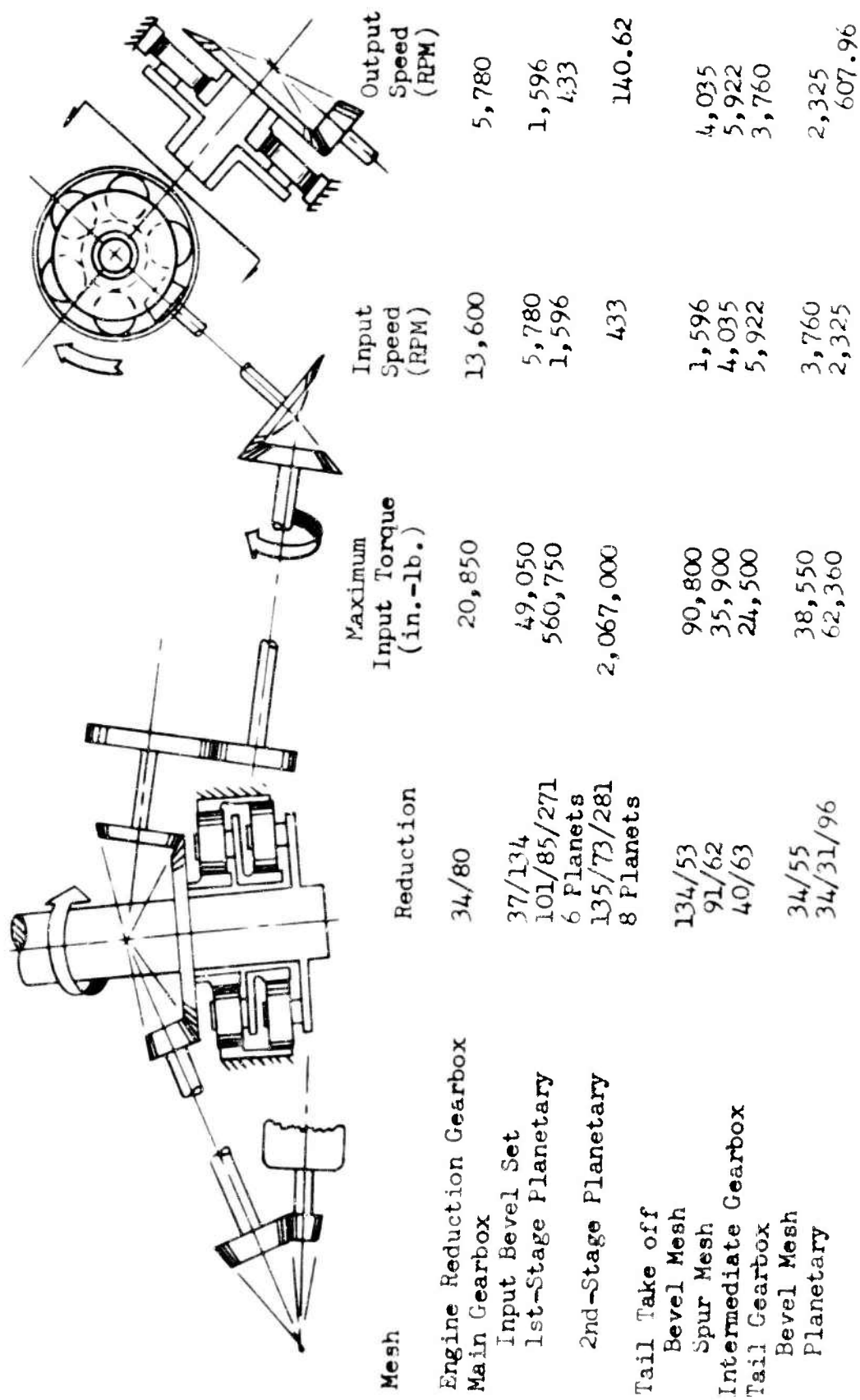
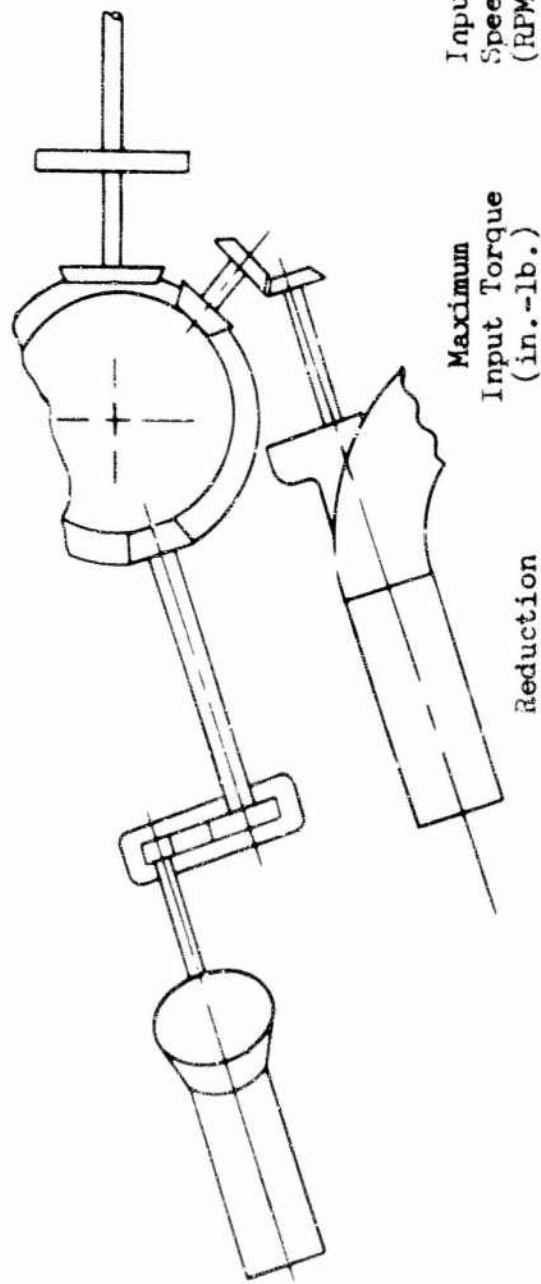


Figure 1. Transmission System Schematic, Front-Drive Engines.



	Reduction	Maximum Input Torque (in.-lb.)	Input Speed (RPM)	Output Speed (RPM)
Engine Reduction Box (Engine Manufacturer's Box)	3.22:1	14,900	19,320	6,000
Main Gearbox				
Outboard Engine Input Bevel	36/36	47,000	6,000	1,595
Inboard Engine) Main Bevel	37/139	47,000	6,000	1,596
Outboard Engine) Set				
Tail Take off				
Bevel Set	139/55	90,800	1,596	4,035
Spur Mesh	91/62	35,900	4,035	5,922
Planetary Stages	11.3:1	560,750	1,596	140.62
Intermediate Gearbox	40/63	24,500	5,922	3,760
Tail Gearbox	6.18:1	36,550	3,760	607.9

Figure 2. Transmission System Schematic, Rear-Drive Engines.

MAIN GEARBOX

Discussion

For the front-drive engine installation of Figure 1, the main gearbox has been designed with the two aft engine speed reductions integrated into the main case as right angle spiral bevel gears of 2.36:1 ratio. (The forward engines utilize individual engine reduction boxes of similar ratio.)

The power from all four engines has been combined through separate spiral bevel meshes at a common driven gear. The ratio of this set is 37/134. Two planetary stages, incorporating 6 and 8 planets, respectively, drive the 95-foot-diameter main rotor at 141 RPM (700 feet per second).

The tail rotor system drive pinion meshes with the main driven bevel gear forming a 3.96:1 speed increase. A spur gear mesh in turn increases the speed to drive the tail rotor drive shaft hypercritically at 5,922 RPM.

At the low operating stresses indicated in Appendix III, a relatively high degree of bevel gear reliability ($R \geq .999$) should be obtained with the following bevel gear proportions.

Input Set - No. 1 and No. 4 Engines

	Pinion	Gear
Number of Teeth	34	80
Diametral Pitch	5.529	
Face Width	2.650	
Pitch Diameter	6.149	14.469
Face Contact Ratio	2.112	
Pressure Angle	$\phi = 20^\circ$	
Mean Spiral Angle	$\psi = 20^\circ$	
Shaft Angle	$\Sigma = 90^\circ$	
Pitch Angle	$\gamma = 23^\circ 2'$	$\Gamma = 66^\circ 58'$

	Pinion	Gear
Hand of Spiral	RH	LH
Direction of Rotation	CCW	CW
Second Stage Bevel Reduction		
Number of Teeth	37	134
Diametral Pitch	4.092	
Face Width	3.25	
Pitch Diameter	9.042	32.747
Face Contact Ratio	1.699	
Pressure Angle	$\phi = 20^\circ$	
Mean Spiral Angle	$\psi = 20^\circ$	
Shaft Angle	$\Sigma = 74^\circ 22'$	
Pitch Angle	$\gamma = 13^\circ 54'$	$\Gamma = 60^\circ 28'$
Hand of Spiral	RH	LH
Direction of Rotation	CCW	CW

To transfer power to the tail rotor, a bevel pinion meshes with the above 134 tooth gear, in turn driving the tail take off spur gear. Tail take off pinion proportions are as follows:

Number of Teeth	53
Diametral Pitch	4.092
Face Width	1.750
Pitch Diameter	12.952
Face Contact Ratio	1.038
Pressure Angle	$\phi = 20^\circ$

Mean Spiral Angle $\psi = 23^{\circ}26'$

Shaft Angle $\Sigma = 80^{\circ}36'$

Pitch Angle $\gamma = 20^{\circ}8'$

Hand of Spiral RH

Direction of Rotation CCW

Tail Take off Spur Gears

The required tail take off spur gear face width has been determined using the stress levels indicated on page 18.

Design Data

$$T_{in} = (63,025)(2,300)/4,035$$

$$T_{in} = 35,900 \text{ in.-lb.}$$

$$b_{pinion} = 62$$

$$N_{gear} = 91$$

$$F_d = 6$$

$$w_t = \frac{2T}{D} = \frac{2 \times 35,900}{(62/6)}$$

$$w_t = 6,950 \text{ lb.}$$

Allowable Stresses

$$PLV = .262 (D)(RPM)$$

$$PLV = (.262)(62/6)4,035$$

$$PLV = 10,900 \text{ fpm}$$

$$F_b = 35,750 + .704 \times 10,900$$

$$F_b = 28,070 \text{ psi}$$

$$F_c = 140,000 \text{ psi}$$

Face Width Calculations

$$N = 62$$

$$D_{pin} = 10.333$$

$$X = .195$$

$$K = 1.03$$

$$F.W._b = \frac{1.5 \times 6,950 \times 1.03}{28,070 \times .195}$$

$$F.W._b = 1.96$$

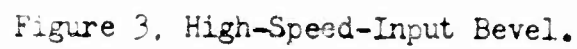
$$F.W._h = \frac{21 \times 10^6 \times 6,950 (1/10.3333 + 1/15.1667)}{(.707)(140,000)^2}$$

$$F.W._h = 1.715$$

Therefore, required spur gear face width to provide sufficient overlap and insure operation within allowable stress levels is 1.970 inch.

Stress Analysis

The dynamic components of the main gearbox have been analyzed for vibratory bending and/or steady torsion where applicable. This analysis is presented on the following pages.


$$\begin{aligned} \text{O.D.} &= 3.74 & Z &= 3.41 \\ \text{I.D.} &= 2.85 & K_t &= 2.65 \\ M &= 1.85 \sqrt{1,710^2 + 3,520^2} = 7,240 \text{ in.-lb.} \\ f_b &= \frac{K_t M}{Z} = \frac{(2.65)(7,240)}{3.41} \\ f_b &= 5,630 \text{ psi} \\ F_{en} &= 19,500 \text{ psi} \\ \text{M.S.} &= \frac{F_{en}}{f_b} - 1 = \frac{19,500}{5,630} - 1 \\ \text{M.S.} &= +2.46 \end{aligned}$$

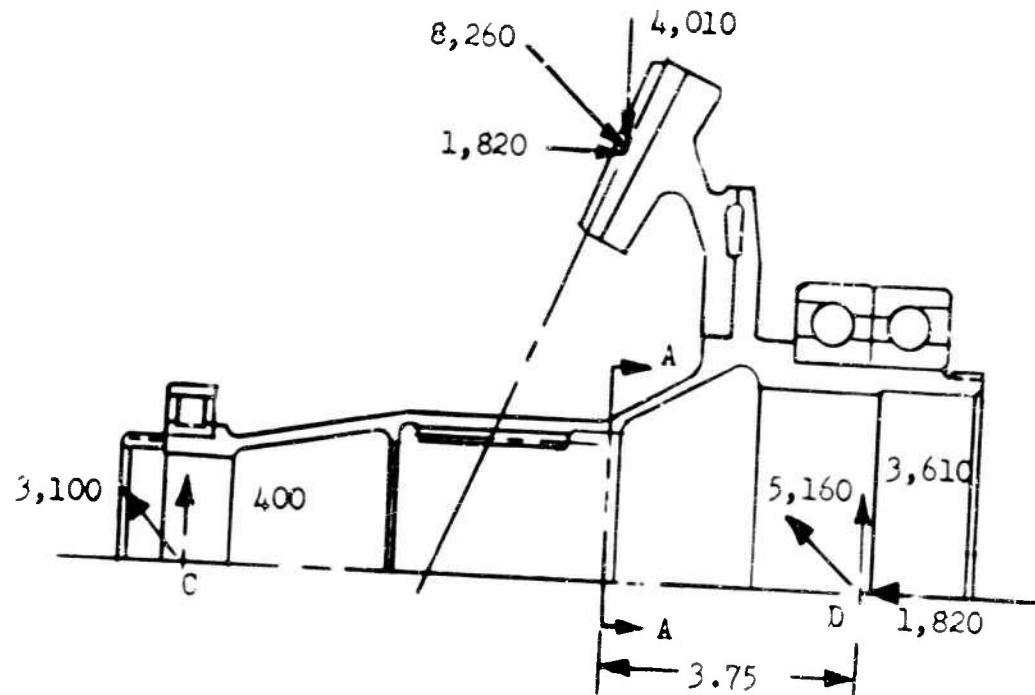


Figure 4 . High-Speed-Driven Bevel.

Critical Section A-A

$$\overline{\text{O.D.}} = 4.50$$

$$Z = 2.286$$

$$\overline{\text{I.D.}} = 4.18$$

$$K_t = 1.70$$

$$M = 3.75 \sqrt{(5,160)^2 + (3,610)^2} = 23,620 \text{ in.-lb.}$$

$$f_b = \frac{K_t M}{Z} = \frac{1.70 (23,620)}{2.286} = 17,570 \text{ psi}$$

$$F_{en} = 19,500 \text{ psi}$$

$$\text{M.S.} = \frac{F_{en}}{f_b} - 1 = \frac{19,500}{17,570} - 1$$

$$\text{M.S.} = +.10$$

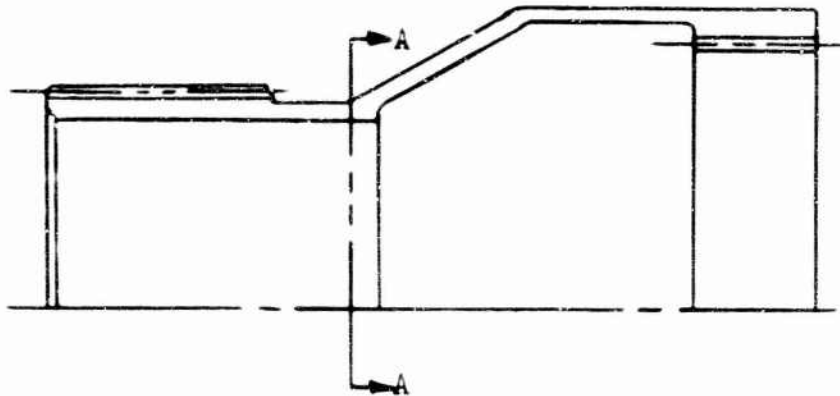


Figure 5. Quill Shaft (Input Bevel to Freewheel Shaft).

Critical Section A-A

$$\overline{\text{O.D.}} = 3.80$$

$$Z = 1.421$$

$$\overline{\text{I.D.}} = 3.52$$

$$T = \frac{63,000 (4,500)}{5,780} = 49,050 \text{ in.-lb.}$$

$$f_s = \frac{T}{2Z} = 49,050 / 2 (1.421) = 17,250 \text{ psi}$$

$$\text{M.S.} = \frac{115,000}{1.15 (2) (17,250)} - 1$$

$$\text{M.S.} = +1.90$$

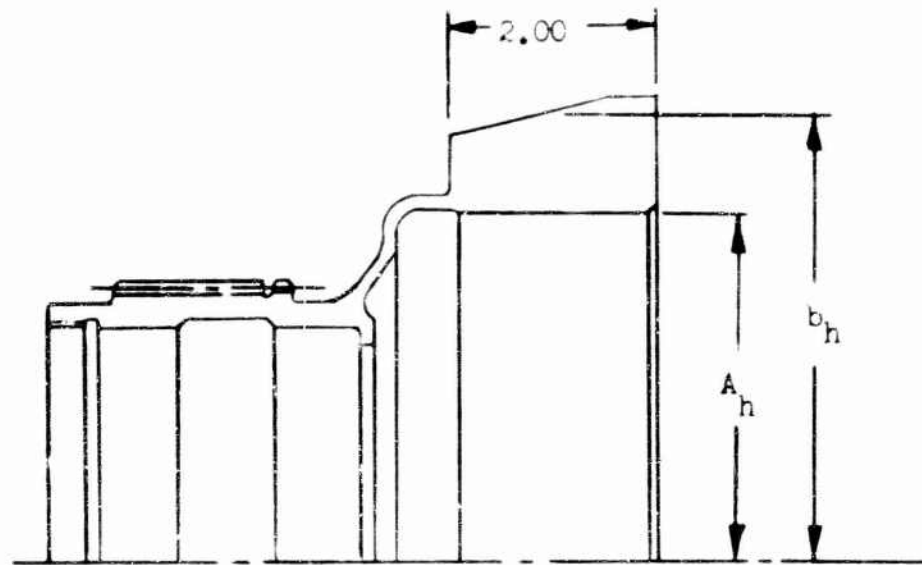


Figure 6. Freewheel Housing.

Critical sections through housing are at roller contact points.

$$\psi_f = \text{Full Load Nip Angle} = 5^\circ$$

$$P_h = \text{Roller Radial Load} = 24,670 \text{ lb.}$$

$$P_t = \text{Roller Tangential Load} = P_h \tan \left(\frac{\psi_f}{2} \right) = 1,080 \text{ lb.}$$

$$P_a = \text{End Load at any cross section of roller housing, lb.}$$

$$\theta = \frac{\pi}{\text{No. Rollers}} = \frac{\pi}{14} = .2244 \text{ rad.} = 12^\circ 51'$$

$$l = 2.00$$

$$A_h = 6.50$$

$$b_h = 8.36$$

$$M_{\max} = -\frac{P_h}{2} \left[A_h + \frac{(b_h - A_h)}{2} \right] \left(\frac{1}{\theta} - \cot \theta \right) - \frac{P_t}{2} \frac{(b_h - A_h)}{2}$$

$$= -24,670 \left[6.50 + \frac{(8.36 - 6.50)}{2} \right] \left[\frac{1}{.2244} - \cot 12^\circ 51' \right] -$$

$$\frac{1,080}{2} \frac{(8.36 - 6.50)}{2}$$

$$M_{\max} = -7,150 \text{ in.-lb.}$$

$$P_a = \frac{P_h}{2} \cot \theta + \frac{P_t}{2} = \frac{24,670}{2} \cot 12^\circ 51' + \frac{1,080}{2}$$

$$= 54,610 \text{ lb.}$$

$$A_{\text{ring}} = (b_h - A_h) \ell = (8.36 - 6.50) (2.00)$$

$$= 3.72 \text{ in.}^2$$

$$f_a = \frac{P_a}{A_{\text{ring}}} = \frac{54,610}{3.72} = 14,680 \text{ psi}$$

$$f_b = \frac{6M}{\ell (b_h - A_h)^2} = \frac{6(7,150)}{2(8.36 - 6.50)^2} = 6,200 \text{ psi}$$

$$F_{tu} = 136,000; F_{bu} = 201,000$$

$$M.S.\text{ult} = \frac{1}{1.5 \left(\frac{f_t}{f_{tu}} + \frac{f_b}{f_{bu}} \right)} - 1 = \frac{1}{1.5 \left(\frac{14,680}{136,000} + \frac{6,200}{201,000} \right)} - 1$$

$$= +3.80$$

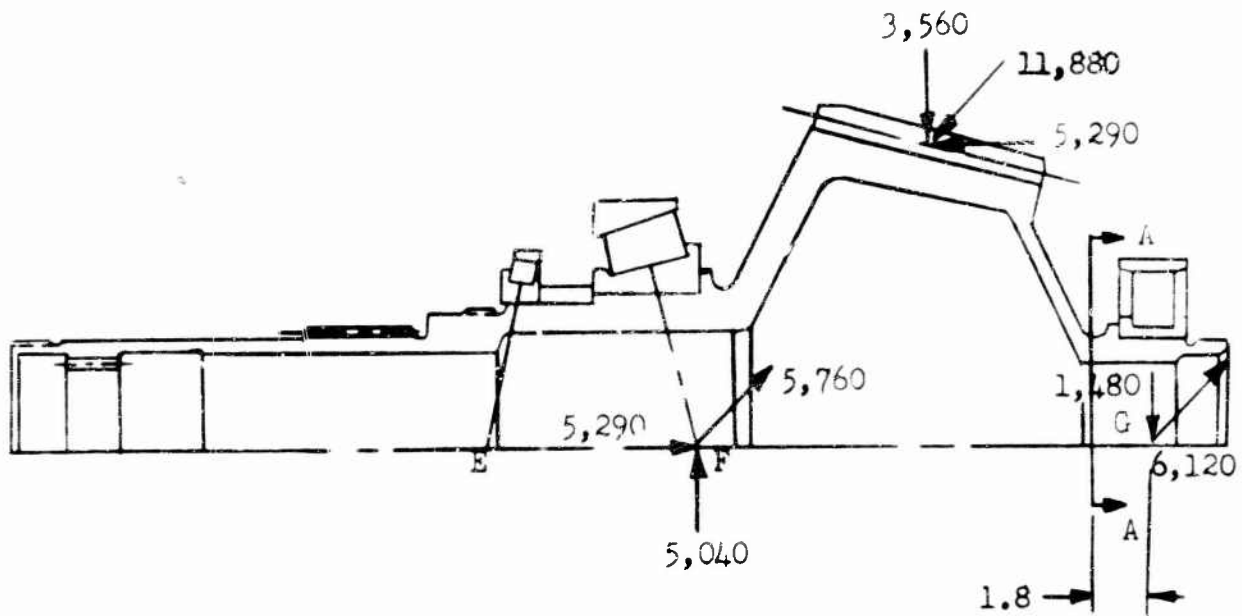


Figure 7. Input Bevel Pinion.

Critical Section A-A

$$\overline{\text{O.D.}} = 3.18 \quad Z = 2.166$$

$$\overline{\text{I.D.}} = 2.38 \quad K_t = 1.77$$

$$M = 1.8 \sqrt{(6,120)^2 + (1,480)^2}$$

$$M = 11,320 \text{ in.-lb.}$$

$$f_b = \frac{K_t M}{Z} = \frac{1.77 (11,320)}{2.166} = 9,270 \text{ psi}$$

$$F_{en} = 19,800 \text{ psi}$$

$$M.S. = \frac{F_{en}}{f_b} - 1 = \frac{19,800}{9,270} - 1$$

$$M.S. = + 1.13$$

Outer Shaft

To indicate the design adequacy of the outer shaft, section A-A of Figure 8 has been analyzed. In the critical loading condition, shown on page 35, three engines transmit torque to the main rotor shaft while 2,300 horsepower are supplied to the tail take off bevel gear shaft.

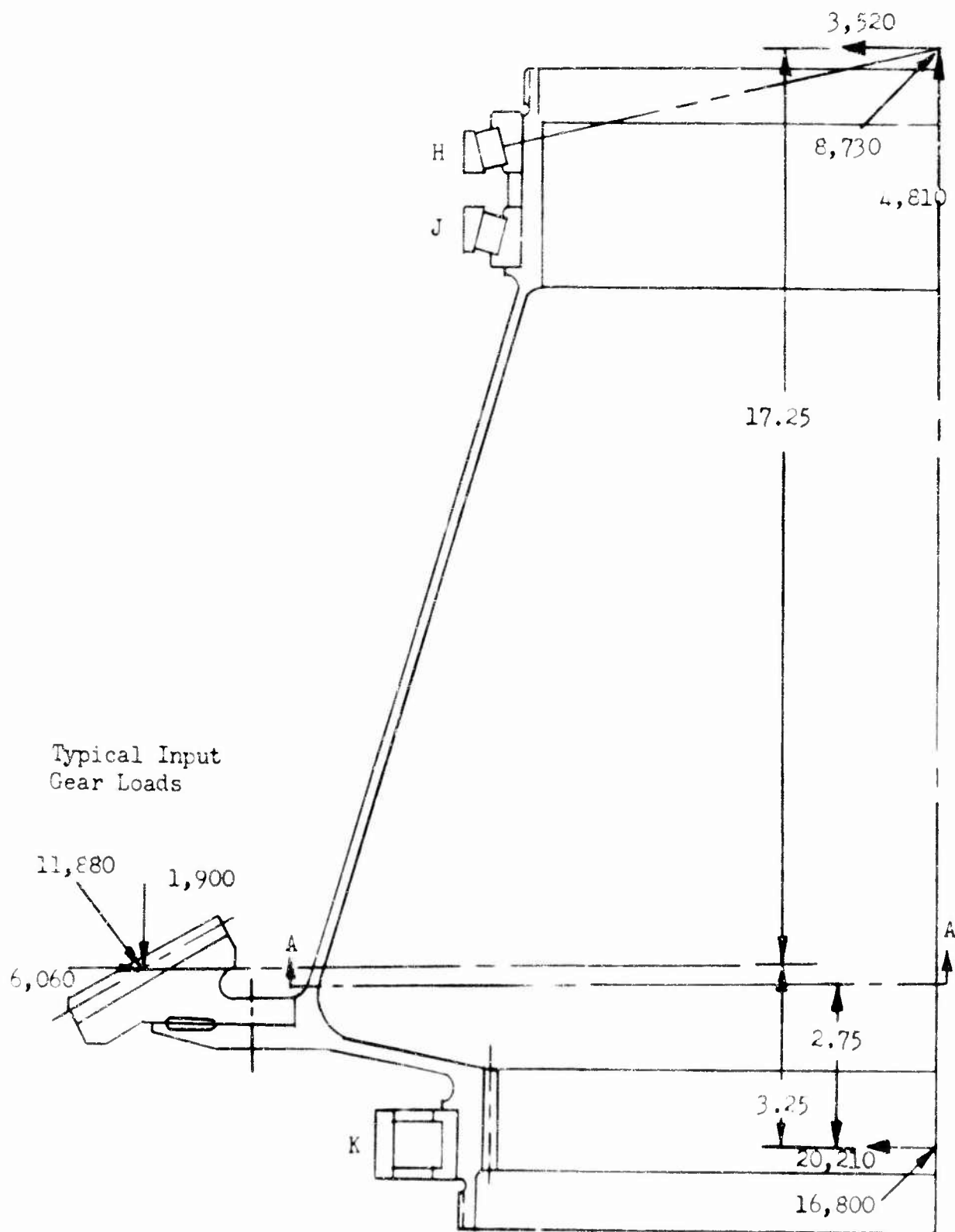
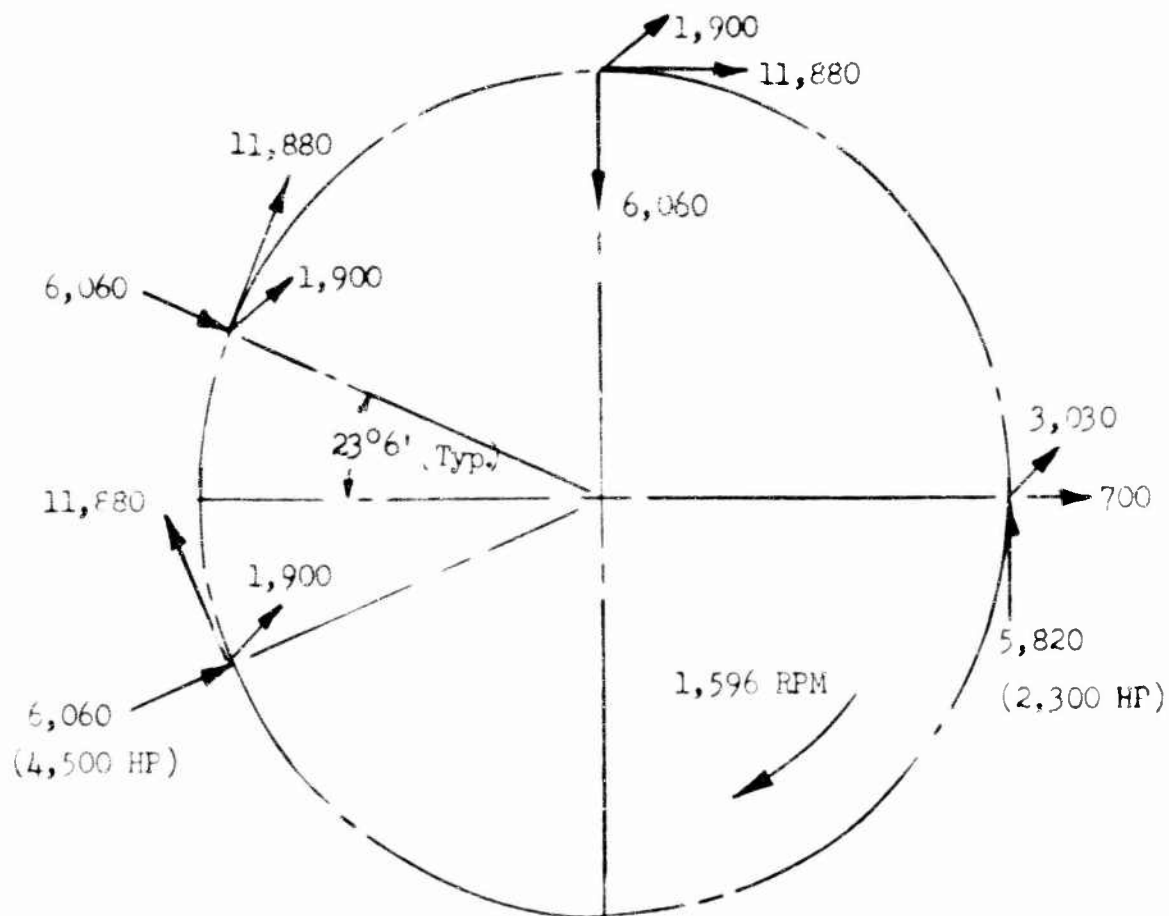


Figure 8. Outer Shaft.



Section A-A of Figure 8.

Critical Section A-A

$$\overline{O.D.} = 23.84 \qquad Z = 80.68$$

$$\overline{I.D.} = 23.47 \qquad K_t = 2.35$$

$$M = 2.75 \sqrt{(20,210)^2 + (16,800)^2}$$

$$M = 72,270 \text{ in.-lb.}$$

$$f_b = \frac{K_t M}{Z} = \frac{2.35 (72,270)}{80.68}$$

$$f_b = 2,100 \text{ psi}$$

$$F_{en} = 15,000 \text{ psi}$$

$$M.S. = \frac{F_{en}}{f_b} - 1 = \frac{15,000}{2,100} - 1 = + 6.14$$

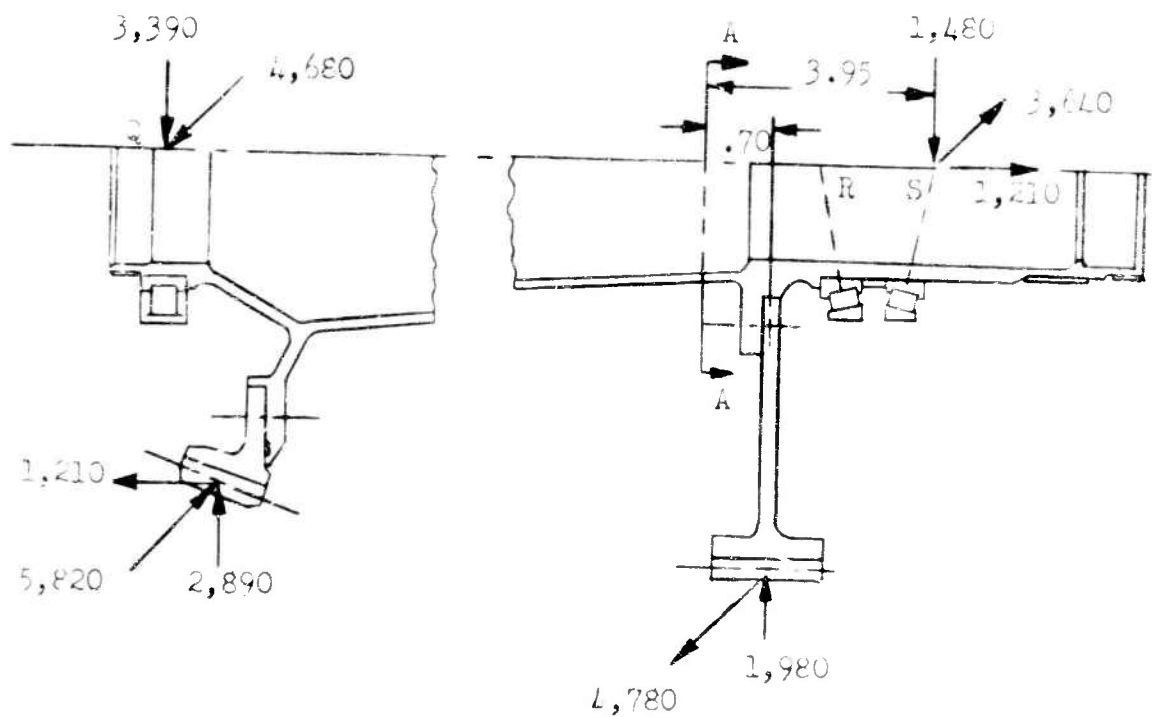


Figure 9. Tail Take off Bevel Gear Shaft

Critical Section A-A

$$\overline{O.D.} = 4.37$$

$$Z = 2.442$$

$$\overline{I.D.} = 4.00$$

$$k_t = 2.01$$

$$M_{HOR} = (-3,640)(3.95) + (4,780)(.7) = -11,030 \text{ in.-lb.}$$

$$M_{VERT} = (-1,480)(3.95) + (1,980)(.7) = -4,460 \text{ in.-lb.}$$

$$M = \sqrt{(11,030)^2 + (4,460)^2}$$

$$M = 11,900 \text{ in.-lb.}$$

$$f_b = \frac{K_t M}{Z} = \frac{2.01 (11,900)}{2.442}$$

$$f_b = 9,790 \text{ psi}$$

$$F_{en} = 19,500 \text{ psi}$$

$$M.S. = \frac{19,500}{9,790} - 1$$

$$M.S. = +.99$$

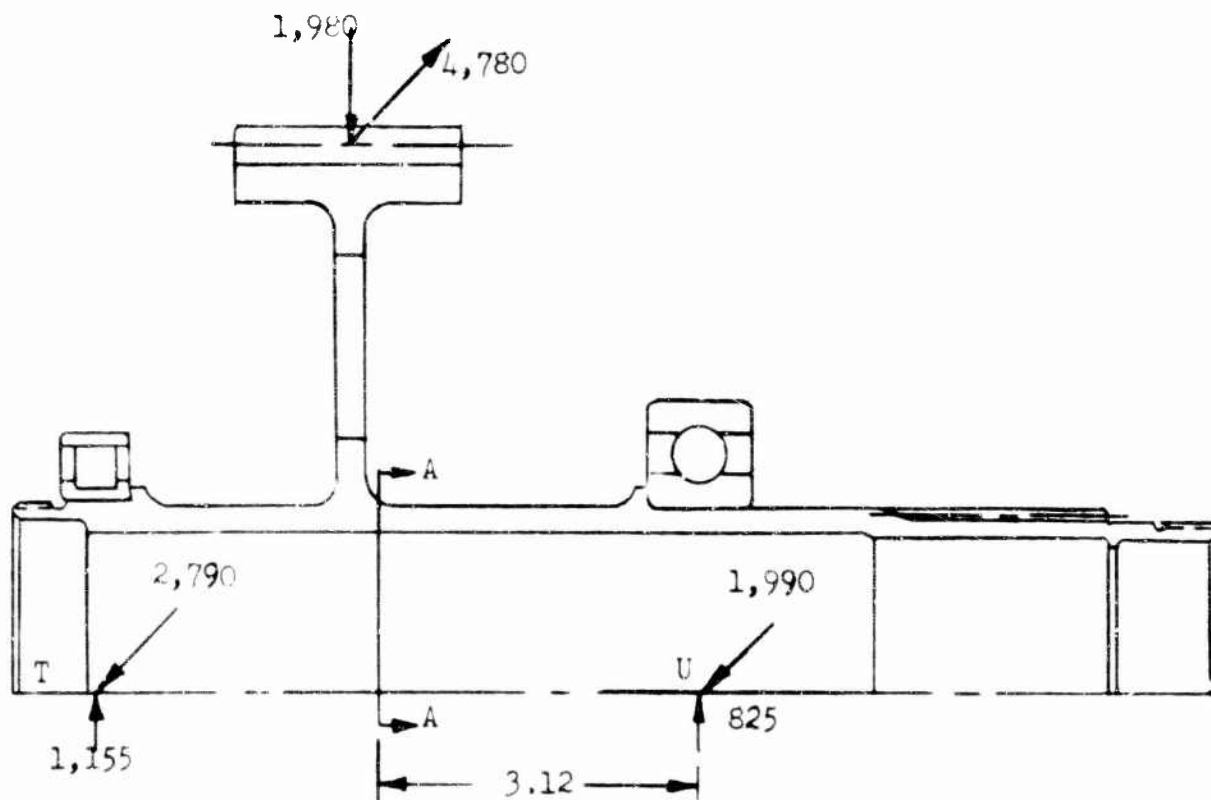


Figure 10. Tail Take off Spur Gear Shaft.

Critical Section A-A

$$\overline{O.D.} = 3.48$$

$$Z = 1.599$$

$$\overline{I.D.} = 3.03$$

$$K_t = 1.56$$

$$M = 3.12 \sqrt{(1,990)^2 + (825)^2}$$

$$M = 6,750 \text{ in.-lb.}$$

$$f_b = \frac{K_t M}{Z} = \frac{(6,750)(1.56)}{1.599}$$

$$f_b = 6,590 \text{ psi}$$

$$F_{en} = 19,500 \text{ psi}$$

$$M.S. = \frac{F_{en}}{f_b} - 1 = \frac{19,500}{6,590} - 1$$

$$M.S. = + 1.96$$

Bearing Analysis, Computer Solution

The lives of the high-speed-input triplex and quadruple ball bearing sets, accompanying roller bearings, and the first- and second-stage planetary pinion bearings were obtained using an independently developed general bearing life solution. In this solution, elastic yielding of the shaft and supporting structure is considered, as well as centrifugal and gyroscopic moment loading of the rolling elements under high-speed operating conditions. A 7090 computer has been used to achieve a numerical solution by iterative techniques.

Ball Bearings

The B-10 lives of the triplex and quadruple high-speed bearing sets can be determined using the following equations.

Capacity

The capacity of a ball bearing race contact for one million (10^6) revolutions and 90 percent probability of survival is given by the relationship

$$Q_{cq} = A \left[1 - k \frac{W_{sq}}{W_{rq}} \right]^{\phi} \left[\frac{2f}{2f-1} \right]^{.41} \left[\frac{(1 \mp \gamma \cos \beta_q)^{1.39}}{(1 \pm \gamma \cos \beta_q)^{.33}} (\gamma^{0.3} d e^{-n-1/3}) \right]^*$$

Note: For inner race contact use upper signs.
For outer race contact use lower signs.

B-10 Life

The lives of the inner and outer raceways for a given bearing in a triplex or quadruple bearing set with inner race rotation, expressed in hours for a 90 percent probability of survival, are given by the following equations.

$$B_{Li}^{L_i} = \frac{\text{Inner Raceway (n)} \quad 10^6}{60(\text{RPM}) \frac{1}{n} \sum_{q=1} \left(\frac{P_{iq}}{Q_{cq}} \right)^3}$$

*Note: Nomenclature for bearing analysis is presented on page 43.

Outer Raceway

$$BL_o = \frac{10^6}{60(\text{RPM}) \left[\frac{1}{n} \sum_{q=1}^n \left(\frac{P_{oq}}{Q_{cq}} \right)^{10/3} \right]^{.9}}$$

The life of one complete bearing of the set is expressed as follows:

$$BL = \left[\left(\frac{1}{BL_o} \right)^{10/9} + \left(\frac{1}{BL_1} \right)^{10/9} \right]^{-.9}$$

The life of the entire set of (n) bearings is given by:

$$L_{\text{set}} = \left[\left(\frac{1}{BL_1} \right)^{10/9} + \left(\frac{1}{BL_2} \right)^{10/9} + \dots + \left(\frac{1}{BL_n} \right)^{10/9} \right]^{-.9}$$

Roller Bearings

The B-10 life of high-speed roller bearings and planetary pinion bearings can be determined by the following equations.

Capacity

The capacity of a cylindrical roller or planetary pinion bearing race contact for one million revolutions and 90 percent probability of survival is given by the following equation.

$$Q'_{cq} = A' \frac{[1 + \gamma]^{29/27}}{[1 - \gamma]^{1/4}} \gamma^{2/9} d^{29/27} \rho_e^{7/9} n^{-1/4} \quad *$$

* See note on page 39.

The lives of the inner and outer raceways for high-speed roller bearings and planetary pinion bearings expressed in hours for 90 percent probability of survival is calculated as follows:

Raceway I

$$R^{L_I} = \frac{10^6}{60 \text{ (RPM)} \left[\frac{1}{n} \sum_{q=1}^n \left(\frac{P_{Iq}}{Q'_{cq}} \right)^{9/2} \right]^{8/9}}$$

Raceway II

$$R^{L_{II}} = \frac{n \cdot 10^6}{60 \text{ (RPM)} \sum_{q=1}^n \left(\frac{P_{2q}}{Q_{cq}} \right)^4}$$

Note: In the case of the high-speed cylindrical roller bearings accompanying the triplex and quadruple sets, raceway I becomes the outer race and P_{Iq} becomes P_{Oq} , while raceway II becomes the inner raceway and P_{IIq} becomes P_{Iq} .

In the case of planetary pinion bearings, raceway I becomes the inner raceway and P_{Iq} becomes P_{Iq} , while raceway II becomes the outer raceway and P_{IIq} becomes P_{Oq} .

The life equation of a complete high-speed cylindrical roller bearing or planetary pinion bearing, expressed in hours for 90 percent probability of survival, takes the following form:

$$R^L = \left[\left(\frac{1}{R^{L_0}} \right)^{9/8} + \left(\frac{1}{R^{L_1}} \right)^{9/8} \right]^{-8/9}$$

In the case of planetary pinion bearing, the deflection of the pinion gear and bearing inner race due to gear separating loads is accounted for in the bearing life analysis.

The above bearing life analysis is similar to that presented in ASME paper number 59-lub-10, "A General Theory for Elastically Constrained Ball and Radial Roller Bearings Under Arbitrary Load and Speed Conditions", by A. B. Jones, October 20, 1959.

The computer lives of the bearing applications described below are based on the bearing life analysis presented herein.

#1 and #4 high-speed inputs, Reference Figure 3, page 27

219-size triplex set, $L = 3,714$ hours

312-size roller bearing, $L = 6,209$ hours

#2 and #3 high-speed inputs, Reference Figure 17, page 73

216-size quadruple set, $L = 4,072$ hours

216-size roller bearing, $L = 14,848$ hours

} Engine Reduction
Gearbox

First-stage planetary pinion bearings:

Diameter over rollers = 12.20

Bore = 9.1

Length = 3.25

$L = 10,656$ hours

Second-stage planetary pinion bearings:

Diameter over rollers = 10.4

Bore = 7.36

Length = 6.0

$L = 4,474$ hours

Nomenclature

A	=	A fatigue constant for ball bearings
A^s	=	A fatigue constant for roller bearings
E	=	Pitch diameter of bearing, inch
B^L	=	Fatigue life for ball bearings, hours
R^L	=	Fatigue life for roller bearings, hours
RPM	=	Speed of rotating race
P_{oq}, P_{iq}	=	Dynamic rolling element loads at outer and inner race contacts, pounds
Q_{cq}, Q'_{cq}	=	Capacity of a ball and roller race contact for 90 percent probability of survival to 10^6 revolutions of inner race, pounds
ℓ_e	=	Effective length of roller, inch
d	=	Ball diameter, inch
f	=	Ratio of transverse radius of ball race to ball diameter
n	=	Number of balls in the system
β	=	Initial contact angle of ball bearing after mounting - degrees
γ	=	Ratio of d/ℓ_e
L_i	=	Inner raceway fatigue life, hours
L_o	=	Outer raceway fatigue life, hours

Subscript q refers to conditions at the q^{th} rolling element position.

TABLE 6
BEARING LIFE SUMMARY,
MAIN GEARBOX

Bearing Type	Location	Page No.	Fig. No.	Locat. Letter	Life (Hr.)
Triples Set	High-Speed-Input Bevel	27	3	A	3,714
Roller	High-Speed-Input Bevel	27	3	B	6,209
Roller	Driven Bevel - 1st Stage	28	4	C	8,070
Duplex Set	Driven Bevel - 1st Stage	28	4	D	5,420
Tapered Roller	Input - Main Bevel	32	7	E	∞
Tapered Roller	Input - Main Bevel	32	7	F	4,610
Roller	Input - Main Bevel	32	7	G	5,990
Tapered Roller	Outer Shaft	34	8	H	3,860
Tapered Roller	Outer Shaft	34	8	J	∞
Roller	Outer Shaft	34	8	K	8,340
Roller	1st-Stage Planetary	-	-	L	10,656
Roller	2nd-Stage Planetary	-	-	M	4,474
Roller	Main Rotor Shaft	58	13	N	4,950
Triples Set	Main Rotor Shaft	58	13	P	3,410
Roller	Tail Take off Bevel	36	9	Q	15,200
Tapered Roller	Tail Take off Bevel	36	9	R	∞
Tapered Roller	Tail Take off Bevel	36	9	S	10,950
Roller	Tail Take off	37	10	T	19,610
Ball	Tail Take off	37	10	U	5,990

Note: All bearings in the primary drive train (engine through main rotor) with B-10 lives of less than 5,000 hours will be made from vacuum processed 52100 steel.

Planetary Gear Reductions

The planetary reduction stages have been designed with separate upper and lower cage (carrier) plates connected by means of clamped spacers and the preload journal of the planet pinion bearings. Both the primary and secondary planetary reduction stages are shown in Figure 54 of Appendix I.

With this design, the components are designed to stress levels consistent with good reliability. Deflections of the carrier plates are accommodated by cutting corrective helix angles in the sun and ring gears, crowning and providing tip relief in the mating gear teeth. This design practice has produced reliable, efficient, and lightweight designs of simple planetary stages in use in current production helicopter transmissions.

Determination of the required face widths and planetary cage plate thicknesses follows.

Planetary Stages - Gear Face Width Calculations

Determination of the required face widths will be based on allowable bending (Lewis) and compressive (Hertz) stresses, as given on page of this report. Bending and compressive stresses have been calculated using the following equations:

$$f_b = \frac{1.5 W_t K}{(F.W.) X}$$

$$f_c^2 = \frac{21 \times 10^6 W_t}{\sin 2\phi (F.W.)} (1/D \text{ pinion} \pm 1/D \text{ gear})$$

Note: + for external mesh, - for internal mesh

First-Stage Planetary Data

	No. Teeth (-N)	Pitch Diameter (-D)
Sun	101	16.8333
Planet	85	14.1667
Ring	271	45.1667

Number of Planet Pinions (N_{pp})	= 6
Pressure Angle (ϕ)	= $22^{\circ}30'$
Sun Gear Speed	= 1,596 RPM
Gear Tooth Design Power	= 14,200 HP

Allowable Stresses

$$\begin{aligned} \text{PLV} &= \frac{.524 \times \text{RPM sun} \times (D_s + D_p) \times N_s \times N_r}{2 \times (N_s + N_p) \times (N_s + N_r)} \\ &= \frac{.524 \times 1,596 \times (16.8333 + 14.1667) \times 101 \times 271}{2 \times (101 + 85) \times (101 + 271)} \end{aligned}$$

$$\text{PLV} = 5,130 \text{ fpm}$$

$$F_b = 31,500 - 0.625 \times \text{PLV} \quad (\text{Reference page } 18)$$

$$= 31,500 - 0.625 \times 5,130$$

$$F_b = 28,290 \text{ psi}$$

$$F_c = 140,000 \text{ psi} \quad (\text{Reference page } 18)$$

Loading

$$\text{Torque} = \frac{63,025 \times 14,200}{1,596}$$

$$\text{Torque} = 560,750 \text{ in.-lb.}$$

$$W_t = \frac{2 \times \text{Torque}}{D_s} = \frac{2 \times 560,750}{16.8333}$$

$$W_t = 66,600 \text{ lb.}$$

$$W_t/\text{Mesh} = W_t/6 = 11,100 \text{ lb.}$$

Face Width - Sun Gear

$$X = (\text{function of pitch \& number of teeth}) = .2125$$

$$K = (\text{function of root radius}) = 1.05$$

$$F.W.b = \frac{1.5 W_t K}{F_b(\text{allowable})^X}$$

$$F.W._b = \frac{1.5 \times 11,100 \times 1.05}{28,290 \times .2125}$$

$$F.W._b = 2.91 \text{ in.}$$

$$F.W._c = \frac{21 \times 10^6 W_t}{\sin 2 \phi F_c^2 (\text{allowable})} \quad (1/D_p + 1/D_s)$$

$$= \frac{21 \times 10^6 \times 11,100}{0.707 \times (140,000)^2} (1/14.1667 + 1/16.8333)$$

$$F.W._c = 2.19 \text{ in.}$$

Face Width - Planet Pinion

$$X = .207$$

$$K = 1.017$$

$$F.W._b = \frac{1.5 \times 11,100 \times 1.017}{28,290 \times 0.207}$$

$$F.W._b = 2.89 \text{ in.}$$

Face Width - Ring Gear

$$X = 0.284$$

$$K = 1.12$$

$$F.W._b = \frac{1.5 \times 11,100 \times 1.12}{28,290 \times 0.284}$$

$$F.W._b = 2.32 \text{ in.}$$

$$F.W._c = \frac{21 \times 10^6 \times 11,100}{0.707 \times 140^2 \times 10^6} (1/14.1667 - 1/45.1667)$$

$$F.W._c = .82 \text{ in.}$$

Second-Stage Planetary Data

	Teeth - N	Pitch Diameter - D
Sun	135	22.500
Planet	73	12.1667
Ring	281	46.8333
Number of Planet Pinions (N _{pp})	= 8	
Pressure Angle	φ	= 22°30'
Sun RPM	= 433.3	
Gear Design Horsepower	= 14,200	

Allowable Stresses

$$PLV = \frac{0.524 \times 433.3 \times (22.50 + 12.1667) \times 135 \times 281}{2 \times (135 + 73) \times (135 \div 281)}$$

$$PLV = 1,725 \text{ fpm}$$

$$F_b = 31,500 - 0.625 \times 1,725$$

$$F_b = 30,420 \text{ psi}$$

$$F_c = 140,000 \text{ psi}$$

Loading

$$\text{Torque} = \frac{63,025 \times 14,200}{433.3}$$

$$\text{Torque} = 2.065 \times 10^6 \text{ in.-lb.}$$

$$W_t/\text{Mesh} = \frac{2 \times \text{Torque}}{D_s \times 8} = \frac{2 \times 2.065 \times 10^6}{22.5 \times 8}$$

$$W_t/\text{Mesh} = 22,950 \text{ lb.}$$

Face Width - Sun Gear

$$X = .2143$$

$$K = 1.05$$

$$F.W._b = \frac{1.5 \times 22,950 \times 1.05}{30,420 \times 0.2143}$$

$$F.W._b = 5.55 \text{ in.}$$

$$F.W._c = \frac{21 \times 10^6 \times 22,950}{0.707 \times 140^2 \times 10^6} (1/12.1667 + 1/22.500)$$

$$F.W._c = 4.40 \text{ in.}$$

Face Width - Planet Pinion

$$X = .202$$

$$K = 1$$

$$F.W._b = \frac{1.5 \times 22,950 \times 1}{30,420 \times 0.202}$$

$$F.W._b = 5.60 \text{ in.}$$

Face Width - Ring Gear

$$X = .284$$

$$K = 1.13$$

$$F.W._b = \frac{1.5 \times 22,950 \times 1.13}{30,420 \times 0.284}$$

$$F.W._b = 4.50 \text{ in.}$$

$$F.W._c = \frac{21 \times 10^6 \times 22,950}{0.707 \times 140^2 \times 10^6} (1/12.1667 - 1/46.8333)$$

$$F.W._c = 2.12 \text{ in.}$$

TABLE 7
PLANETARY GEAR DATA

Component	Required Face Width Bending (in.)	Required Face Width Compression (in.)	Face Width Selected (in.)	Actual Bending Stress (psi)	Actual Compressive Stress (psi)
First Stage					
Sun Gear	2.91	2.19	3.00	27,400	121,800
Planet Pinion	2.99	2.19	2.90	28,200	121,800
Ring Gear	2.32	.82	2.60	25,300	83,000
Second Stage					
Sun Gear	5.55	4.40	5.70	29,700	124,600
Planet Pinion	5.60	4.40	5.60	30,400	124,600
Ring Gear	4.50	2.12	5.30	25,900	96,000

The calculated planetary gear face widths are summarized in Table 7 on page 50. Also presented are the actual gear face widths chosen for sufficient overlap to assure that operating stresses are consistent with calculated values.

Planetary Cage (Carrier) Plate

In the symmetrical, double-plate planetary configuration, plate thickness is determined by either of two design limitations - maximum allowable bending stress or maximum allowable plate deflection. Operational experience has indicated that these two design criteria are sufficient to determine the required plate thicknesses. Plate thicknesses for the two reduction stages will be determined by the use of the following equations.

$$f_b = \frac{12T}{N_{pp} D_s L} \frac{(0.5L - .4d)(g + t)}{(O.D. - I.D. - 1.2 d) t^2}$$

$$\lambda = \frac{16 T}{D_s \cdot N_{pp} (O.D. - I.D.) E \cdot L^2} \frac{(0.5L - .4d)^3 (g + t)}{t^3}$$

Plate thickness calculations for each stage are as follows.

First Stage

$$\begin{aligned} T &= 560,750 \text{ in.-lb.} \\ \text{RPM}_{\text{sun}} &= 1,596 \\ N_{pp} &= 6 \\ g &= 3.30 \text{ in.} \\ N_s &= 101 \\ N_p &= 85 \\ N_r &= 271 \\ D_s &= 16.8333 \text{ in.} \\ D_p &= 14.1667 \text{ in.} \end{aligned}$$

$$d = 11.35 \text{ in.}$$

$$\overline{\text{O.D.}} \\ \text{plates} = 44.6 \text{ in.}$$

$$\overline{\text{I.D.}} \\ \text{plates} = 17.3 \text{ in.}$$

$$E = 30 \times 10^6$$

$$L = (D_s + D_p) \sin (\pi / N_{pp}) \\ = (16.8333 + 14.1667) \sin (180/6)$$

$$L = 15.50 \text{ in.}$$

$$f_b = \frac{(12)(560,750)(0.5 \times 15.5 - 0.4 \times 11.35) (g + t)}{(6)(16.8333)(15.5)(44.6 - 17.3 - 1.2 \times 11.35) t^2}$$

$$f_b = (1,008) \frac{g + t}{t^2}$$

$$\lambda = \frac{(16)(560,750)(0.5 \times 15.5 - 0.4 \times 11.35)^3 (g + t)}{(16.8333)(6)(44.6 - 17.3)(30 \times 10^6)(15.5)^2 t^3}$$

$$\lambda = (14.94 \times 10^{-6}) \frac{g + t}{t^3}$$

Substitution (in the above equations) of the allowable plate stress and maximum plate deflection limits as given on page 19 results in a first-stage carrier plate thickness of $t = 0.400$ inch.

The relation of the first-stage carrier plate stress and deflection for various plate thicknesses is shown graphically in Figure 11, page 55.

Second Stage

$$\begin{aligned}T &= 2.067 \times 10^6 \text{ in.-lb.} \\RPM_{sun} &= 433 \\N_{pp} &= 8 \\g &= 6 \text{ in.} \\N_s &= 135 \\N_p &= 73 \\N_r &= 281 \\D_s &= 22.50 \text{ in.} \\D_p &= 12.1667 \text{ in.} \\D &= 9.35 \text{ in.} \\\overline{O.F.} &= 46.30 \text{ in.} \\\overline{I.D.} &= 23.00 \text{ in.} \\E &= 30 \times 10^6 \text{ psi} \\L &= (22.5 + 12.1667) \sin (180/8) \\L &= 13.266 \text{ in.}\end{aligned}$$

Inspection of the second-stage dimensions and required design parameters in the plate stress and deflection equations results in the following relations.

$$\begin{aligned}f_b &= (2,488) \frac{g + t}{t^2} \\\lambda &= (36.16 \times 10^{-6}) \frac{g + t}{t^3}\end{aligned}$$

Substitution (in the preceding equations) of the allowable plate stress and maximum plate deflection limits, as given on page 19, results in a second-stage carrier plate thickness of 0.610 inch. The relation of the second-stage carrier plate stress and deflection for various plate thicknesses is shown graphically in Figure 12, page 56.

To compensate for the deflection in the first- and second-stage carrier plates in this design, a corrective right-hand helix angle of 0.0005 to 0.0008 inch per inch should be cut on the sun and ring gears of each stage.

Planetary Design Using Titanium

As indicated on page 17, the contractor has successfully used titanium alloy (6 Al-4V) for planetary cage plates on several production aircraft. Maintaining the present design limits ($f_b = 42,000$ psi and $\lambda = .001$ inch per inch) for titanium carriers and spacers, the following weight saving was realized:

	Wt. Saving
1st-Stage	53 lb.
2nd-Stage	87 lb.
Total	<hr/> 140 lb.

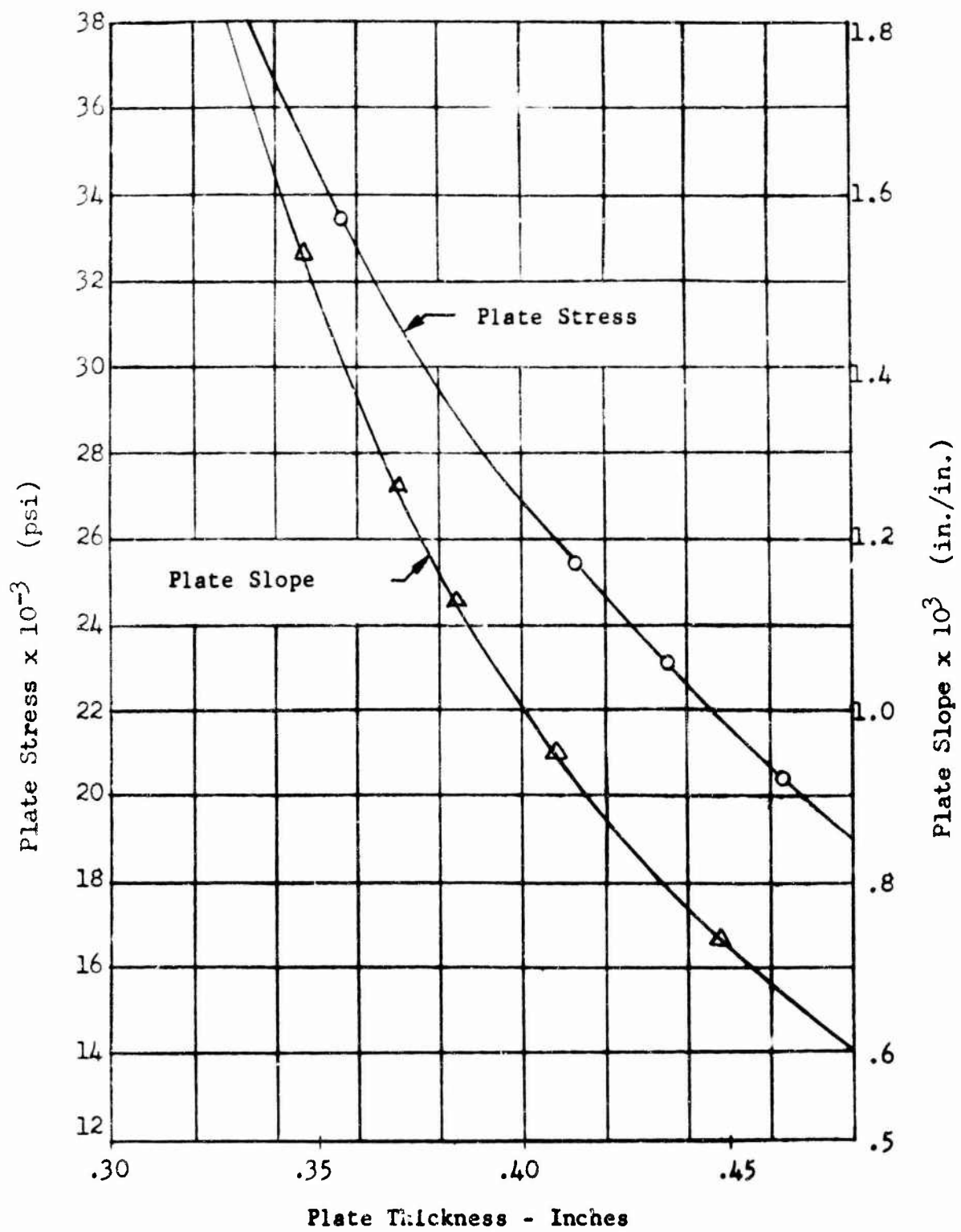


Figure 11. Stress and Deflection Versus Planetary Plate Thickness, First Stage.

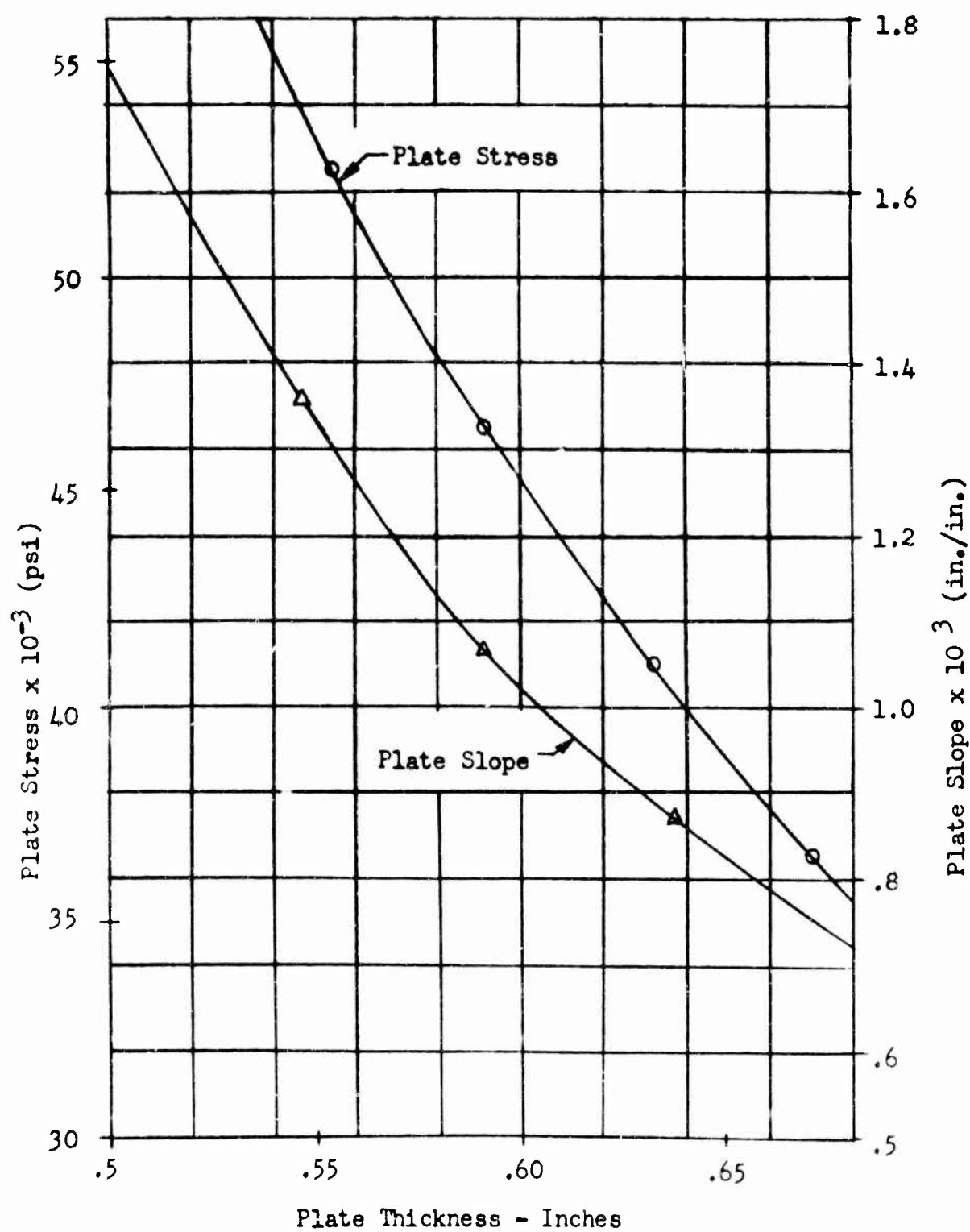


Figure 12. Stress and Deflection Versus Planetary Plate Thickness, Second Stage.

Main Rotor Shaft

The transmission of torque to the main rotor during all operational flight regimes subjects the main rotor shaft to vibratory loads which result from the flapping motion of the blades. As the lift vector is tilted to obtain horizontal force components, a moment and force is induced on the hub which is transmitted to the shaft through the hub attachment. As the shaft rotates relative to these loads, the moments and forces are cyclic and proportional to the flapping angle β . In addition to these loads, a steady vertical force, approximately equal to the aircraft gross weight (G.W.), is also transmitted to the shaft.

To design the rotor shaft for an adequate service interval, a load-time schedule (flapping spectrum) and a stress-time relation (S-N curve) have been established. The flapping spectrum depicts the main rotor blade flapping angle β and its anticipated frequency of occurrence. Table 4, page 12, presents the anticipated flapping spectrum for the single-rotor heavy-lift helicopter of Reference 3. The S-N curve for the main rotor shaft is shown in Figure 14, page 64. These S-N data incorporate a reliability factor ($R = .9999$) and a size effect factor based on volume.

Using the cumulative damage theory, an iterative calculation is made to establish an endurance flapping angle β_e which must be considered to obtain the desired service life (in this case = 3,600 hours) when the load spectrum is applied to the S-N curve. The main rotor shaft, Figure 13, page 58, has been designed for infinite service life at the load level corresponding to β_e .

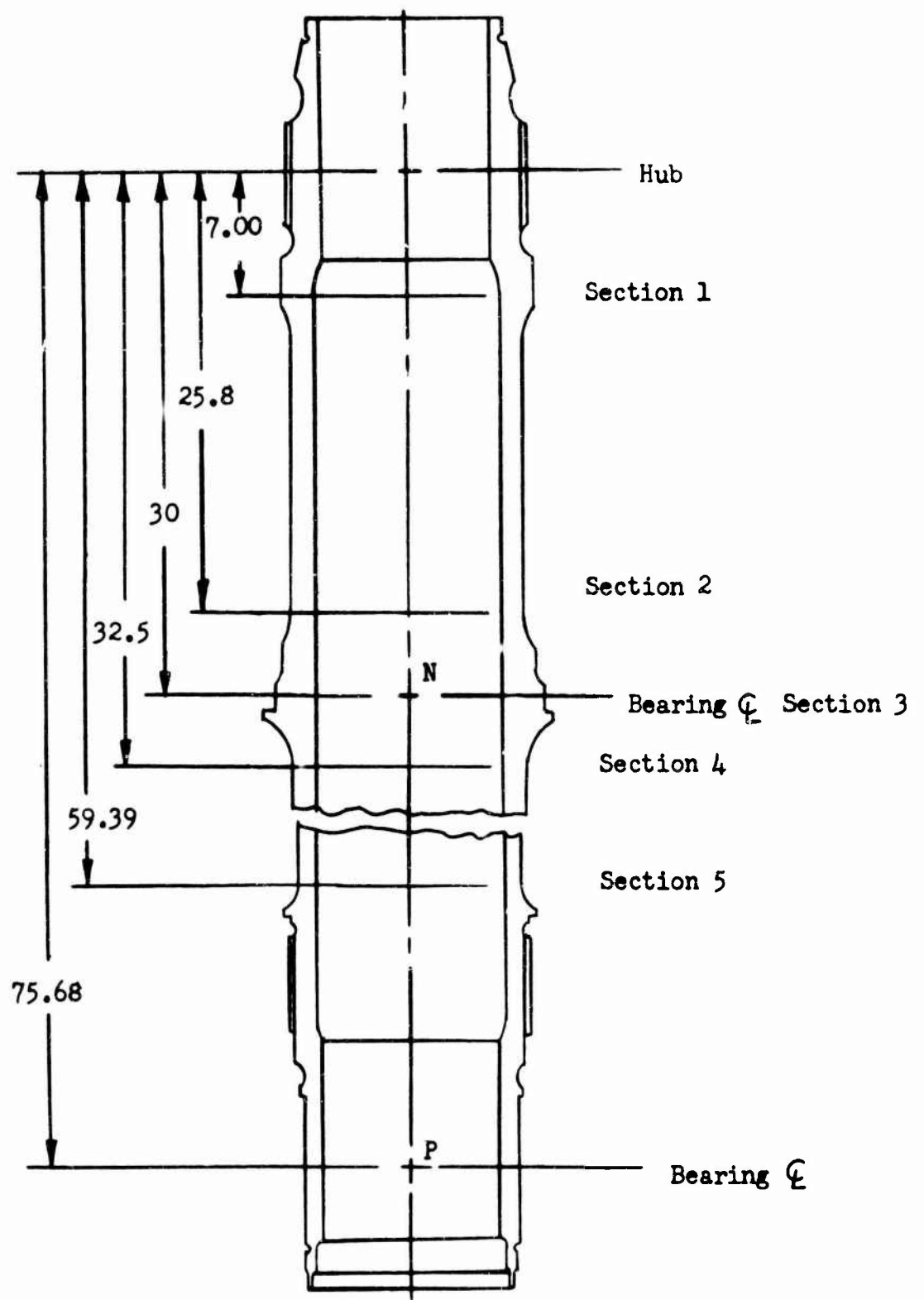


Figure 13. Main Rotor Shaft.

Design Data

G.W.	= 86,900 lb.
Horsepower	= 14,200
RPM	= 140.6
Number of Blades b	= 6
Hinge Offset e	= 30 in.
Forward Inclination of Shaft i_s	= 3 degrees
Blade Centrifugal Force F_c	= 153,000 lb.
C.G. Range	= 50 in.
Endurance Flapping Angle β_e	= 10.00 degrees
Tan β_e	= .1763
Hub Constant K	= $(b/2)e F_c = 13.8 \times 10^6$ in.-lb./rad.
Hub Moment M_h	= $\frac{(b/2)e F_c \beta_e}{57.3} = \frac{K \beta_e}{57.3}$
M_h	= 2.408×10^6 in.-lb.
Horizontal Force H	= $G.W. \times \tan \beta_e = 15,320$ lb.
Shaft Material:	SAE 4340 steel

$$F_{tu} = 200,000 \text{ psi}$$

$$F_{en} = 21,800 \text{ psi (Reference Figure 14 , page 64)}$$

Stress Analysis

All section numbers refer to those sections shown on Figure 13 ,
page 58 .

Section 1, cone seat

$$\overline{O.D.} = 15.16 \text{ in.}$$

$$\overline{I.D.} = 11.12 \text{ in.}$$

$$Z = 235.6 \text{ in.}^3$$

$$X = 7 \text{ in.}$$

$$K_t = 1.88$$

$$M = 2.408 \times 10^6 + 15,320 \times 7 = 2.515 \times 10^6 \text{ in.-lb.}$$

$$f_b = K_t M/Z = 1.88 \times 2.515 \times 10^6 / 235.6$$

$$f_b = 20,070 \text{ psi}$$

Section 2, fillet above upper bearing

$$\overline{O.D.} = 14.16 \text{ in.}$$

$$\overline{I.D.} = 11.12 \text{ in.}$$

$$Z = 172.7 \text{ in.}^3$$

$$X = 25.8 \text{ in.}$$

$$K_t = 1.33$$

$$M = 2.408 \times 10^6 + 15,320 \times 25.8$$

$$M = 2.803 \times 10^6 \text{ in.-lb.}$$

$$f_b = 1.33 \times 2.803 \times 10^6 / 172.7$$

$$f_b = 21,580 \text{ psi}$$

Section 3, bearing seat

$$\overline{O.D.} = 16.14 \text{ in.}$$

$$\overline{I.D.} = 11.12 \text{ in.}$$

$$Z = 319.8 \text{ in.}^3$$

$$X = 30 \text{ in.}$$

$$K_t = 2.34$$

$$M = 2.408 \times 10^6 + 15,320(30) = 2.867 \times 10^6 \text{ in.-lb.}$$

$$f_b = \frac{(2.34)(2.867 \times 10^6)}{319.8}$$

$$f_b = 20,970 \text{ psi}$$

Section 4, fillet below bearing

$$\overline{O.D.} = 13.80 \text{ in.}$$

$$\overline{I.D.} = 11.12 \text{ in.}$$

$$Z = 149.2 \text{ in.}^3$$

$$X = 32.5 \text{ in.}$$

$$K_t = 1.20$$

$$M = \left[2.408 \times 10^6 + 15,320(30) \right] \frac{75.68 - 32.50}{45.68}$$

$$M = 2.711 \times 10^6 \text{ in.-lb.}$$

$$f_b = \frac{(1.20)(2.711 \times 10^6)}{149.2} = 21,800 \text{ psi}$$

$$f_b = 21,800 \text{ psi}$$

Section 5, end of lower taper

$$\overline{O.D.} = 12.90 \text{ in.}$$

$$\overline{I.D.} = 11.12 \text{ in.}$$

$$Z = 94.4 \text{ in.}^3$$

$$X = 59.38 \text{ in.}$$

$$K_t = 1.50$$

$$M = \left[2.408 \times 10^6 + 15,320(30) \right] \frac{75.68 - 59.38}{45.68}$$

$$M = 1.023 \times 10^6 \text{ in.-lb.}$$

$$f_b = \frac{1.5 \times 1.023 \times 10^6}{94.4} = 16,250 \text{ psi}$$

$$f_b = 16,250 \text{ psi}$$

Assuming the maximum transient flapping angle of 12 degrees, a static analysis of Section 5 follows:

$$f_b = 16,250 \text{ psi} \times \frac{12.0}{10.0}$$

$$f_b = 19,500 \text{ psi}$$

$$T_{\max} = \frac{63,025 \times 14,200}{140.6}$$

$$T_{\max} = 6.365 \times 10^6 \text{ in.-lb.}$$

$$f_s = \frac{T}{2Z}$$

$$f_s = \frac{6.365 \times 10^6}{2 \times 94.4} = 33,710 \text{ psi}$$

$$f_a = P/A \approx G.W./A = 86,900/33.58$$

$$f_a = 2,590 \text{ psi}$$

$$\text{Margin of Safety, M.S.} = \frac{F_{tu}}{1.5 \sqrt{(f_a + f_b)^2 + 4(f_s)^2}} \quad -1$$

$$\text{M.S.} = \frac{200,000}{1.5 \sqrt{(2,590 + 19,500)^2 + 4(33,710)^2}} \quad -1$$

$$\text{M.S.} = + .88$$

Life Analysis

A life analysis on the highest stressed shaft section (Section 4) for the 20-ton heavy-lift mission, which is the most severe, has been made as follows.

% Time	Flapping Angle (Degrees)	Stress (psi)	Cycles to Fracture (See Fig. 14, pg. 64)
.01	12.00	26,160	1.27×10^5
.54	11.50	25,070	1.96×10^5
.40	10.07	21,960	46.10×10^5
.80	7.20	15,700	

The shaft life, by the cumulative damage theory, is:

$$L = \frac{100}{\frac{\%t_1}{l_1} + \frac{\%t_2}{l_2} + \frac{\%t_3}{l_3} + \dots + \frac{\%t_n}{l_n}} \quad (\text{Cycles})$$

$$= \frac{100}{\frac{.01}{1.27 \times 10^5} + \frac{.54}{1.96 \times 10^5} + \frac{.40}{46.10 \times 10^5}}$$

$$= \frac{100 \times 10^5}{.292}$$

$$L = 342 \times 10^5 \text{ cycles}$$

$$L = 4,050 \text{ hours at } R = 0.9999$$

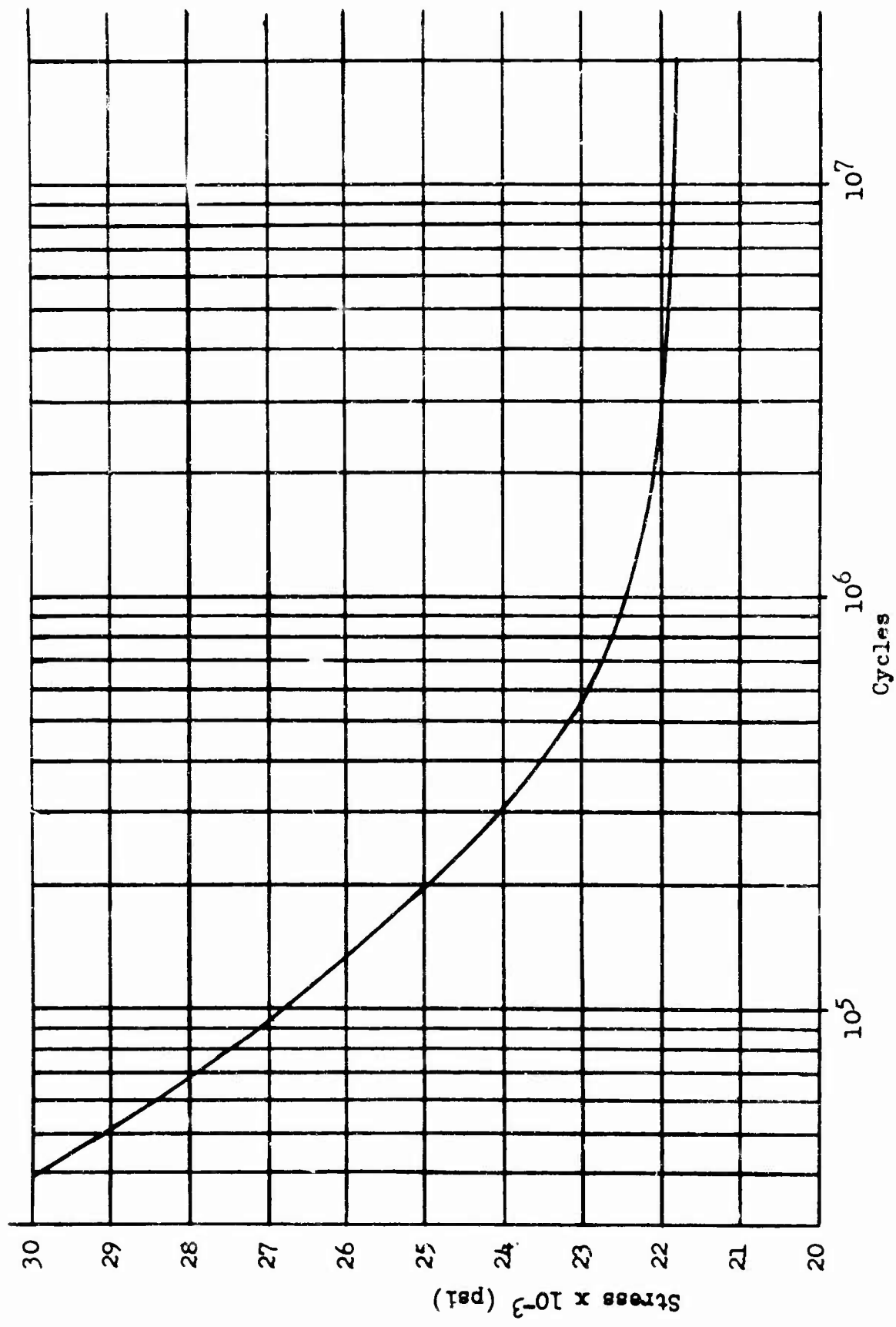


Figure 14. S-N Curve, 4340 Steel, $F_{tu} = 200,000$ psi (Main Rotor Shaft).

To investigate the weight saving that could be realized by fabricating the main rotor shaft from 6Al-4V titanium alloy, a preliminary comparative design analysis was conducted. The analysis indicated a possible weight saving of 340 pounds in the main rotor shaft.

Overrunning Clutch

Each main gearbox input pinion drive incorporates a roller-type free-wheel unit which automatically disengages an engine should it suffer partial or complete loss of power. This unit also allows for engine to main rotor release during autorotation.

A cross section of this unit is shown in Figure 15. page 66. The roller-type clutch functions on the principle of relative speeds. The overrunning condition is achieved by a variation in relative speed between the inner and outer members of the freewheel unit.

In normal operation, the rollers roll up an inclined plane (cam flats) and are wedged between the cam and the outer housing.

The freewheel unit required for the HLH input drives are similar in size to those currently in use in the Army CH-54A crane helicopter. Test and service experience on units of this size indicate no developmental problems should be realized in either direct drive or overrunning operation. In fact, the contractor has accumulated sufficient overrunning experience to justify shutting down engines to accomplish the 1,500-n.m. ferry mission.

A structural analysis of the overrunning clutch outer housing is presented on page 30.

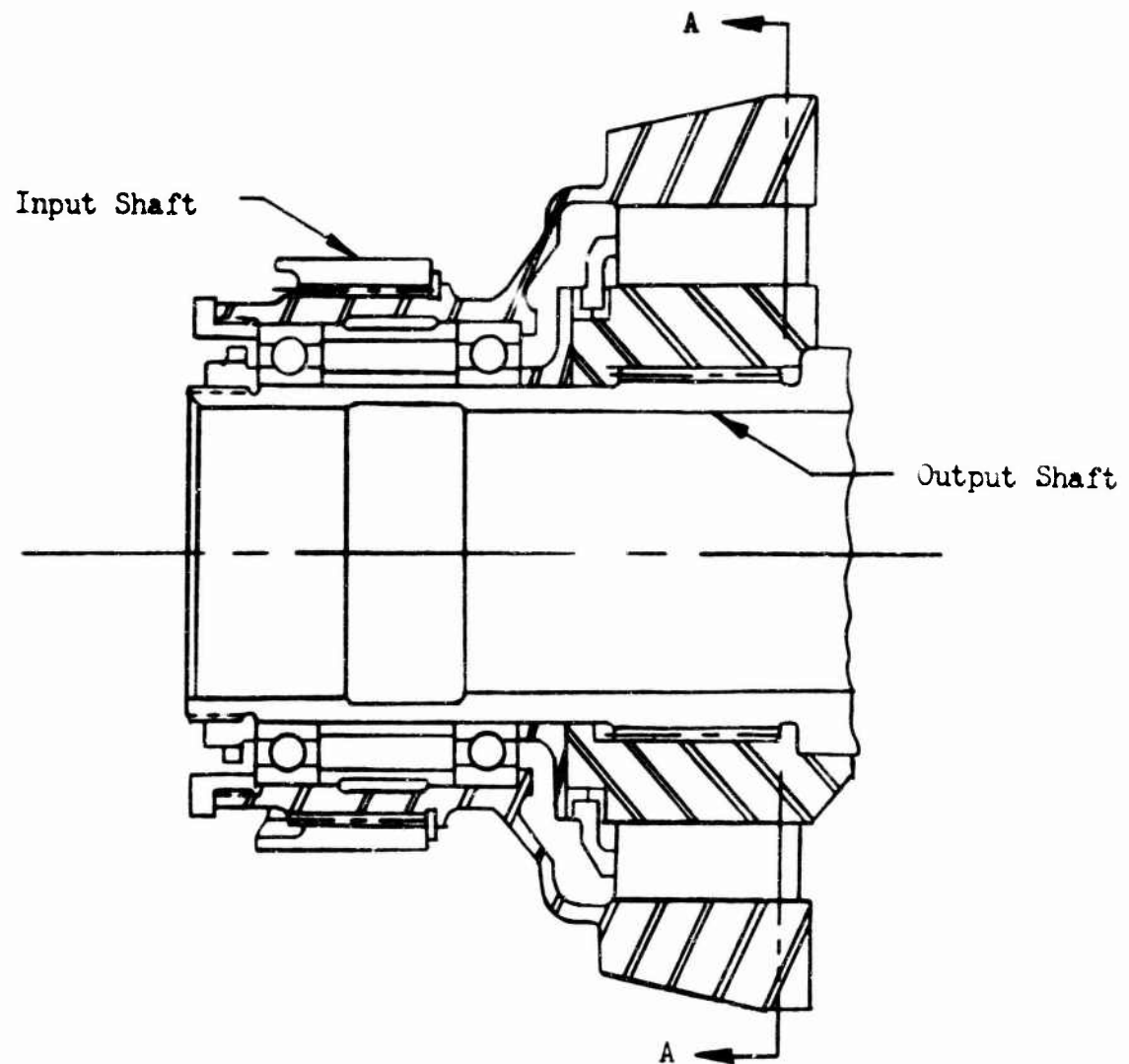
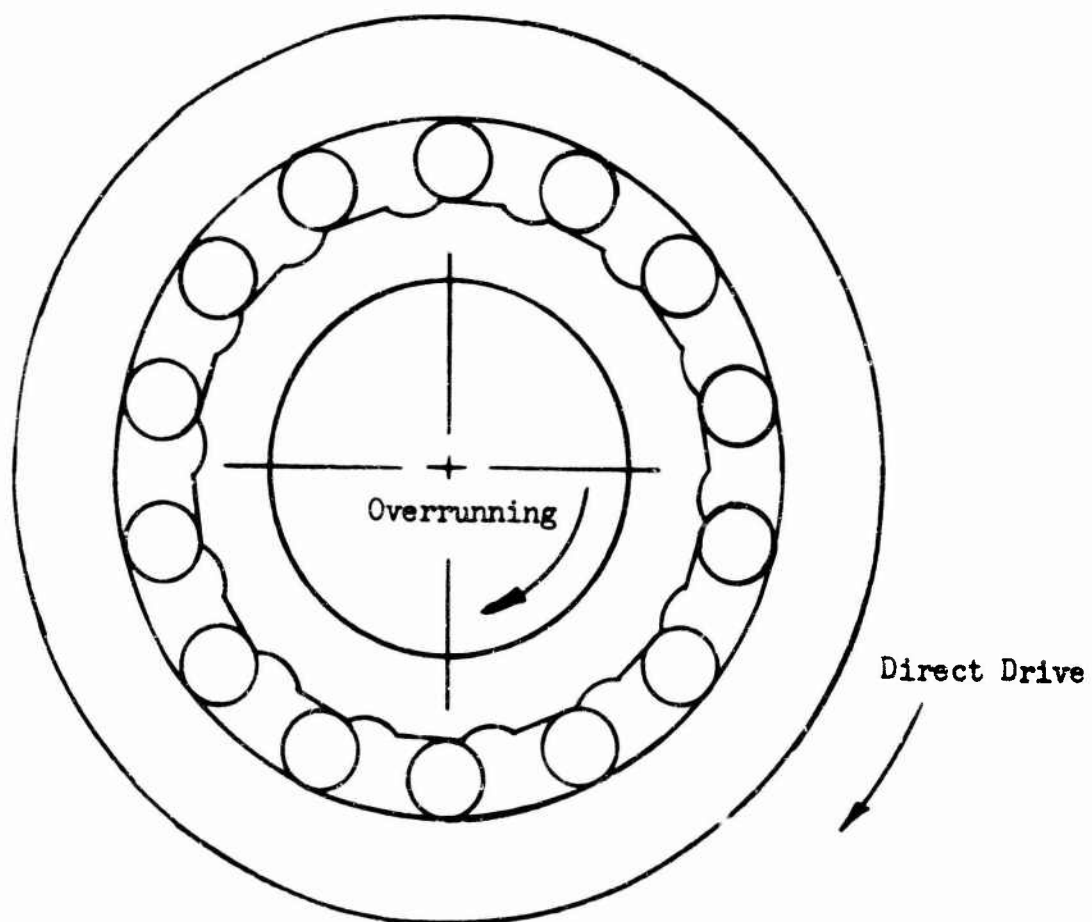


Figure 15. Roller-type Freewheel Unit



Section A-A of Figure 15.

Lubrication and Efficiency Analysis

The primary consideration of the design of a lubrication system for this gearbox and previous helicopter main transmissions is to provide cooling oil to remove heat generated due to friction generated at gear meshes and bearings and to provide lubricity to support tooth and bearing loads.

The preliminary analysis presented in this report establishes a systematic approach to the design of an integrated lubrication system for each transmission component. This approach is based upon extensive test and production experience with a considerable number of helicopter transmissions. This transmission utilizes carburized and ground gears, precision bearings, and close tolerance machined dynamic parts and housings. Experience indicates the losses through gear meshes, including the associated bearings, to be 1/2 percent per mesh; for planetary gear trains 3/4 percent and the total gearbox churning losses to be 3/4 percent.

Efficiency Analysis

Input Bevel Mesh (2 places)	(.005)(4,000)(2) =	40.0
Main Bevel Mesh (4 places)	(.005)(4,000)(4) =	80.0
Accessory Bevel Mesh	(.005)(300) =	1.5
1st-Stage Planetary	(.0075)(14,200) =	106.5
2nd-Stage Planetary	(.0075)(14,200) =	106.5
Tail take off Bevel Mesh	(.005)(1,500) =	7.5
Tail take off Spur Mesh	(.005)(1,500) =	7.5
Churning Losses	(.0075)(16,000) =	120.00

$$FHP(\text{friction HP}) = \overline{469.5}$$

$$\text{Estimated Efficiency} = \frac{16,000 - 469.5}{16,000} (100) = 97.1\%$$

Total Heat Generated, (QG)

$$\begin{aligned} QG &= 2,545 \text{ FHP} \\ &= (2,545)(469.5) \\ &= 1,195,000 \text{ BTU/HR.} \end{aligned}$$

From past helicopter experience, at least 15 percent of the total heat generated in a main gearbox is conducted through the gear case and radiated to the surrounding area. Therefore, the necessary main gearbox oil cooler can be designed to reject 85 percent of the total gearbox heat generated at maximum power.

Heat Rejection Rate - Oil Cooler

$$\begin{aligned} Q_{o.c.} &= .85 Q_G \\ &= (.85)(1,195,000) \\ &= 1,015,000 \text{ BTU/HR.} \end{aligned}$$

The transmission oil cooler and blower design is summarized on page 149 of this report.

Cooling Oil Required

Oil flow requirements are based upon the following parameters:

1. Use MIL-L-7808 oil in this transmission.
2. Oil in at 176°F.
3. Oil out of gearbox at 230°F.

Main Gearbox

$$\begin{aligned} W_o &= \frac{C_e (42.4)(F_{HP})}{(.1337)(C_p)(\rho_o \Delta T)} \quad \text{GPM} \\ &= (.565) \frac{(42.4)(469.5)}{(.1337)(.528)(54.4)(54)} = 54.5 \text{ GPM} \end{aligned}$$

Oil Pump

On the basis of the above main gearbox oil flow requirement, a 35-60-gallon-per-minute vane pump operating at 1,800 revolutions per minute is required. This size and type of pump has been selected for optimum serviceability, quality, and low cost. The location of the pump and associated lubrication system components are outlined on the lubrication schematic for the main gearbox, Figure 16, page 70.

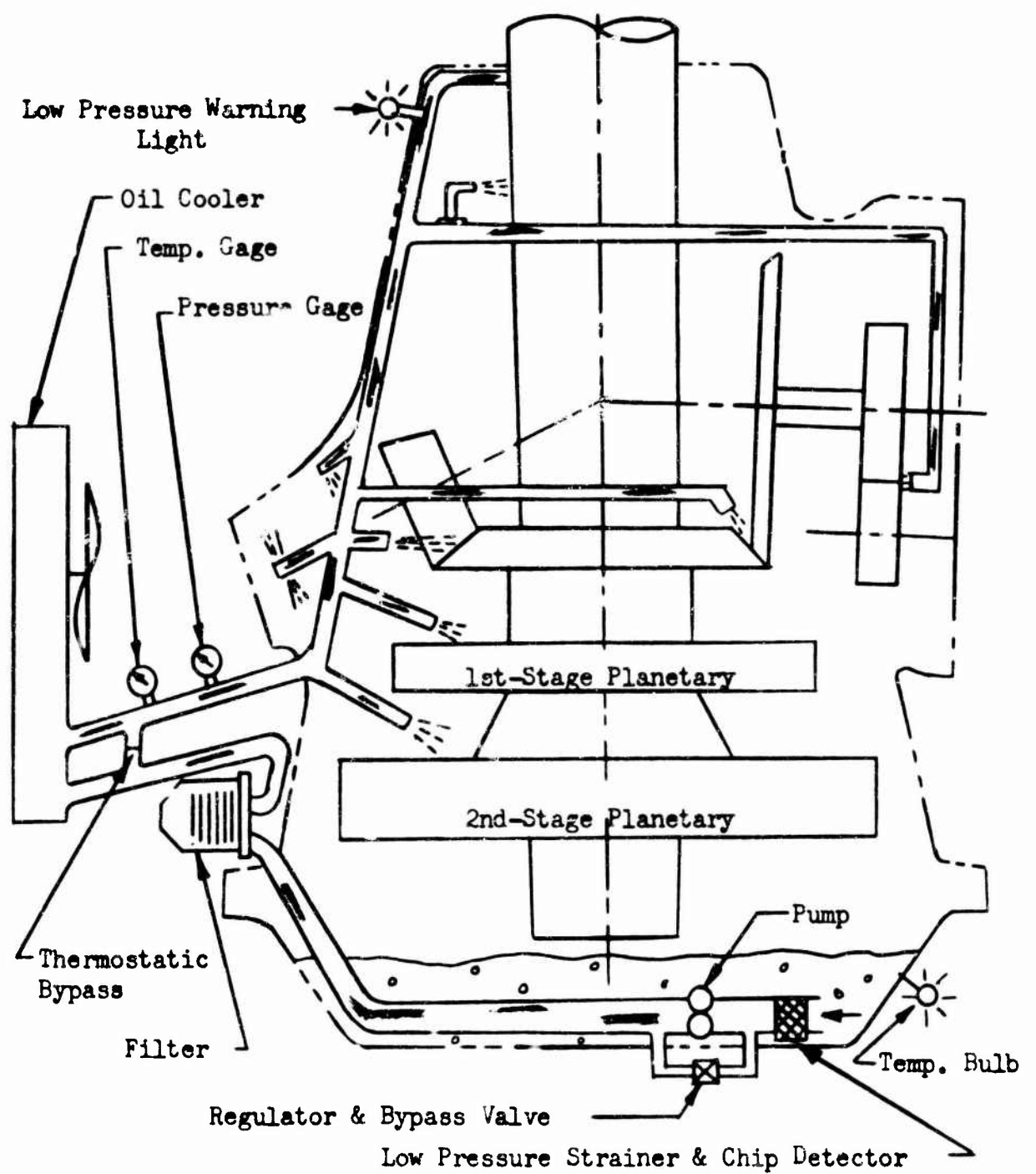


Figure 16. Lubrication System, Main Gearbox.

TABLE 8
WEIGHT SUMMARY,
MAIN GEARBOX

	Assembly Weight (lb.)	Total Weight (lb.)
Input Assembly - No. 1 Engine	306	
Input Assembly - No. 2 Engine	223	
Input Assembly - No. 3 Engine	223	
Input Assembly - No. 4 Engine	300	
Outer Shaft Assembly	332	
First-Stage Planetary Assembly	852	
Second-Stage Planetary Assembly	1,867	
Ring Gear	248	
Main Rotor Shaft	1,270	
Main Rotor Shaft Bearings and Support Assembly	668	
Driven Tail Take Off Bevel Gear and Housing Assembly	108	
Driven Tail Take Off Spur Gear and Housing Assembly	38	
Main Housing, Liner. & Stud Assembly	495	
Sump Housing and Pump Assembly	60	
		6,990

ENGINE REDUCTION GEARBOX - TWO FORWARD ENGINES

To achieve the angular change required by the system configuration and reduce the speed of the main gearbox input shaft, reduction gearboxes are attached to the two forward engines, as shown in Figure 51 of Appendix I. These boxes consist of a spiral bevel gear reduction of 80/34 (2.35:1) and accessory drives for the tachometer, fuel control, and a lubricating pump.

As indicated by the stresses given Appendix III, acceptable operation will be obtained using the following spiral bevel gear proportions:

	Pinion		Gear
Number of Teeth	34		80
Diametral Pitch		5.529	
Face Width		2.650	
Pitch Diameter	6.149		14.469
Face Contact Ratio		1.841	
Pressure Angle		$\phi = 20^\circ$	
Mean Spiral Angle		$\psi = 20^\circ$	
Shaft Angle		$\Sigma = 29^\circ 30'$	
Pitch Angle	$\gamma = 8^\circ 41'$		$\Gamma = 20^\circ 49'$
Hand of Spiral	RH		LH
Direction of Rotation	CCW		CW

As outlined on page 42, the input pinion bearing lives, determined by computer solution, are 4,072 and 14,848 hours for the 216 quadruple set and the 216 roller bearing, respectively.

Output gear bearing lives are as follows:

Cylindrical Roller	(65 x 120 x 23 mm)	4,340 hours
Preload (smaller) Tapered Roller	(L814749, L814710)	>> 100,000 hours
Tapered Roller	(33472/33287)	19,000 hours

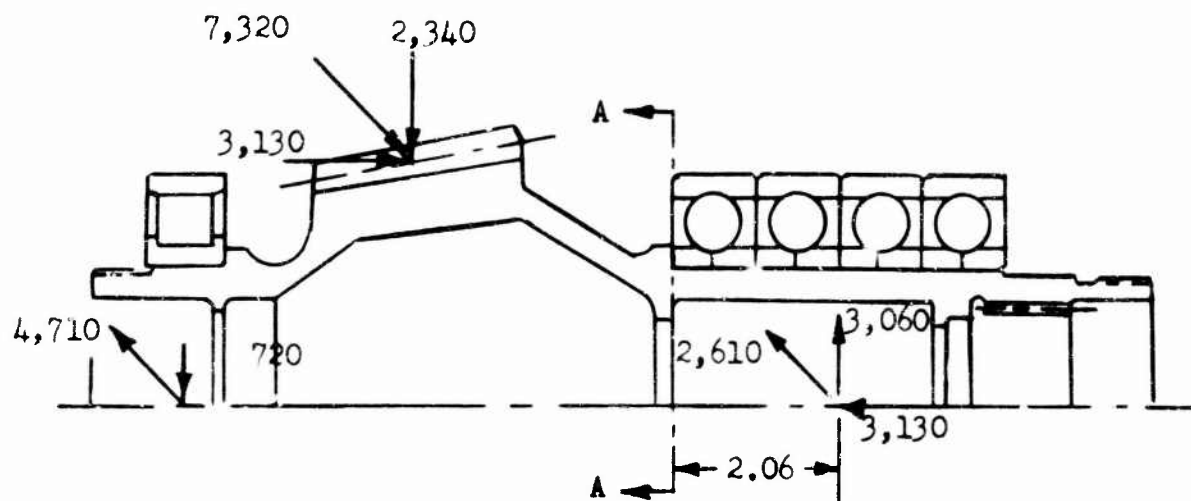


Figure 17. Pinion, Engine Reduction Gearbox.

Critical Section A-A

$$\overline{O.D.} = 3.25 \quad Z = 1.947$$

$$\overline{I.D.} = 2.62 \quad K_t = 2.48$$

$$M = 2.06 \sqrt{(2,610)^2 + (3,060)^2}$$

$$M = 8,280 \text{ in.-lb.}$$

$$f_b = \frac{K_t M}{Z} = \frac{(2.48)(8,280)}{(1.947)}$$

$$f_b = 10,550 \text{ psi}$$

$$F_{en} = 19,500 \text{ psi}$$

$$M.S. = \frac{F_{en}}{f_b} - 1 = \frac{19,500}{10,550} - 1$$

$$M.S. = + .85$$

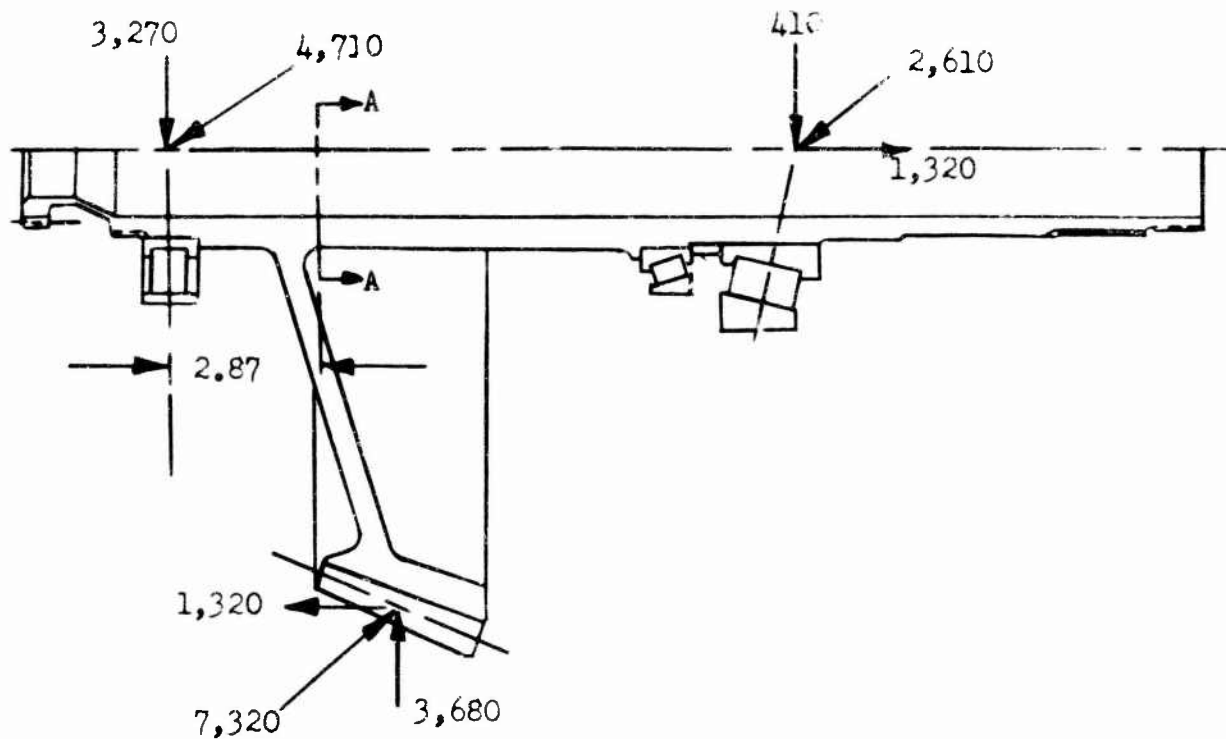


Figure 18. Output Gear Shaft, Engine Reduction Gearbox.

Critical Section A-A

$$\text{O.D.} = 3.00 \quad Z = 2.073$$

$$\text{I.D.} = 2.05 \quad K_t = 1.39$$

$$M = 2.87 \sqrt{(3,270)^2 + (4,710)^2}$$

$$M = 16,460 \text{ in.-lb.}$$

$$f_b = \frac{K_t M}{Z} = \frac{(1.39)(16,460)}{2.073}$$

$$f_b = 11,040 \text{ psi}$$

$$F_{en} = 19,500 \text{ psi}$$

$$\text{M.S.} = \frac{F_{en}}{f_b} - 1 = \frac{19,500}{11,040} - 1$$

$$\text{M.S.} = +.77$$

Lubrication and Efficiency Analysis

The primary consideration of the design of a lubrication system for this gearbox and previous helicopter transmissions is to provide cooling oil to remove heat generated due to friction losses at gear meshes and bearings and to provide lubricity to support tooth and bearing loads.

The preliminary analysis presented in this report establishes a systematic approach to the design of an integrated lubrication system for each transmission component. This approach is based upon extensive test and production experience with a considerable number of helicopter transmissions. This transmission utilizes carburized and ground gears, precision bearings, and close-tolerance, machined dynamic parts and housings. Experience indicates the losses through gear meshes, including the associated bearings, to be 1/2 percent per mesh and the total gearbox churning loss to be 1/2 percent.

Efficiency Analysis

$$\begin{aligned}\text{Input Bevel Mesh} &= (.005)(4,000) = 20.0 \\ \text{Churning Losses} &= (.005)(4,000) = 20.0 \\ &\quad \text{FHP (friction HP)} \quad 40.0 \\ \text{Estimated Efficiency} &= \frac{4,000-40}{4,000} \times 100 = 99\%\end{aligned}$$

Total Heat Generated (QG)

$$\begin{aligned}Q_G &= 2,545 \times \text{FHP} \\ &= (2,545)(40) \\ &= 101,800 \text{ BTU/HR.}\end{aligned}$$

From past helicopter experience at least 15 percent of the total heat generated in an engine reduction gearbox is conducted through the gear case and radiated to the surrounding area. Therefore, the necessary oil cooler can be designed to reject 85 percent of the total gearbox heat generated at maximum power.

Heat Rejection Rate - Oil Cooler

$$\begin{aligned} Q_{o.c.} &= .85 Q_G \\ &= (.85)(101,800) \\ &= 86,500 \text{ BTU/HR.} \end{aligned}$$

The transmission oil cooler and blower design is summarized on page 149 of this report.

Cooling Oil Required

Oil flow requirements are based upon the following parameters:

1. Use MIL-L-7808 oil in this transmission.
2. Oil in at 176°F.
3. Oil out of gearbox at 230°F.

$$\begin{aligned} \text{Therefore, } W_o &= \frac{C_e (42.4) \text{ FHP}}{(.1337) C_p \rho_o \Delta T} \quad \text{GPM} \\ &= \frac{(.565)(42.4)(40)}{(.1337)(.528)(54.4)(54)} \\ &= 4.64 \text{ GPM} \end{aligned}$$

Oil Pump

On the basis of the above engine reduction gearbox oil flow requirement, a 5-10-gallon-per-minute vane pump operating at 2,800 revolutions per minute is required. This size and type of pump has been selected for optimum serviceability, quality, and low cost. The location of this pump and associated lubrication system components are outlined on Figure 19, page 77.

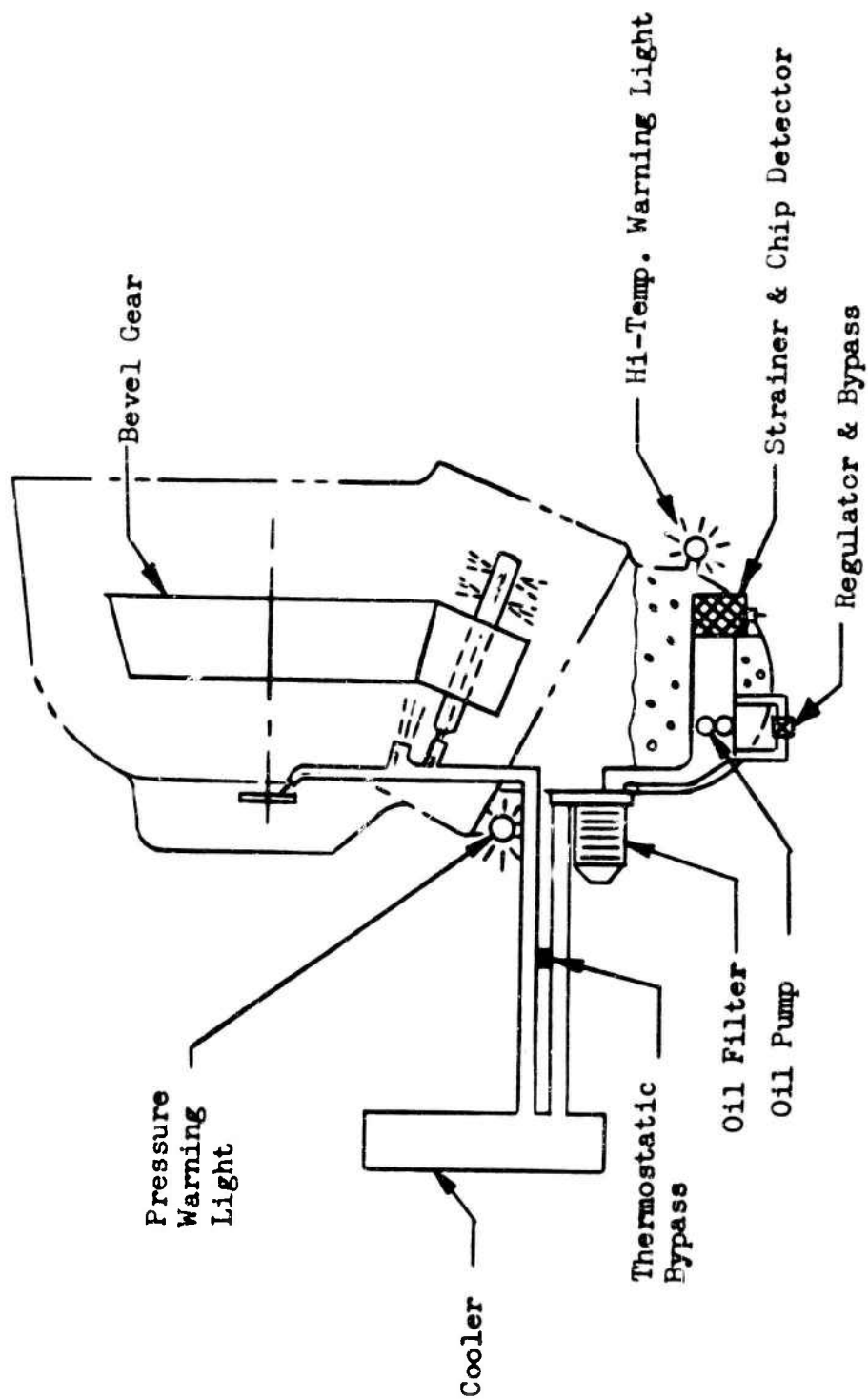


Figure 19. Lubrication System, Engine Reduction Gearbox.

TABLE 9
WEIGHT SUMMARY,
ENGINE REDUCTION GEARBOX

Component	Unit Weight (lb.)	Assembly Weight (lb.)	Total Weight (lb.)
Center Housing Assembly		41	
Front Cover Assembly		23	
Fuel Control Shaft Assembly (L.H. Installation Only)		3	
Input Pinion Assembly		51.5	
Input Pinion	18.7		
Bearings	17		
Housing and Liner Assembly	9.2		
Miscellaneous	6.6		
Output Gear Assembly		79.5	
Output Gear	47.3		
Bearings	8.8		
Housing and Liner Assembly	9.4		
Coupling	7.0		
Miscellaneous	7.0		
			198

INPUT DRIVE SHAFT - MAIN GEARBOX

To compensate for momentary over-torques that may occur from free turbine engines, the engine reduction gearbox to main gearbox shaft system is designed to transmit limit power equal to twice normal rated power. Utilizing one flexible, viscous damped bearing support, the drive shaft system has been designed so that its operating speed is between the first and second critical speeds. Shaft vibration is isolated from the fuselage by the viscous damped bearing support. The flexibility of the bearing support enables the use of a rigid coupling to connect the two shaft sections. Flexible disk couplings are used adjacent to the gearboxes. The shaft sections are of equal length for ease of manufacturing and logistics.

The shafts are fabricated from 2024-T3 aluminum alloy tubing. The size is selected to transmit the required power, provide the required critical speeds, be lightweight, and yet be amenable to manufacture.

The critical speeds are determined using a method developed by N. O. Myklestad (Reference 8). The principle upon which the method is based is that a frequency, or critical speed, and curve shape are assumed and computations for shear and bending moment are progressively carried out from one end of the shaft to the other. A tabular form of computation is used with a series of concentrated loads representing the shaft. Successive approximations using assumed values of frequency and curve shape are accomplished using a 7094 computer. When the assumed value of frequency corresponds to one of the modes, the selected boundary conditions of the curve shape have been met.

Computation Equations:

The shaft is considered to be pinned at the ends and has no damping imposed.

$$\text{Shear } i + 1 = \text{Shear } i + (\text{Moment } i)(\text{frequency})^2(\text{deflection } i)$$

$$\text{Moment } i + 1 = \text{Moment } i + (\text{Length of Beam } i)(\text{Shear } i)$$

i and $i + 1$ represent two adjacent stations

Boundary Conditions:

$$\text{Shear}_0 = 1 \qquad \text{Shear}_n = 1$$

$$\text{Moment}_0 = 0 \qquad \text{Moment}_n = 0$$

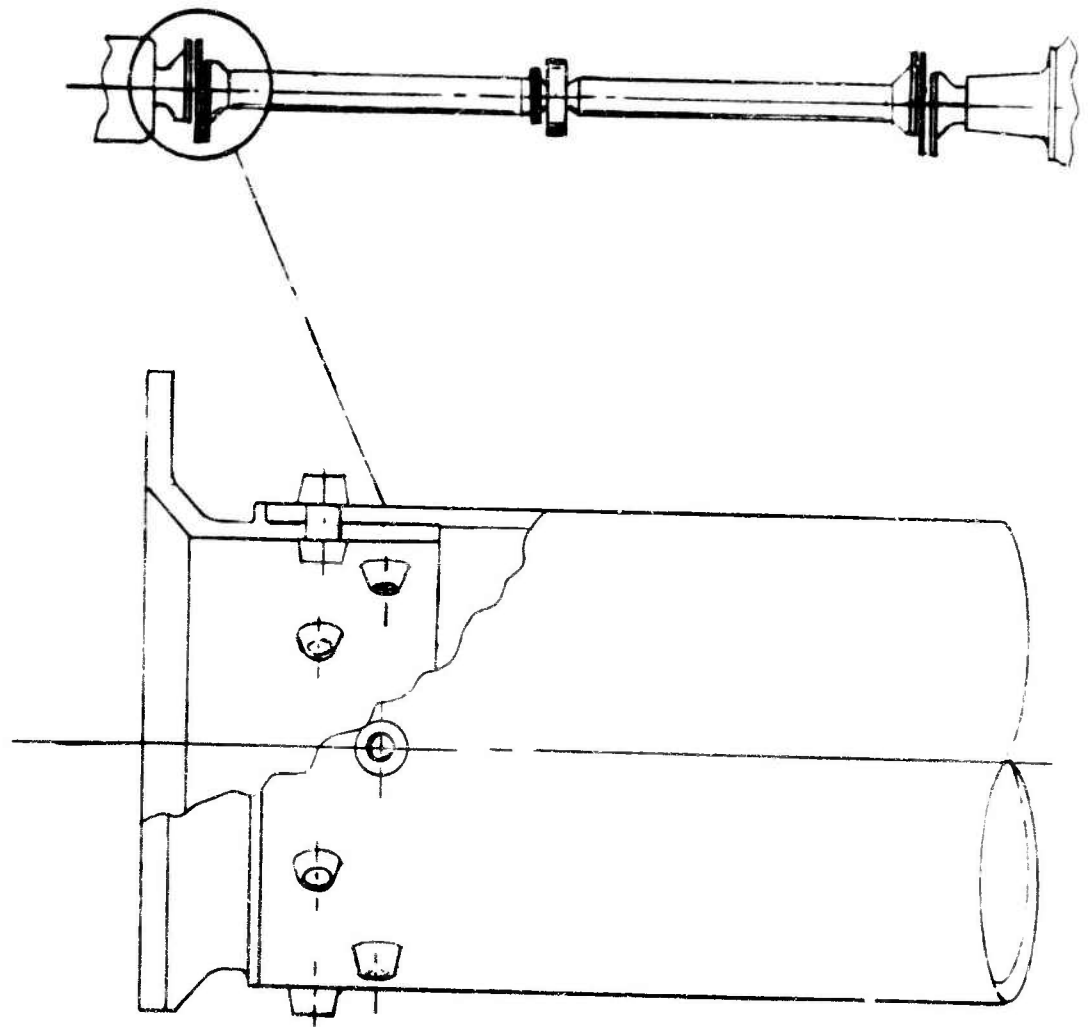


Figure 20. Typical Drive Shaft End Fitting.

Stress Analysis of Shafting

Stress developed at critical shaft sections for limit power is calculated to determine design adequacy.

$$\text{Maximum HP per Engine} = 4,500$$

$$\text{Operating Speed} = 5,780 \text{ RPM}$$

Distance between engine output coupling and gearbox input coupling is 115 inches.

$$T = \frac{2 \times 63,025 \times \text{HP}}{\text{RPM}}$$

$$T = \frac{2 \times 63,025 \times 4,500}{5,780}$$

$$T = 98,477 \text{ in.-lb.}$$

$$\overline{\text{O.D.}} = 5.500$$

$$\overline{\text{I.D.}} = 5.170$$

Center of Shaft

$$Z = 3.581$$

$$f_s = \frac{T}{2 \times Z}$$

$$f_s = \frac{98,477}{2 \times 3.581}$$

$$f_s = 13,750 \text{ psi}$$

$$F_{st} = 24,000 \text{ psi (Reference 4)}$$

$$\text{M.S.} = \frac{F_{st}}{1.5 \times f_s} - 1$$

$$\text{M.S.} = \frac{24,000}{1.5 \times 13,750} - 1$$

$$\text{M.S.} = + .16$$

Shaft End Connection

No. of .344 dia. lock bolt holes = 6

$$f_s = \frac{98,477}{2 \times 2.517}$$

$$f_s = 19,556 \text{ psi}$$

$$F_{sy} = 23,100 \text{ psi (Reference 4)}$$

$$\begin{aligned} \text{M.S.} &= \frac{F_{sy}}{1.15 \times f_s} - 1 \\ &= \frac{23,100}{1.15 \times 19,556} - 1 \end{aligned}$$

$$\text{M.S.} = + .03$$

Shaft Critical Speeds

Shaft critical speeds are computed using Myklestad's method as described in the introductory paragraphs. The viscous damped bearing support has a lateral spring rate of two hundred pounds per inch. The shaft is divided into ten equal concentrated mass increments with a concentrated mass at the bearing support.

$$N_{c1} = 2,136 \text{ RPM}$$

$$N_{c2} = 10,608 \text{ RPM}$$

The input drive shaft is therefore operating supercritically at 5,780 RPM.

TABLE 10
ITEMIZED WEIGHT OF ONE INPUT DRIVE SHAFT SYSTEM

Component	Weight Analysis	Weight (lb.)
Weight of Shaft	$\frac{\text{Wt.}}{\text{In. Length}} \times \text{Length} = .277 \times 115$	31.8
Weight of Flexible Disk Couplings	Unit Wt. x No. of Couplings = 7.7 x 2	15.4
Weight of Rigid Couplings	Unit Wt. x No. of Couplings = 6.8 x 1	6.8
Weight of Bearing Support and Attaching Hardware	Unit Wt. x No. of Bearing Supports = 4.7 x 1	4.7
Total weight of one input drive shaft system =		58.7

ACCESSORY DRIVE SHAFT

The accessory drive shaft has been designed to transmit the maximum power required by all accessories (summarized on page 87). Based on previous experience, an overload factor of 2.0 has been applied to the maximum input torque to the accessory gearbox to assure structural adequacy for all operating conditions.

The shaft assembly has been designed to be a single span, with a flexible disk type coupling on each end to allow parallel misalignment of the gearboxes.

Since the power is relatively low, and the shaft span is short (35 inches), supercritical operation is not warranted. The shaft has therefore been designed such that its first critical speed is at least 1.50 times its operating speed.

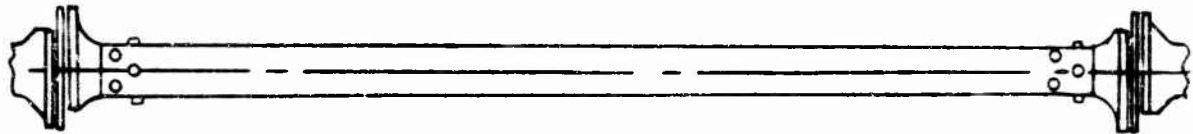


Figure 21. Accessory Drive Shaft.

Stress Analysis

The stresses developed at the critical shaft sections for the overload torque of twice maximum accessory power are calculated to determine the design adequacy as follows:

Maximum Accessory Power = 300 at 6,022 RPM (Reference page 87)

Shaft Span (between couplings) = 35 inches

$$T = \frac{63,025 \times \text{HP}}{\text{RPM}} \times \text{overload factor}$$

$$T = \frac{63,025 \times 300 \times 2}{6,022}$$

$$T = 6,280 \text{ in.-lb.}$$

$$\text{O.D.} = 1.875$$

$$\overline{\text{I.D.}} = 1.557$$

Center of Shaft

$$Z = .252$$

$$f_s = \frac{T}{2xZ}$$

$$f_s = \frac{6,280}{2x.252}$$

$$f_s = 12,500 \text{ psi}$$

$$F_{tu} = 29,000 \text{ psi} \quad (\text{Reference 4})$$

$$\text{M.S.} = \frac{F_{tu}}{1.5xf_s} - 1$$

$$\text{M.S.} = \frac{29,000}{1.5x12,500} - 1$$

$$\text{M.S.} = + .55$$

Shaft End Connection

$$f_s = \frac{T}{2xZ} \quad ; \quad Z = .180, \text{ based on two rows of four } 0.323\text{-diameter rivet holes}$$

$$f_s = \frac{6,280}{2x.180}$$

$$f_s = 16,500 \text{ psi}$$

$$F_{sy} = 23,100 \text{ psi} \quad (\text{Reference 4})$$

$$\text{M.S.} = \frac{F_{sy}}{1.15xf_s}$$

$$\text{M.S.} = \frac{23,100}{1.15x16,500}$$

$$\text{M.S.} = + .22$$

Shaft Critical Speed

Shaft critical speed is computed using the basic equation for a beam pinned at the ends. The gear mountings inside of the gearboxes must be rigid in order to use this simplified method of analysis.

$$N_{cn} = \frac{60}{2\pi} \omega_n$$

$$\omega_n = \frac{a_n}{L^2} \sqrt{\frac{E EI}{\rho_a A}} \quad (\text{Reference 8, page 217})$$

$$a_1 = 9.87 \text{ for } \omega_1$$

$$E = 10.5 \times 10^6$$

$$\rho_a = .100$$

$$N_{c1} = \frac{9.87}{L^2} \sqrt{\frac{386 \times 10.5 \times 10^6 I}{.100 A}}$$

$$N_{c1} = \frac{19.2 \times 10^6}{L^2} \sqrt{\frac{I}{A}}$$

$$N_{c1} = \frac{19.2 \times 10^6 \times .626}{35^2}$$

$$N_{c1} = 9,820 \text{ RPM}$$

TABLE 11
ITEMIZED WEIGHT OF ACCESSORY DRIVE SHAFT

Component	Weight Analysis	Weight (lb.)
Weight of Shaft	$\frac{\text{Wt.}}{\text{In. Length}} \times \text{Length} = .060 \times 35$	2.10
Weight of Flexible Disk Couplings	Unit Wt. x No. of Couplings = 1.03×2	2.06
Total Weight of Accessory Shaft Assembly		4.16

ACCESSORY GEARBOX

The transmission system study considered here has accessory drives as outlined below. The accessories have been mounted on a separate accessory gearbox, as depicted on Figure 58, page 245. The study included provisions for all necessary accessories driven on the ground by using an auxiliary power turbine that operates either with the rotor locked or rotating and delivers 80 horsepower.

Accessory Drives

	<u>Max. HP</u>	<u>Avg. HP</u>
Primary Servo Pump	30	10
Secondary Servo Pump	30	10
Two Generators (30 KVA)*	149	53
Utility Pump	70	20
Hoist Pump	20	6
Rotor Tachometer	<u>1</u>	<u>1</u>
TOTALS	300 HP	100 HP

Auxiliary Power Supply (T62T-16A) 80 HP

*Note: Both generator drives were designed for 50 percent generator overload. Only one generator is driven by the auxiliary power supply. The other is driven only when the rotor is turning. (See Figure 58).

Lubrication and Efficiency Analysis

The primary consideration of the design of a lubrication system for this gearbox and previous helicopter transmissions is to provide cooling oil to remove heat generated due to friction losses at gear meshes and bearings and to provide lubricity to support tooth and bearing loads.

The preliminary analysis presented in this report establishes a systematic approach to the design of an integrated lubrication system for each transmission component. This approach is based upon extensive test and production experience with a considerable number of helicopter transmissions. This transmission utilizes carburized and ground gears, precision bearings, and close-tolerance, machined dynamic parts and housings. Experience indicates the losses through gear meshes, including the associated bearings, to be 1/2 percent per mesh, and the total gearbox churning loss to be 1/2 percent.

Efficiency Analysis

Accessory Gearbox

Generator - Utility Mesh	(.005)(225)	=	1.13
Utility - Hoist Mesh	(.005)(155)	=	.78
Hoist - Primary Servo Mesh	(.005)(135)	=	.68
Primary - Secondary Servo Mesh	(.005)(30)	=	.15
Primary Servo - Generator Mesh	(.005)(74)	=	.37
Churning Losses	(.005)(300)	=	1.50
	F_{HP} (friction HP)		<u>4.61</u>

$$\text{Estimated Efficiency} = \frac{300 - 4.61}{300} \times 100 = 98.4\%$$

Total Heat Generated (Q_G)

$$\begin{aligned} Q_G &= 2,545 F_{HP} \\ &= 2,545 \times 4.61 \\ &= 11,700 \text{ BTU/HR.} \end{aligned}$$

Based upon current aircraft experience on accessory gearboxes, with low friction power losses and relatively large gear case surface area, the case rejection rate is great enough to dissipate the generated heat provided the oil is circulated via an oil pump.

Cooling Oil Required

Oil flow requirements are based upon the following parameters:

1. Use MIL-L-7808 oil in this transmission.
2. Oil in at 176°F.
3. Oil out of gearbox at 230°F.

Therefore,

$$\begin{aligned} W_o &= \frac{C_e (42.4) F_{HP}}{(.1337) C_p \rho_o \Delta T} \quad \text{GPM} \\ &= \frac{(1) (42.4) (4.61)}{(.1337) (.528) (54.4) (54)} \\ &= 0.95 \text{ GPM} \end{aligned}$$

Oil Pump

On the basis of the above accessory gearbox oil flow requirement, a 2-gallon-per-minute vane pump operating at 5,179 revolutions per minute is required. This size and type of pump has been selected for optimum serviceability, quality, and low cost. The arrangement of this pump and associated lubrication system components is outlined on Figure 22, page 90.

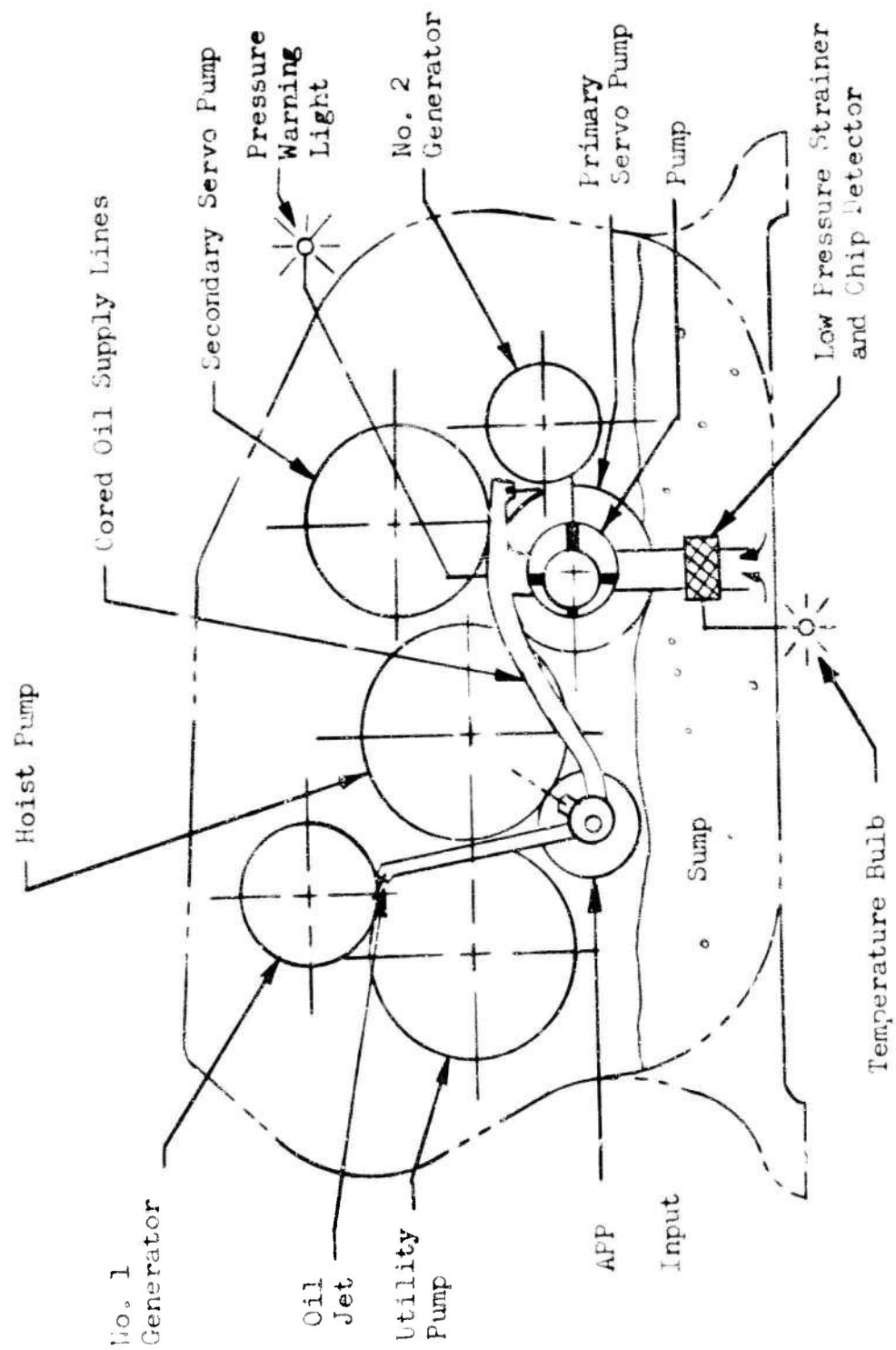


Figure 22. Lubrication System, Accessory Gearbox.

TABLE 12
WEIGHT SUMMARY,
ACCESSORY GEARBOX

	Unit Weight (lb.)	Assembly Weight (lb.)	Total Weight (lb.)
Housing Assembly		57.8	
Housing Liner and Stud Assembly	24.0		
Input Gear	4.0		
Input Flange	0.5		
Utility Gear	2.0		
Hoist Gear	2.3		
Lube Pump Gear	1.6		
Gen. Right Gear	2.2		
2nd Servo Gear	1.2		
Auxiliary Power Supply Gear	1.0		
Freewheel Unit	3.0		
Miscellaneous	16.0		
Front Cover Assembly		22.2	
Cover Liner & Stud Assembly	21.0		
Lubrication Pump Assembly	1.2		
		TOTAL WEIGHT	80.0

HYPERCRITICAL TAIL ROTOR DRIVE SYSTEM

Tail Drive Shafting

Fuselage - Tail Cone Shafting

The fuselage - tail cone shaft system connecting the main and intermediate gearboxes has been designed to transmit the maximum anticipated transient power to the tail rotor. Based on extensive experience on large single rotor aircraft, this peak (or limit) tail rotor power is approximately 25 percent of the maximum input power to the main transmission. Hypercritical speed operation of this shaft system has been selected to achieve a lightweight installation. This system requires only two viscous damped bearing supports spaced to efficiently minimize shaft vibrations when transient speeds coincide with the shaft natural frequencies (critical speeds). The operating speed of the shaft (5,922 RPM) is between the seventh and eighth critical speeds during flight operation.

As shown in Figure 51, page 229, the shafting consists of three sections, with the longest section limited to 23 feet to facilitate manufacturing and handling.

Shaft Critical Speeds

The critical speeds of the shaft system are computed by the Myklestad method of analysis, as described in the introductory paragraphs on critical speed analysis for the input drive shaft on page 79. The two viscous damped bearing supports each have a lateral spring rate of 200 pounds per inch. The shaft is divided into 36 equal concentrated mass increments with an additional concentrated mass at each bearing support. The first eight critical speeds are summarized as follows:

<u>N_{cn}</u>		<u>RPM</u>
N _{c1}	=	254
N _{c2}	=	557
N _{c3}	=	1,052
N _{c4}	=	1,770
N _{c5}	=	2,640
N _{c6}	=	3,940
N _{c7}	=	5,370
N _{c8}	=	6,765

The analysis predicts the normalized shaft deflections (related to a maximum deflection unit of 1 inch).* Since operational speed is between the seventh and eighth critical speeds, these mode shapes are plotted in Figure 23, page 95 .

*reference 8, page 115.

Number of Supports

Although the hypercritical drive shaft design presented herein incorporates two viscous damped bearing supports (Reference Figure 23, page 95), analysis indicates that only one support is required for hypercritical operation between the seventh and eighth critical speeds. The investigations of Reference 7 verify this conclusion. However, two damped supports have been utilized for HLH to provide a fail-safe tail drive shaft design. If one damper should malfunction, the system will operate successfully, although at a somewhat higher amplitude than that anticipated for the two-bearing system.

Damping Coefficient - Viscous Damped Support

The damping coefficient $-c-$ for the viscous damped bearing support is equal to 10 pounds second per inch for the seventh critical speed. Analysis indicates that this coefficient is satisfactory for all other modes.

Bending Stress Calculations

The following analysis establishes that the viscous damped hypercritical drive shaft installation possesses enough restraint to adequately control shaft resonance at operating speed with shaft unbalances resulting from normal manufacturing tolerances.

A normal mode approach is used to define the forces caused by different sources of unbalance. These forces are applied to the damped normal modes of the shaft at the critical frequencies adjacent to operating speed. The normalized shaft bending moment distribution derived earlier by the Myklestad analysis is dimensioned by the modal response to determine the actual bending moment expected in operation.

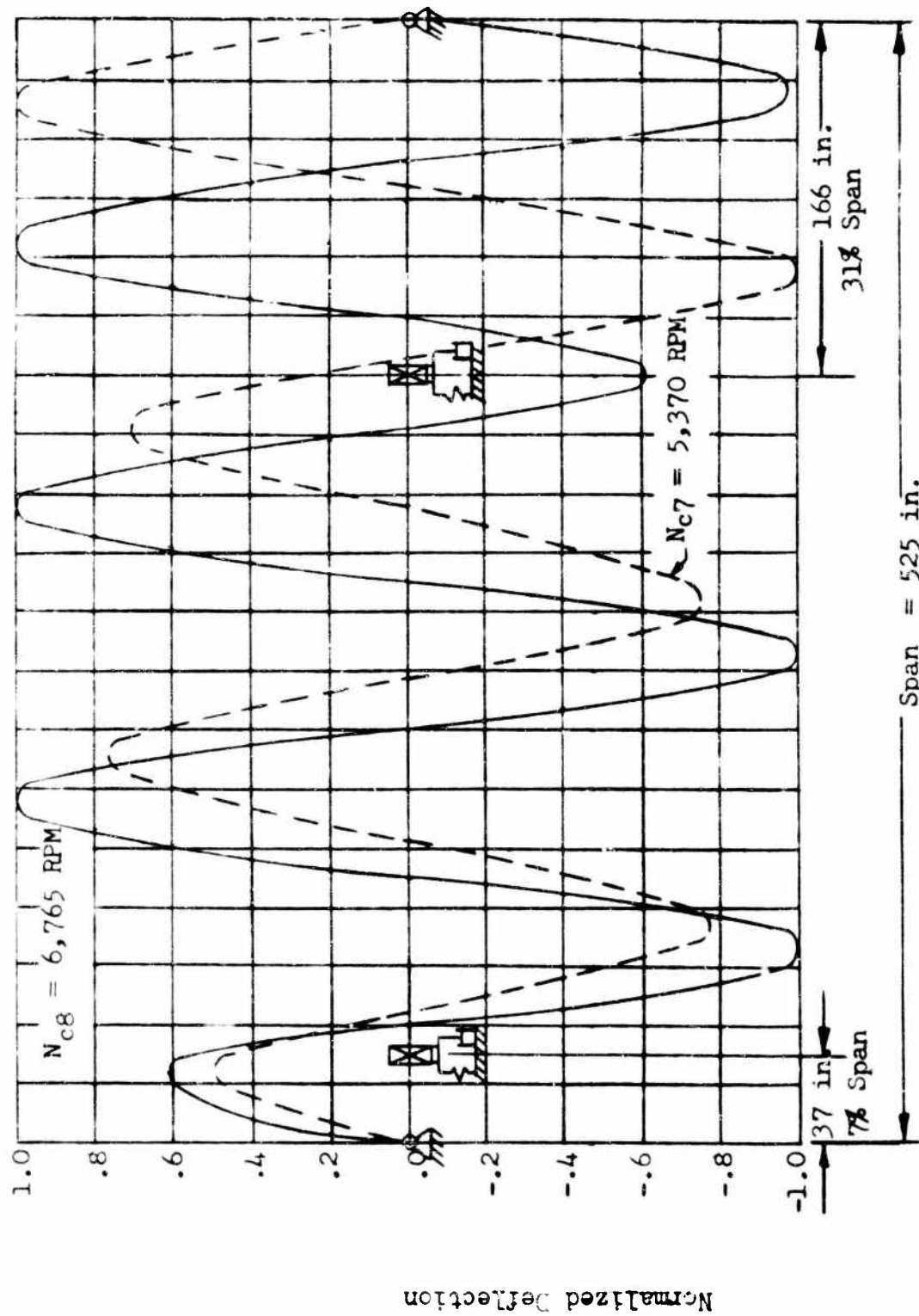
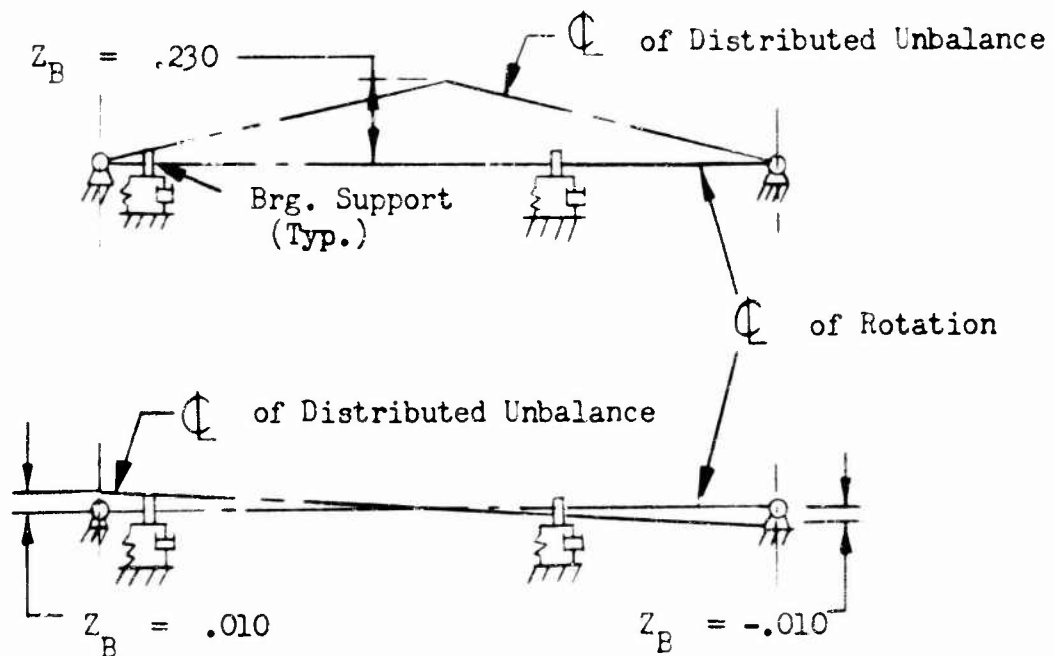


Figure 23. Normalized Tail Drive Shaft Deflection
(Fuselage - Tail Cone Shafting)

The two types of shaft system unbalance distribution are illustrated below, showing the theoretical maximum unbalance distribution for a production shaft assembly. The first type of unbalance distribution is caused by the maximum allowable runout in production shafting, while the second is caused by assembly tolerances between the bearing and shaft center lines.



The first type of distribution affects only the odd number mode shapes ($N_1, N_3 \dots$ etc.) while the second affects only the even number mode shapes ($N_2, N_4 \dots$ etc.). Maximum shaft bending stress is calculated as outlined in Reference 2, for steady operation at the seventh and eighth critical speeds. Since operational speed is between these two conditions, operational stress will be below that calculated. The mode shape for any particular critical speed remains fixed in a plane that whirls at the same RPM as the shaft. The bending stress is thus constant at a particular critical speed.

Critical Speed (N_c)

$$N_{c7} = 5,370 \text{ RPM} \quad N_{c8} = 6,765 \text{ RPM}$$

% of Critical Damping

$$\xi = \frac{2 c \pi \sum x^2 \text{ Brgs. } 100}{\sum x^2 \text{ Shaft Increments}}$$

46.7%

46.5%

Magnification Factor

$$\frac{x}{x_0} = \frac{1}{2 \xi (1 - \xi^2)^{1/2}}$$

1.22

1.22

Principle Eccentricity, P.E., =

$$\frac{4 \sqrt{2} z_B}{(n \pi)^2}$$

$$\frac{4 \sqrt{2} z_B}{n \pi}$$

$$\frac{4 \sqrt{2} (.230)}{(7 \pi)^2}$$

$$\frac{4 \sqrt{2} (.010)}{8 \pi}$$

.00266 in.

.00225 in.

Maximum Deflection

$$\delta = \frac{x}{x_0} (\text{P.E.}) \frac{1}{\sqrt{2}}$$

.0023 in.

.0019 in.

Maximum Bending Moment*

$$M_B = \left[\frac{\text{Bending Moment}}{\text{Inch of Deflection}} \right] \delta \quad 1.07 \times 10^5 (.0023) \quad 1.29 \times 10^5 (.0019)$$

246 in.-lb.

245 in.-lb.

Maximum Bending Stress

$$f_b = \frac{M_B}{Z} = \frac{M_B}{2.437}$$

101 psi

100 psi

* Value of bending moment per inch of deflection obtained from computer analysis predicting normalized shaft deflections.

Static Substantiation of Shafting

Stresses developed at critical shaft sections for limit tail rotor power have been calculated to verify the design adequacy. The bending stresses calculated in the previous section have a negligible effect on the fatigue or static strength of the shaft.

$$\text{Limit HP to tail rotor} = 4,000$$

$$\text{Operating Speed} = 5,922 \text{ RPM}$$

$$\begin{array}{l} \text{Distance between main} \\ \text{and intermediate gear-} \\ \text{box couplings} \end{array} = 525 \text{ in.}$$

$$T = \frac{63,025 \times \text{HP}}{\text{RPM}}$$

$$T = \frac{63,025 \times 4,000}{5,922}$$

$$T = 42,570 \text{ in.-lb.}$$

$$\overline{\text{O.D.}} = 5.000$$

$$\overline{\text{I.D.}} = 4.714$$

Center of Shaft

$$Z = 2.427$$

$$f_s = \frac{T}{2Z}$$

$$f_s = \frac{42,570}{2 \times 2.427}$$

$$= 8,770 \text{ psi}$$

$$F_{st} = 16,500 \text{ psi} \quad (\text{Reference 4})$$

$$\text{M.S.} = \frac{F_{st}}{1.5 \times f_s} - 1$$

$$\text{M.S.} = \frac{16,500}{1.5 \times 8,770} - 1$$

$$M.S. = +.25$$

Shaft End Connection

No. of .344-dia. lock bolt holes = four per row (two rows)

$$Z = 2.209$$

$$f_s = \frac{T}{2 Z}$$

$$f_s = \frac{42,570}{2 \times 2.209}$$

$$f_s = 9,600 \text{ psi}$$

$$F_{sy} = 23,100 \text{ psi} \quad (\text{Reference 4})$$

$$M.S. = \frac{F_{sy}}{1.15 \times f_s} - 1$$

$$M.S. = \frac{23,100}{1.15 \times 9,600} - 1$$

$$M.S. = +1.08$$

Pylon Drive Shaft

The pylon drive shaft transmits the same power as the tail drive shaft, but at 3,760 RPM rather than at 5,922 RPM. It is designed to transmit the power using the specified safety factors. As is done on the engine input drive shaft, one flexible, viscous damped bearing support is used at the center of the span, and operational speed is between the first and second critical speeds. The critical speeds are computed by using Myklestad's method of analysis, as described in the introductory paragraph on critical speed analysis for the input drive shaft.

Stress Analysis of Shafting

Stress developed at critical shaft sections for limit power is calculated to determine design adequacy.

$$\text{Limit HP to tail rotor} = 4,000$$

$$\text{Operating speed} = 3,760 \text{ RPM}$$

$$\text{Distance between intermediate and tail gearbox couplings} = 136 \text{ in.}$$

$$T = \frac{63,025 \times \text{HP}}{\text{RPM}}$$

$$T = \frac{63,025 \times 4,000}{3,760}$$

$$T = 67,000 \text{ in.-lb.}$$

$$\overline{O.D.} = 5.250$$

$$\overline{I.D.} = 4.982$$

Center of Shaft

$$Z = 2.686$$

$$f_s = \frac{T}{2 \times Z}$$

$$f_s = \frac{67,000}{2 \times 2.686}$$

$$f_s = 12,500 \text{ psi}$$

$$F_{st} = 21,000 \text{ psi} \quad (\text{Reference 4})$$

$$M.S. = \frac{F_{st}}{1.5 \times f_s} - 1$$

$$M.S. = \frac{21,000}{1.5 \times 12,500} - 1$$

$$M.S. = +.12$$

Shaft End Connection (Reference Figure 20, page 80)

No. of .344 dia. lock bolt holes = five per row (two rows)

$$Z = 2.399$$

$$f_s = \frac{T}{2 \times Z}$$

$$f_s = \frac{67,000}{2 \times 2.399}$$

$$f_s = 14,000 \text{ psi}$$

$$F_{sy} = 23,100 \text{ psi} \quad (\text{Reference 4})$$

$$M.S. = \frac{F_{sy}}{1.15 \times f_s} - 1$$

$$M.S. = \frac{23,100}{1.15 \times 14,000} - 1$$

$$M.S. = +.44$$

Shaft Critical Speeds

Shaft critical speeds are computed by the Myklestad method of analysis, as described in the introductory paragraph on critical speed analysis for the input drive shaft. The viscous damped bearing support has a lateral spring rate of 200 pounds per inch. The shaft is divided into 10 equal concentrated mass increments with a concentrated mass at the bearing support.

$$N_{c1} = 1,531 \text{ RPM}$$

$$N_{c2} = 7,300 \text{ RPM}$$

The pylon drive shaft is operating supercritically at 7,760 RPM, since the first mode is 1,531 RPM and the second is 7,300.

TABLE 13
ITEMIZED WEIGHT,
TAIL DRIVE SHAFTING.

Item	Weight Analysis	Weight (lb.)
Fuselage - Tail Cone Shafting		
Shaft	$\frac{\text{Wt.}}{\text{Inch Length}} \times \text{Length} = .202 \times 525$	106.
Flexible Disk Couplings	Unit Wt. x No. of Couplings = 6.3×2	12.6
Rigid Couplings	Unit Wt. x No. of Couplings = 5.5×2	11.0
Bearing Supports & Attaching Hardware	Unit Wt. x No. of Bearing Supports = 4.7×2	<u>9.4</u>
Weight - fuselage - tail cone shafting		139.0
Pylon Drive Shaft		
Weight of Shaft	$\frac{\text{Wt.}}{\text{Inch Length}} \times \text{Length} = .228 \times 136$	31.1
Weight of Flexible Disk Couplings	Unit Wt. x No. of Couplings = 7.7×2	15.4
Weight of Rigid Couplings	Unit Wt x No. of Couplings = 6.8×1	6.8
Weight of Bearing Supports and Attaching Hardware	Unit Wt. x No. of Bearing Supports = 4.7×1	<u>4.7</u>
Weight, Pylon Drive Shaft		58.0
Total Weight - Tail Drive Shafting		197

Intermediate Gearbox

As shown in Figure 56, Appendix I, the angular change between the tail cone and pylon drive shafting is accomplished in an intermediate gearbox located at the intersection of these shaft axes. To obtain as much reduction as is practical, a 63/40 (1.575:1) ratio spiral bevel gear set was selected. An acceptable face contact ratio of 1.571 was achieved using the following gear proportions. As indicated in Appendix III, relatively low operating stresses are obtained for this gear set.

	Pinion		Gear
Number of Teeth	40		63
Diametral Pitch		4.000	
Face Width		2.000	
Pitch Diameter	10.000		15.750
Face Contact Ratio		1.571	
Pressure Angle		$\phi = 20^\circ$	
Mean Spiral Angle		$\psi = 28^\circ$	
Shaft Angle		$\Sigma = 125^\circ 54'$	
Pitch Angle	$\gamma = 39^\circ 20'$		$\Gamma = 86^\circ 34'$
Hand of Spiral	RH		LH
Direction of Rotation	CCW		CW

Gearing Data

$$\phi = 20^\circ 0'$$
$$\tan \phi = .36397$$

$$\psi = 28^\circ 0'$$
$$\sin \psi = .46947$$
$$\cos \psi = .88295$$

$$\gamma = 39^\circ 20'$$
$$\sin \gamma = .63383$$
$$\cos \gamma = .77347$$

$$\Gamma = 86^\circ 34'$$
$$\sin \Gamma = .99821$$
$$\cos \Gamma = .05989$$

$$D_{\text{mean}} (\text{pinion}) = D_p - F \sin \gamma$$
$$= 10.000 - 2 \times 0.63383$$

$$D_{\text{mean}} (\text{pinion}) = 8.73 \text{ in.}$$

Note: Loads shown are for prorated power (875 HP).

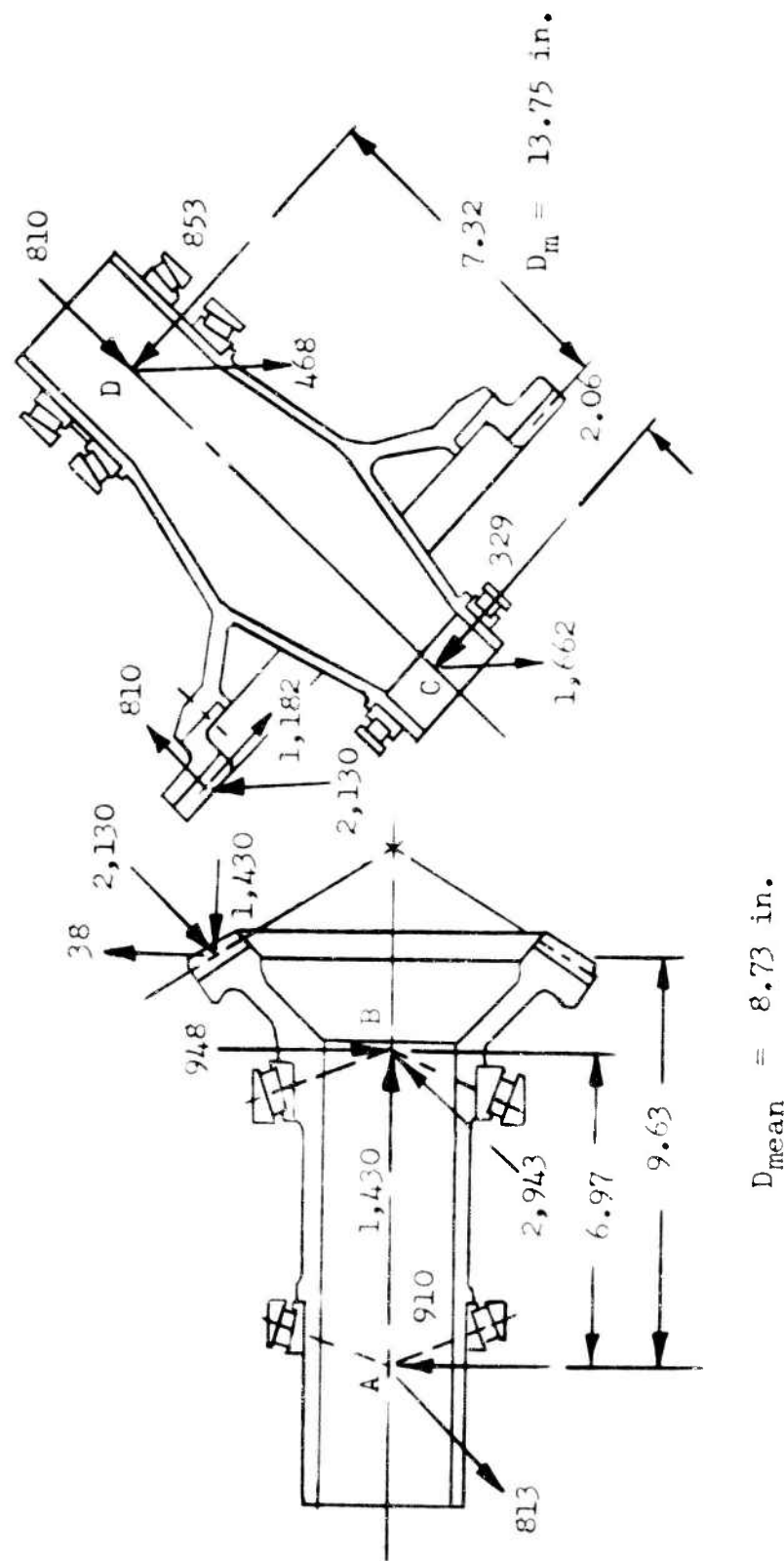


Figure 24. Intermediate Gearbox Shafting

$$D_{\text{mean}} (\text{gear}) = 8.73 \times (63/40)$$

$$D_{\text{mean}} (\text{gear}) = 13.75 \text{ in.}$$

Input Pinion, Figure 24

Horsepower	875
Input Speed	5,922 RPM
Mean Diameter	8.73 in.

$$\text{Torque} = \frac{63,025 \times \text{HP}}{\text{RPM}} = \frac{63,025 \times 875}{5,922}$$

$$\text{Torque} = 9,300 \text{ in.-lb.}$$

$$W_t = \frac{2T}{D_{\text{mean}}} = \frac{2 \times 9,300}{8.73}$$

$$W_t = 2,130 \text{ lb.}$$

$$W_x = W_t \frac{(\tan \phi \sin \gamma + \sin \psi \cos \gamma)}{\cos \psi}$$

$$W_x = 2,130 \frac{(.36397 \times .63383 + .46947 \times .77347)}{.88295}$$

$$W_x = 1,430 \text{ lb.}$$

$$W_r = W_t \frac{(\tan \phi \cos \gamma - \sin \psi \sin \gamma)}{\cos \psi}$$

$$W_r = 2,130 \frac{(.36397 \times .77347 - .46947 \times .63383)}{.88295}$$

$$W_r = -38 \text{ lb.}$$

$$R_A = \frac{\sqrt{(2,130 \times 2.66)^2 + (38 \times 2.66 + 1,430 \times 4.365)^2}}{6.97}$$

$$R_A = 1,220 \text{ lb.}$$

$$R_B = \frac{\sqrt{(2,130 \times 9.63)^2 + (38 \times 9.63 + 1,430 \times 4.365)^2}}{6.97}$$

$$R_B = 3,090 \text{ lb.}$$

Bearing Selection - Input Pinion

At "A", tapered roller bearing 31306/34478.

$$K_A = 1.3$$

$$BRR = 3,580 \text{ lb.}$$

At "B", tapered roller bearing HM617049/HM617010.

$$K_B = 1.35$$

$$BRR = 10,500 \text{ lb.}$$

$$\frac{.47 R_B}{K_B} = \frac{.47 \times 3,090}{1.35} = 1,076 \text{ lb.}$$

$$\frac{.47 R_A}{K_A} + \text{Thrust} = \frac{.47 \times 1,220}{1.3} + 1,430 = 1,871 \text{ lb.}$$

Therefore, since $1,076 < 1,871$

$$RE_B = 0.53 R_B + K_B \left(\frac{.47 R_A}{K_A} + \text{Thrust} \right)$$

$$RE_B = .53 \times 3,090 + 1.35 \times 1,871$$

$$RE_B = 4,164 \text{ lb.}$$

$$RE_A = R_A = 1,220 \text{ lb.}$$

The B-10 life of tapered roller bearings may be found by the use of the following equation:

$$L = 3,000 \times (BRR/RE)^{10/3} \times (500/\text{RPM}) \text{ hours}$$

$$L_A = 3,000 \times (3,580/1,220)^{10/3} \times (500/5,922)$$

$$L_A = 9,170 \text{ hours}$$

$$L_B = 3,000 \times (10,500/4,164)^{10/3} \times (500/5,922)$$

$$L_B = 5,550 \text{ hours}$$

Output Gear, Figure 24

$$\begin{aligned}W_x &= W_t \frac{(\tan \phi \sin \Gamma - \sin \psi \cos \Gamma)}{\cos \psi} \\&= 2,130 \frac{(.36397 \times .99821 - .46947 \times .05989)}{.88295}\end{aligned}$$

$$W_x = 810 \text{ lb.}$$

$$\begin{aligned}W_s &= W_t \frac{(\tan \phi \cos \Gamma + \sin \psi \sin \Gamma)}{\cos \psi} \\&= 2,130 \frac{(.36397 \times .05989 + .46947 \times .99821)}{.88295}\end{aligned}$$

$$W_s = 1,182 \text{ lb.}$$

$$R_C = \frac{\sqrt{(2,130 \times 7.32)^2 + (1,182 \times 7.32 - 810 \times 6.875)^2}}{9.38}$$

$$R_C = 1,695 \text{ lb.}$$

$$R_D = \frac{\sqrt{(2,130 \times 2.06)^2 + (1,182 \times 2.06 + 810 \times 6.875)^2}}{9.38}$$

$$R_D = 973 \text{ lb.}$$

Bearing Selection - Output Gear

At "C", locate a roller bearing, 70 x 110 x 20 mm, with a basic dynamic capacity of 15,700 lb. The B-10 life is expressed by the following formula:

$$\text{B-10 life} = \frac{(C/P)^{10/3} 10^6}{\text{RPM} \times 60}$$

$$L_C = \frac{(15,700/1,695)^{10/3} 10^6}{3,760 \times 60}$$

$$L_C = 7,410 \text{ hours}$$

At "D-E", two tapered roller bearings 34306/34478 back-to-back.

$$K_D = 1.30$$

$$BRR = 3,580 \text{ lb.}$$

$$\text{Thrust} = 810 \text{ lb.}$$

$$\frac{.47 R_D}{K_D} = \frac{.47 \times 973}{1.3} = 352 \text{ lb.}$$

Since $810 > 352$, bearing "D" reacts the radial load and bearing "E" is used for preload.

$$\begin{aligned} RE_D &= .53 R_D + K_D \times \text{thrust} \\ &= .53 \times 973 + 1.3 \times 810 \end{aligned}$$

$$RE_D = 1,570 \text{ lb.}$$

$$L_D = 3,000 \times (3,580/1,570)^{10/3} \times (500/3,760)$$

$$L_D = 6,220 \text{ hours}$$

$$L_E = >> 100,000 \text{ hours}$$

Lubrication and Efficiency Analysis

The primary consideration of the design of a lubrication system for this gearbox and previous helicopter transmissions is to provide cooling oil to remove heat generated due to friction losses at gear meshes and bearings and to provide lubricity to support tooth and bearing loads.

The preliminary analysis presented in this report establishes a systematic approach to the design of an integrated lubrication system for each transmission component. This approach is based upon extensive test and production experience with a considerable number of helicopter transmissions. This transmission utilizes carburized and ground gears, precision bearings, and close tolerance machined dynamic parts and housings. Experience indicates the losses through gear meshes, including the associated bearings, to be 1/2 percent per mesh, and the total gearbox churning loss to be 1/2 percent.

Efficiency Analysis - Intermediate Gearbox

$$\text{Bevel Mesh} = (.005)(1,500) = 7.5$$

$$\text{Churning Losses} = (.005)(1,500) = \underline{7.5}$$

$$F_{\text{HP}} \text{ (friction HP)} = 15.0$$

$$\text{Estimated Efficiency} = \frac{1,500 - 15}{1,500} \times 100 = 99\%$$

Total Heat Generated, (Q_G)

$$\begin{aligned} Q_G &= 2,545 \times F_{\text{HP}} \\ &= (2,545)(15) \\ &= 38,175 \text{ BTU/HR} \end{aligned}$$

From past helicopter experience, at least 15 percent of the total heat generated in an intermediate gearbox is conducted through the gear case and radiated to the surrounding area. Therefore, the necessary oil cooler can be designed to reject 85 percent of the total gearbox heat generated at maximum power.

Heat Rejection Rate, Oil Cooler

$$\begin{aligned} Q_{o.c.} &= .85 Q_G \\ &= (.85)(38,175) \\ &= 32,450 \text{ BTU/HR} \end{aligned}$$

The transmission oil cooler and blower design is summarized on page 149 of this report.

Cooling Oil Required

Oil flow requirements are based upon the following parameters:

1. Use MIL-L-7808 oil in this transmission.
2. Oil in at 176°F.
3. Oil out of gearbox at 230°F.

Therefore,

$$\begin{aligned} W_o &= \frac{C_e (42.4) F_{HP}}{(.1337) C_p \rho_o \Delta T} \text{ GPM.} \\ &= \frac{(.565)(42.4)(15)}{(.1337)(.528)(54.4)(54)} \\ &= 1.74 \text{ GPM.} \end{aligned}$$

Oil Pump

On the basis of the above intermediate gearbox oil flow requirement, a 2-5-gallon-per-minute vane pump operating at 3,760 revolutions per minute is required. This size and type of pump has been selected for optimum serviceability, quality, and low cost. The location of this pump and associated lubrication system components is outlined on lube schematic Figure 25.

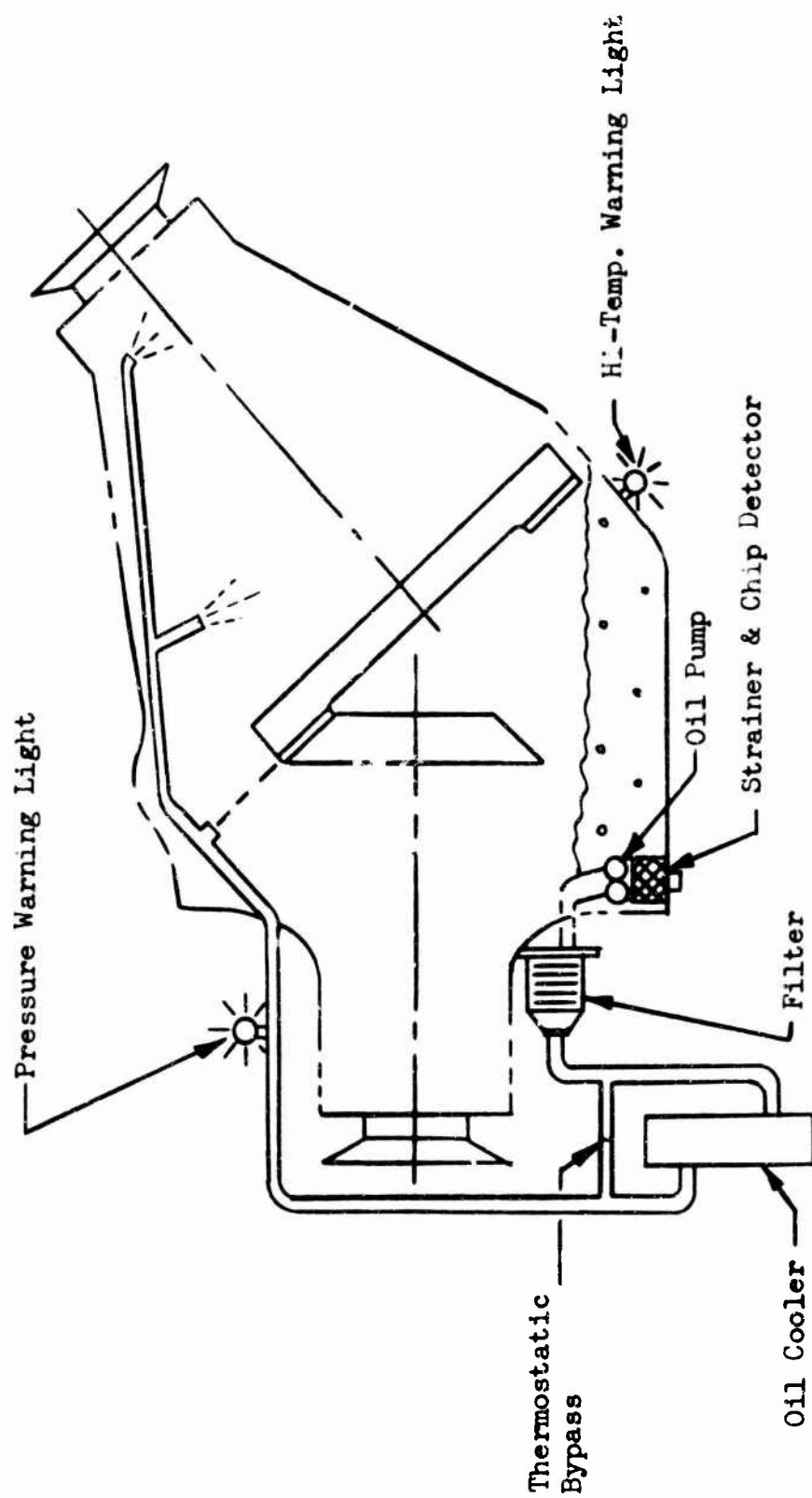


Figure 25 . Lubrication System, Intermediate Gearbox.

TABLE 14
WEIGHT SUMMARY,
INTERMEDIATE GEARBOX

Item	Unit Weight (lb.)	Assembly Weight (lb.)	Total Weight (lb.)
Input Section		49.1	
Housing	9.5		
Input Pinion	21.8		
Bearings	7.8		
Miscellaneous	10.0		
Center Housing & Stud Assembly		13.6	
Output Section		69.8	
Housing	7.7		
Output Gear	46.0		
Bearings	5.6		
Miscellaneous	10.5		
Oil Pump & Quill Shaft		4.5	
			137.

Tail Rotor Gearbox

To transfer power from the pylon drive shaft operating at 3,760 RPM to the tail rotor at 607 RPM involves a 90° shaft angle change and a total speed reduction of 6.18:1.

Since the required speed reduction cannot be achieved in the single spiral bevel gear mesh, an additional reduction must be employed. To minimize gear sizes and weight, the design study indicated that the maximum reduction should be accomplished at the last possible reduction stage to maintain minimum transmitted torque through as many reduction stages as is feasible. To provide multiple mesh load sharing and minimize the number of reduction stages, a single stage planetary adjacent to the tail rotor was the lightest, most efficient solution.

A planetary reduction of 3.82:1 was achieved using a sun gear input and fixed ring gear with the cage, or planet carrier, driving the tail rotor shaft. This, in addition to a spiral bevel gear ratio of 55/34 (1.62:1), furnishes the desired reduction. Figure 57 of Appendix I shows the tail gearbox arrangement described above.

Calculated operating stresses for the tail gearbox spiral bevel gears are presented in Appendix III for the design load conditions. At these stress levels a reliability of $R \approx .999$ will be obtained.

	Pinion		Gear
Number of Teeth	34		55
Diametral Pitch		3.676	
Face Width		2.632	
Pitch Diameter	9.249		14.962
Face Contact Ratio		1.726	
Pressure Angle		$\phi = 20^\circ$	
Mean Spiral Angle		$\psi = 25^\circ$	
Shaft Angle		$\Sigma = 90^\circ$	
Pitch Angle	$\gamma = 31^\circ 43'$		$\Gamma = 58^\circ 17'$
Hand of Spiral	RH		LH
Direction of Rotation	CCW		CW

Bevel Gear Data

$$\phi = 20^{\circ}0'$$
$$\tan \phi = .36397$$

$$\psi = 25^{\circ}0'$$
$$\sin \psi = .42262$$
$$\cos \psi = .90631$$

$$\gamma = 31^{\circ}43'$$
$$\sin \gamma = .52572$$
$$\cos \gamma = .85066$$

$$D_{\text{mean}} (\text{pinion}) = D_p - F \sin \gamma$$
$$= 9.249 - 2.632 \times 0.52572$$

$$D_{\text{mean}} (\text{pinion}) = 7.865 \text{ in.}$$

$$D_{\text{mean}} (\text{gear}) = 7.865 \times 55/34$$

$$D_{\text{mean}} (\text{gear}) = 12.723 \text{ in.}$$

Input Pinion, Figure 26

Horsepower	875
Input Speed	3,760 RPM
Mean Diameter	7.865 in.

$$\text{Torque} = \frac{63,025 \times 875}{3,760} = 14,670 \text{ in.-lb.}$$

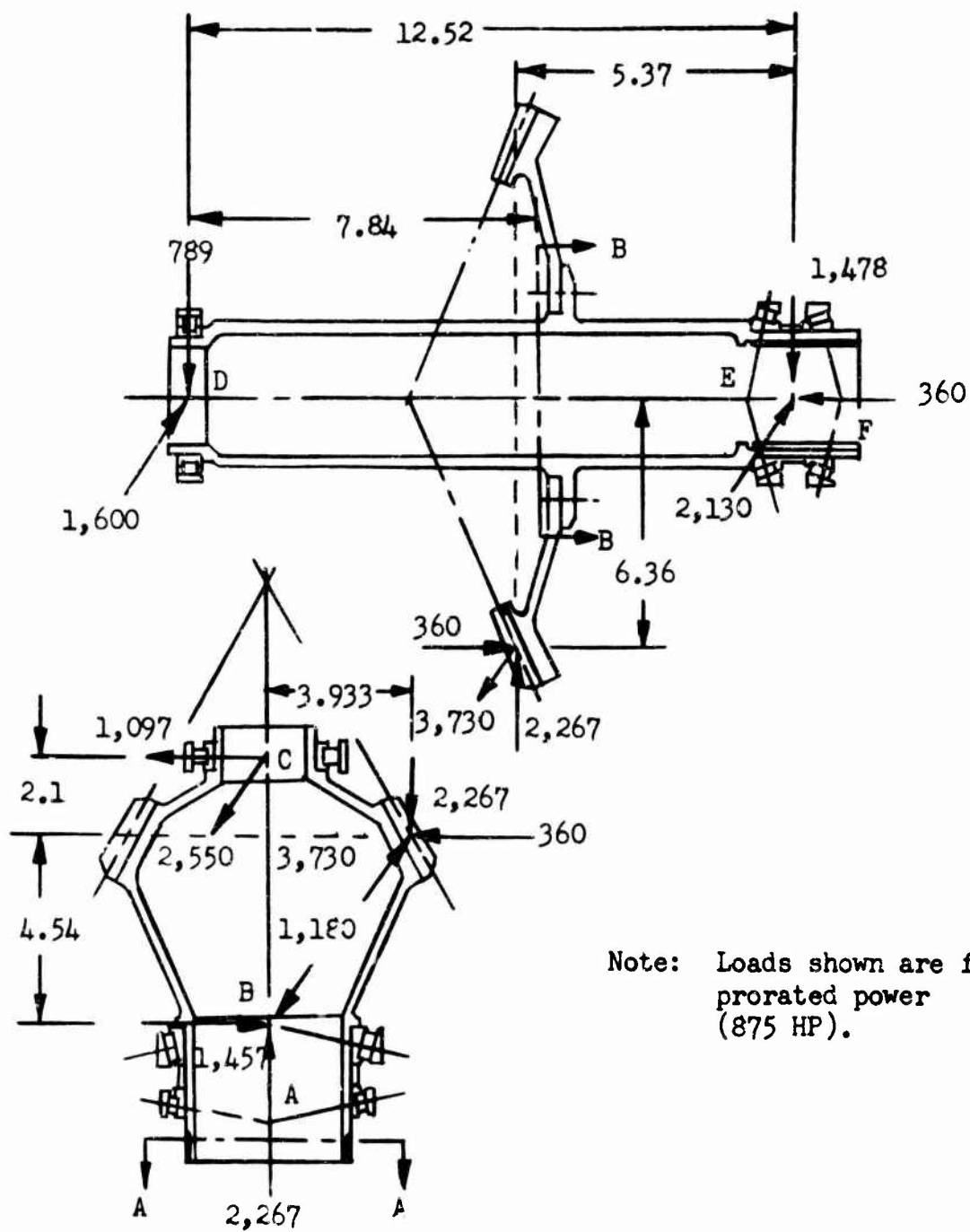
$$W_t = \frac{2 \times T}{D_{\text{mean}}} = \frac{2 \times 14,670}{7.865}$$

$$W_t = 3,730 \text{ lb.}$$

$$W_x = W_t \left(\frac{\tan \phi \sin \gamma + \sin \psi \cos \gamma}{\cos \psi} \right)$$

$$W_x = 3,730 \left(\frac{.36397 \times .52572 + .42262 \times .85066}{.90631} \right)$$

$$W_x = 2,267 \text{ lb.}$$



Note: Loads shown are for
prorated power
(875 HP).

Figure 26 . Bevel Gear Shafts, Tail Gearbox.

$$W_s = W_t \frac{(\tan \phi \cos \delta - \sin \psi \sin \delta)}{\cos \psi}$$

$$W_s = 3,730 \frac{(.35397 \times .85066 - .42262 \times .52572)}{.90631}$$

$$W_s = 360 \text{ lb.}$$

$$R_B = \frac{\sqrt{(3,730 \times 2.1)^2 + (2,267 \times 3.933 + 360 \times 2.1)^2}}{6.64}$$

$$R_B = 1,875 \text{ lb.}$$

$$R_C = \frac{\sqrt{(3,730 \times 4.54)^2 + (2,267 \times 3.933 - 360 \times 4.54)^2}}{6.64}$$

$$R_C = 2,770 \text{ lb.}$$

Bearing Selection - Input Pinion, Figure 26

At "A", the preload bearing, a tapered roller bearing L 521949/
L 521910 and at "B", a tapered roller bearing 48190/48120,

$$K_A = 1.49$$

$$BRR_A = 4,100 \text{ lb.}$$

$$K_B = 1.16$$

$$BRR_B = 7,800 \text{ lb.}$$

$$\frac{.47 R_B}{K_B} = \frac{0.47 \times 1,875}{1.16} = 760 \text{ lb.}$$

$$\text{Thrust} = 2,267 \text{ lb.}$$

Therefore, since thrust > 760

$$RE_B = 0.53 \times 1,875 + 1.16 \times 2,267$$

$$RE_B = 3,620 \text{ lb.}$$

$$RE_A = 0$$

$$L_A = >> 100,000 \text{ hours}$$

$$L_B = 3,000 \times (7,800/3,620)^{10/3} \times (500/3,760)$$

$$L_B = 5,130 \text{ hours}$$

At "C", a roller bearing 65 x 120 x 23 mm. with a basic dynamic capacity of 23,300 lb.,

$$L_C = \frac{(23,300/2,770)^{10/3} 10^6}{3,760 \times 60}$$

$$L_C = 5,410 \text{ hours.}$$

Output Gear, Figure 26

As this is a right angle bevel mesh, the axial and separating loads on the pinion are reversed for the gear.

$$W_x \text{ gear} = W_s \text{ pinion} = 360 \text{ lb.}$$

$$W_s \text{ gear} = W_x \text{ pinion} = 2,267 \text{ lb.}$$

$$W_t = 3,730 \text{ lb.}$$

$$R_D = \frac{\sqrt{(3,730 \times 5.37)^2 + (2,267 \times 5.37 - 360 \times 6.36)^2}}{12.52}$$

$$R_D = 1,785 \text{ lb.}$$

$$R_{E-F} = \frac{\sqrt{(3,730 \times 7.15)^2 + (2,267 \times 7.15 + 360 \times 6.36)^2}}{12.52}$$

$$R_{E-F} = 2,590 \text{ lb.}$$

Bearing Selection, Output Gear

At "D", a 95 x 130 x 18 mm. roller bearing, capacity = 16,100 lb.

$$L_D = \frac{(16,100/1,785)^{10/3} 10^6}{2,325 \cdot 60}$$

$$L_D = 11,050 \text{ hours}$$

At "E-F", two tapered roller L521910/L521949 bearings, back-to-back,

$$K = 1.49$$

$$BRR = 4,100 \text{ lb.}$$

$$\text{Thrust} = 360 \text{ lb.}$$

$$\frac{.47 \times 2,590}{1.49} = 817$$

$$\text{Thrust} < 817$$

$$RE_E = \frac{R}{2} + 1.064 \times K_E \times \text{Thrust}$$

$$= \frac{2,590}{2} + 1.064 \times 1.49 \times 360$$

$$= 1,866 \text{ lb.}$$

$$RE_F = \frac{R}{2} - 1.064 \times K_E \times \text{Thrust}$$

$$= \frac{2,590}{2} - 1.064 \times 1.49 \times 360$$

$$= 724 \text{ lb.}$$

$$L_E = 3,000 \times (4,100/1,866)^{10/3} \times 500/2,325$$

$$L_E = 8,830 \text{ hours}$$

$$L_F = 3,000 \times (4,100/724)^{10/3} \times 500/2,325$$

$$L_F = >> 100,000 \text{ hours}$$

Tail Rotor Shaft - Bearing Loading and Selection

The loads imposed on the bearings result from the head moment $-M_h$ - caused by the flapping motion of the blades, the thrust developed by the tail rotor to counteract main rotor torque, a lateral force equal to the product of thrust multiplied by the prorated tail rotor flapping angle, and the weight of the components. To be conservative, all of these applied forces are considered coplanar.

Design Data

$$\text{RPM} = 608$$

$$b = 6$$

$$e = 6.6 \text{ in.}$$

$$F_c = 36,740 \text{ lb.}$$

$$K = 727,400 \text{ in.-lb./rad.}$$

$$\beta \text{ prorated} = 2.42^\circ$$

$$\text{Main Rotor HP}_{\text{prorated}} = 7,370$$

$$\text{Main Rotor RPM} = 140.6$$

$$\text{Distance, Main Rotor to Tail Rotor, } d = 714 \text{ in.}$$

$$\text{Weight of Hub and Blades} = 500 \text{ lb.}$$

$$\text{Weight of Planetary} = 100 \text{ lb.}$$

$$M_h = K \frac{\beta_{\text{prorated}}}{57.3} = \frac{(727,400)(2.42)}{57.3} = 30,700 \text{ in.-lb.}$$

$$\text{Thrust} = \frac{\text{Main Rotor Torque}_{\text{prorated}}}{d} = \frac{63,025 \times 7,370}{140.6 \times 714}$$

$$\text{Thrust} = 4,620 \text{ lb.}$$

$$H = \text{Thrust} \times \tan \beta_{\text{prorated}} = 4,620 \times .042$$

$$H_{\text{prorated}} = 194 \text{ lb.}$$

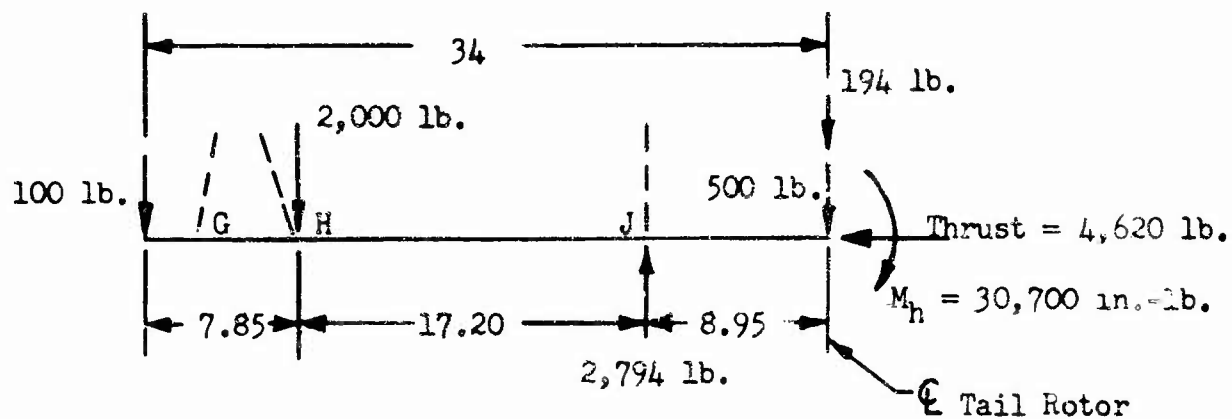


Figure 27 Tail Rotor Shaft Loading.

Bearing Selection

$$R_H = \frac{694 \times 8.95 + 30,700 - 25.05 \times 100}{17.20}$$

$$R_H = 2,000 \text{ lb.}$$

$$R_J = \frac{694 \times 26.15 + 30,700 - 7.85 \times 100}{17.20}$$

$$R_J = 2,794 \text{ lb.}$$

At G & H, tapered roller bearings 48393/48320,

$$\text{BRR} = 12,800$$

$$K = 1.82$$

$$\frac{.47 R_H}{K_H} = \frac{.47 \times 2,000}{1.82} = 515.$$

Since $515 < \text{Thrust}$,

$$R_G = 0 \text{ (bearing "G" acts as a preload bearing)}$$

$$R_H = .53 \times 2,000 + 1.82 \times 4,620$$

$$R_H = 9,470 \text{ lb.}$$

$$L_G = >> 100,000 \text{ hours}$$

$$L_H = 3,000 \times (12,800/9,470)^{10/3} \times 500/608$$

$$L_H = 6,750 \text{ hours}$$

At J, a 130 x 200 x 33 ball bearing,
basic dynamic capacity = 18,400 lb.

$$L_J = \frac{(18,400/2,794)^3}{608} \frac{10^6}{60}$$

$$L_J = 7,800 \text{ hours}$$

Planetary - Gear Face Width Calculations

Determination of the required face width is based on bending (Lewis) and compressive (Hertz) stresses given respectively by the following equations.

$$f_b = \frac{1.5 W_t K}{(F.W.) X}$$

$$f_c^2 = \frac{21 \times 10^6 W_t (1/D_{pinion} \pm 1/D_{gear})}{\sin 2\phi (F.W.)}$$

Note: + for external mesh
- for internal mesh

Planetary Data:

	No. Teeth -N	Pitch Diameter -D
Sun Gear	34	5.6667
Planet Pinion	31	5.1667
Ring Gear	96	16.0000

Number of Planet Pinions $N_{pp} = 5$

Pressure Angle $\phi = 22^{\circ}30'$

Sun RPM $= 2,325$

Gear Design HP $= 2,300$

Allowable Stresses

$$\begin{aligned} PLV &= \frac{0.524 \text{ RPM sun } (D_s + D_p) N_s N_r}{2 (N_s + N_p) (N_s + N_r)} \\ &= .524 \frac{(2,325)(5.6667 + 5.1667)(34)(96)}{2(34 + 31)(34 + 96)} \end{aligned}$$

$$PLV = 2,550 \text{ fpm}$$

$$\begin{aligned} F_b &= 31,500 - 0.625 \times PLV \\ &= 31,500 - 0.625 \times 2,550 \end{aligned}$$

$$F_b = 29,900 \text{ psi}$$

$$F_c = 140,000 \text{ psi}$$

Loading

$$\text{Torque} = 63,025 (2,300)/2,325 = 62,360 \text{ in.-lb.}$$

$$W_t = 2 \times \text{Torque}/D_s = 2(62,360)/5.6667 = 22,000 \text{ lb.}$$

$$W_t/\text{Mesh} = 22,000/5 = 4,400 \text{ lb.}$$

Face Width, Sun Gear

$$X \text{ (Function of pitch and number of teeth)} = .1661$$

$$K \text{ (Function of root radius)} = 1.00$$

$$\begin{aligned} F.W._b &= \frac{1.5 W_t K}{F_b X} \\ &= \frac{1.5 (4,400)(1)}{(29,900)(.1661)} \end{aligned}$$

$$F.W._b = 1.33 \text{ in.}$$

$$\begin{aligned} F.W._c &= \frac{21 \times 10^6 W_t}{\sin 2\phi F_c^2} (1/D_p + 1/D_s) \\ &= \frac{21 \times 10^6 \times 4,400}{.707(196 \times 10^8)} (1/5.6667 + 1/5.1667) \end{aligned}$$

$$F.W._c = 2.47 \text{ in.}$$

Face Width, Planet Pinion

$$X = .1616$$

$$K = 1.0$$

$$F.W._b = \frac{1.5(4,400)(1)}{29,900(.1616)}$$

$$F.W._b = 1.37 \text{ in.}$$

Face Width, Ring Gear

$$X = .30$$

$$K = 1.05$$

$$F.W._b = \frac{1.5 (4,400)(1.05)}{(29,900) (.30)}$$

$$F.W._b = 0.773 \text{ in.}$$

$$F.W._c = \frac{21 \times 10^6 \times 4,400}{.707 \times 196 \times 10^8} \left(\frac{1}{5.1667} - \frac{1}{16} \right)$$

$$F.W._c = 0.875 \text{ in.}$$

The calculated planetary gear face widths are summarized in Table 15 below. Also presented are the actual gear face widths chosen for sufficient overlap to assure that operating stresses are consistent with calculated values.

TABLE 15
PLANETARY GEAR SUMMARY,
TAIL ROTOR GEARBOX

Component	Required Face Width Bending (in.)	Required Face Width Compression (in.)	Face Width Selected (in.)	Actual Bending Stress (psi)	Actual Compressive Stress (psi)
Sun Gear	1.33	2.47	2.60	15,300	139,000
Planet Pinion	1.37	2.47	2.50	16,400	139,000
Ring Gear	.78	.88	1.25	18,650	110,000

Planetary Cage Plate Analysis

The design criteria used in determining the tail gearbox planetary plate thickness is identical to that shown on page 19 for the main transmission planetary plates.

Plate Thickness

$$T = 62,350 \text{ in.-lb.}$$

$$\text{RPM}_{\text{sun}} = 2,325$$

$$N_{\text{pp}} = 5$$

$$g = 2.75 \text{ in.}$$

$$N_s = 34$$

$$N_p = 31$$

$$N_r = 96$$

$$D_s = 5.667 \text{ in.}$$

$$D_p = 5.1667 \text{ in.}$$

$$d = 3.400 \text{ in.}$$

$$\overline{\text{O.D.}}_{\text{plates}} = 15.63 \text{ in.}$$

$$\overline{\text{I.D.}}_{\text{plates}} = 6.1 \text{ in.}$$

$$E = 30 \times 10^6 \text{ psi}$$

$$L = (D_s + D_p) \sin \pi / N_{\text{pp}} = 10.8337 \sin 36^\circ = 6.368$$

$$f_b = \frac{12(62,350)(0.5 \times 6.368 - .4 \times 3.4)}{5(5.667)(6.368)(15.63 - 6.1 - 1.2 \times 3.4)} \left[\frac{g + t}{t^2} \right]$$

$$f_b = 1,390 \times \frac{g + t}{t^2}$$

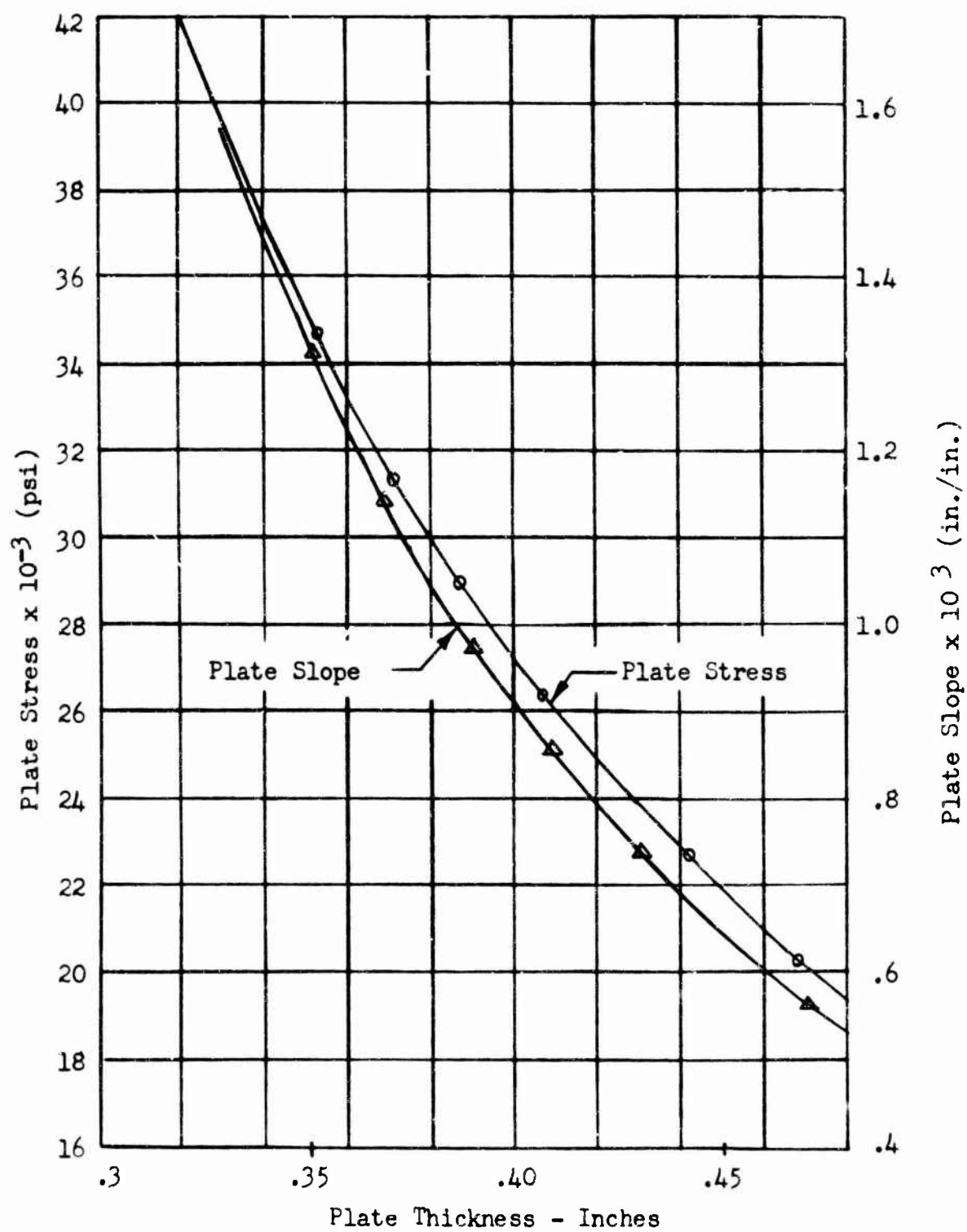


Figure 28. Stress and Deflection Versus Planetary Plate Thickness, Tail Gearbox.

$$\lambda = \frac{16(62,350)(0.5 \times 6.368 - .4 \times 3.4)^3}{5.667(5)(15.63 - 6.1)(30 \times 10^6)(6.368)^2} \left[\frac{g + t}{t^3} \right]$$

$$\lambda = 18.44 \times 10^{-6} \times \frac{g + t}{t^3}$$

Substitution of the allowable plate stress and maximum plate deflection limitations in the above equations results in a carrier plate thickness of 0.400 inch (Reference page 19).

The relation of the carrier plate stress and deflection for various plate thicknesses is shown graphically in Figure 28, page 126. To compensate for the deflection in the carrier plates, a corrective left hand helix angle of 0.0005 to 0.0008 inch per inch should be cut on the sun and ring gears.

Planetary Pinion Bearing Selection

Determination of the planet pinion bearing lives is similar to the procedure developed on page 40 for the main gearbox. By limiting the maximum deflection of the outer and inner races to 0.025 inch and 0.005 inch, respectively, experience indicates that agreement between calculated and actual bearing lives will be obtained.

Planetary Data

HP _{prorated}	=	875
N _{pp}	=	5
P _d	=	6
D _s	=	5.6667 in.
D _p	=	5.1667 in.
D _R	=	16.000 in.
RPM _{sun}	=	2,325

$$RIM_{\text{planet}} = 1,880$$

Loading

$$T = 63,025 \times 875/2,325 = 23,720 \text{ in.-lb.}$$

$$W_t = \frac{2 T}{N_{pp} D_s}$$

$$W_t = \frac{2 \times 23,720}{5 \times 5.6667}$$

$$W_t = 1,675 \text{ lb.}$$

$$W_s = W_t \tan \phi \quad \text{where } \phi = 22^\circ 30'$$

$$W_s = 695 \text{ lb.}$$

Outer Race Deflection

The planet pinion tooth backup and inside diameter is determined by either the backup requirement (1.1 times the whole depth of the tooth) or that thickness required to limit the outer race deflection to 0.025 inch. First deflection determination is made on the basis of required backup.

$$\overline{I.D.}_{pp} = 4.750 - (1.1)(2) 2.25/6$$

$$\overline{I.D.}_{pp} = 3.925 \text{ in.}$$

The deflection of the outer and inner bearing races will be analyzed using the following equations:

$$\delta = (0.149) \frac{W_s D_m^3}{E I} \quad (\text{Reference 5, page 156})$$

$$\delta = (7.45 \times 10^{-9})(W_s/F.W.)(D_m/t)^3$$

$$\delta = (7.45 \times 10^{-9})(695/2.5)(4.337/.412)^3$$

$$\delta = 0.00241 \text{ in.}$$

Bearing Selection

Install two rows of rollers, 0.35 diameter by 1.00 inch long.

$$\text{Maximum number of rollers (Z)} \approx \frac{(\overline{\text{I.D.}}_{\text{pp}} - D_{\text{roller}})}{D_{\text{roller}} + t_{\text{cage rib}}}$$

$$Z \approx \frac{(3.925 - .35)}{.35 + .15}$$

$$Z = 22 \text{ rollers/row}$$

The basic load rating for a roller bearing is given by

$$C_b = 5,500 (L_{\text{eff rollers}} \times \text{No. of Rows})^{7/9} (\text{Rollers per row})^{3/4} \times (D_{\text{roller}})^{29/27}$$

(Reference 1, page 1)

$$C_b = 5,500 (.9 \times 2)^{7/9} (22)^{.75} (.35)^{29/27}$$

$$C_b = 28,600 \text{ lb.}$$

$$\text{Radial Equivalent (RE)} = 1.2 (2) W_t$$

$$= 1.2 \times 2 \times 1,675$$

$$\text{RE} = 4,020 \text{ lb.}$$

$$L = \frac{(28,600/4,020)^{10/3} 10^6}{1,800 \times 60}$$

$$L = 6,200 \text{ hours}$$

Inner Race Deflection

$$\overline{\text{O.D.}} = 3.225 \text{ in.}$$

$$\overline{\text{I.D.}} = 2.62 \text{ in.}$$

$$\delta = (7.45 \times 10^{-9}) (695/2.7) (2.923/.302)^3$$

$$\delta = 0.00174 \text{ in.}$$

Stress Analysis of Shafting

Stresses developed at various shaft sections will be determined for critical loading conditions to indicate the design adequacy of the gearbox shafting.

Input Pinion (Figure 26, page 115)

Since the input pinion shaft configuration was largely determined by gearing and manufacturing requirements, the resulting bending stresses are negligible. The stresses developed at Section A-A are the result of transmitted horsepower and nut torque.

$$T = 38,550 \text{ in.-lb. (Figure 1, page 21)}$$

$$P_{\text{spline}} = 16/32$$

$$N = 66$$

$$D_p = 4.125 \text{ in.}$$

$$\text{Major Dia. (O.D.)} = 4.125 + 1/16 = 4.1875 \text{ in.}$$

$$\overline{\text{I.D.}} = 3.7 \text{ in.}$$

$$A = (\pi/4)(D_p^2 - \overline{\text{I.D.}}^2)$$

$$A = 2.59 \text{ in.}^2$$

$$J = (\pi/32)(4.125^4 - 3.7^4)$$

$$J = 9.92 \text{ in.}^4$$

$$f_s = \frac{T \overline{\text{O.D.}}}{2J}$$

$$f_s = \frac{38,550 \times 4.1875}{2 \times 9.92}$$

$$f_s = 8,150 \text{ psi}$$

$$\text{Maximum Nut Torque} = 500 \text{ ft.-lb.} = 6,000 \text{ in.-lb.}$$

$$D_{\text{threads}} = 4 \text{ in.}$$

$$f_a = P/A, \text{ where } P = T/.2D \text{ threads}$$

$$f_a = \frac{T_{\text{nut}}}{.2 A D}$$

$$f_a = \frac{6,000}{(.2)(2.59)(4)}$$

$$f_a = 2,900 \text{ psi}$$

$$\text{M.S. ult} = \frac{F_{tu}}{1.5 \sqrt{(f_a + f_b)^2 + 4(f_s)^2}} \quad -1$$

$$= \frac{136,000}{1.5 \sqrt{2,900^2 + 4(8,150)^2}} \quad -1$$

$$\text{M.S. ult} = + 4.48$$

Bevel Gear Shaft (Figure 26, page 115)

As the loading indicated on Figure 26 is for prorated powers, the reactions must be increased by the ratio of maximum to prorated horsepower (2,300/875). Section BB is critical in fatigue.

$$M = 7.84 \times \sqrt{1,600^2 + 789^2} \quad (2,300/875)$$

$$M = 36,800 \text{ in.-lb.}$$

$$\overline{\text{O.D.}} = 4.62$$

$$\overline{\text{I.D.}} = 4.10$$

$$Z = 3.67$$

$$K_t = 1.55$$

$$f_b = M/Z$$

$$f_b = 36,800/3.67$$

$$f_b = 10,000 \text{ psi}$$

$$F_{en} = 19,500 \text{ psi}$$

$$M.S. = \frac{F_{en}}{K_t f_b} - 1$$

$$M.S. = \frac{19,500}{1.55 \times 10,000} - 1$$

$$M.S. = + 0.258$$

Tail Rotor Shaft

The design of the tail rotor shaft is based on a fatigue analysis similar to that of the main rotor shaft. The imposed loads are similar to those used in the tail rotor shaft bearing analysis on page 119 except ~~maximum~~ tail rotor horsepower (2,300 HP) is considered and the flapping angle is 5 degrees.

$$M_h = \frac{K \beta_e}{57.3}$$

$$M_h = \frac{727,400(5)}{57.3}$$

$$M_h = 63,480 \text{ in.-lb.}$$

$$T_h = \frac{14,200}{7,370} (4,620) = 8,900 \text{ lb.}$$

$$H = 8,900 \times \tan \beta_e, \text{ where } \beta_e = 5^\circ$$

$$H = 780 \text{ lb.}$$

$$F_{tu} = 136,000 \text{ psi}$$

$$F_{en} = 19,500 \text{ psi}$$

Section CC (Located as shown in Figure 29, page 135)

$$\overline{O.D.} = 4.875$$

$$\overline{I.D.} = 4.000$$

$$Z = 6.22$$

$$K_t = 1.5$$

$$M = 63,480 + (780 \times 7.1) + (500 \times 7.1)$$

$$M = 72,600 \text{ in.-lb.}$$

$$f_b = M/Z$$

$$f_b = 72,600/6.22$$

$$f_b = 11,700 \text{ psi}$$

$$M.S. = \frac{19,500}{1.5 \times 11,700} - 1$$

$$M.S. = + 0.11$$

Section DD (Located as shown in Figure 29, page 135)

$$\overline{O.D.} = 5.200$$

$$\overline{I.D.} = 4.550$$

$$Z = 5.71$$

$$K_t = 1.3$$

$$\begin{aligned}
 A &= 4.97 \text{ in.}^2 \\
 M &= 63,480 + (1,280 \times 8.95) - \\
 &\quad (100 \times 25.05) \frac{15.20}{17.20} + (100 \times 23.05) \\
 M &= 68,500 \text{ in.-lb.} \\
 f_b &= \frac{68,500}{5.71} \\
 f_b &= 12,000 \text{ psi} \\
 \text{Axial Force} &= \text{Bolt torque} - \text{thrust}
 \end{aligned}$$

Twelve 3/8- diameter bolts clamp the tail rotor hub, cones, and bearing assembly.

$$\begin{aligned}
 \text{Maximum Nut Torque} &= 405 \text{ in.-lb.} \\
 P_{\text{nut torque}} &= \frac{12 T}{.2 D} \\
 &= \frac{12 \times 405}{.2 \times .375} \\
 P_{\text{nut torque}} &= 64,800 \text{ lb.} \\
 \text{Net Axial Force} &= 64,800 - 8,900 \\
 \text{Net Axial Force} &= 55,900 \text{ lb.} \\
 f_a &= 55,900 / 4.97 = 11,250 \text{ psi} \\
 M.S. &= \frac{1}{\frac{f_a}{f_{ty}} + \frac{K_t f_b}{F_{en}}} - 1 \\
 &= \frac{1}{\frac{11,250}{115,000} + \frac{1.3 \times 12,000}{19,500}} - 1 \\
 M.S. &= + 0.11
 \end{aligned}$$

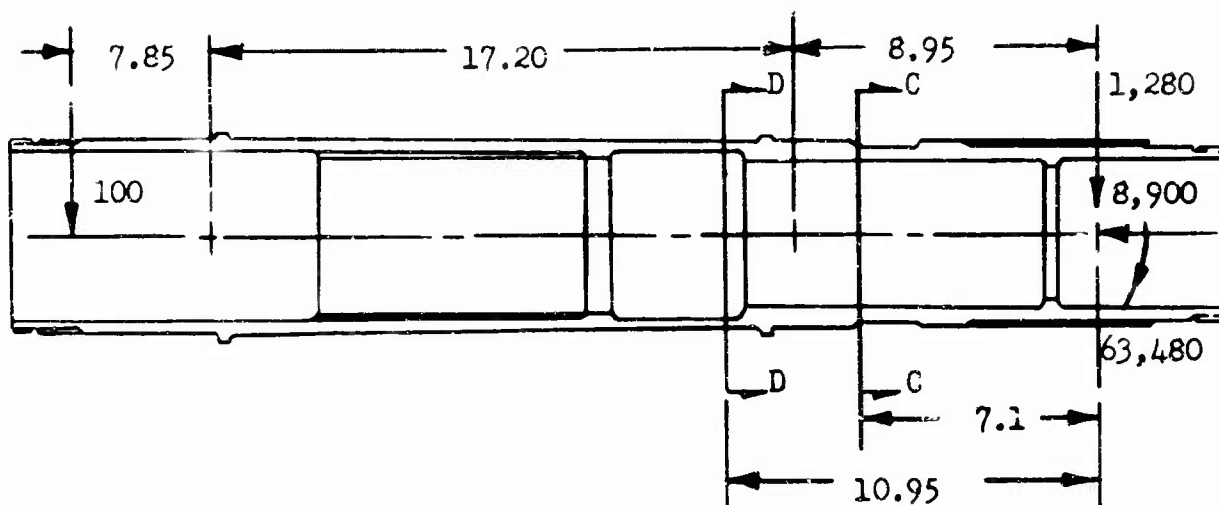


Figure 29. Tail Rotor Shaft.

Since analysis indicates a positive margin of safety at critical shaft sections, an unlimited service time will be obtained on this component.

Planetary and Tail Rotor Shaft Design Using Titanium

Incorporating titanium for the planetary carrier plates, spacers, and tail rotor shaft as proposed for the main gearbox on page 54, the following weight saving could be realized:

	Wt. Saving
Planetary	6.6
Tail Rotor Shaft	18.
Total	24.6 lb.

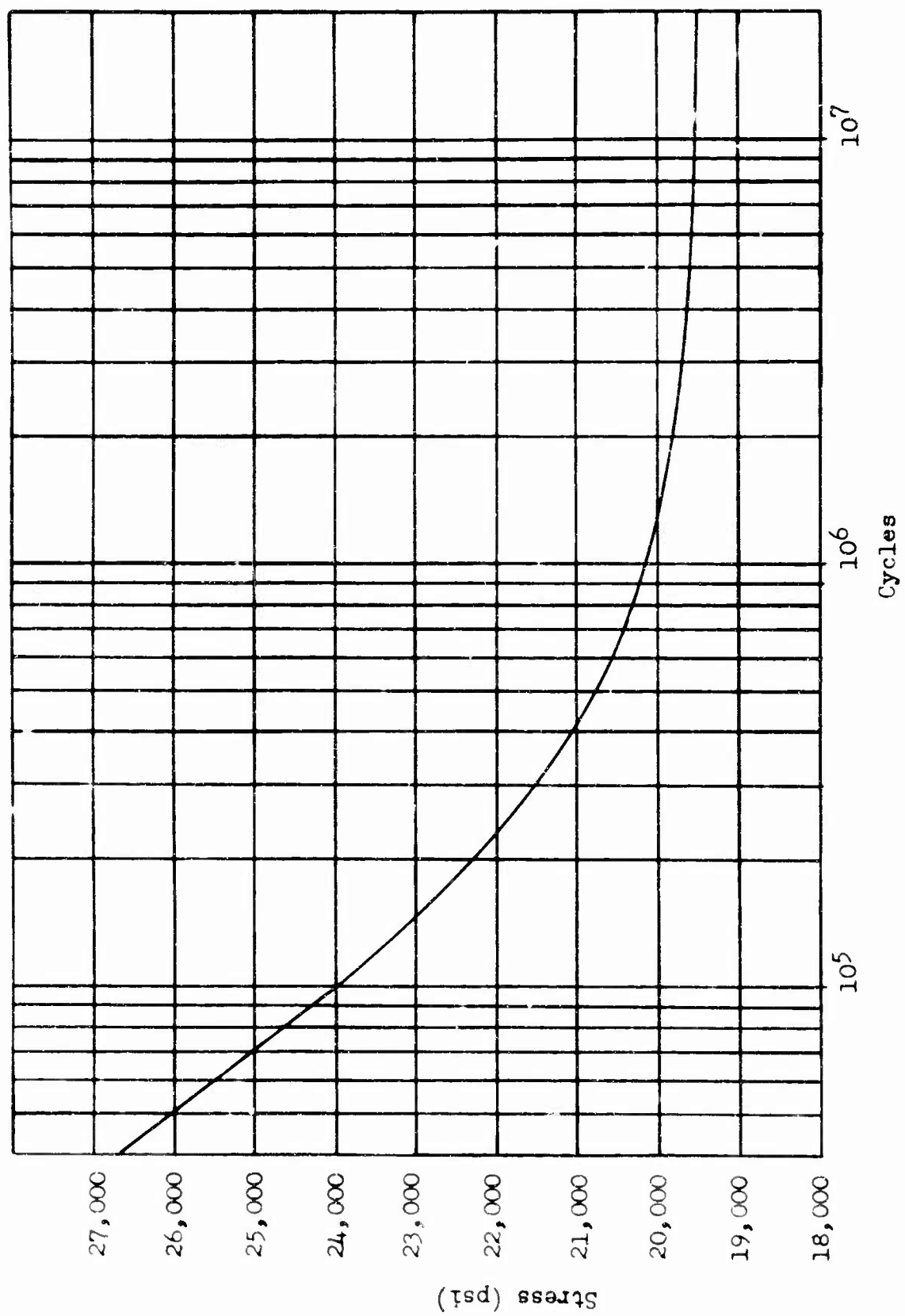


Figure 30. S-N Curve, 931A Carburized Steel (R_c 30-40 Core Hardness).

Lubrication and Efficiency Analysis

The primary consideration of the design of a lubrication system for this gearbox and previous helicopter transmissions is to provide cooling oil to remove heat generated due to friction losses at gear meshes and bearings and to provide lubricity to support tooth and bearing loads.

The preliminary analysis presented in this report establishes a systematic approach to the design of an integrated lubrication system for each transmission component. This approach is based upon extensive test and production experience with a considerable number of helicopter transmissions. This transmission utilizes carburized and ground gears, precision bearings, and close tolerance machined dynamic parts and housings. Experience indicates the losses through gear meshes, including the associated bearings, to be 1/2 percent per mesh, for planetary gear trains 3/4 percent, and the total gearbox churning loss to be 3/4 percent.

Efficiency Analysis, Tail Gearbox

Bevel Mesh	=	(.005)(1,500)	=	7.5
Planetary	=	(.0075)(1,500)	=	11.25
Churning Losses	=	(.005)(1,500)	=	<u>7.5</u>
				F _{HP} (friction HP) 26.25

$$\text{Estimated Efficiency} = \frac{1,500 - 26.25}{1,500} \times 100 = 98.25\%$$

Total Heat Generated (Q_G):

$$\begin{aligned} Q_G &= 2,545 \times F_{HP} \\ &= (2,545)(26.25) \\ &= 66,800 \text{ BTU/HR.} \end{aligned}$$

From past helicopter experience for exposed tail gearbox housings, the heat rejection is 0.250 British Thermal Unit per hour per square inch per degree centigrade.

Therefore,

$$\begin{aligned} Q_{\text{case}} &= UA \Delta T_c \\ &= (.250)(2,027)(30) = 15,220 \text{ BTU/HR.} \end{aligned}$$

The necessary oil cooler can be designed to reject the net heat rejected to cooler ($Q_{o.c.}$).

$$\begin{aligned} Q_{o.c.} &= Q_G - Q_{\text{case}} \\ &= 66,800 - 15,220 \\ &= 51,580 \text{ BTU/HR.} \end{aligned}$$

The transmission oil cooler and blower design is summarized on page 149 of this report.

Cooling Oil Required

Oil flow requirements are based upon the following parameters:

1. Use MIL-L-7808 oil in this transmission.
2. Oil in at 176°F.
3. Oil out of gearbox at 230°F.

Therefore,

$$\begin{aligned} W_o &= \frac{(.66)(42.4) \text{ FHP}}{(.1337)(c_p)(\rho_o) \Delta T} \quad \text{GPM} \\ &= \frac{(.66)(42.4)(26.25)}{(.1337)(.528)(54.4)(54)} = 2.76 \text{ GPM.} \end{aligned}$$

Oil Pump

On the basis of the above tail gearbox oil flow requirement, a 5-10-gallon-per-minute vane pump operating at 2,800 revolutions per minute is required. This size and type of pump has been selected for optimum serviceability, quality, and low cost. The location of this pump and associated lubrication system components are outlined on the lube schematic of Figure 31, page 139.

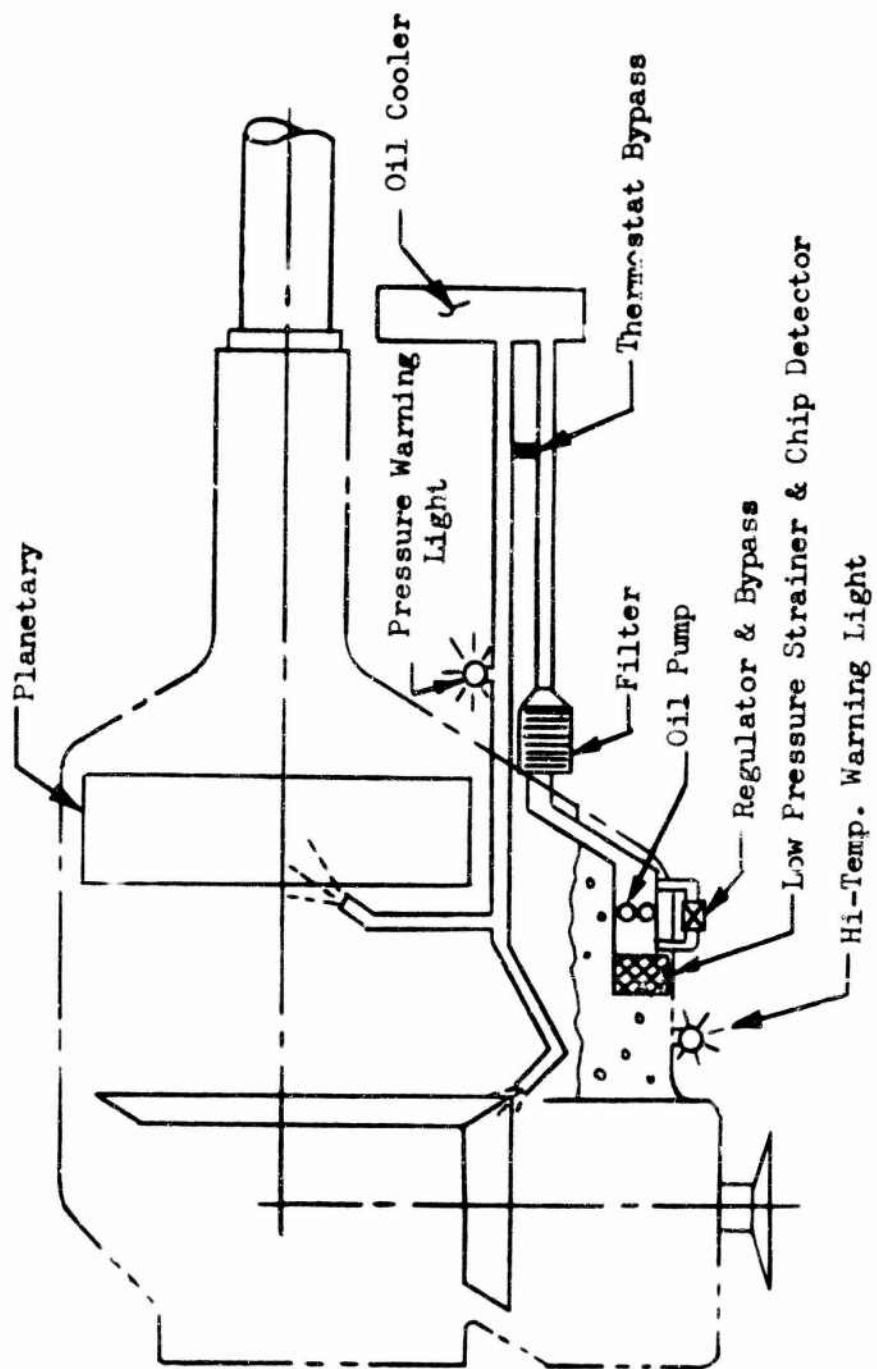


Figure 31. Lubrication System, Tail Rotor Gearbox .

TABLE 16
WEIGHT SUMMARY
TAIL ROTOR GEARBOX

Item	Unit Weight (lb.)	Assembly Weight (lb.)	Total Weight (lb.)
Input Section		39.3	
Housing	6.0		
Input Pinion	21.2		
Bearings	3.0		
Miscellaneous	4.1		
Center Housing & Gear Assembly		83	
Housing	25.3		
Output Gear	32.0		
Gear Shaft	15.1		
Bearings	5.9		
Miscellaneous	4.7		
Planetary Assembly		97.8	
Sun Gear	10		
Planet Pinions	30		
Ring	18.3		
Thrust Washers	2.3		
Planetary Plates	13		
Bearings & Journals	15.6		
Miscellaneous	8.6		
Output Shaft & Housing Assembly		103.8	
Housing	21.8		
Output Shaft	50.5		
Bearings	23.3		
Miscellaneous	8.2		
Oil Pump & Quill Shaft		9.1	
			333.

ROTOR BRAKE

Introduction

The heavy-lift helicopter rotor brake system has been designed, consistent with previous Crane-type helicopter braking requirements, to stop the rotor within a reasonable time with all engines shut down. In addition, sufficient torque capacity has been provided to hold all engines within the ground idle regime.

Brake Requirements

The brake design requirements to meet the above conditions are assumed as follows:

Delay Time	=	25 seconds
Braking Time	=	15 seconds
Total Stopping Time	=	40 seconds
Full Rotor Speed	=	141 RPM
Speed of Rotor Brake Disc	=	4,035 RPM
Output Torque of Each Engine at Ground Idle Throttle Setting	=	350 ft.-lb.
Engine Output Speed	=	13,600 RPM

Design Loads

Rotor System Inertia:	J	=	138,000 ft.-lb. sec. ²
Number of Blades:	b	=	6
Diameter - Main Rotor Head:	D_{MRH}	=	95 ft.
Blade Section (Chord):	C	=	2.95 ft.
Mass Density of Air:	ρ	=	.00237 slugs/ft. ³
Rotor Angular Velocity:	ω	=	$\pi \times \text{RPM}/30$
Section Profile - Drag Coef.:	C_{do}	=	.01

Design Analysis

To achieve a rotor braking system compatible with the available space envelope, it is necessary to proportion the total stopping time between a delay (or coast down) and a braking interval. This decision of stopping time is determined by the following analysis.

Rotor Decay

The profile drag torque may be represented by:

$$Q = 1.1 b \frac{1}{2} \rho \omega^2 C \cdot C_{do} \frac{D^4}{64} \text{ (ft.-lb.)}$$

Substituting,

$$Q = 3.275 (\text{RPM})^2.$$

The natural decay of the rotor may be represented by:

$$\Delta t = - \frac{2\pi J}{60} \int_{141}^{\text{RPM}} \frac{d(\text{RPM})}{Q} = - \frac{2\pi J}{60} \int_{141}^{\text{RPM}} \frac{d(\text{RPM})}{3.275 (\text{RPM})^2}$$

where Δt is time.

Substituting and simplifying gives

$$\text{RPM} = \frac{10^3}{7.63 + .227 (\Delta t)}.$$

This expression represents the natural rotor decay and is plotted on Figure 32.

Brake Torque

The decelerating torque acting on the main rotor may be represented by

$$T = -3.275 (\text{RPM})^2 - T_B$$

where T_B is the brake torque.

For a 25-second delay the rotor speed, from the natural rotor decay curve, is 75 RPM. Therefore:

$$\Delta t = - \frac{2\pi J}{60} \int_{75}^0 \frac{d(\text{RPM})}{3.275 (\text{RPM})^2 + T_B}.$$

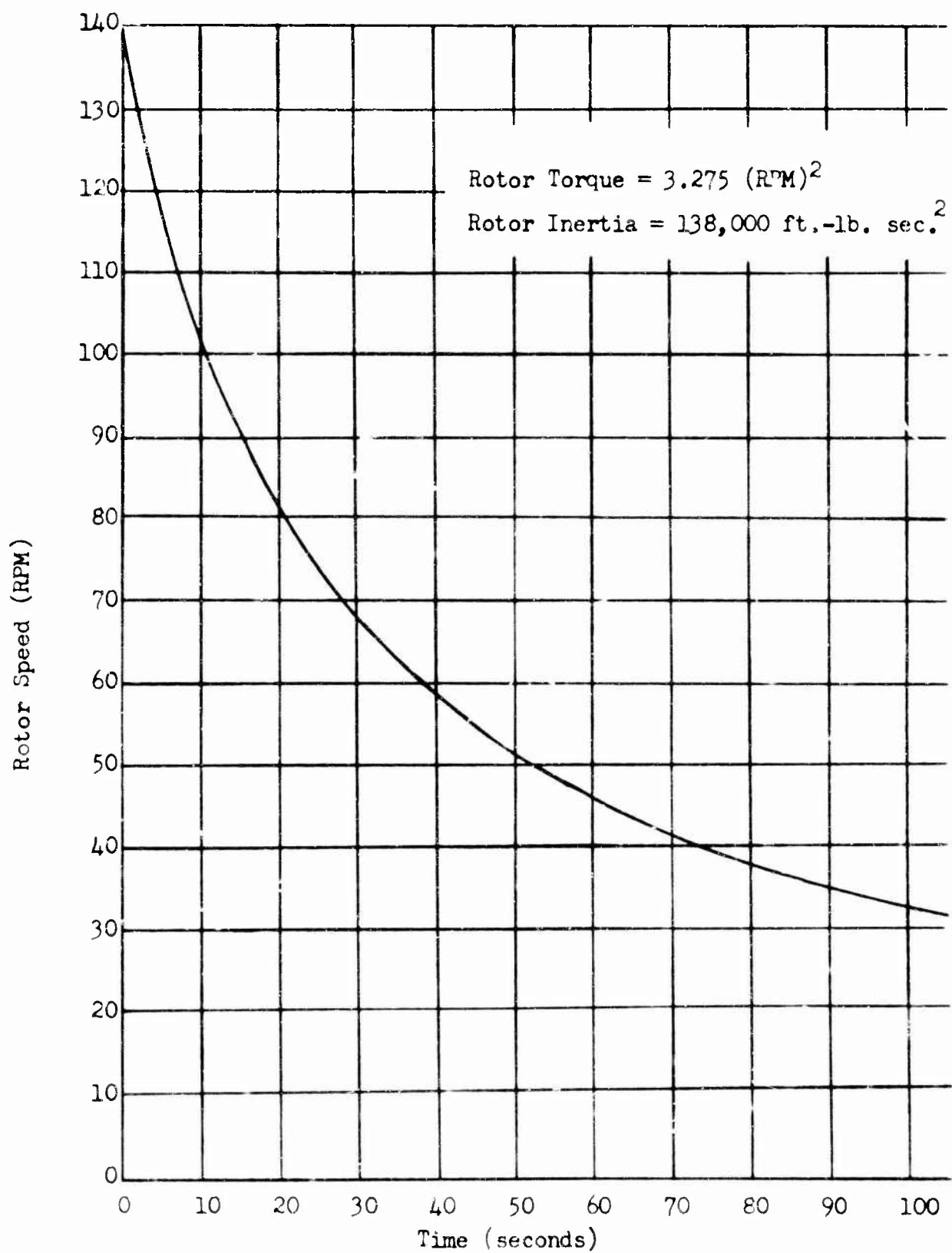


Figure 32. Main Rotor Decay Curve.

$$\Delta t = \frac{14,450}{\sqrt{3.275 T_B}} \left(\tan^{-1} \frac{75 \sqrt{3.275 T_B}}{T_B} \right)$$

This expression is plotted on Figure 34.

Kinetic Energy

The angle through which the rotor turns in coming to a stop is given by:

$$\Delta \theta = - \frac{2\pi}{60} \frac{2\pi J}{60} \int_{RPM}^0 \frac{(RPM) d(RPM)}{3.275 (RPM)^2 + T_B}$$

$$\Delta \theta = - 231.1 \ln \frac{T_B/3.275}{(RPM)^2 + T_B/3.275}$$

Thus the kinetic energy may be represented by:

$$K.E. = T_B (\Delta \theta).$$

Substituting,

$$K.E. = -231.1 (T_B) \ln \frac{T_B/3.275}{5,625 + T_B/3.275}$$

This is plotted on Figure 34.

Therefore, in order to stop the rotor system in 40 seconds, the rotor brake must be capable of developing a brake torque of 2,190 foot pounds and absorbing and dissipating 3.7×10^6 foot pounds of kinetic energy, as shown in the curves of Figure 34.

Engine Idle Torque

For an engine of this horsepower, the locked free turbine shaft torque with gas generator at ground idle, $T_i = 350$ ft.-lb.

The torque required to hold four engines is:

$$T_e = 4(350) \frac{13,600}{4,035}$$

$$T_e = 4,800 \text{ ft.-lb. at the rotor brake}$$

Rotor Brake Design

The rotor brake is a hydraulically actuated disc brake of the variable displacement type in which lining wear is compensated for by increased volume of operating fluid.

Pistons	Three 2 $\frac{1}{4}$ in. diameter/housing
Piston Area	23.75 in. ²
Effective Radius	6.5 in.
Maximum Rubbing speed	7,800 sfpm
Operating Pressure (dynamic)	690 psi
Operating Pressure (static)	1,480 psi
Coefficient of Friction	0.25
Disc Thickness	.710 in.
Disc Inside Diameter	8 in.
Disc Outside Diameter	16 in.
Disc Weight	32 lb.
Brake Housing	26 lb.
Total Weight	58 lb.

Rotor Brake System

A schematic of the rotor brake actuating system is shown in Figure 33 , page 146. The weight of this system is 60 pounds.

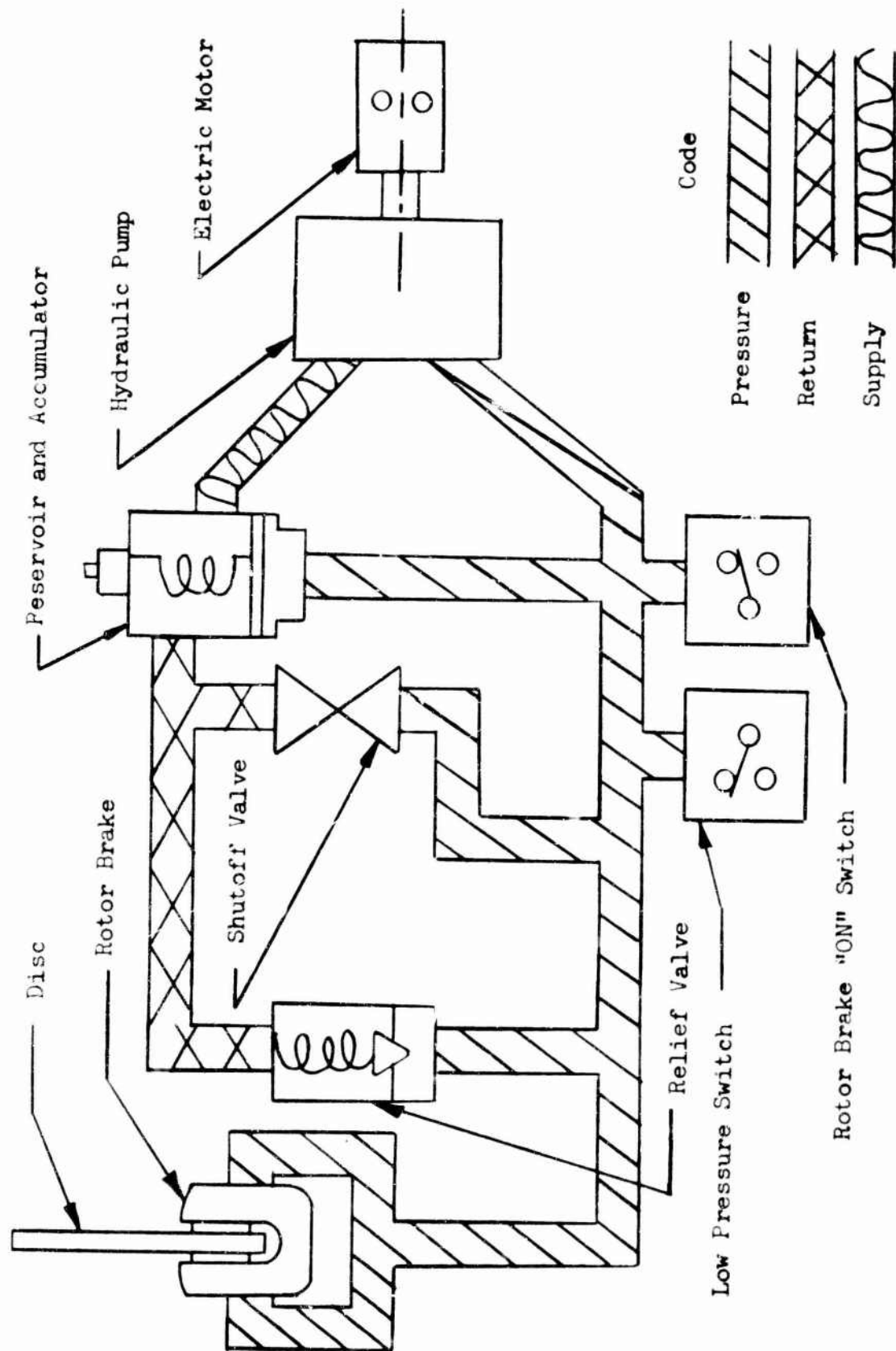


Figure 33. Rotor Brake System.

Kinetic Energy (ft.-lb. $\times 10^{-6}$) (K.E.)

$$K.E. = 231.1 (T_B) \ln \left[\frac{T_B/3.275}{RPM^2 + T_B/3.275} \right]$$

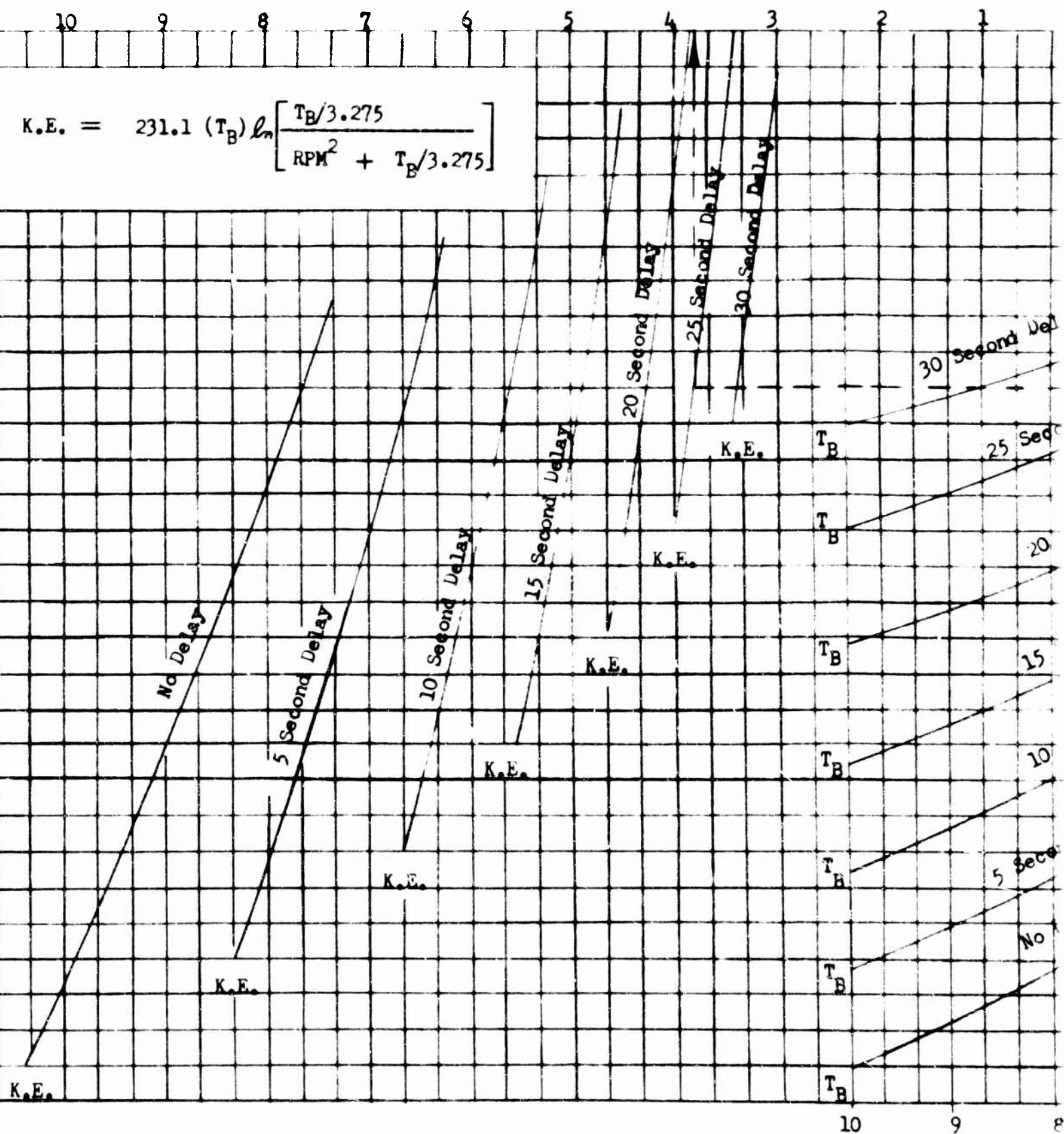
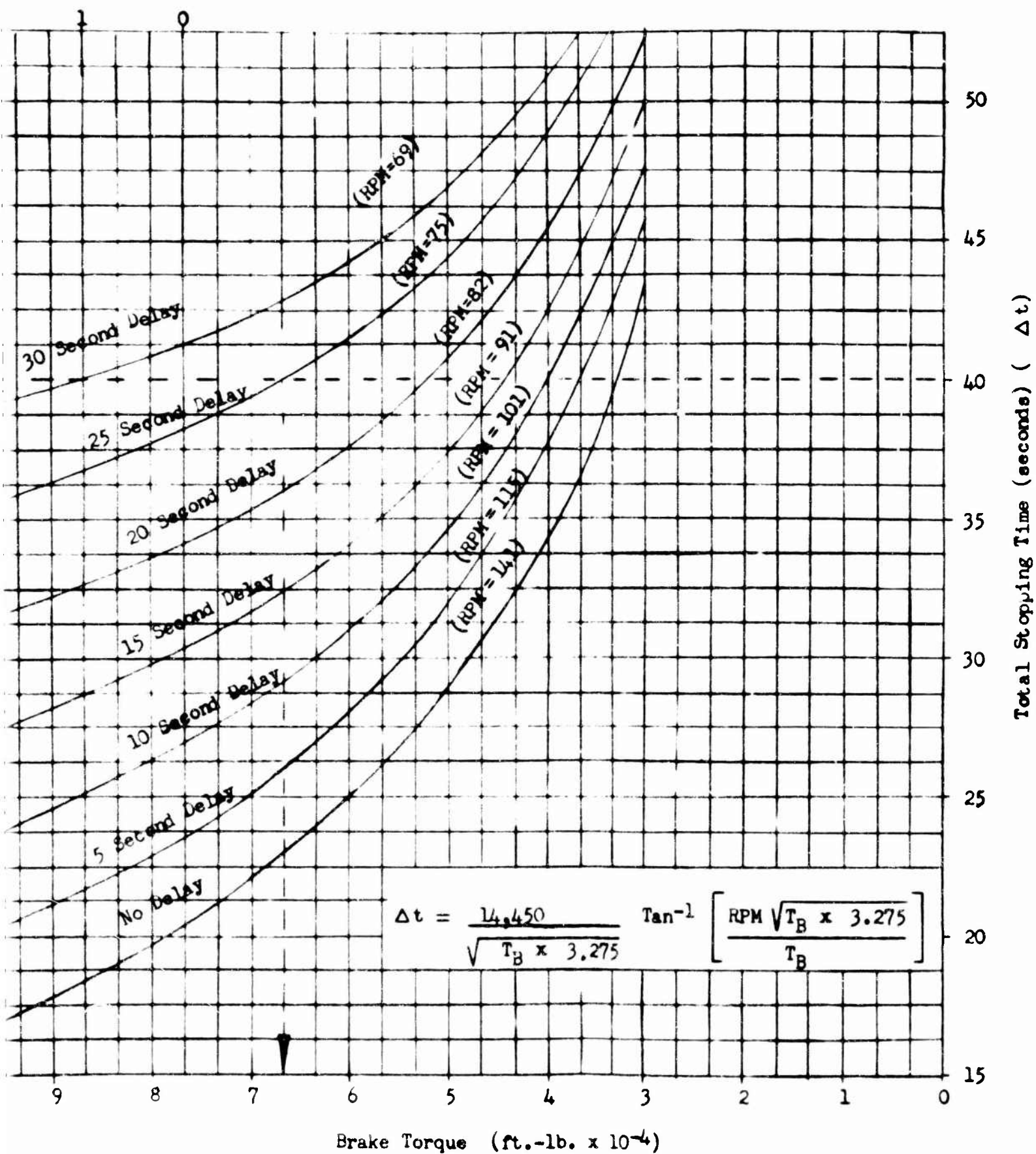


Figure 34. Rotor Brake Requirements. (Brake Torque and Kinetic Energy)



ake Torque and Kinetic Energy Versus Stopping Time).

B

OIL COOLER AND BLOWER SUMMARY

The main gearbox and associated tail, intermediate, and engine reduction gearboxes will pump hot oil to oil/air heat exchangers similarly constructed of aluminum plate and fin design. Oil temperature and pressure relief controls are integrated into the outlet port. A vane axial blower is used to provide the source of cooling air. Cooler capacities are summarized in Table 17 below.

TABLE 17
OIL COOLER CAPACITIES AND WEIGHTS

Item	Engine Reduction Gearbox	Main Gearbox	Intermediate Gearbox	Tail Gearbox
Cooler Heat Rejection Rate, BTU/HR.	86,500	1,015,000	32,450	51,600
Cooler Weight, lb.	8.1	76.5	4.7	4.7
Blower Weight, lb.	11.9	43.5	25.3	36.3
Total Weight, lb.	20.0	120.0	30.0	41.0

TABLE 18
COMPONENT WEIGHT SUMMARY,
BASIC TRANSMISSION SYSTEM*

						Total Weights **
Component	Reduction Ratio	Output Speed (RPM)	Quantity Per Aircraft	Estimated (lb.)	Total ** Calculated (lb.)	
Primary Drive						
Engine Reduction Gearbox	2.353	5,780	2	366	396	
Main Gearbox	41.0	140.6	1	7,400	6,990 ***	
Input Drive Shaft	—	—	2	208	118	
Accessory Gearbox	—	—	1	100	80	
Accessory Drive Shaft	—	—	1	7	4	
Hypercritical Tail Rotor Drive System						
Intermediate Gearbox	1.575	3,760	1	207	137	
Tail Gearbox	6.18	607	1	325	333 ***	
Tail Drive Shafting	—	—	1	210	197	

TABLE 18 (continued)

Total Weights **				
Component	Reduction Ratio	Output Speed (RPM)	Quantity Per Aircraft	Total ** Estimated (lb.) Calculated (lb.)
Lubrication System: (Incl. Coolers, Blowers & Oil)				
Eng. Red. Gearbox	—	—	2	45
Oil 3 Gal.	—	—	2	40
Cooler & Blower	—	—	—	—
Main Gearbox	—	—	—	—
Oil 30 Gal.	—	—	1	225
Cooler & Blower	—	—	—	120
Intermediate Gearbox	—	—	—	—
Oil 2 Gal.	—	—	1	15
Cooler & Blower	—	—	—	30
Tail Gearbox	—	—	—	—
Oil 3 Gal.	—	—	1	23
Cooler & Blower	—	—	—	41
Rotor Brake	—	—	1	58
Total				8,852

* Service Time = 3,600 hours minimum at R = .999

** Gearbox Weights are Dry Weights

*** The use of 6-4 Titanium alloy planetary plates, spacers, main rotor shaft, and tail rotor shaft would result in an additional weight saving as follows:

Main Gearbox 480.0 lb.

Tail Gearbox 24.6 lb.

* Service Time = 3,600 hours minimum at R = .999

** Gearbox Weights are Dry Weights

*** The use of 6-4 Titanium alloy planetary plates, spacers, main rotor shaft, and tail rotor shaft would result in an additional weight saving as follows:

Main Gearbox 480.0 lb.

Tail Gearbox 24.6 lb.

ALTERNATE TRANSMISSION SYSTEM DESIGNS,
MAIN ROTOR DRIVE TRAIN

The maximum main rotor power requirement of 14,200 horsepower (Table 2 page 10) for the single rotor heavy-lift helicopter of Reference 3 warranted examination of alternate transmission system concepts to reduce gearbox component weight and improve overall transmission system efficiency, if at all possible. The calculated efficiency of the basic (or conventional) engine to main rotor drive train against which the proposed alternate designs were evaluated was calculated at nearly 96.6 percent, as summarized in Table 19, page 159.

Among the concepts that have been compared with the "basic" main gearbox design of pages 23 to 71 were systems incorporating the harmonic drive, the roller gear drive, and redundant power paths in the main power train. The design analysis of these alternate gearing concepts has been presented in the following pages.

HARMONIC DRIVE

The harmonic drive concept was considered for application in the primary or main rotor drive in the heavy-lift helicopter transmission, as shown in the schematic of Figure 35 on the following page. Reference 9 was used as the basis of this harmonic drive design.

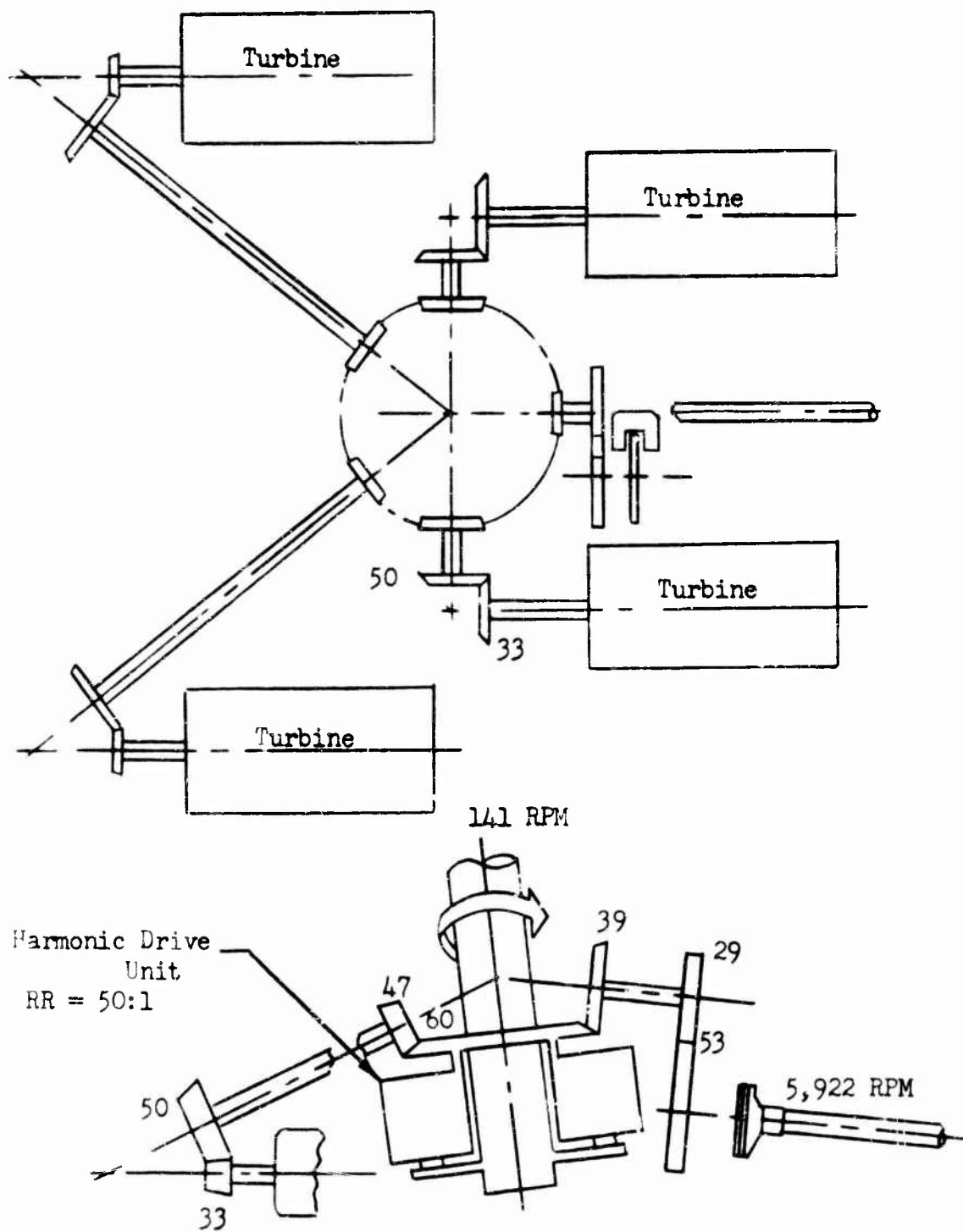


Figure 35 . Transmission System Schematic With Harmonic Drive.

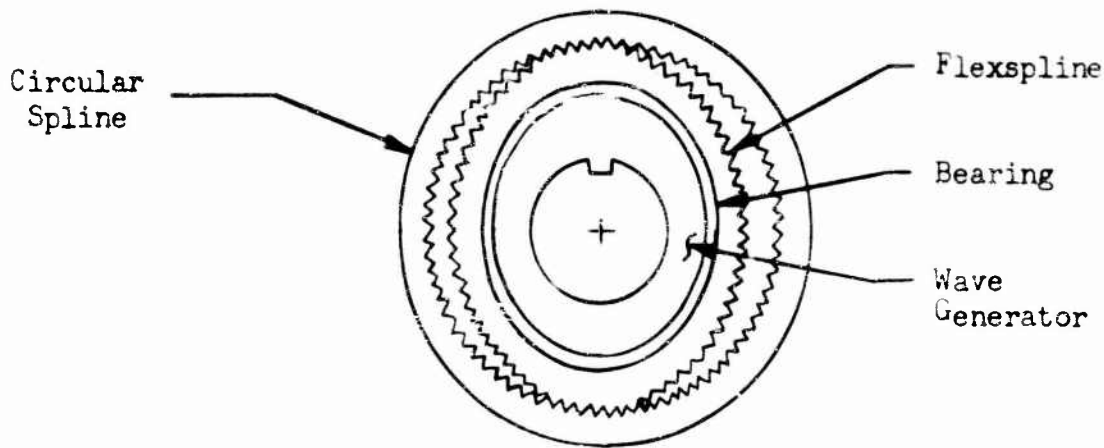


Figure 36. Harmonic Drive Elements.

Harmonic Drive Design Analysis

$$\begin{aligned}
 T_{\text{output}} &= \frac{\text{HP} \times 63,025}{\text{RPM}} \\
 &= \frac{14,200 \times 63,025}{140.62} \\
 &= 6.36 \times 10^6 \text{ in.-lb.}
 \end{aligned}$$

Based on the recommendation of Reference 9, page 35, a diametral pitch of 64 was used for the design comparison.

$$P_d = 64$$

Extrapolating Figure 3, page 11, of Reference 9, as shown in Figure 37, page 155, a circular spline pitch diameter for a 14,200 horsepower unit was obtained.

$$D_c = 53$$

$$\text{Reduction ratio} = \text{RR} = 50:1$$

$$\text{Number of teeth in flexspline} = N_f = 53 \times 64 = 3,392$$

$$\text{Tooth difference} = N_d = \frac{N_f}{\text{RR}} = \frac{3,392}{50} = 67.85$$

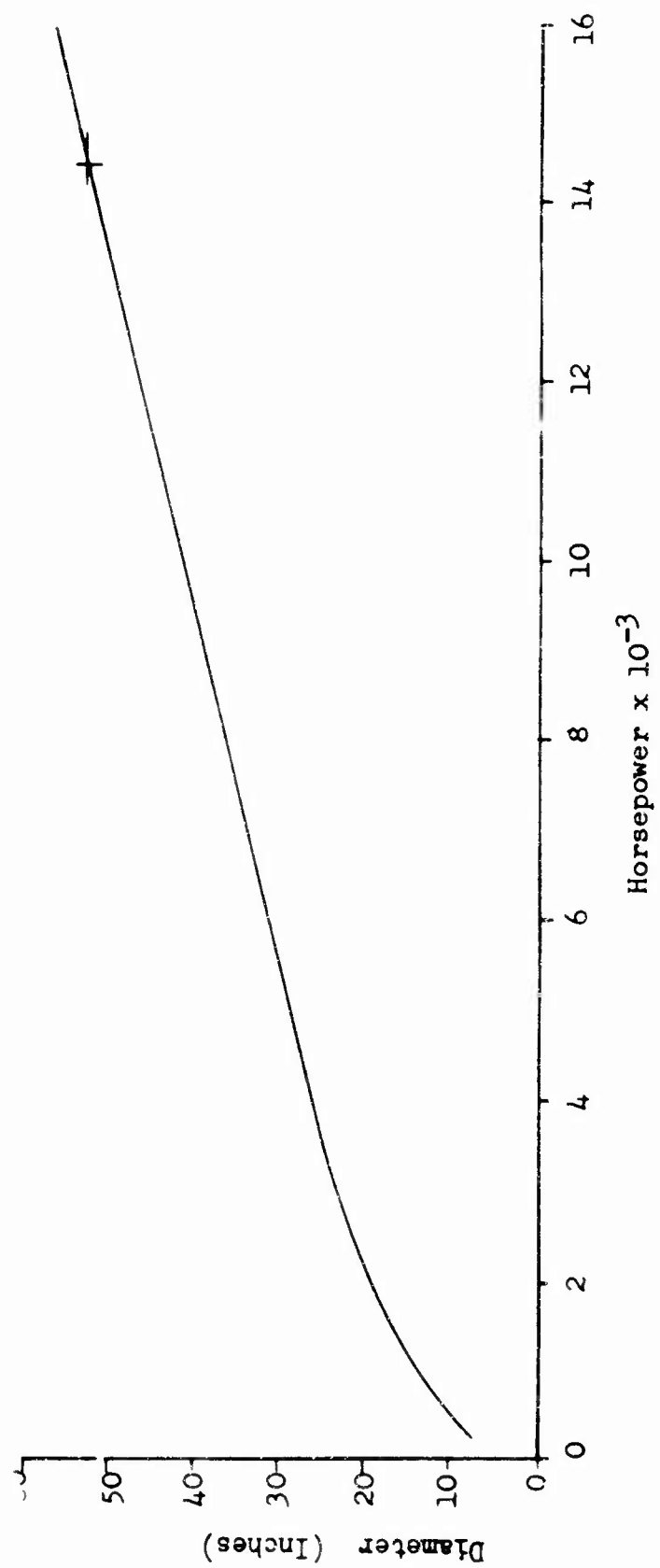


Figure 37. Horsepower Versus Diameter, Harmonic Drive.

$$\begin{aligned}
\text{Number of teeth in circular spline} &= N_o = 3,392 - 68 = 3,324 \\
\text{Flexspline pitch diameter} &= D_f = \frac{N_o}{P_d} = \frac{3,324}{64} = 51.94 \text{ in.} \\
\text{Face Width (F.W.)} &= 25 \text{ in.} \\
\text{Dedendum} &= \frac{1.2}{P_d} + .002 = .0208 \text{ in.} \\
\text{Root Dia. (D}_R\text{)} &= 51.94 - 2(.0208) = 51.898 \text{ in.} \\
\text{Bed thickness (t}_b\text{)} &= .166 \text{ in.} \\
\text{Inside Dia. (I.D.)} &= 51.898 - 2(.166) = 51.566 \text{ in} \\
\text{Mean Bed Dia. (D}_b\text{)} &= 51.566 + .166 = 51.732 \text{ in.}
\end{aligned}$$

Flexspline Deflection

$$D_c - D_f = 53 - 51.94 = 1.06 \text{ in.}$$

Flexspline Deflection Stress

$$\begin{aligned}
f_f &= \frac{3E (D_c - D_f) t_b}{D_b^2} \\
&= \frac{3(30 \times 10^6)(1.06)(.166)}{(51.73)^2}
\end{aligned}$$

$$f_f = 5,950 \text{ psi}$$

Flexspline Load Stress

$$\begin{aligned}f_t &= \frac{T}{D_b A_r} \\&= \frac{T}{D_b \times F.W. \times t_b} \\&= \frac{6.36 \times 10^6}{(51.73)(25)(.166)} \\f_t &= 29,600 \text{ psi}\end{aligned}$$

Flexspline Tooth Shear Stress

$$\begin{aligned}f_s &= \frac{T}{(.1)D_f^2 (F.W.)} \\&= \frac{6.36 \times 10^6}{(.1)(51.94)^2(25)} \\f_s &= 940 \text{ psi}\end{aligned}$$

Flexspline Bell Face Shear Stress

$$\begin{aligned}f_s &= \frac{2T}{D_b A} \\A &= D_b t_b = (51.73)(.166) = 27 \text{ in.}^2 \\f_s &= \frac{(2)(6.36 \times 10^6)}{(51.73)(27)} \\&= 9,100 \text{ psi}\end{aligned}$$

Flexspline Torsion Stress

$$f_s = \frac{16 T D_R}{(D_R^4 - I.D.^4)}$$
$$= \frac{(16)(6.36 \times 10^6)(51.9)}{(51.9^4 - 51.57^4)}$$

$$f_s = 11,900 \text{ psi}$$

Since the stress calculated in this unit approximate those presented in Reference 9, a weight and efficiency analysis of the 14,200 horsepower harmonic drive unit was made as follows:

Weight and Efficiency

An estimated weight of 3,200 pounds was obtained for the heavy-lift helicopter harmonic drive unit by extrapolating the weight versus horsepower curve of Reference 9, Figure 5, page 13, to 14,200 horsepower.

In extending this curve, a linear relationship between weight and power was optimistically assumed beyond the 6,000-horsepower unit. This weight did not reflect the weight penalty incurred by decreasing the reduction ratio from 85:1 (unit of Reference 9) to 50:1. As the reduction ratio is decreased, the difference in size between the circular spline and the flexspline increased, causing the harmonic drive assembly to acquire greater mass. The weight and horsepower extended curve is presented as Figure 38, page 160.

The efficiency of a harmonic drive unit transmitting 14,200 horsepower was calculated using the following equation presented on page 80 of Reference 9.

$$\begin{aligned} \text{Harmonic Drive HP Loss} &= (2.3 \times 10^{-7})(\text{output torque})^{5/6}(\text{input RPM}) \\ &= (2.3 \times 10^{-7})(6.36 \times 10^6)^{5/6}(7,031) \\ &= 770 \text{ HP} \end{aligned}$$

$$\begin{aligned} \text{Harmonic Drive Efficiency} &= \frac{(14,200 - 770)(100)}{14,200} \\ &= 94.58\% \end{aligned}$$

TABLE 19
COMPARISON OF DRIVE TRAIN
EFFICIENCIES

Source of Losses	Loss equation (Quan)(%/100)(HP)	Losses with Two- stage Planetary (HP)	Losses with Harmonic Drive (HP)
Engine Red. Box (2 places)	(2)(.010)(4,000)	80	80
Input Bevel Mesh (2 Places)	(2)(.005)(4,000)	40	40
Main Bevel Mesh (4 places)	(4)(.005)(4,000)	80	80
Accessory Bevel Mesh	(1)(.005)(300)	1.5	1.5
First-stage Planetary	(1)(.0075)(14,200)	106.5	-
Second-stage Planetary	(1)(.0075)(14,200)	106.5	-
Harmonic Drive	(1)(.0542)(14,200)	-	770
Tail Take off Bevel	(1)(.005)(1,500)	7.5	7.5
Tail Take off Spur	(1)(.005)(1,500)	7.5	7.5
Windage and Churning	(.0075)(16,000)	120.0	-
Windage and Churning	(.0075)(2)(16,000) 37	-	29
Total Losses		<u>549.5</u>	<u>1,015.5</u>
Overall Engine to Main Rotor Drive Train Efficiency		96.57%	93.65%

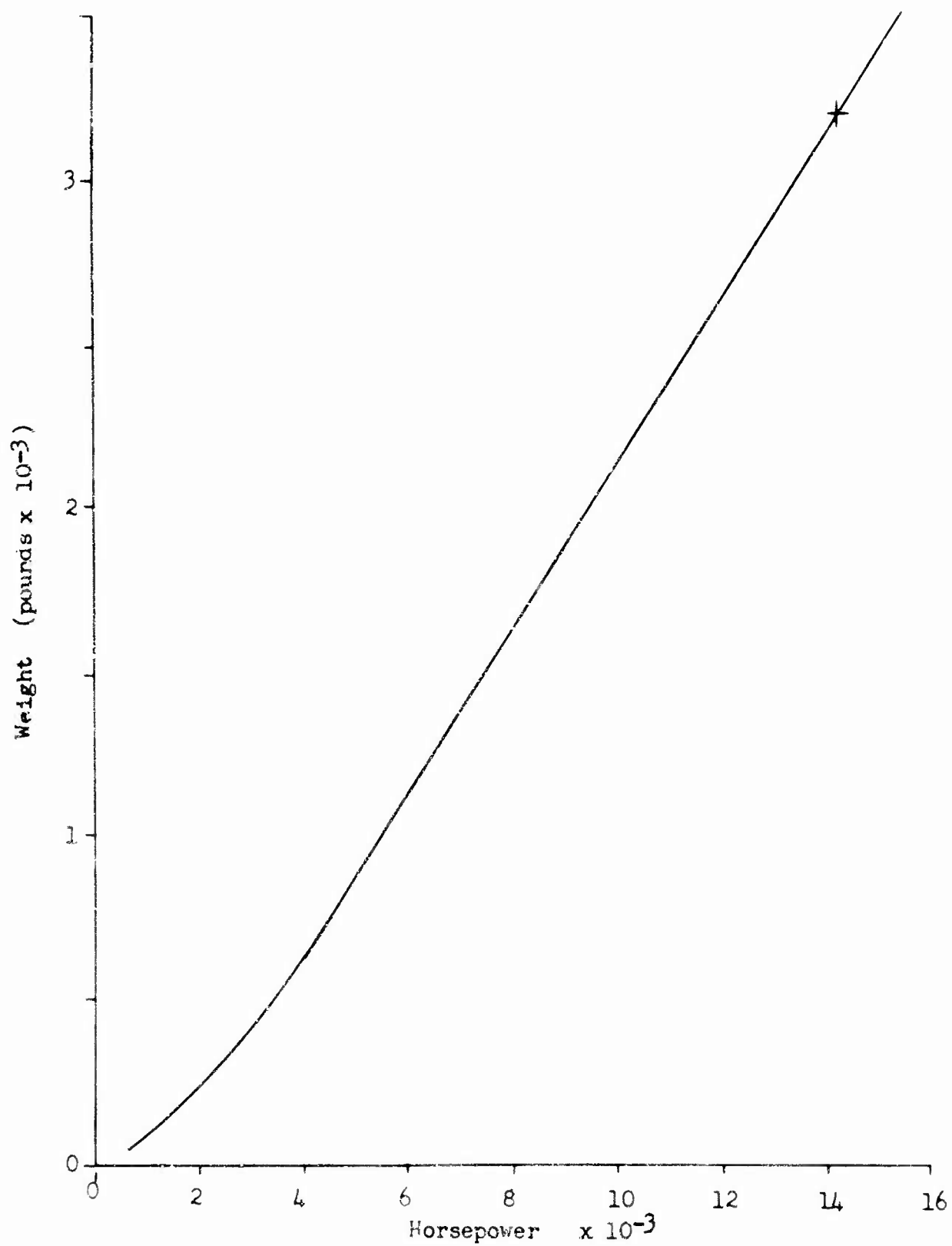


Figure 38. Horsepower Versus Weight, Harmonic Drive.

This efficiency was used in Table 19, page 159, to determine the power loss in a system incorporating the harmonic drive. Table 19 indicates the losses in a drive train using a two-stage planetary system versus one using a harmonic drive unit. The respective efficiencies were calculated using the following equation.

$$\% \text{ Efficiency} = \frac{(\text{input HP} - \text{HP loss})(100)}{(\text{input HP})}$$

Primary Drive Train with a Two-stage Planetary

$$= \frac{(16,000 - 549.5)(100)}{16,000} = 96.57\%$$

Primary Drive Train with a Harmonic Drive

$$= \frac{(16,000 - 1,015.5)(100)}{16,000} = 93.65\%$$

A relative weight comparison between the two systems was made using the ratio of gross weight to installed horsepower as the comparative parameter.

$$\frac{\text{LB.}}{\text{HP}} = \frac{\text{G.W.}}{\text{Installed HP}}$$

$$= \frac{86,000}{16,000}$$

$$\frac{\text{LB.}}{\text{HP}} = 5.4$$

The difference in horsepower loss from Table 19, page 159 is:

$$\text{HP loss} = 1,015.5 - 549.5 = 466$$

Optimistically assuming (despite contrary evidence) that the difference in weight (plus 290 pounds) between the harmonic drive unit and the two stage planetary can be made up in the bevel gear reduction stages in the gearbox, the net weight penalty incurred in the heavy-lift transmission using the harmonic drive unit was a function of its lower efficiency or

$$\begin{aligned}\text{weight penalty} &= (\text{losses}) \left(\frac{\text{lb.}}{\text{HP}} \right) \\ &= (466 \text{ HP}) (5.4) \\ &= 2,515 \text{ lb.}\end{aligned}$$

ROLLER GEAR DRIVE

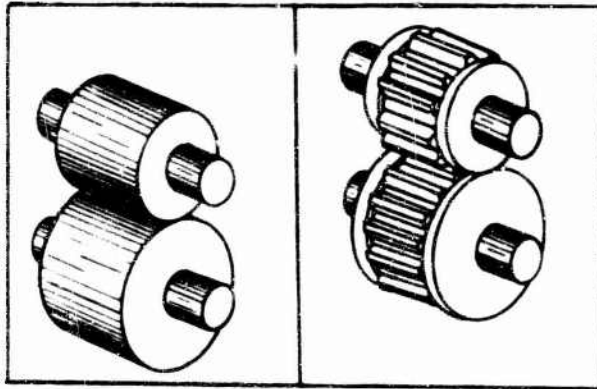
Several different arrangements of the roller gear drive have been considered for incorporation in the primary gear train (engine to main rotor drive) of this heavy-lift-helicopter transmission system.

Although the roller gear drive concept is relatively new and untried in actual aircraft application as of the date of this report, tests conducted on two 46 to 1 bench test units at 200 HP at 28,000 input RPM for 1,000 hours show excellent results. An additional 180 hours were accumulated on the same hardware at 300 HP. Data obtained during these tests indicated that the efficiency and weight-to-power ratio of the roller gear drive warrant its consideration in this study.

Although the size of unit required for the 12- to 20-ton helicopter is beyond the current roller gear drive "state of the art," it is anticipated that, by the initiation of fabrication of the heavy-lift transmission, units of suitable size can be proved feasible.

Discussion

As shown in Figure 39, the roller gear drive evolved from a pure



friction roller drive. The center portion of the rolling surfaces have been replaced with gear teeth, leaving the outside diameters aligned with the pitch diameters of the gears. The torque, therefore, is carried primarily through the gears and the radial position of the gears is determined by the rollers and the relation of gear separating load to roller preload.

Figure 39. Roller and Roller Gear Elements.

An evaluation of the roller gear drive has been accomplished using the front drive engine propulsion system of Appendix I, Figure 51. Of the three systems considered, two 12.2-to-1 ratios and a 30-to-1 ratio, the latter was selected because of compatibility with the balance of power train. Schematics of this system are shown in Figures 40 and 41.

As in the basic front drive engine transmission system, reduction gearboxes are mounted directly to the forward engines. These units incorporate a 37/67 spiral bevel gear set. All four main gearbox input shafts turn at 7,510 RPM and combine through separate spiral bevel pinions to a common driven bevel gear at 4,219 RPM.

Design Analysis

The 30-to-1 roller gear drive transmission consists of a sun roller, three rows of planets, and a stationary ring gear. As the planets are rotating with output speed, the reduction ratio is 29, which becomes 30 as a result of rotating spider. In each row there are ten stepped roller gear planets. The gear roller planets elements are press fitted and electron-beam welded. This novel assembly method rendered considerable weight savings. The sizes of the gears and other gear design and stress data are given in Table 20. Due to high pitch line velocity of input sun roller dictated by the given RPM and minimum sun gear size necessary to accommodate rotor shaft, helical gears were selected through the drive, except output ring gears. The bending stress calculations are for spur gears, assuming that identical stresses could be obtained

for helical gears with some adjustment of tooth form and the number of teeth. Double helical gear teeth are suitable for roller gear drive due to split gear design, and they eliminate the necessity to provide other axial support for all rotating gear elements. The helical gears will not cause any drive assembly problem, as the drive is assembled from inside. The toggle angles for gear rows were selected of a size permitting this type of assembly. The sun gear is axially assembled last, employing a special assembly tool - a cam device which preloads and expands all planets radially to overcome gear addendum and supporting roller dimension interference.

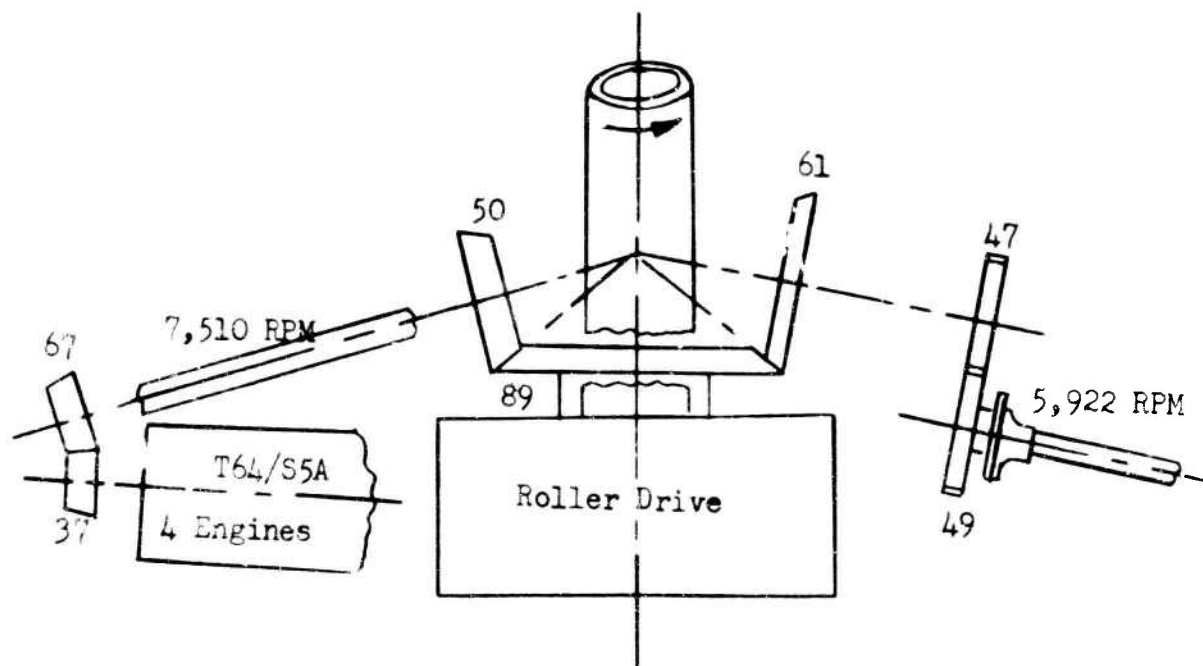
The reaction bending moment is absorbed by two spider rings of special structure. The main support stud between two rings is a stationary pin carrying the bearings. To minimize the twist in the rotating cage, 20 support bolts are employed - 10 in a gap between the last row of gears and 10 through the second row of planet centers. The bending stress in the support studs at full load is less than 25,000 psi. The total deflection is minimized by the fact that the roller gear cluster, preloaded by ring gear separation forces, has inherent rigidity. The roller gear cluster assemblies tend to stay parallel. The torsional deflection of the two support rings (the cage) and its effect to the roller gear assembly can be minimized purposely by assembling the unloaded cage in a distorted position so that at maximum load the assembly will stay parallel.

The support rollers are 5/16 inch long on each side (total, 5/8 inch). The size was selected to keep surface stresses on rollers below 300,000 psi. Experience obtained with roller gear drive testing has proved that good load sharing properties on teeth contacts is obtained by locating the roller gear planets carrying studs within .001 inch to .002 inch. The cage support rings act as a drive assembly fixture. To save weight, heavy-duty needle bearings were used. The bearings with increased length to 3 inches will be good for a B-10 life of 8,100 hours (vacuum-melted material is used).

In the existing design, spur gears can be used instead of helical gears, but due to high Hertz stress level, the Y_1-X_1 and Y_2-X_2 gear sizes should be increased totally about 2 inches. With this axial increase, the total drive weight will be increased 250 pounds. In this case, shoulders on the rolling cylinder should be provided for axial stability.

TABLE 20
ROLLER GEAR DESIGN SUMMARY

Gear	Pitch Dia. (in.)	No. Teeth	P.A. Normal (deg.)	Helix Angle (deg.)	Dia. Pitch	Face Width (in.)	Bending Stress (psi)	Compressive Stress (psi)
I	16.555	149	25°	22.5°	9	1.912	20,100	71,600
II	6.777	61	25°	22.5°	9	1.912	19,100	
III	2.694	18	25°	22.5°	6.682	1.700	23,700	131,900
IV	8.082	54	25°	22.5°	6.682	1.700	20,500	
V	3.771	19	25°	22.5°	5.039	2.375	26,600	136,600
VI	12.106	61	25°	22.5°	5.039	2.375	20,900	
VII	6.548	23	25°	0°	3.512	5.50	27,500	134,700
VIII	48.113	169	25°	0°	3.512	5.50	15,800	



Component	Reduction	Input RPM	Output RPM
Engine Reduction Gearbox	37/67	13,600	7,510
Main Gearbox			
Input Bevel Set (4 Inputs)	50/89	7,510	4,219
Roller Gear Drive	30.08:1	4,219	140
Tail Take off Bevel Mesh	61/89	4,219	6,150
Tail Take off Spur Mesh	47/49	6,150	5,922

Figure 40. Roller Gear Drive Transmission System.

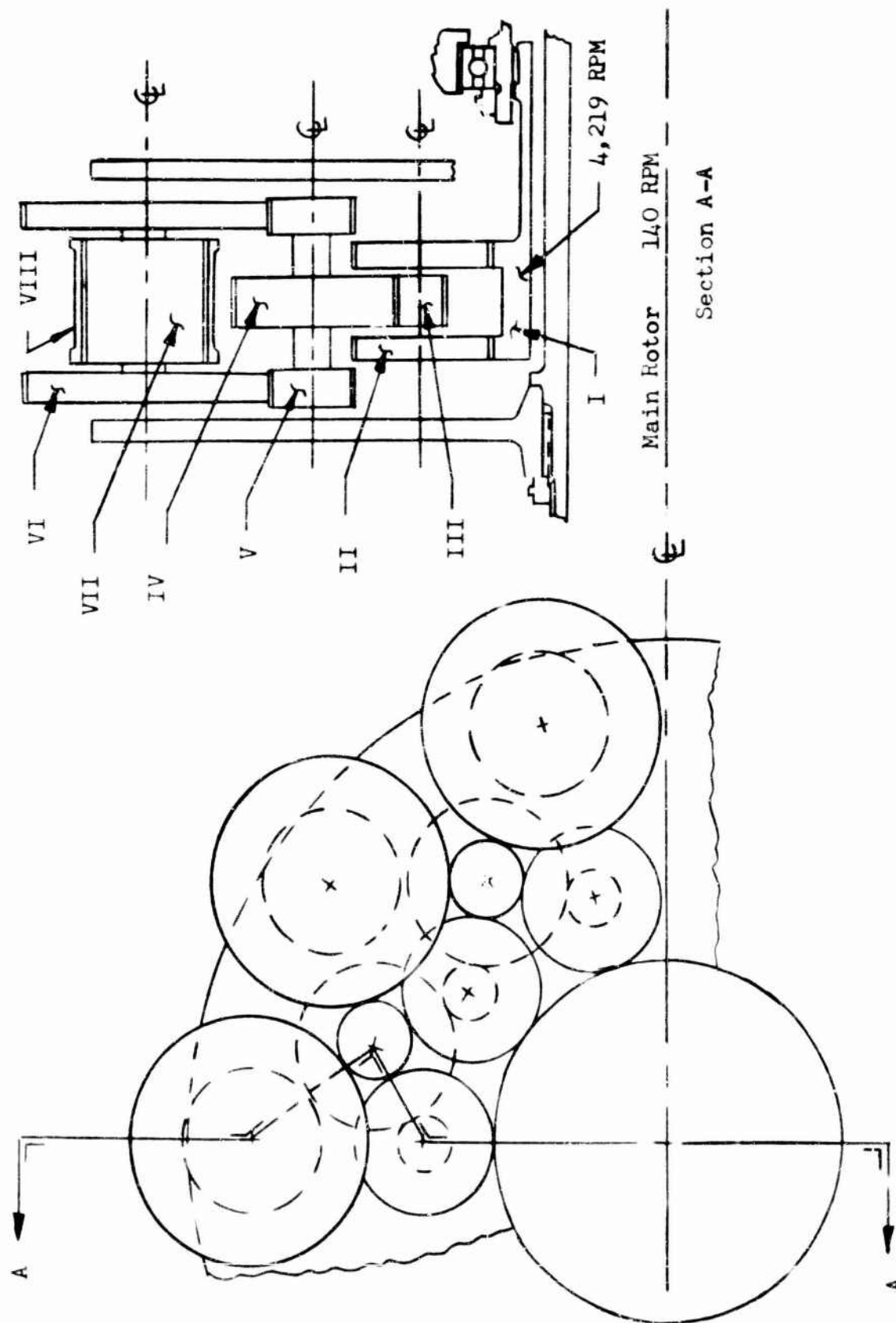


Figure 41. 30:1 Roller Gear Drive Schematic

Weight Analysis

The calculated weight of the 30:1 roller gear drive unit, shown schematically in Figure 41, is as follows:

Items	Description	Weight (lb.)
I	Sun Gear and Splines	93
II & III	First-Row Planets	162
IV & V	Second-Row Planets	291
VI & VII	Third-Row Planets	1,112
VIII	Ring Gear	307
	Rotating Spider (Cage)	597
	TOTAL	<u>2,560</u>

The estimated weight of a main gearbox incorporating the roller drive with gearing ratios as shown in Figure 40 is:

	Weight (lb.)
Input Bevel Stages	1,030
Outer Shaft Assembly	300
Roller Gear Drive	2,560
Main Rotor Shaft	1,270
Main Rotor Shaft Bearings & Support	668
Tail Take off Assembly	150
Main Housing	495
Oil Sump and Pump	60
	<u>TOTAL 6,533</u>

Weight savings over basic main gearbox:

$$\begin{aligned}W_T &= 6,990 - 6,533 \\&= 457 \text{ pounds.}\end{aligned}$$

Efficiency Analysis

The efficiency of the roller gear drive was based on empirical data obtained during tests on the NA-1 46:1 unit:

Rt. Angle Bevel Input Mesh	(.005)(4,000)(2)	=	40.0
Input Bevel Mesh	(.005)(4,000)(4)	=	80.0
Accessory Bevel Mesh	(.005)(300)(1)	=	1.5
Roller Gear Drive	(.010)(14,200)(1)	=	142.0
Tail Take off Bevel Mesh	(.005)(1,500)(1)	=	7.5
Tail Take off Spur Mesh	(.005)(1,500)(1)	=	7.5
Churning Losses	(.0075)(16,000)	=	120.0
		F_{HP}	<u>398.5</u>

REDUNDANT DRIVE MAIN GEARBOX

A redundant power path concept has been investigated to determine a configuration compatible with the HLH design and competitive with the other transmission arrangements studied in this report. The concept evolving from the evaluation is shown in Figure 42. This design consists of two similar gear trains located one above the other, each transmitting power to the main rotor shaft from two engines located outboard of the gearbox.

The gear ratios for this drive are summarized in Table 21 .

TABLE 21
REDUCTION RATIOS,
REDUNDANT DRIVE MAIN TRANSMISSION

Assembly/Item	Reduction	Input RPM	Output RPM
Input Assy. (Angle Box) (Engine Reduction Box)	3.136	13,600	4,336.7
2nd-Stage Bevel Set	3.136	4,336.7	1,383
3rd-Stage Spur	2.474	1,383	558.9
4th-Stage Planetary	3.96	558.9	141.1
Tail Take off			
Bevel Mesh	1.92	1,383	4,035
Spur Mesh	1.47	4,035	5,922

Efficiency Analysis

In the other front drive engine power train concepts evaluated, the initial bevel reduction stage of two engines has been incorporated within the main gearbox as right angle bevel drives. Therefore, to be compatible with other efficiency analyses, the effect of two engine reduction boxes must be included in the overall efficiency analysis.

Redundant Main Gear Box

1st-Stage Bevel Mesh	=	(.005)(4,000)(4)	=	80.0
2nd-Stage Bevel Mesh	=	(.005)(4,000)(4)	=	80.0
Spur Mesh	=	(.005)(4,000)(4)	=	80.0
Planetary	=	(.0075)(7,100)(2)	=	106.5
Tail Take off Bevel Mesh	=	(.005)(1,500)(1)	=	7.5
Spur Mesh	=	(.005)(300)(1)	=	1.5
Accessory Drive	=	(.005)(300)(1)	=	1.5
Churning Losses	=	(.010)(16,000)	=	160.0
TOTAL				<u>517.0</u>

$$\text{Overall Efficiency} = \frac{(16,000 - 517.0)}{16,000} (100\%)$$

$$= 96.8\%$$

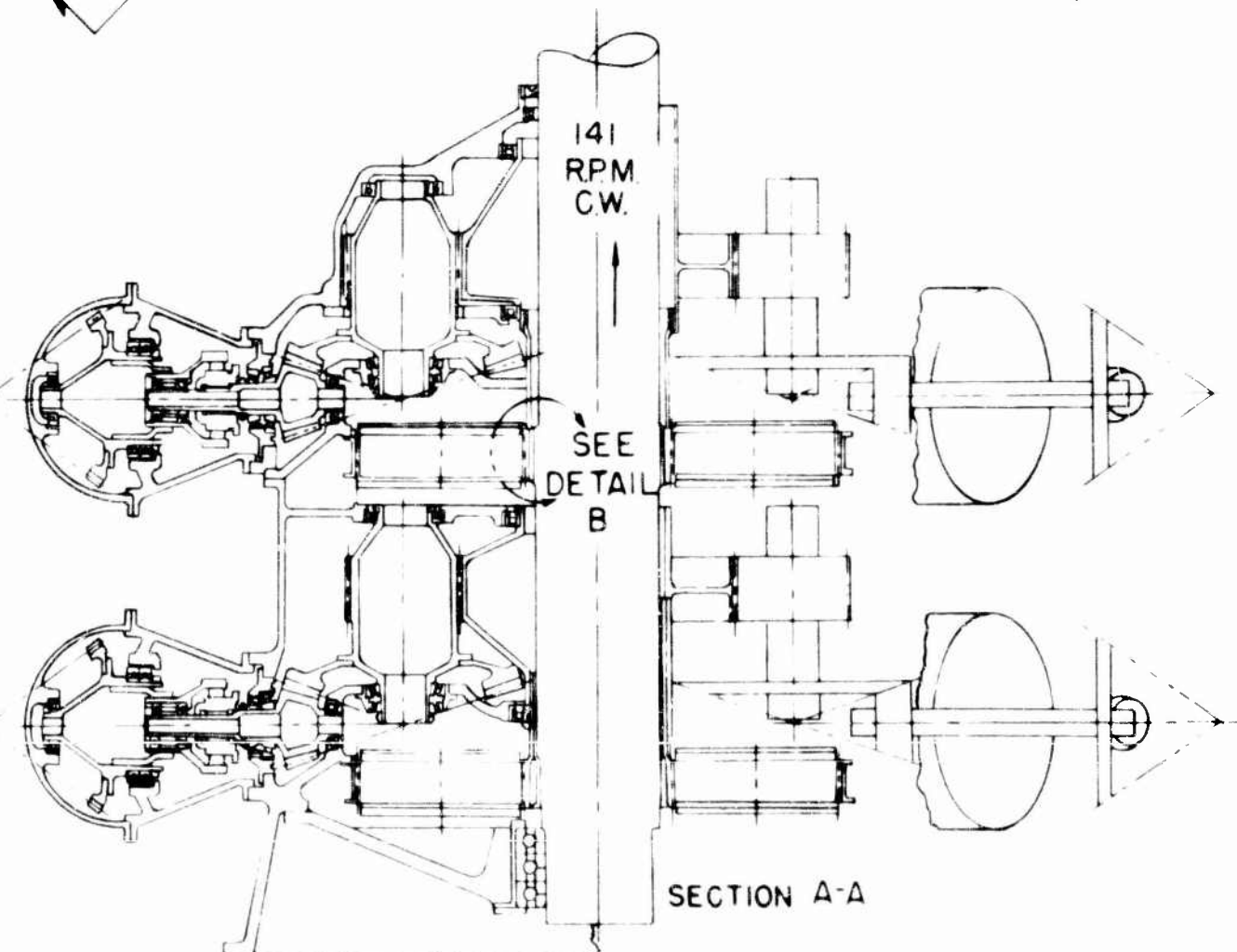
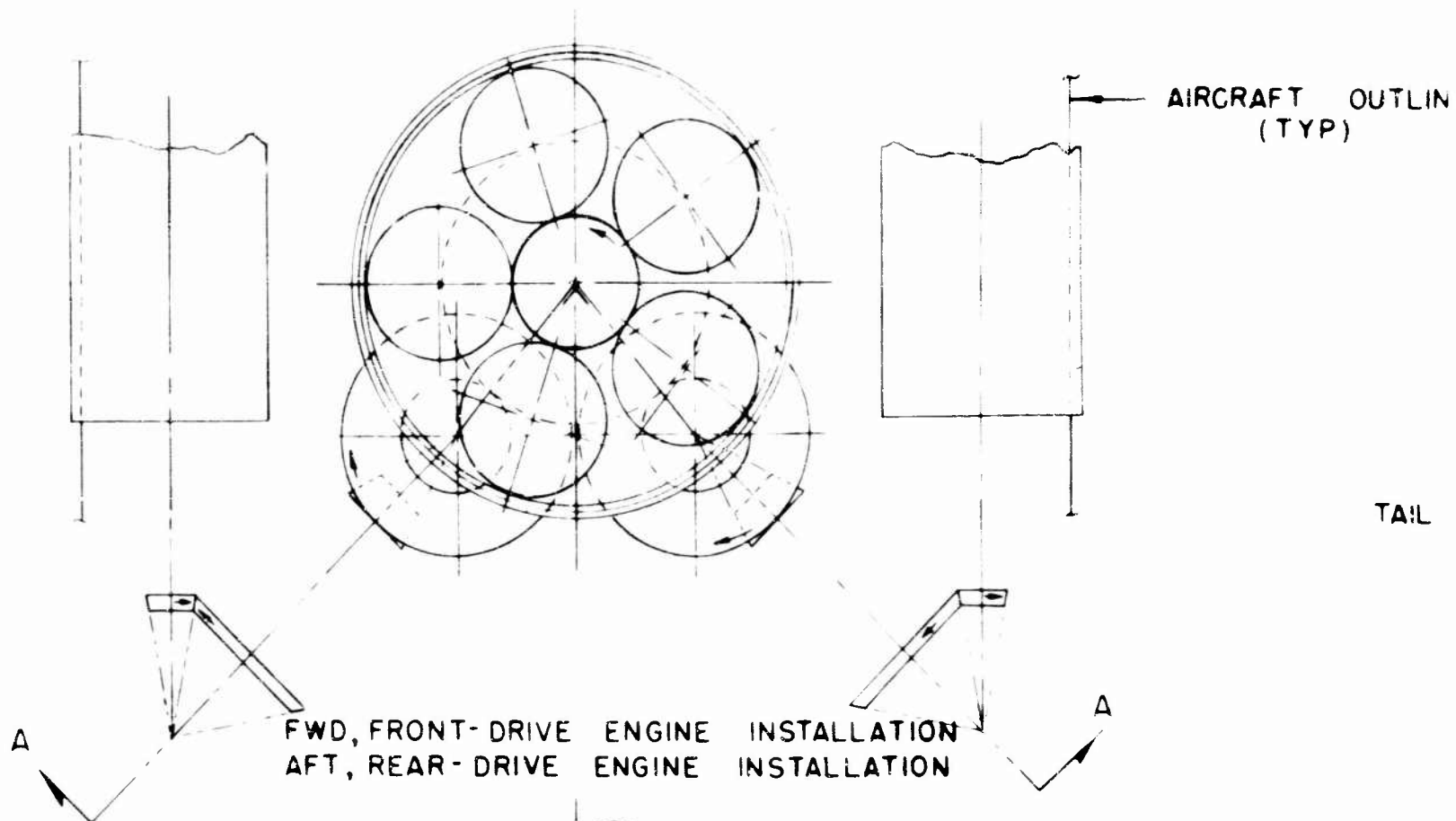
Comparing the redundant gearbox to the basic gearbox as before,

$$\begin{aligned} \text{Effective Wt. Penalty} &= (5.4)(517.0 - 469.5) \\ &= 257 \text{ lb.} \end{aligned}$$

TABLE 22
WEIGHT SUMMARY.
REDUNDANT DRIVE MAIN TRANSMISSION

Assembly/Item	No. Req'd.	Wt. Each (lb.)	Wt. Total (lb.)
Input Assy. (Angle Box)	4	270	1,080
2nd-Stage Bevel Gear	4	99	396
3rd-Stage Spur Pinion & Shaft	4	182.5	730
3rd-Stage Bull Spur & Shaft	2	247	494
4th-Stage Planetary	2	1,520	3,040
All Gearbox Bearings (Except Input & Tail Take off)	1	550	550
Main Rotor Shaft	1	1,430	1,430
Tail Take off	1	146	146
Oil Sump, Pump, etc.	1	65	65
Housings	1	625	625
		TOTAL	8,556

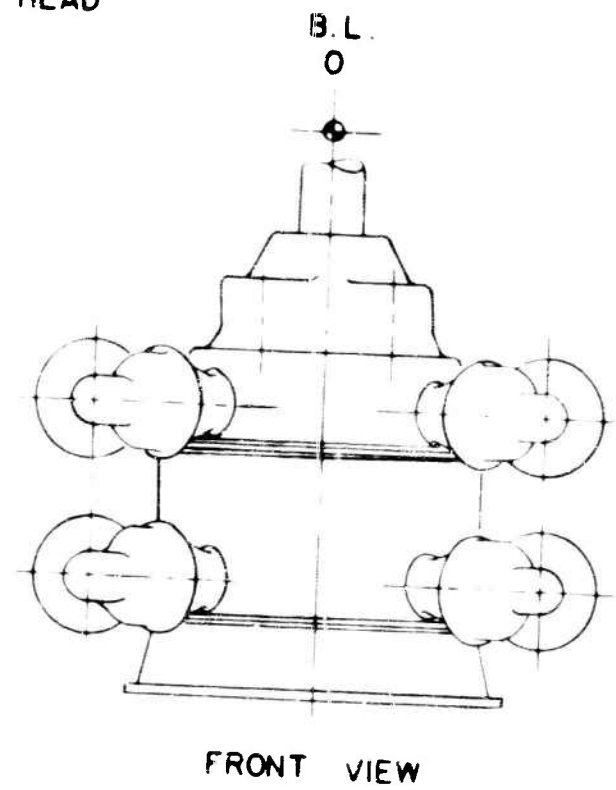
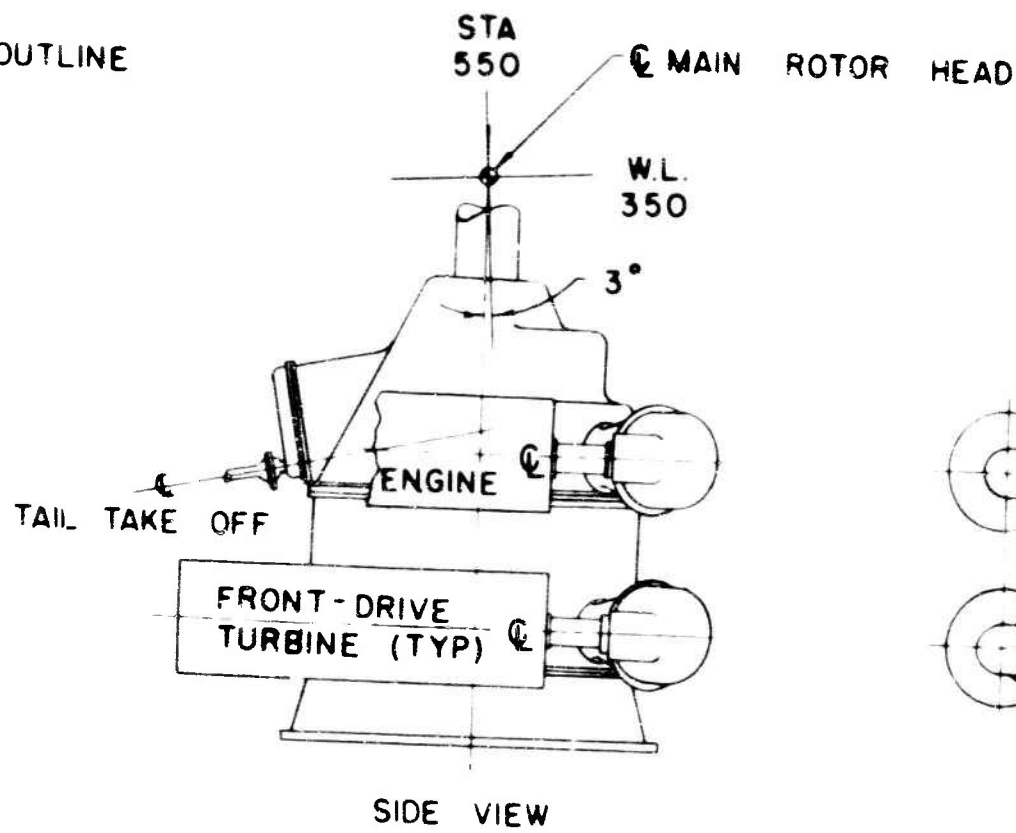
Table 23, page 178, compares the alternate transmission drive concepts to the basic main transmission system.



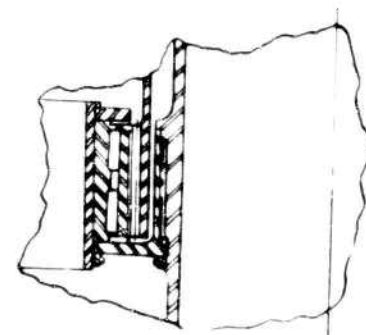
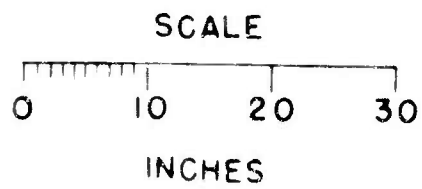
SCALE
0 10
INCH

FIGURE 42

CRAFT OUTLINE
(TYP)



HALF SIZE



DETAIL B

FIGURE 42 REDUNDANT DRIVE MAIN GEARBOX.
HLH-10-22

B

INFINITE INDEXING SPRING CLUTCH

An alternate design to the roller-type overrunning clutch is the infinite indexing spring type unit, as shown in Figure 43, page 176. This unit weighs 14 pounds compared to 34 pounds for the roller-type clutch. A brief description of the spring clutch follows.

The input member is splined to the high-speed quill shaft and the output member is splined to the bevel gear shaft. A double lead spring is mounted between the input and output members so that the first three spring turns are in light interference fit with the outside diameter of the output member, and the remaining twelve turns are in interference fit with the bore of the input member. The heavy ends of the dual lead spring butt against two lugs machined on the input and disposed 180 degrees apart.

As torque is applied at the output member, the friction drag on the first three spring turns (5 inch pounds) causes the spring to expand until all turns are engaged with the output. Torque is transmitted from the input member lugs, through the spring, to the output member.

In the overrunning mode the output member velocity exceeds that of the input. The helix of the spring is such that the relative rotation causes the spring to contract until only the first three turns drag on the output bore. The drag torque level is 5 inch pounds.

A weight analysis showing the possible weight savings per assembly and per aircraft using the spring clutch concept is summarized below.

Component	Weight - lb.	
	Roller Clutch	Spring Clutch
Quill Shaft	5.5	8.5
Bevel Pinion Shaft	34.1	30.8
Servo Quill Shaft	1.4	1.6
Clutch	<u>34.0</u>	<u>14.0</u>
Total Weight	75.0	54.9
Δ Weight per input		20.1
Weight saving per aircraft		80.4

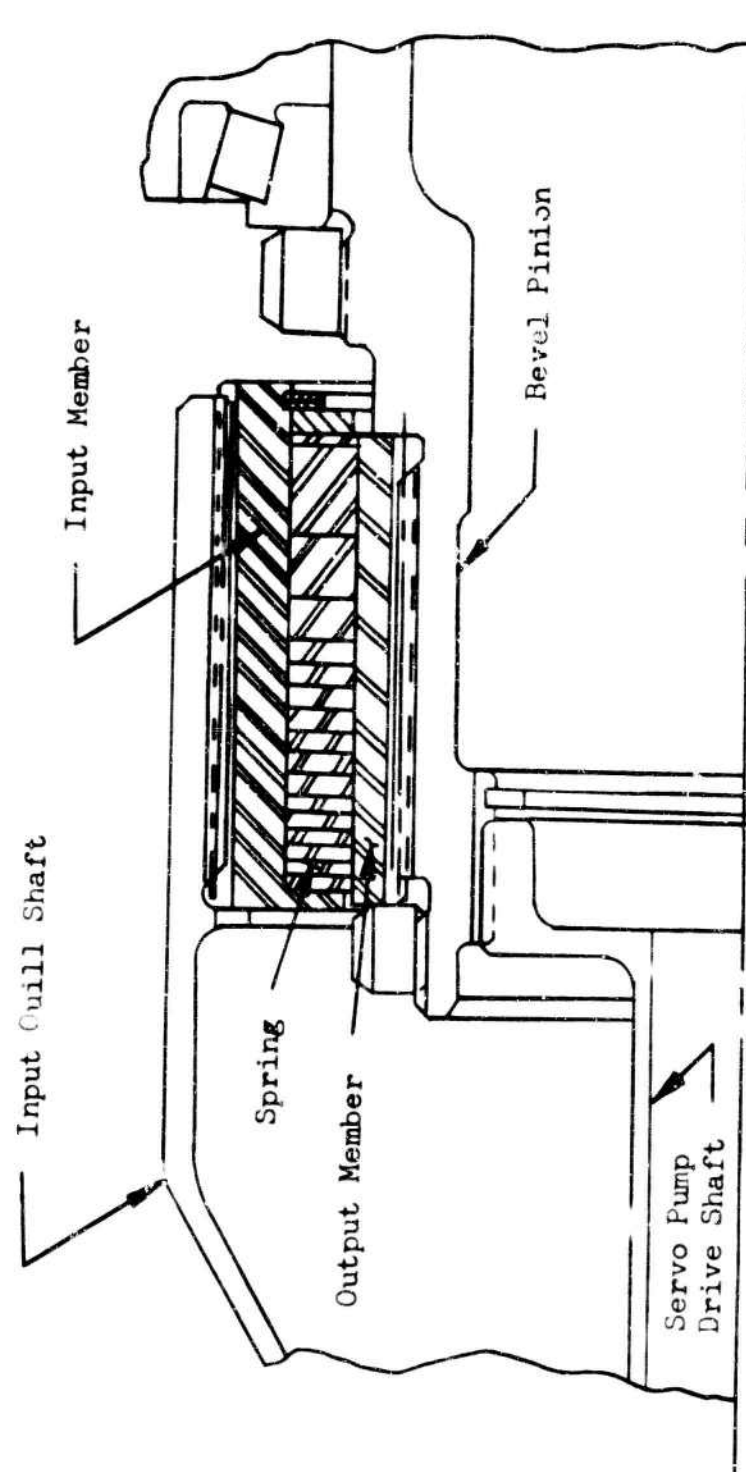


Figure 43. Spring Clutch Installation.

Design Data

The design data utilized in the analysis of the spring clutch were as follows:

Transmission power rating	4,500 HP
Clutch torque rating	49,000 in.-lb.
Operating and/or overrun speed.....	5,780 RPM
Clutch overrun drag torque	5 in.-lb.
Overrun energy loss at 5,780 RPM	343 watts

Based on this information, it is anticipated that the spring clutch concept will operate successfully for all missions of the HLH, including overrunning operation during the 1,500-nautical-mile ferry mission.

TABLE 23
WEIGHT AND EFFICIENCY COMPARISON,
ENGINE TO MAIN ROTOR DRIVE SYSTEMS

	Basic Trans. System	Harmonic Drive System	Roller Drive System	Redundant Drive System
Weight (lb.)				
Engine Red. Gearboxes	396	-	396	-
Main Gearbox	6,990	-	6,533	8,556
System Weight	7,386	Not Determined	6,929	8,556
Power Losses (HP)	549.5	1,015.5	478.5	517
Efficiency (percent)	96.6	93.7	97.0	96.8
Weight Penalty*(lb.)	0	+2,515	-840	+995

* Actual and effective (due to power losses) compared to basic transmission system.

ALTERNATE SUBCRITICAL TAIL ROTOR DRIVE SYSTEMS

To determine the weight advantage of the hypercritical drive system design of pages 92 through 102, alternate subcritical tail drive shaft systems have been designed. Two subcritical systems were designed to transmit the same limit horsepower as the hypercritical tail rotor drive system.

The initial system has been designed to operate at the same speed as the hypercritical speed of pages 92 through 102 (5,922 RPM). The second system is designed for subcritical operation at 3,300 RPM. Critical speeds for both systems are at least 1.25 times the operating speed. The critical speed analysis has been made assuming that each shaft section between the support bearings has pinned ends.

TAIL DRIVE SHAFT SYSTEM (5,922 RPM and 3,760 RPM)

Fuselage - Tail Cone Shafting (5,922 RPM)

For this initial subcritical study, the same intermediate and tail gear-boxes used for the 5,922 RPM hypercritical systems are employed. The shaft assembly will incorporate eight bearing supports spaced at 59 inches and ten flexible disk type couplings.

Stress Analysis

$$T = \frac{63,025 \times \text{HP}}{\text{RPM}}$$

$$T = \frac{63,025 \times 4,000}{5,922}$$

$$T = 42,570 \text{ in.-lb.}$$

Shaft size 4.750 O.D. x .120 wall

Section Through Center of Shaft

$$Z = 1.971$$

$$f_s = \frac{T}{2Z}$$

$$f_s = \frac{42,570}{2 \times 1.971}$$

$$f_s = 10,800 \text{ psi}$$

$$f_{st} = 26,000 \text{ psi (Reference 4)}$$

$$M.S. = \frac{F_{st}}{1.5 \times f_s} - 1$$

$$M.S. = \frac{26,000}{1.5 \times 10,800} - 1$$

$$M.S. = + 0.60$$

Shaft End Connection

$$Z = 1.784 \text{ No. of } .344\text{-dia. lock bolts} = 4 \text{ per row (2 rows)}$$

$$f_s = \frac{T}{2 \times Z}$$

$$f_s = \frac{42,570}{2 \times 1.784}$$

$$f_s = 11,930 \text{ psi}$$

$$F_{sty} = 23,100 \text{ psi (Reference 4)}$$

$$M.S. = \frac{F_{sy}}{1.15 \times f_s} - 1$$

$$M.S. = \frac{23,100}{1.15 \times 11,930} - 1$$

$$M.S. = + 0.68$$

Shaft Critical Speed

$$N_{cl} = \frac{19.2 \times 10^6}{L^2} \sqrt{\frac{I}{A}}$$

$$N_{c1} = \frac{19.2 \times 10^6 \times 1.638}{59.2^2}$$

$$N_{c1} = 8,975 \text{ RPM}$$

Pylon Drive Shafting (3,760 RPM)

The pylon shaft will be of the same size as the supercritical shaft of page 100 with a center bearing support and flexible coupling. The critical speed is at least 1.25 times the operating speed and is calculated by assuming that the span between the bearing and gearbox is pinned at each end. There is a flexible coupling at the bearing support and at each gearbox.

Shaft Critical Speed

$$N_{c1} = \frac{19.2 \times 10^6}{L^2} \sqrt{\frac{I}{A}}$$

$$N_{c1} = \frac{19.2 \times 10^6 \times 1.809}{68^2}$$

$$N_{c1} = 7,511 \text{ RPM}$$

TABLE 24
ITEMIZED WEIGHTS OF SUBCRITICAL SPEED TAIL DRIVE SHAFT SYSTEM,
5,922 RPM FUSELAGE-TAIL CONE SHAFTING,
3,760 RPM PYLON DRIVE SHAFT

Component	Wt. Analysis		Wt. (lb.)
Fuselage-Tail Cone Shafting			
Wt. of Tail Drive Shaft	=	$\frac{\text{Wt.}}{\text{In. Length}} \times \text{Length} = .175 \times 525$	91.9
Wt. of Bearing Supports	=	Unit Wt. x No. Bearing Supports=4.7 x 8	37.6
Wt. of Flexible Disk Couplings at Bearing Support	=	Unit Wt. x No. Couplings=10.9 x 8	87.2
Wt. of Flexible Disk Couplings	=	Unit Wt. x No. Couplings = 6.3 x 2	<u>12.6</u>
Weight of Fuselage-Tail Cone Shafting			229.3
Pylon Drive Shafting			
Wt. of Pylon Drive Shaft	=	$\frac{\text{Wt.}}{\text{In. Length}} \times \text{Length} = .215 \times 136$	29.2
Wt. of Bearing Support	=	Unit Wt. x No. Bearing Supports = 4.7 x 1	4.7
Wt. of Flexible Disk Couplings at Bearing Support	=	Unit Wt. x No. Couplings=10.9 x 1	10.9
Wt. of Flexible Disk Couplings	=	Unit Wt. x No. Couplings = 7.7 x 2	<u>15.4</u>
Weight of Pylon Drive Shafting			60.2
Total Weight - Tail Drive Shaft System			289.5

TAIL DRIVE SHAFT SYSTEM (3,300 RPM and 2,095 RPM)

Fuselage - Tail Cone Shafting (3,300 RPM)

For this alternate subcritical system, an intermediate gearbox of 1.57:1 ratio and tail rotor gearbox of 3.45:1 ratio are employed. As indicated in Table 26, page 188, these units weigh 270 and 390 pounds, respectively. For the fuselage-tail cone drive shafting, six bearing supports spaced at 75 inches and eight flexible couplings have been used.

$$T = \frac{63,025 \times \text{HP}}{\text{RPM}}$$

$$T = \frac{63,025 \times 4,000}{3,300}$$

$$T = 77,485 \text{ in.-lb.}$$

Shaft size 4.500 O.D. x .165 wall

$$\text{I.D.} = 4.170$$

Section Through Center of Shaft

$$Z = 2.349$$

$$f_s = \frac{T}{2 \times Z}$$

$$f_s = \frac{77,485}{2 \times 2.349}$$

$$f_s = 16,500 \text{ psi}$$

$$F_{st} = 27,000 \text{ psi (Reference 4)}$$

$$\text{M.S.} = \frac{F_{st}}{1.5 \times f_s} - 1$$

$$\text{M.S.} = \frac{27,000}{1.5 \times 16,500} - 1$$

$$\text{M.S.} = + 0.09$$

Shaft End Connection

No. of .344 dia.-lock bolt holes = 6 per row (2 rows)

$$Z = 2.005$$

$$f_s = \frac{T}{2 \times Z}$$

$$f_s = \frac{77,485}{2 \times 2.005}$$

$$f_s = 19,300 \text{ psi}$$

$$F_{sy} = 23,100 \text{ psi (Reference 4)}$$

$$\text{M.S.} = \frac{F_{sy}}{1.15 \times f_s} - 1$$

$$\text{M.S.} = \frac{23,100}{1.15 \times 19,300} - 1$$

$$\text{M.S.} = + 0.04$$

Critical Speed

$$N_{cl} = \frac{19.2 \times 10^6}{L^2} \sqrt{\frac{I}{A}}$$

$$N_{cl} = \frac{19.2 \times 10^6 \times 1.534}{75^2}$$

$$N_{cl} = 5,236 \text{ RPM}$$

Pylon Drive Shafting (2,095 RPM)

The pylon drive shaft operates at 2,095 RPM and incorporates at its center a single bearing support and flexible couplings. Flexible couplings are also used at either end. The shaft spans are 68 inches.

$$T = \frac{63,025 \times \text{HP}}{\text{RPM}}$$

$$T = \frac{63,025 \times 4,000}{2,095}$$

$$T = 120,350 \text{ in.-lb.}$$

$$\text{Shaft size} = 6.00 \text{ O.D.} \times .173 \text{ wall}$$

Section Through Center of Shaft

$$Z = 4.294 \text{ No. of } .344\text{-dia. lock bolts} = 4 \text{ per row (2 rows)}$$

$$f_s = \frac{120,350}{2 \times 4.294}$$

$$f_s = 14,000 \text{ psi}$$

$$F_{stu} = 25,000 \text{ psi (Reference 4)}$$

$$\text{M.S.} = \frac{F_{stu}}{1.5 \times f_s} - 1$$

$$\text{M.S.} = \frac{25,000}{1.5 \times 14,000} - 1$$

$$\text{M.S.} = + 0.19$$

Shaft End Connection

$$Z = 4.145$$

$$f_s = \frac{T}{2 \times Z}$$

$$f_s = \frac{120,350}{2 \times 4.145}$$

$$f_s = 14,520 \text{ psi}$$

$$F_{st} = 23,100 \text{ psi (Reference 4)}$$

$$M.S. = \frac{F_{st}}{1.15 \times f_s} - 1$$

$$M.S. = \frac{23,100}{1.15 \times 14,520} - 1$$

$$M.S. = + 0.38$$

Shaft Critical Speed

$$N_{cl} = \frac{19.2 \times 10^6}{L^2} \sqrt{\frac{I}{A}}$$

$$N_{cl} = \frac{19.2 \times 10^6 \times 2.064}{68^2}$$

$$N_{cl} = 8,642 \text{ RPM}$$

TABLE 25
ITEMIZED WEIGHTS OF SUBCRITICAL SPEED TAIL DRIVE SHAFT SYSTEM,
3,300 RPM FUSELAGE-TAIL CONE SHAFTING,
2,095 RPM PYLON DRIVE SHAFT

Components		Wt. Analysis		Wt. (lb.)
Fuselage-Tail Cone Shafting				
Wt. of Tail Drive Shaft	=	$\frac{\text{Wt.}}{\text{In. Length}}$	x Length = .224 x 525	117.6
Wt. of Bearing Supports	=	Unit Wt. x No. of Bearing Supports	= 4.1 x 6	24.6
Wt. of Flexible Disk Couplings at Bearing Supports	=	Unit Wt. x No. Couplings	= 12.8 x 6	76.8
Wt. of Flexible Disk Couplings at the Gearboxes	=	Unit Wt. x No. Couplings	= 11.0 x 2	$\frac{22.0}{241.0}$
Weight of Fuselage-Tail Cone Shafting				
Pylon Drive Shafting				
Wt. of Pylon Drive Shaft	=	$\frac{\text{Wt.}}{\text{In. Length}}$	x Length = .302 x 136	41.1
Wt. of Bearing Support	=	Unit Wt. x No. Bearing Supports	= 4.1 x 1	4.1
Wt. of Flexible Disk Coupling at Bearing Support	=	Unit Wt. x No. of Couplings	= 12.8 x 1	12.8
Wt. of Flexible Disk Coupling at the Gearboxes	=	Unit Wt. x No. of Couplings	= 11.0 x 2	$\frac{22.0}{80.0}$
Weight of Pylon Drive Shafting				
Total Weight - Tail Drive Shaft System				321.0

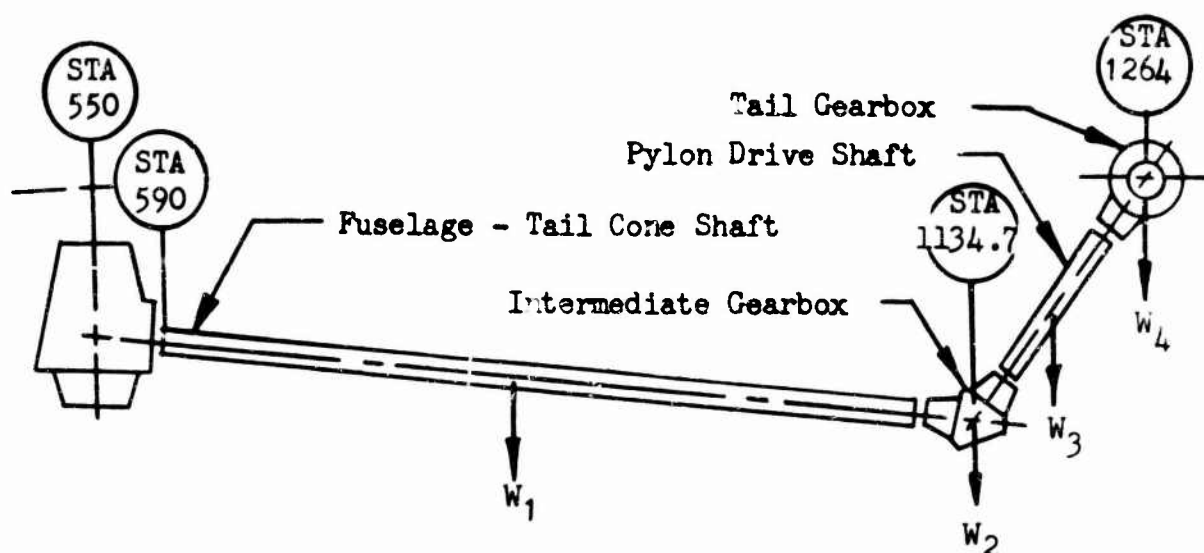


Figure 44. Tail Rotor Drive System Schematic.

TABLE 26
COMPARATIVE WEIGHTS, HYPERCRITICAL VERSUS
SUBCRITICAL SPEED TAIL ROTOR DRIVE SYSTEMS

Type of System		Basic TRD Sys.	Alt. I TRD Sys.	Alt. II TRD Sys.	Alt. III TRD Sys.
Shaft:	Fuselage-Tail Cone	Hypercrit.	Hypercrit.	Subcrit.	Subcrit.
	Pylon Drive	Supercrit.	Subcrit.	Subcrit.	Subcrit.
		(RPM)	(RPM)	(RPM)	(RPM)
Fuselage-Tail Cone Shaft		5,922	5,922	5,922	3,300
Pylon Drive Shaft		3,760	1,085	3,760	2,095
Item	Symbol	Weight (lb.)	Weight (lb.)	Weight (lb.)	Weight (lb.)
Fuselage-Tail Cone Shaft	W_1	139	139	229	241
Pylon Drive Shaft	W_3	58	125	60	80
Intermediate Gearbox	W_2	137	270*	137	175
Tail Gearbox	W_4	333	390**	333	360
Total Weight of System		667	924	759	856

* Intermediate gearbox design is shown in Figure 60, Appendix I.

** Tail gearbox design is shown in Figure 61, Appendix I.

EFFECT ON C.G. OF ALTERNATE TAIL ROTOR DRIVE SYSTEMS

To determine the most advantageous ratio for each tail gearbox in the basic hypercritical system, an analysis of the weights of several gearbox designs and their effect on the aircraft center of gravity range has been made. The data of the first two columns of Table 26 were used as the basis for this analysis.

Moments (about \bar{C} main rotor)			
	Moment Eq.	"Basic" Tail Drive System, Hyper- critical Tail Cone & Pylon	Alt. I Tail Drive System, Hyper- critical-Tail Cone, Subcriti- cal -Pylon
Fuselage-Tail Cone Shaft	$W_1 \times 313$	43,510	43,510
Intermediate Gearbox	$W_2 \times 585$	74,300	157,950
Pylon Drive Shaft	$W_3 \times 650$	37,700	81,250
Tail Gearbox	$W_4 \times 714$	237,760	278,460
	TOTALS	<u>393,270</u>	<u>561,170</u>

$$\text{Weight - Moment Reduction} = \frac{561,170 - 393,270}{12}$$

$$= 13,990 \text{ ft.-lb.}$$

$$\text{Effect on C.G. Range} = \frac{13,990}{86,000}$$

$$= .163 \text{ ft. (1.96 in.)}$$

Hypercritical Versus Subcritical Designs

A comparative weight moment analysis for the basic 5,922 RPM hypercritical -supercritical (pylon) system versus the 3,300 RPM subcritical system (Alternate III) was also made as follows:

Moments (about ϕ main rotor)			
	Moment Eq.	Hypercritical Basic Tail Drive System	Subcritical Tail Drive System (Alt. III)
Fuselage-Tail Cone Shaft	$W_1 \times 313 \text{ in.}$	43,510	75,430
Intermediate Gearbox	$W_2 \times 585 \text{ in.}$	74,300	102,400
Pylon Drive Shaft	$W_3 \times 650$	37,700	52,000
Tail Gearbox	$W_4 \times 714$	237,760	257,000
		<hr/>	<hr/>
	TOTALS	393,270	486,830

$$\text{Weight - Moment Reduction} = \frac{486,830 - 393,270}{12}$$

$$= 7,800 \text{ ft.-lb.}$$

$$\text{Effect on C.G. Range} = \frac{7,800}{86,000}$$

$$= 0.091 \text{ ft. (1.09 in.)}$$

CONTROL SYSTEMS

Introduction

To evaluate the feasibility of integrating the main rotor controls within the heavy-lift helicopter main transmission design, several systems were evaluated. These included a modified Hafner type internal control system and a "double eccentric" internal control system. These were compared to a conventional swash plate system external to the main transmission.

Loads

The control system motions are delivered to the main rotor blades by means of "push rods." These are attached to radius arms about the pitching axis of each blade. In the rotor control systems studied, there are six blades and therefore six push rods. The loads for each control system are given in terms of push rod loads and are equal to:

$$500 \text{ lb.} \pm 3,000 \text{ lb.}$$

For the conventional external control system only, there are applicable servo loads in addition to the push rod loads. These servo mechanisms are used to tilt the conventional swash plates. There are three servos and the servo load is equal to:

$$3,000 \text{ lb.} \pm 5,000 \text{ lb.}$$

MODIFIED HAFNER SYSTEM

Description

The modified Hafner internal control system operates in the following manner: the swash plates are mounted above the main rotor head and are tilted by a pivoting axle, which is regulated by a pivoting rod thru the main rotor shaft. Tilting of the swash plates provides cyclic control, and raising or lowering of the swash plates provides collective control. The actuating servo mechanisms are installed below the main transmission housing, inside the aircraft. A schematic of this control system is shown in Figure 45, on page 192, and a complete drawing appears in Appendix I, Figure 63.

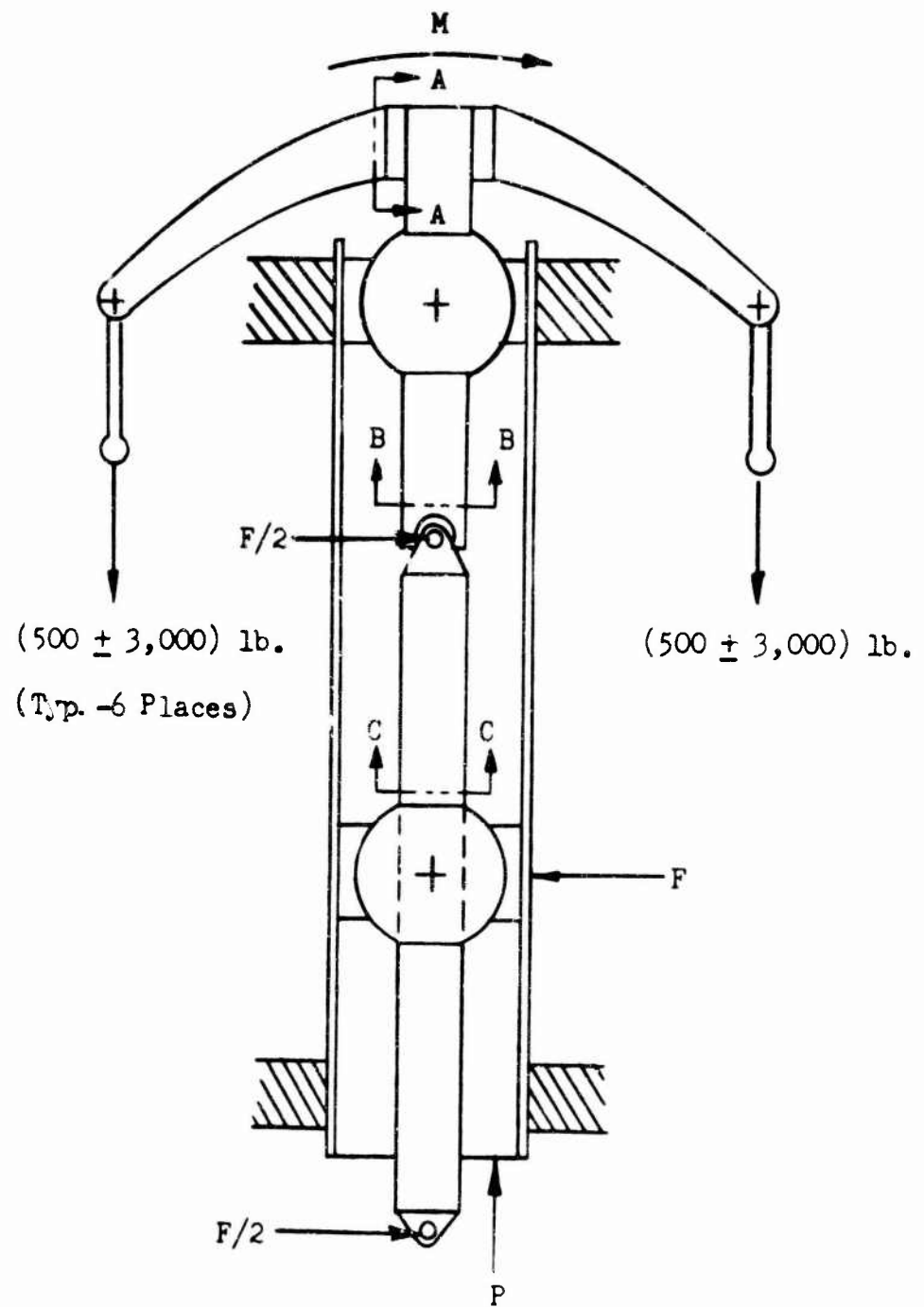
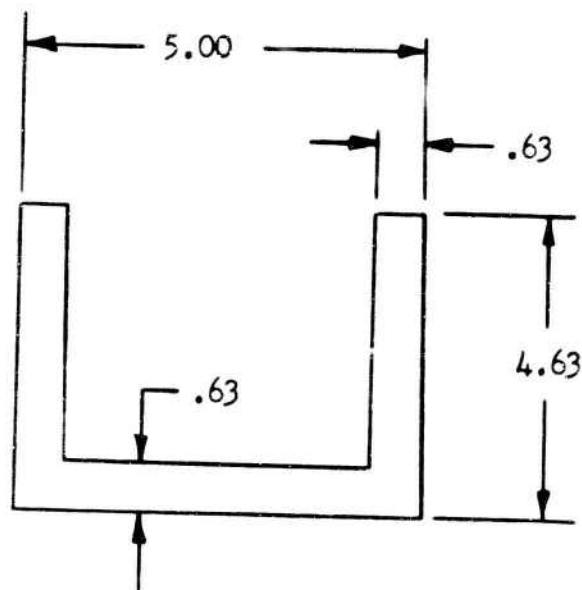


Figure 45. Modified Hafner Internal Control System.

Design Analysis

Referring to Figure 45 on page 192, stress calculations were made on critical sections and the supporting tube, shown in Detail D, as follows:

Section A-A



Section A-A of Figure 45.

$$f_b = \frac{Mc}{I}$$

$$I = 17.24 \text{ in.}^4$$

$$c = 2.89 \text{ in.}$$

Steady Stresses

$$M = 500 \text{ lb.} \times 21 \text{ in.}$$

$$f_b = \frac{500 (21) 2.89}{17.24} = 1,760 \text{ psi}$$

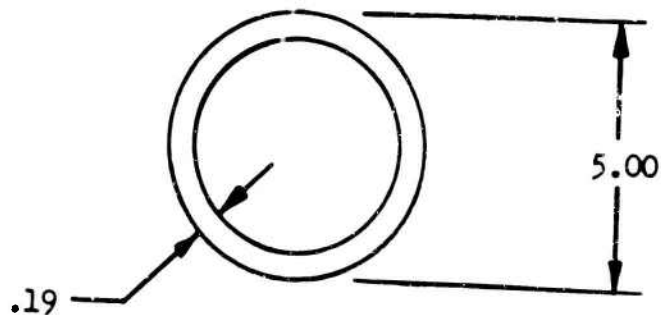
Vibratory Stresses

$$M = 3,000 \text{ lb.} \times 21 \text{ in.}$$

$$f_v = \frac{3,000 (21) 2.89}{17.24} = 10,570 \text{ psi}$$

Referring to the modified Goodman diagram on page 198, the point for section A-A falls well below the line required for infinite life and .9999 reliability.

Section B-B



Section B-B of Figure 45.

$$f_b = \frac{M}{Z}$$

$$Z = 3.28 \text{ in.}^3$$

$$M = 360,000 \text{ in.-lb.}$$

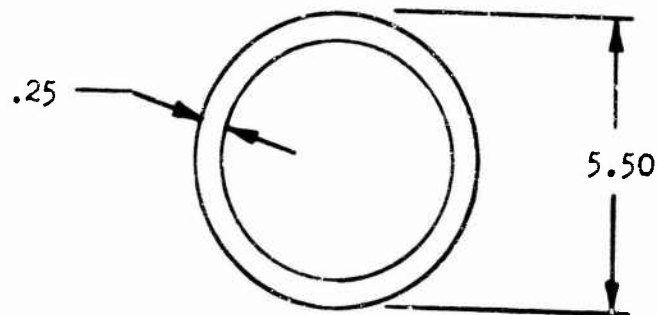
$$f_b = \frac{360,000}{3.28} = 110,000 \text{ psi}$$

$$F_{tu} = 125,000 \text{ psi (for steel)}$$

$$\text{M.S.} = \frac{F_{tu}}{f_b} - 1 = \frac{F_{tu} - f_b}{f_b}$$

$$M.S. = \frac{125,000 - 110,000}{110,000} = + .14$$

Section C-C



Section C-C of Figure 45.

$$f_b = \frac{M}{Z}$$

$$Z = 5.18 \text{ in.}^3$$

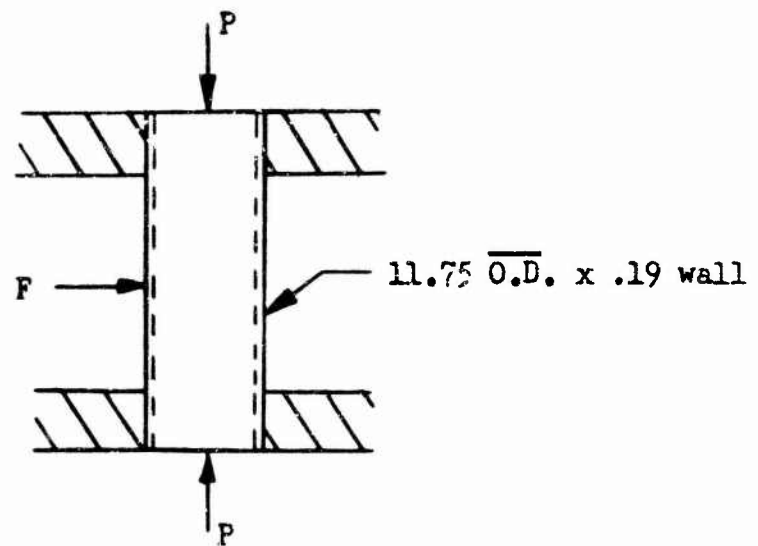
$$M = \frac{40}{24} (360,000) = 600,000 \text{ in.-lb.}$$

$$f_b = \frac{600,000}{5.18} = 116,000 \text{ psi}$$

$$F_{tu} = 125,000 \text{ psi (for steel)}$$

$$M.S. = \frac{125,000 - 116,000}{116,000} = + .078$$

Supporting Tube



Detail D of Figure 45.

$$M = \frac{1}{2} FJ \left(\tan \frac{U}{2} - \frac{1 - \cos U/2}{\sin U/2 \cos U/2} \right) \quad \text{Reference 5, P. 136, Case No. 9.}$$

$$P = 21,000 \text{ lb. max.}$$

$$F = 32,000 \text{ lb.}$$

$$J = \sqrt{\frac{EI}{P}}$$

$$E = 10 \times 10^6 \text{ psi}$$

$$I = 118 \text{ in.}^4$$

$$L = 80 \text{ in.}$$

$$U = L/J$$

$$J = \sqrt{\frac{10^7 (118)}{21,000}} = 237 \text{ in.}$$

$$U = \frac{80}{237} = .338 \text{ rad.}$$

$$M = \frac{32,000 (237)}{2} \left(\tan .169 - \frac{1 - \cos .169}{\sin .169 \cos .169} \right)$$

$$.169 \text{ rad.} = 9.68^\circ = 9^\circ 41'$$

$$M = 16,000 (237) (.17057 - \frac{1 - .98584}{.16814 \times .98584})$$

$$M = 16,000 (237) (.17057 - \frac{.01416}{.16576})$$

$$M = 16,000 (237) (.17057 - .08542)$$

$$M = 16,000 (237) (.08515)$$

$$M = 323,000 \text{ in.-lb.}$$

$$f_b = \frac{Mc}{I}$$

$$c = 5.88$$

$$f_b = \frac{323,000 (5.88)}{118} = 16,100 \text{ psi max.}$$

The maximum bending stress as calculated above is sufficiently below the endurance limit for aluminum to assure infinite life.

Weight

The modified Hafner system as described above weighs 556 pounds. A weight breakdown and comparison appears on page 213.

DOUBLE ECCENTRIC SYSTEM

The double eccentric control system operates as follows: The swash plates are mounted above the main rotor head and cyclic control is obtained by shifting the cyclic swash plate off center with respect to the collective swash plate. This shifting is accomplished by the differential angular rotation of two eccentric torque tubes which extend through the main rotor shaft. Collective control is gained by the raising or lowering of the swash plates together. The actuating servo mechanisms are mounted below the main transmission housing, inside the aircraft. A schematic of this control system is shown in Figure 47 page 199, and a complete drawing appears in Appendix I, Figure 64.

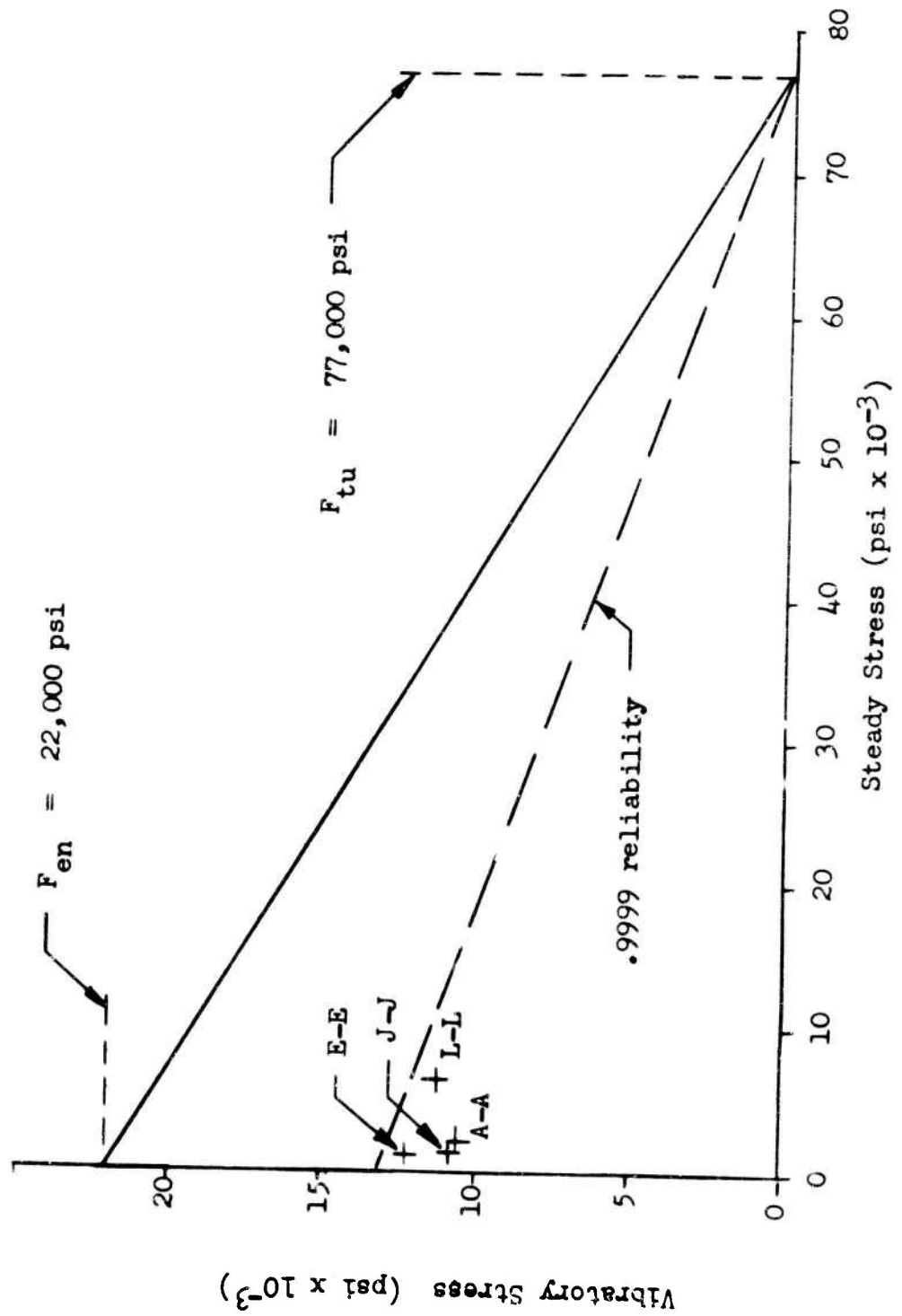


Figure 46. Modified Goodman Diagram for 7075-T6 Aluminum

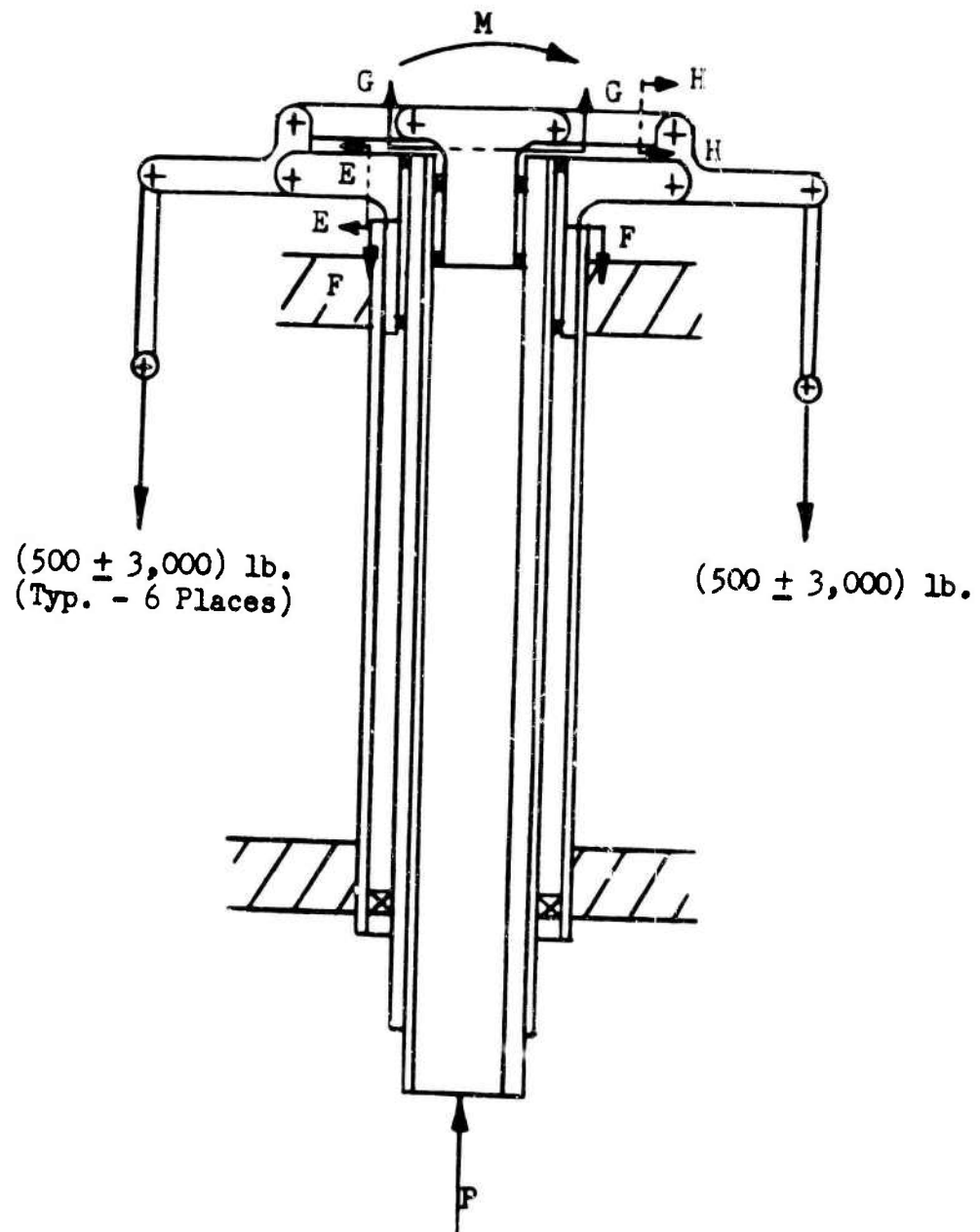
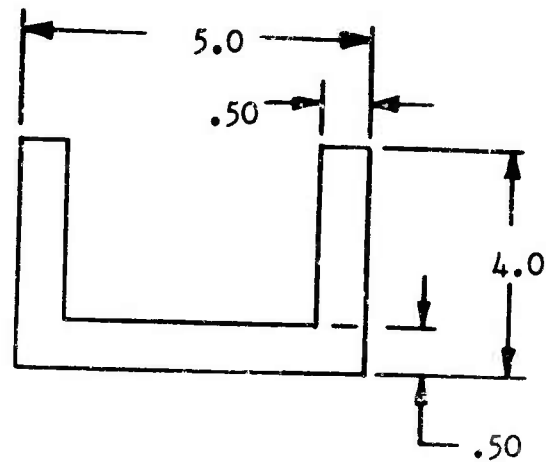


Figure 47. Double Eccentric Internal Control System.

Design Analysis

Referring to Figure 47, page 199, stress calculations were made on critical sections as follows:

Section E-E



Section E-E of Figure 47.

$$f_b = \frac{M c}{I}$$

$$f_c = \frac{P}{A}$$

$$c = 2.59 \text{ in.}$$

$$I = 9.94 \text{ in.}^4$$

$$A = 6.0 \text{ in.}^2$$

$$P = 2,000 \pm 12,000 \text{ lb.}$$

$$M = [(500 \pm 3,000) 13] \text{ in.-lb.}$$

Steady Stresses

$$f_b = \frac{500 (13) 2.59}{9.94} = 1,690 \text{ psi (tension)}$$

$$f_c = \frac{2,000}{6} = 333 \text{ psi (compression)}$$

$$f_a = 1,690 - 333 = 1,357 \text{ psi (tension)}$$

Vibratory Stresses

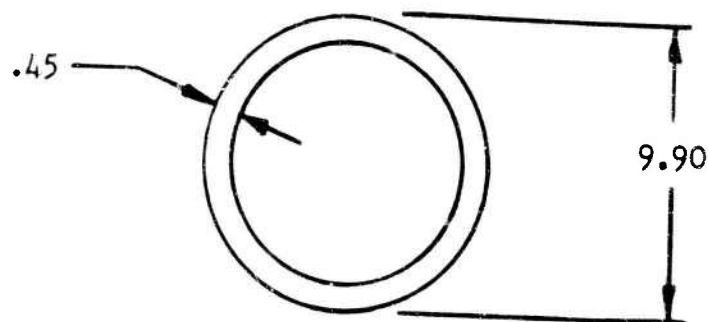
$$f_b = \frac{3,000 (13) 2.59}{9.94} = 10,200 \text{ psi}$$

$$f_c = \frac{12,000}{6.0} = 2,000 \text{ psi}$$

$$f_v = \pm 10,200 \pm 2,000 = \pm 12,200 \text{ psi}$$

Referring to the modified Goodman diagram on page 198, the point for section E-E falls below the line required for infinite life and 0.9999 reliability.

Section F-F



Section F-F of Figure 47.

$$f_b = \frac{M c}{I}$$

$$I = 147.5 \text{ in.}^4$$

$$c = 4.95 \text{ in.}$$

$$M = 360,000 \text{ in.-lb.}$$

$$f_b = \frac{360,000 (4.95)}{147.5} = 12,000 \text{ psi}$$

$$f_c = \frac{P}{A}$$

$$P = 21,000 \text{ lb. max.}$$

$$A = 4.25 \text{ in.}^2$$

$$f_c = \frac{21,000}{4.25} = 4,950 \text{ psi}$$

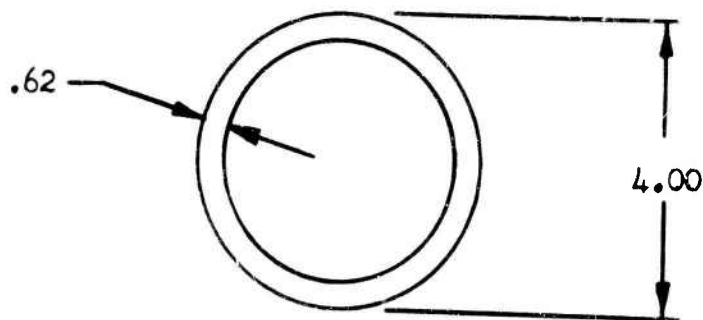
$$f_b + f_c = 12,000 + 4,950$$

$$f_a = 16,950 \text{ psi}$$

$$F_{en} = 22,000 \text{ psi}$$

The combined stresses as calculated for section F-F above are well below the endurance limit for aluminum, and thus infinite life is assured.

Section G-G



Section G-G of Figure 47.

$$F_{tu} = 180,000 \text{ psi}$$

$$F_{en} = 53,000 \text{ psi}$$

$$f_b = \frac{Mc}{I}$$

$$I = 9.80 \text{ in.}^4$$

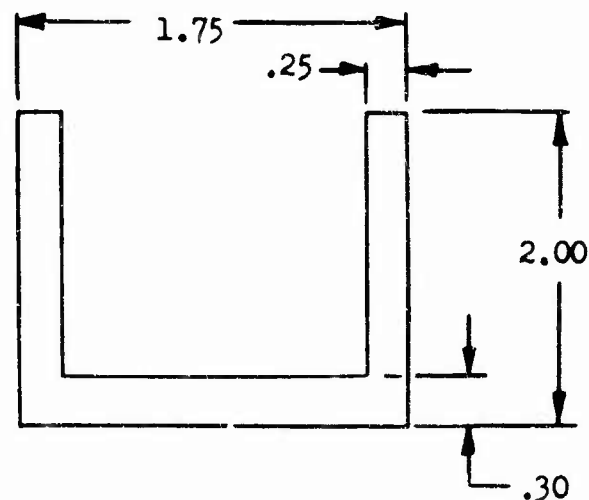
$$c = 2.00 \text{ in.}$$

$$M = 48,000 (3.5) \text{ in.-lb.}$$

$$f_b = \frac{48,000 (3.5) 2.0}{9.8} = 34,000 \text{ psi}$$

The vibratory stresses as calculated above are sufficiently below the endurance limit for steel to assure infinite life.

Section H-H



Section H-H of Figure 47.

$$f_a = \frac{P}{A}$$

$$P = 2,000 \pm 12,000 \text{ lb.}$$

$$A = 1.38 \text{ in.}^2$$

$$P_{\text{max}} = 14,000 \text{ lb.}$$

$$f_a = \frac{14,000}{1.38} = 10,200 \text{ psi max.}$$

$$F_{\text{en}} = 22,000 \text{ psi}$$

The maximum vibratory stress as calculated above is sufficiently below the endurance limit for aluminum to assure infinite life.

Weight

The double eccentric internal control system as described above weighs 424 pounds. A weight breakdown and comparison appears on page 213 .

CONVENTIONAL SYSTEM

Description

The conventional external control system operates as follows: the swash plates are tilted and raised or lowered by servo mechanisms outside the transmission housing to provide cyclic and collective control, respectively. A schematic of this control system is shown in Figure 48 on the following page, and a drawing appears in Appendix I, Figure 65.

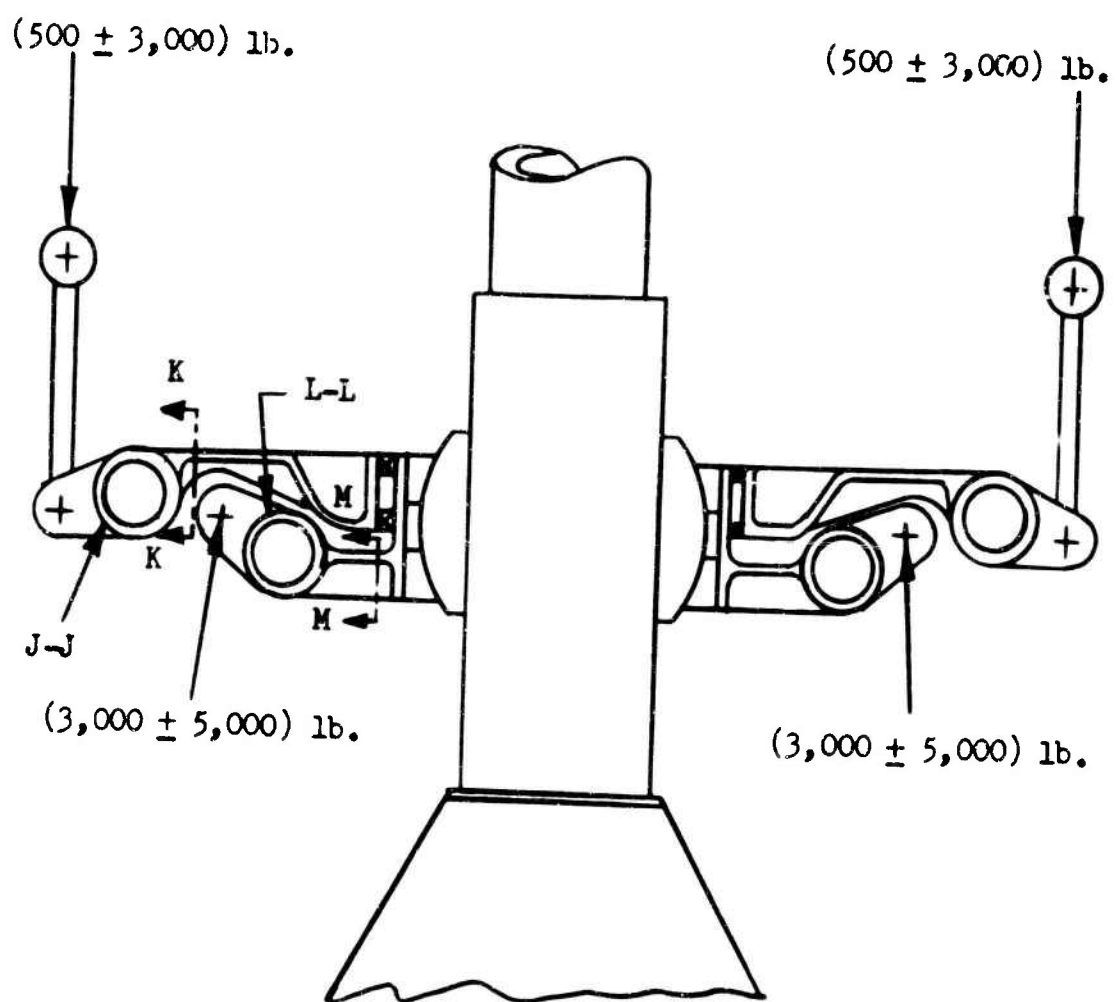


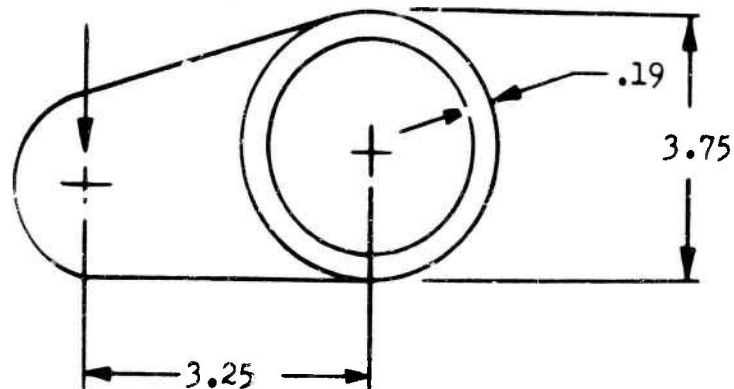
Figure 48. Conventional External Control System.

Design Analysis

Referring to Figure 48, page 205, stress calculations were made on critical sections as follows:

Section J-J

(500 ± 3,000) lb.
(Typ. - 6 Places)



Section J-J of Figure 48.

$$f_b = \frac{McR}{I} \quad (\text{Reference 5, Page 231.})$$

$$I = 3.25 \text{ in.}^4$$

$$c = 1.88 \text{ in.}$$

$$R = 26.5 \text{ in.}$$

Steady stresses in the torus section of the rotating swash plate are:

$$M = \frac{500 (3.25) 6}{26.5 (\pi)} = (0.234)(500) \text{ in.-lb./in.}$$

$$M = 117 \text{ in.-lb./in.}$$

$$f_b = \frac{(117)(1.88)(26.5)}{3.25}$$

$$f_b = 1,790 \text{ psi.}$$

The vibratory stresses in the torus section of the rotating swash plate are:

$$M = 3000(.234) \text{ in.-lb./in.}$$

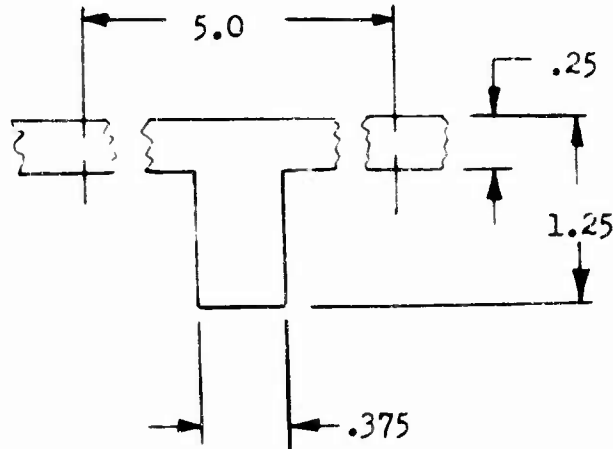
$$M = 702 \text{ in.-lb./in.}$$

$$f_v = \frac{702 (1,790)}{117}$$

$$f_v = 10,750 \text{ psi}$$

Referring to the modified Goodman diagram on page 198, the point for section J-J falls well below the line required for infinite life and .9999 reliability.

Section K-K



Section K-K of Figure 48.

Assuming that the connection between the rotating torus and the inner ring of the rotating swash plate is a flat plate, the following calculations were made.

$$f = \frac{3W}{2\pi t^2} \left[1 - \frac{2r^2}{R^2 - r^2} \left(\log \frac{R}{r} \right) \right] \quad \begin{array}{l} \text{(Reference 5,} \\ \text{Page 200} \\ \text{Case 20.)} \end{array}$$

$$f_{\text{allowable}} = 10,000 \text{ psi}$$

$$R = 21 \text{ in.}$$

$$r = 11 \text{ in.}$$

$$W = 18,000 \text{ lb.}$$

Substituting these values in the preceding equation and solving for $t_{\text{reqd.}}$,

$$t_{\text{reqd.}}^2 = \frac{(3)(18,000)}{(2)(\pi)(10,000)} \left[1 - \frac{2(11)^2}{21^2 - 11^2} \left(\log \frac{21}{11} \right) \right]$$

$$t_{\text{reqd.}} = .662 \text{ in.}$$

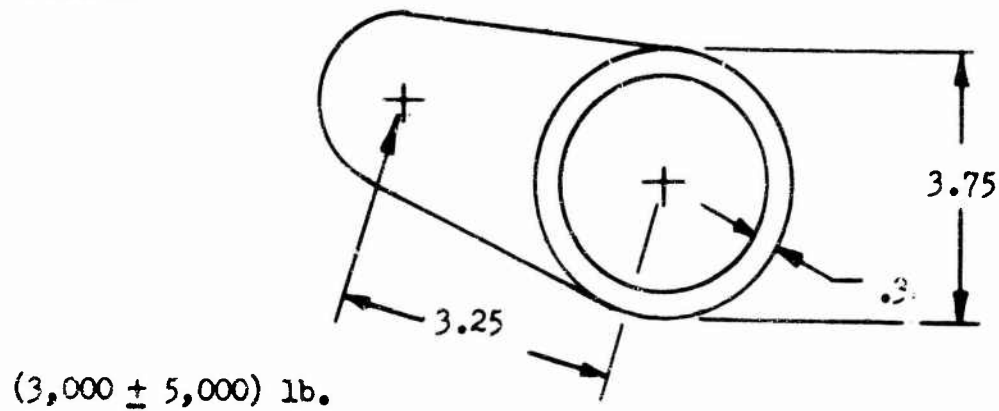
The moment of inertia for the assumed plate is:

$$I = \frac{5}{12} (.662)^3 \quad (\text{for a 5-in. typical section})$$

$$I = 0.121 \text{ in.}^4$$

$$I_{\text{actual}} = 0.153 \text{ in.}^4$$

Section L-L



Section L-L of Figure 48.

$$f_b = \frac{McR}{I} \quad (\text{Reference 5, Page 231.})$$

$$I = 5.17 \text{ in.}^4$$

$$c = 1.88 \text{ in.}$$

$$R = 16.25 \text{ in.}$$

The steady stresses in the torus section of the stationary swash plate are:

$$M = \frac{3,000 (3.25) (6)}{16.25 (\pi)} = .382 (3,000) \text{ in.-lb./in.}$$

$$M = 1,146 \text{ in.-lb./in.}$$

$$f_b = \frac{(1,146) (1.88) (16.25)}{5.17}$$

$$f_b = 6,775 \text{ psi}$$

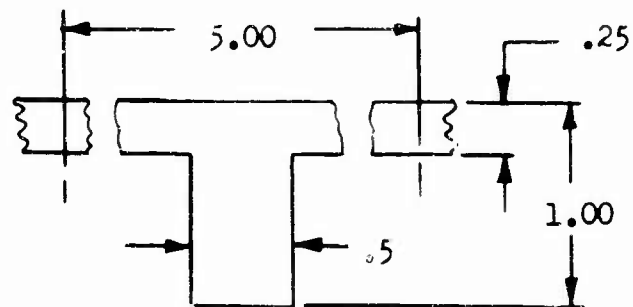
The vibratory stresses in the torus section of the stationary swash plate are:

$$M = (.382) 5,000 = 1,910 \text{ in.-lb./in.}$$

$$f_v = \frac{1,910 (6.775)}{1,246} = 11,300 \text{ psi}$$

Referring to the modified Goodman diagram on page 198, the point representing section L-L falls below the line required to assure infinite life and .9999 reliability.

Section M-M



Section M-M of Figure 48.

Assuming that the connection between the stationary torus and the inner ring of the stationary swash plate is a flat plate, the following calculations were made:

$$f = \frac{3W}{2 \pi t^2} \left[\frac{1 - \frac{2 r^2}{R^2 - r^2}}{\left(\log \frac{R}{r} \right)} \right] \quad \text{(Reference 5, Page 200, Case 20.)}$$

$$f_{\text{allowable}} = 10,000 \text{ psi}$$

$$R = 15 \text{ in.}$$

$$r = 10 \text{ in.}$$

$$W = 20,000 \text{ lb.}$$

Substituting these values in the preceding equation and solving for t_{reqd} ,

$$t_{\text{reqd}}^2 = \frac{(3)(20,000)}{2(\pi)10,000} \left[1 - \frac{2(10^2)}{15^2 - 10^2} \log \frac{15}{10} \right]$$

$$t_{\text{reqd}} = 0.58 \text{ in.}$$

The moment of inertia for the assumed plate is:

$$I = \frac{(5)(.58)^3}{12}$$

$$I_{\text{reqd}} = 0.081 \text{ in.}^4 \text{ (for a 5-inch typical section).}$$

$$I_{\text{actual}} = 0.096 \text{ in.}^4 \text{ (for a 5-inch typical section)}$$

Weight

The conventional external control system as described above weighs 467 pounds. A weight breakdown and comparison with the other alternate control systems is given on page 213.

COMPARATIVE DRAG ANALYSIS

The exposed frontal area for each of the three control systems studied has been determined by analysis to be:

Hafner System	2.26 ft. ²
Double Eccentric System	2.22 ft. ²
Conventional System	3.12 ft. ²

The drag on each system due to the exposed frontal area may be expressed as:

$$D = A \left(\frac{1}{2} \rho V^2 \right)$$

where

$$A = \text{ft.}^2$$

$$\rho = .002378 \text{ slugs/ft.}^3$$

$$V = 95 \text{ KT} \times 1.688$$

$$V = 160 \text{ ft./sec.}$$

The horsepower lost due to this drag is expressed by:

$$HP_{\text{lost}} = \frac{DV}{550}$$

where

$$D = \text{lb.}$$

$$V = 160 \text{ ft./sec}$$

System	Drag (lb.)	Effective Power Loss (HP)
Hafner System	68.5	19.9
Double Eccentric System	67.4	19.6
Conventional System	94.6	28.0

Evaluation

The integration of the rotor controls within the heavy-lift helicopter transmission design is desirable for an aerodynamically "clean" and efficient system design. Evaluation of the systems herein considered reveals some advantages and disadvantages of each. The Hafner system (Figure 45) provides a simple system in which the motions of a pilot's stick can easily be translated into the proper control motions required as inputs to this system. However, the Hafner system proved to be heavier than any of the others.

The "double eccentric" system (Figure 45) is lighter than the Hafner and equivalent in weight to the conventional, but this system requires a complex relationship between the motions of a pilot's "stick" and the motions required to actuate this system properly.

The conventional system is one of proven reliability and the weight compares favorably with the other systems considered; however, aerodynamic efficiency will be sacrificed with this design, since it is entirely external to the transmission housing.

TABLE 27
SUMMARY,
WEIGHTS COMPARISON, CONTROL SYSTEMS STUDY (POUNDS)

Part Name	External Conventional System	Internal Hafner System	Internal Double Eccentric System
Rotary Swash Plate	200	92	-
Stationary Swash Plate	100	28	-
Rotary Scissors	7	2	2
Stationary Scissors	20	-	-
Controls Rods	30	18.5	42
Guide Shaft	40	-	-
Swash Plate Ball & Races	34	-	-
Bearings	36	15	30
Collective Shaft	-	89	50
Cyclic Rod	-	85	-
Cyclic Axle	-	30	-
Spherical Brg. & Races	-	161	-
Bearing Retainer	-	18	-
Nuts, Retaining	-	17.5	30
Cyclic Shaft	-	-	40
Collective Swash Plate	-	-	120
Cyclic Swash Plate	-	-	30
Pitch Links	-	-	50
Gimbal Drive	-	-	3
Journals	-	-	27
TOTALS	467	556	424

PERFORMANCE

Introduction

The table on the following pages presents the final weight breakdown for the single-rotor heavy-lift helicopter for which this transmission system design study was conducted. As in Reference 3, the weights given for the components are based on a load factor of at least 2.5 at a gross weight of 86,000 pounds (20-ton payload).

It should be noted that no refinements were made in any portion of the transmission or control system designs presented in this report to reflect the effect of this difference between the final gross weights of 86,037 (front-drive engines) and 85,863 (rear-drive engines) and the preliminary assumption of 86,000 pounds.

WEIGHT AND BALANCE ANALYSIS

The balance characteristics of the 12-to 20-ton single rotor helicopters of Figure 50 and 52 have been calculated to be as follows:

	Gross Weight (lb.)	Center of Gravity Location (station)*	
		Front Drive (Fig. 50)	Rear Drive (Fig. 52)
12-Ton Transport	74,097	550.3	549.0
20-Ton Heavy Lift	86,037	550.0	548.9
1,500 n.m. Ferry	98,587	550.9	549.9

*Note: The design C.G. limits for this aircraft are as follows:

Station	
Fwd. C.G. Limit	533.6
Aft C.G. Limit	<u>583.6</u>
Total C.G. Range	50.0

The balance analysis summarized above was based on the final weight analysis presented on the following pages.

Item	Weight (lb.)
Rotor Group (Less Controls)	11,100
Tail Group	975
Transmission System (Front-Drive Engine Install.)	8,852
Main Gearbox	6,990
Intermediate Gearbox	137
Tail Gearbox	333
Accessory Gearbox and Shaft	84
Engine Reduction Gearbox (2)	396
Input Drive Shaft	118
Tail Drive Shaftering	197
Lube Systems	539
Rotor Brake	58
Hydraulic Controls (Brake)	60
Supports	400
Body Group (incl. stabilizer)	5,600
Flight Controls (incl. automatic flight control system and main rotor controls)	2,015
Hydraulic and Electrical	1,390
Alighting Gear	4,060
Main Landing Gear	2,120
Landing Gear Support	1,420
Nose Gear	450
Tail Skid	70
Engine Section (cowling mounting & fire walls)	560
Power Plant Group (front-drive engine)	4,000
Engines (4) T-64/S5A	3,060
Induction System	60
Exhaust System	60
Fuel System	475
Starting System	130
Cooling System	---
Lube System	140
Engine Controls	75
Electronics (incl. VHF, FM, ADF, VOR, IFR, and radar altimeter)	290
Instruments	300
Flight	85
Engine	160
Trans., Hyd., etc.	55

TABLE 28 (continued)

Item	Weight (lb.)
Furnishings	350
Personnel Accommodations	180
Emergency Accommodations	90
Air Conditioning	80
Anti-icing (Engine Inlet)	50
Auxiliary Power Unit (T 62 T -16A)	165
Four-point Winching System (40,000# Capability at L.F. = 2.5)	1,500
Weight Empty	41,667
HEAVY-LIFT MISSION	
Useful Load for Heavy-Lift Mission	44,370
Crew (3)	600
Fuel-Usable (20-n.m. radius)	
Including 10% Reserve	3,700
Oil-Usable	20
Unusable	50
Payload	40,000
Gross Weight for Heavy-Lift Mission	86,037
12-TON TRANSPORT MISSION	
Useful Load (for transport mission)	32,430
Crew (3)	600
Fuel-For 100-n.m. radius	
(w/10% Reserve)	7,760
Oil-Usable	20
Unusable	50
Payload	24,000
Gross Weight (for transport mission)	74,097
1,500-N.M. FERRY MISSION	
Useful Load (Ferry Mission)	56,920
Crew (3)	600
Fuel	53,750
Auxiliary Tanks	2,500
Oil	70
Payload	0
Gross Weight (for Ferry Mission)	98,587

TABLE 29
COMPARISON
TRANSMISSION SYSTEM WEIGHTS
FRONT AND REAR DRIVE ENGINES

	Front Drive Engines			Rear Drive Engines		
	No.	Unit Wt. (lb.)	Total Wt. (lb.)	No.	Unit Wt. (lb.)	Total Wt. (lb.)
Engines	4	765	3,060	4	732	2,928
Engine Reduction Gearboxes	2	198	396	4	90	360
Main Gearbox	1	6,990	6,990	1	6,990	6,990
Input Drive Shaft	2	59	118	4	28	112
Accessory Gearbox and Shaft	1	84	84	1	84	84
Tail Drive Shafting	1	197	197	1	197	197
Intermediate Gearbox	1	137	137	1	137	137
Tail Gearbox	1	333	333	1	333	333
Lube Systems	1	539	539	1	539	539
Rotor Brake	1	58	58	1	58	58
TOTAL			11,912			11,738

Note: For the rear-drive engine installation of Figure 53, (engine model 548-C2), the heavy-lift aircraft total gross weights are approximately 174 pounds less for all three missions.

MISSION PERFORMANCE VERIFICATION

To verify that the helicopter design considered herein meets the required performance levels, the final aircraft mission weights have been utilized to establish actual performance levels.

The required horsepower to hover at 6,000 feet, 95°F, is given by

$$\text{SHP} = \frac{(0.0437) \text{ G.W.}^{3/2}}{D} + .02755 (\text{G.W.})$$

$$\text{SHP} = 11,320$$

where

$$\text{G.W.} = 74,097 \text{ lb.}$$

$$D = 95 \text{ feet.}$$

Fuel requirements for the 1,500-nautical-mile ferry mission were established as follows:

Four engines utilized for warm-up, take off, and climb - 2 minutes

Three engines operating for 27 percent of mission

Two engines operating for 73 percent of mission

	Pounds Fuel
Warm-up, Take off, and Climb	
$1.05 \times .482 \times (2/60) \times 16,000$	= 270
Cruise - 3 Engines	
$1.05 \times .55 (222/60) \times 6,660$	= 14,100
Cruise - 2 Engines	
$1.05 \times .494 \times (596/60) \times 6,600$	= 34,000
	<hr/> 48,370

$$\text{Total fuel required} = 48,370 / .9 = 53,750 \text{ lb.}$$

METHODS OF MANUFACTURING

The fabrication of transmission components for the heavy-lift helicopter can be accomplished by using present manufacturing methods. Equipment is now available at most facilities used for gear train subcontract work for the helicopter industry.

In the few cases where machinery of larger capacity is required, these units are available in the machine tool market and can be procured within the anticipated heavy-lift helicopter transmission design cycle so that no delays in lead time will result.

The following is a list of equipment proposed for use for the large dynamic elements of the gearboxes. In only two cases will subcontractors have to procure larger equipment.

Item	Size	Equipment	Availability
Spiral Bevel Gears	Up to 32" diameter	#27 Gleason Grinder	In use
	Greater than 36" diameter	#137 Gleason Grinder	1 year
Internal Ring Gears	Up to 40" diameter	Detroit Grinder	In use
	Up to 58" diameter	Maag Cutter Maag Grinder	1 year
Main Rotor Shaft	16" diameter x 80" length	Turning Operation- Lodge & Shipley Tracer Lathe Boring Operation- Lodge & Shipley Tracer Lathe & Barnes Gun Drill	In use

As indicated in the materials section, page 16 through 19, it is proposed that all housings be fabricated from cast or forged magnesium alloys where at all feasible. Other than the main gearbox main housing, all castings and forgings are within existing foundry performance. As shown in Figure 49, the heavy-lift helicopter main transmission is approximately a 50 percent extrapolation in physical size over the contractor's CH-54A crane type main transmission. It is anticipated that current casting and heat-treating methods will provide castings of quality equal to that of production aircraft.

An alternate manufacturing method to be evaluated during the design phase is the design and fabrication of major housings in subsections, and the joining of these sections by heli-arc or electron beam welding techniques prior to heat treating. A second alternative would employ bolted connections to join the separate subsections. Some weight penalty must be anticipated if this practice is employed.

Other than those items listed above (equipment availability and casting fabrication) the contractor can foresee no high-risk items involved in the fabrication of the transmission system for the heavy-lift helicopter. In fact, many of the components can be considered to be off-the-shelf items. For example, the contractor is currently operating gearboxes equal in size and power capacity to the spiral bevel engine reduction gearboxes, the accessory gearbox, the freewheel units, and input bevel sections of the main gearbox, as well as the input drive shafting.

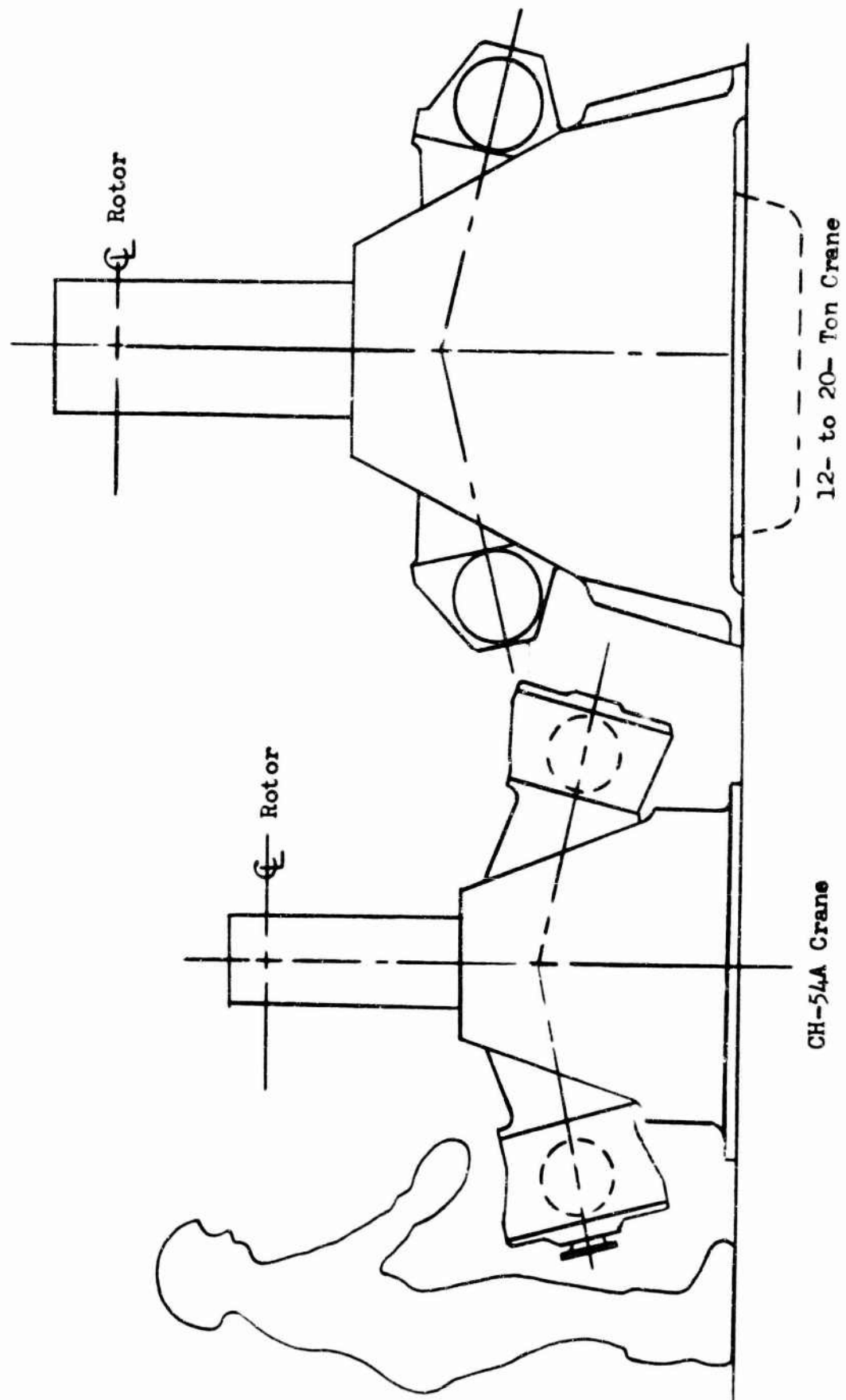


Figure 49. Comparative Sizes, Main Transmissions.

BIBLIOGRAPHY

1. AFBMA Standards, Method of Evaluating Load Ratings for Roller Bearings, Section No. 11, The Anti-Friction Bearing Manufacturers Association, Incorporated, New York, New York, page 1.
2. French, M.J., "Balancing High Speed Rotors at Low Speeds", The Engineer, (British Publication) Volume 215, Number 5605, June 28, 1963, pp. 1154 - 1159.
3. Jepson, D., U.S. Army Crane Helicopter Parametric Study 12-20 Ton Payload, SER-50273, Sikorsky Aircraft, Stratford, Connecticut, June 29, 1962, 125 pages.*
4. Metallic Materials and Elements for Flight Vehicle Structures (MIL-HDBK-5), Department of Defense, Washington 25, D.C., August 1962.
5. Roark, Raymond J., Formulas for Stress and Strain, Third Edition, McGraw-Hill Book Company, Incorporated, New York, New York, 1954.
6. Strength of Bevel and Hypoid Gears, Gleason Works, Rochester, New York, 1955, page 30.
7. Technical Documentary Report No. ASD-TDR-62-728, Part I, Design Criteria for High-Speed Power-Transmission Shafts, Flight Accessories Laboratory, Directorate of Aeromechanics, Aeromautical Systems Division, Air Force Systems Command, Wright-Patterson Air Force Base, Ohio, August 1962.
8. Thompson, William T., Mechanical Vibrations, Second Edition, Prentice-Hall, Incorporated, Englewood Cliffs, New Jersey, June 1959, pages 186 and 216.
9. TRECOM Technical Report 64-12, Feasibility Investigation of Harmonic Drive Speed Reducers for Helicopter Applications, U.S. Army Aviation Material Laboratories, Fort Eustis, Virginia (formerly U.S. Army Transportation Research Command), May 1964.

*Note: Item 3 is not being furnished as subject data under this contract, but is merely a reference that has been made available to the Government on a limited rights basis in accordance with ASPR 3-506 in response to TC REC-RC, dated 1 February 1962. Its further distribution is subject to Sikorsky Aircraft Division of United Aircraft Corporation approval.

DISTRIBUTION

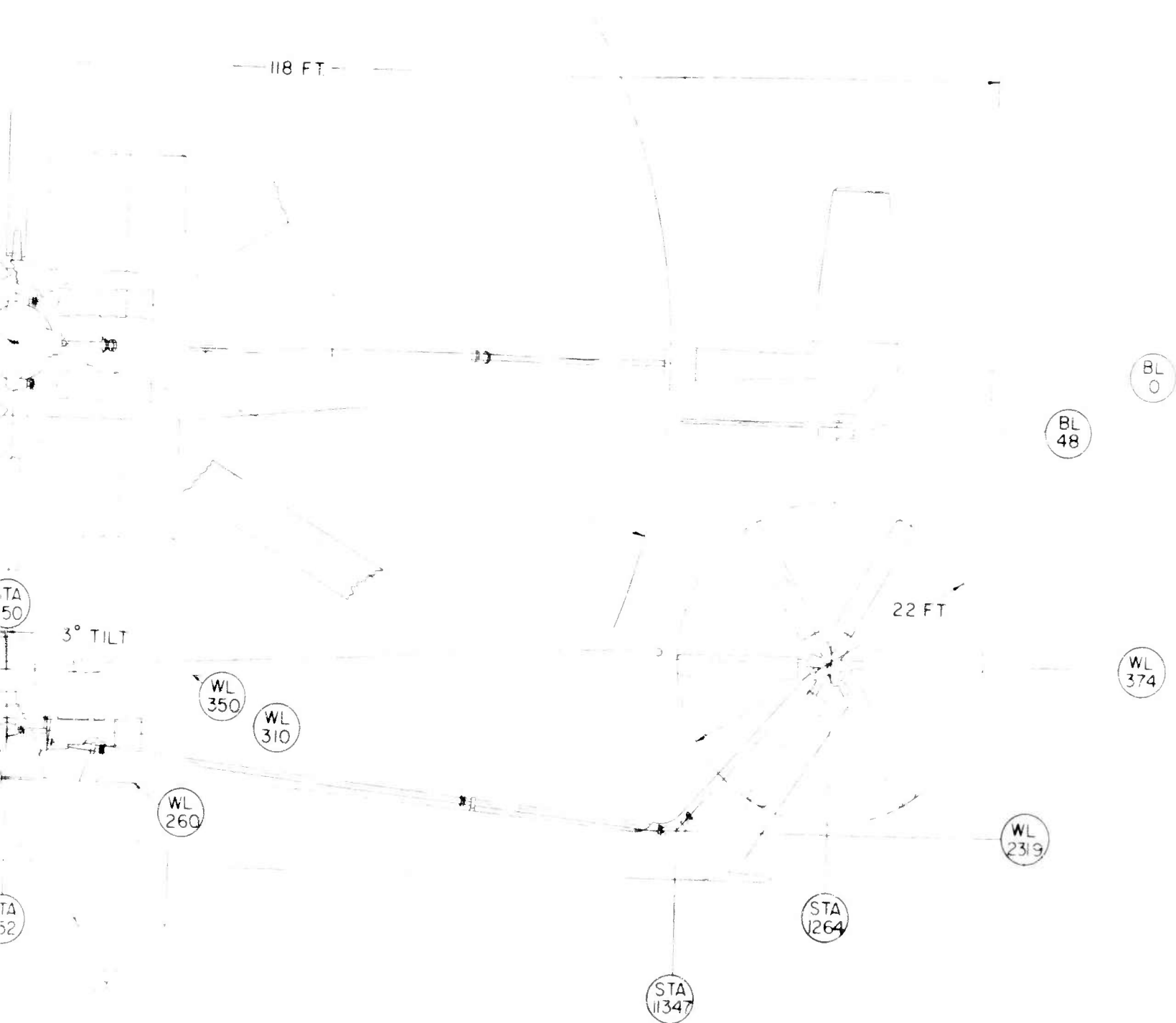
US Army Materiel Command	16
US Army Mobility Command	3
US Army Aviation Materiel Command	2
Office of Ordnance, ODDR&E	1
Chief of R&D, DA	3
US Army Aviation Materiel Laboratories	24
US Army R&D Group (Europe)	1
US Army Engineer R&D Laboratories	2
US Army Limited War Laboratory	1
US Army Human Engineering Laboratories	1
US Army Research Office-Durham	1
US Army Test and Evaluation Command	1
US Army Engineer Waterways Experiment Station	1
US Army Combat Developments Command, Fort Belvoir	1
USACDC Armor Agency	1
US Army Combat Developments Command Transportation Agency	1
US Army Combat Developments Command Experimentation Command	1
US Army War College	1
US Army Transportation School	1
US Army Aviation School	1
US Army Aviation Test Board	1
US Army Aviation Test Activity	1
Air Force Flight Test Center, Edwards AFB	1
US Army Transportation Engineering Agency	1
US Army General Equipment Test Activity	1
US Army Field Office, AFSC Andrews AFB	1
Air Force Systems Command, Wright-Patterson AFB	2
Air Force Avionics Laboratory, Wright-Patterson AFB	1
Air Force Flight Dynamics Laboratory, Wright-Patterson AFB	1
Air Proving Ground Center, Eglin AFB	1
Chief of Naval Operations	1
Bureau of Ships, DN	1
Bureau of Naval Weapons	1
Bureau of Supplies and Accounts, DN	1
Chief of Naval Research	2
US Naval Supply R&D Facility	1
US Naval Air Station, Patuxent River	1
Marine Corps Liaison Officer, US Army Transportation School	1
Ames Research Center, NASA	1
Lewis Research Center, NASA	1
Manned Spacecraft Center, NASA	1
NASA Representative, Scientific and Technical Information Facility	2
Defense Documentation Center	20
US Patent Office	1
US Government Printing Office	1

APPENDIX I

TRANSMISSION SYSTEM DRAWINGS



FIGURE 50 12- TO 20-TON
FRONT-DRIVE TRUCK



N CRANE
TURBINE INSTALLATION. HLH-10

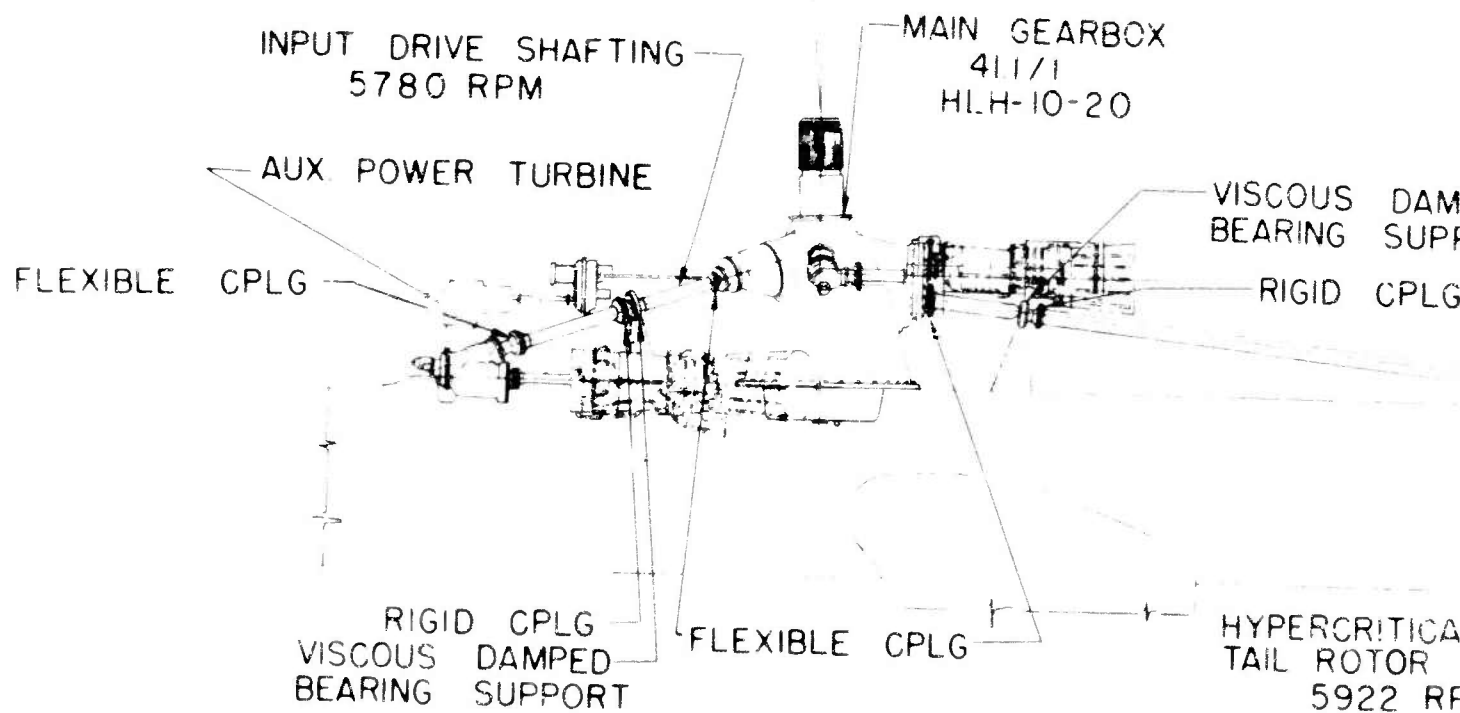
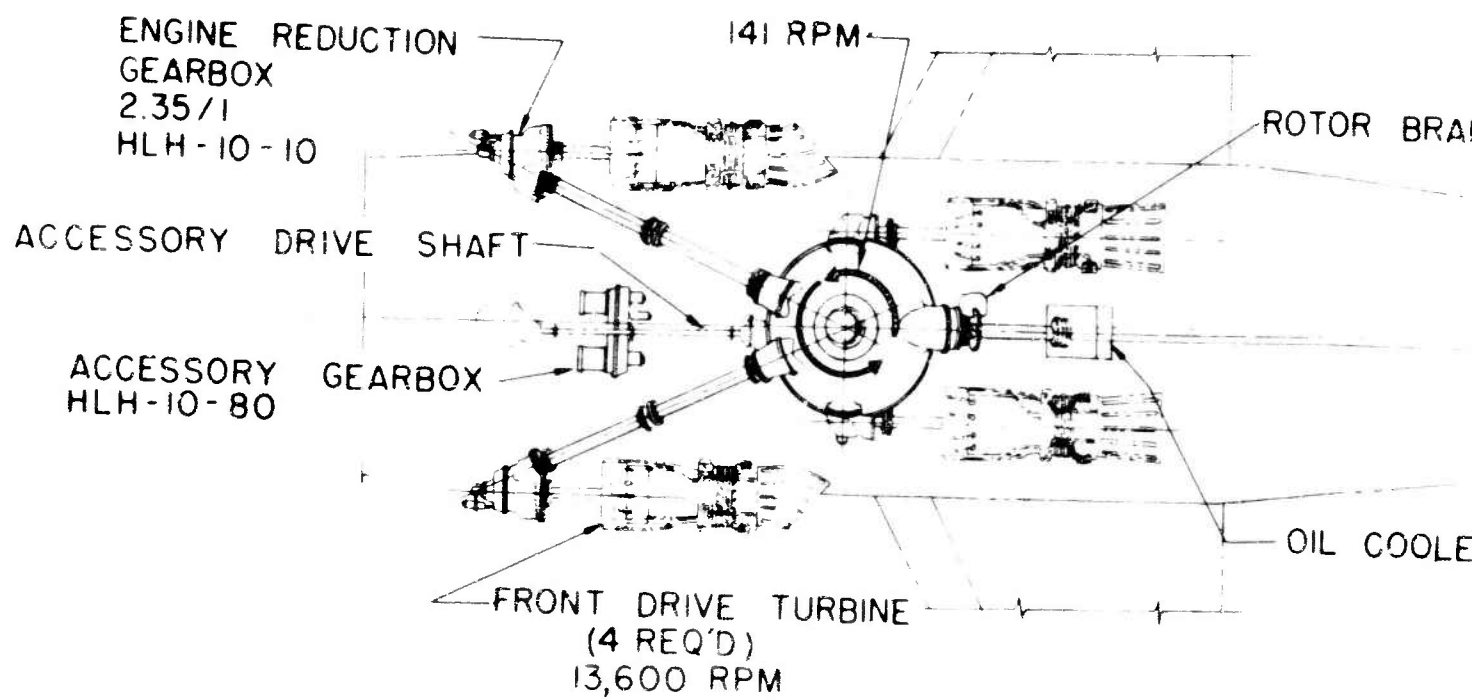


FIGURE 51. 12
TRANSMISSION
FRONT- DRIVE
HLH-10-1

BRAKE

OLER

TAIL ROTOR GEARBOX
6.18/1
HLH-10-60

DAMPED
SUPPORT
PLG

OIL COOLER
PYLON DRIVE SHAFT
3760 RPM
607 RPM

RIGID CPLG
VISCIOUS DAMPED
BEARING SUPPORT

FLEXIBLE CPLG

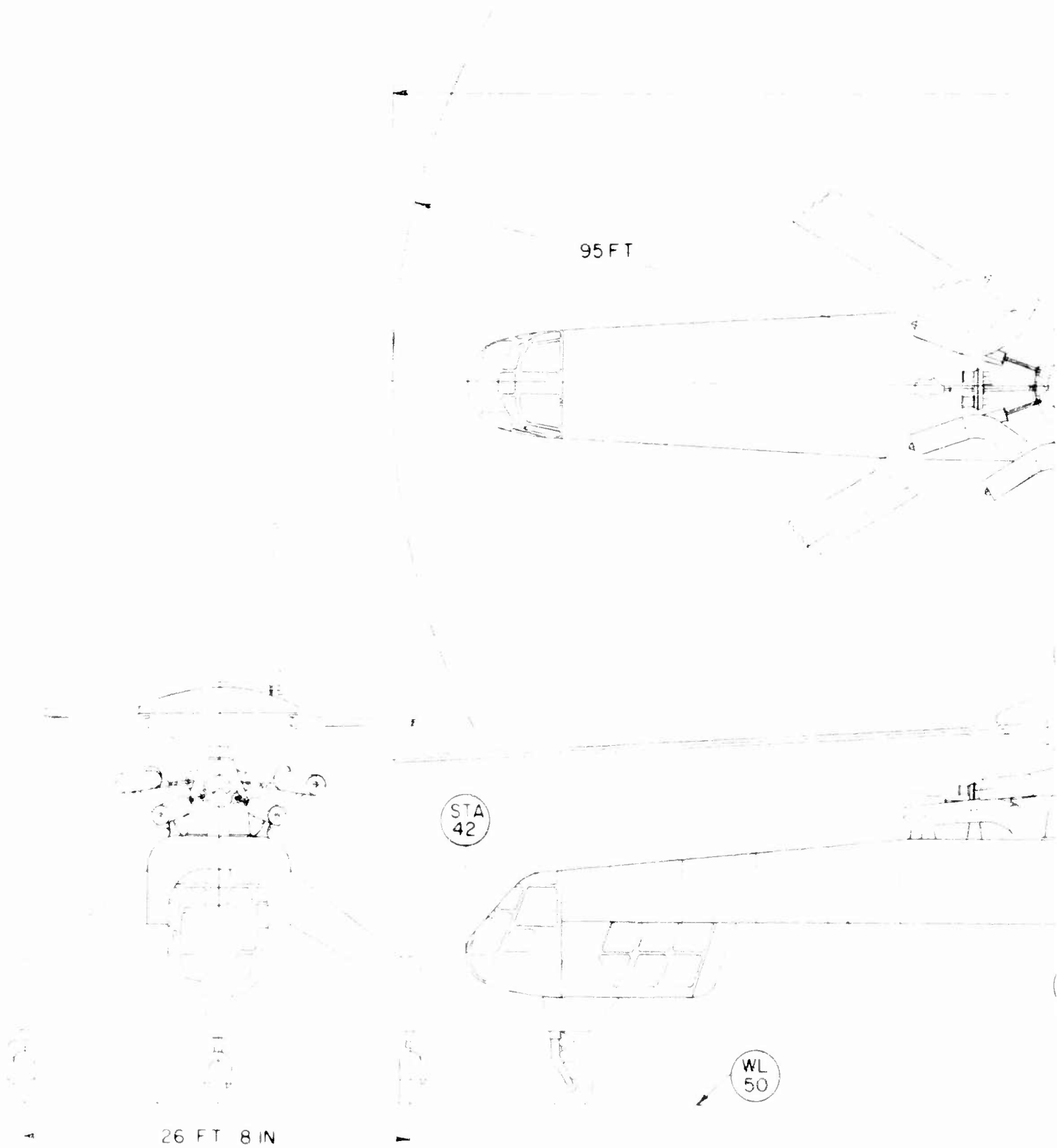
OIL COOLER

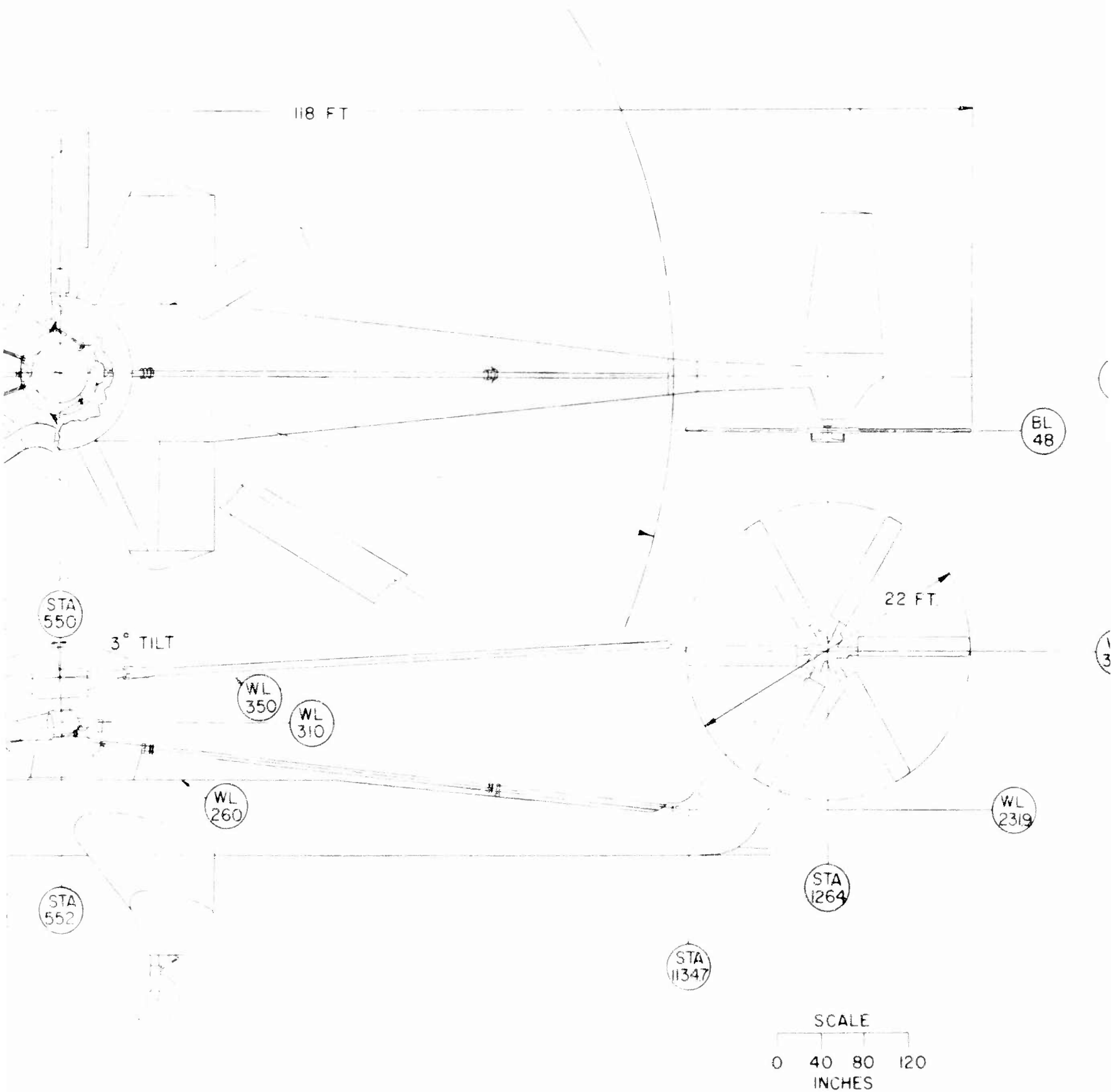
FICAL
OR DRIVE SHAFTING
RPM

FLEXIBLE CPLG

INTERMEDIATE
GEARBOX
HLH-10-40
1.57/1

12- TO 20- TON CRANE
ON SYSTEM SCHEMATIC,
VE TURBINE INSTALLATION.





TO 20-TON CRANE
CAR-DRIVE TURBINE INSTALLATION. HLH-20

ENGINE MANUFACTURER'S
REDUCTION GEARBOX
3.22 / 1

141 RPM.

FLEXIBLE CPLG.

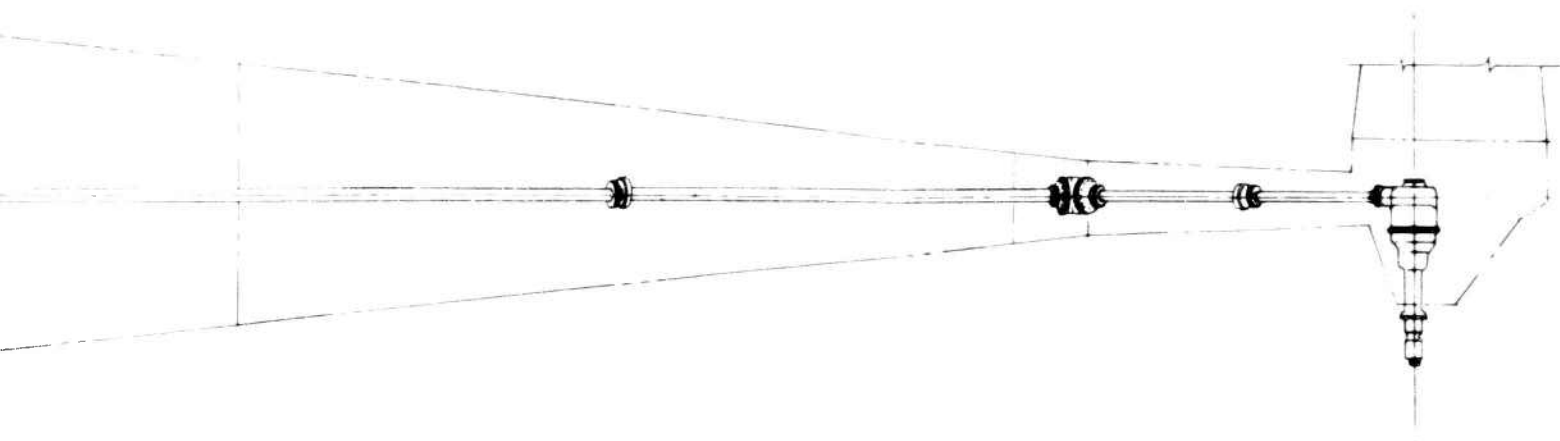
INPUT DRIVE SHAFT
6,000 RPM

REAR DRIVE TURBINE
(4 REQ - 19,320 RPM)

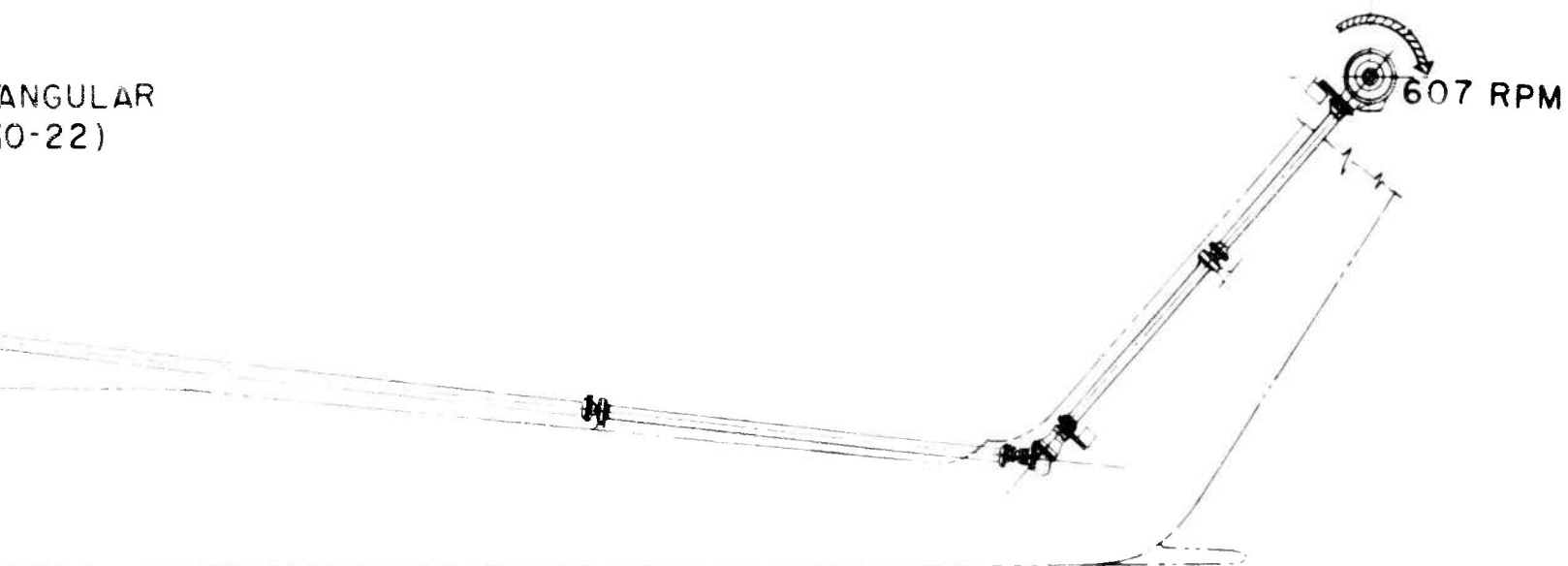
MAIN GEARBOX
42.67 / 1 HLH-10-20
MODIFIED TO INCL. AN
INPUT DRIVES (HLH-20-

TRANSMIS
(SAME AS FI

FIGURE 53.
TRANSMISSIO
REAR- DRIVE
HLH-20-1

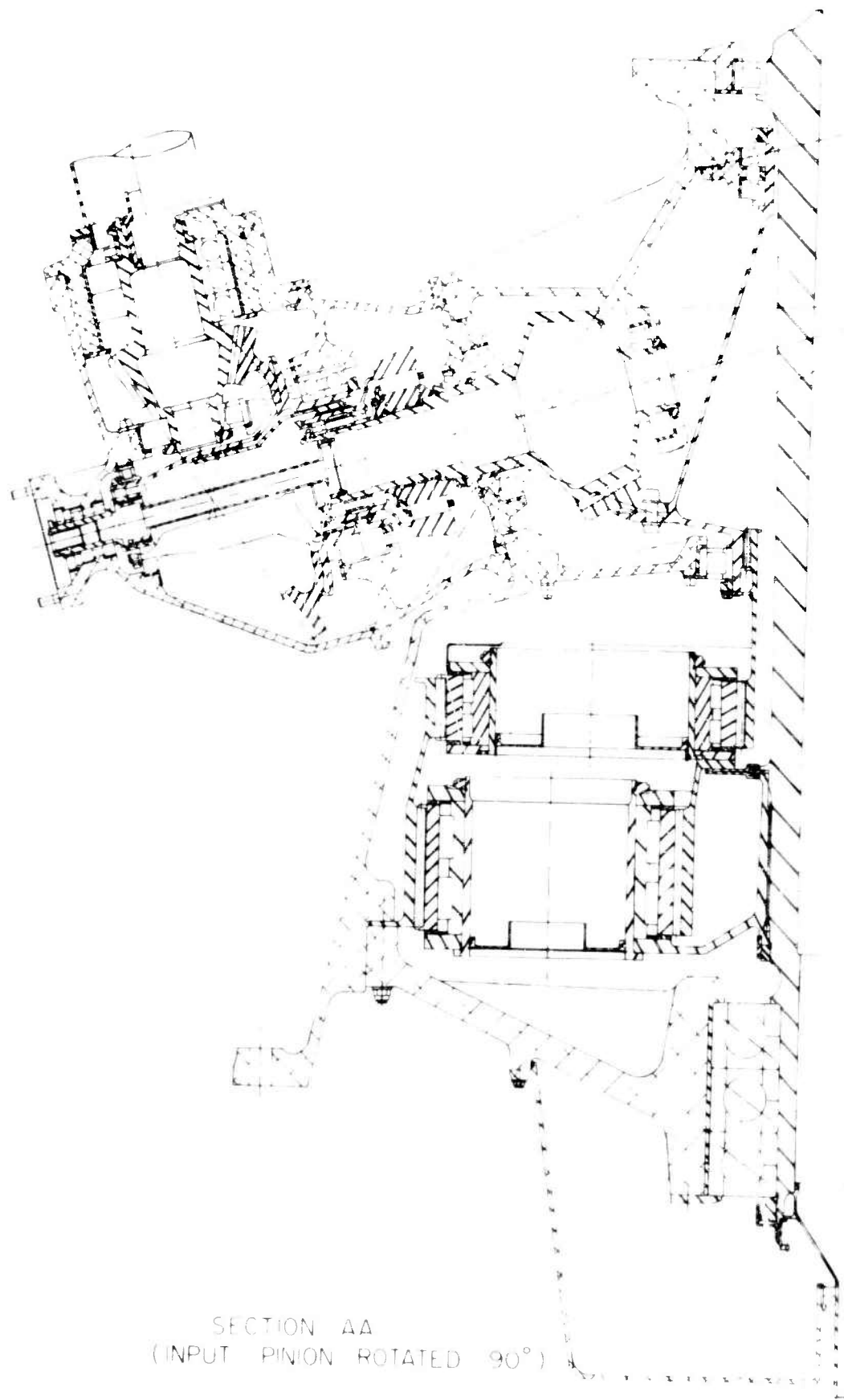


ANGULAR
(O-22)



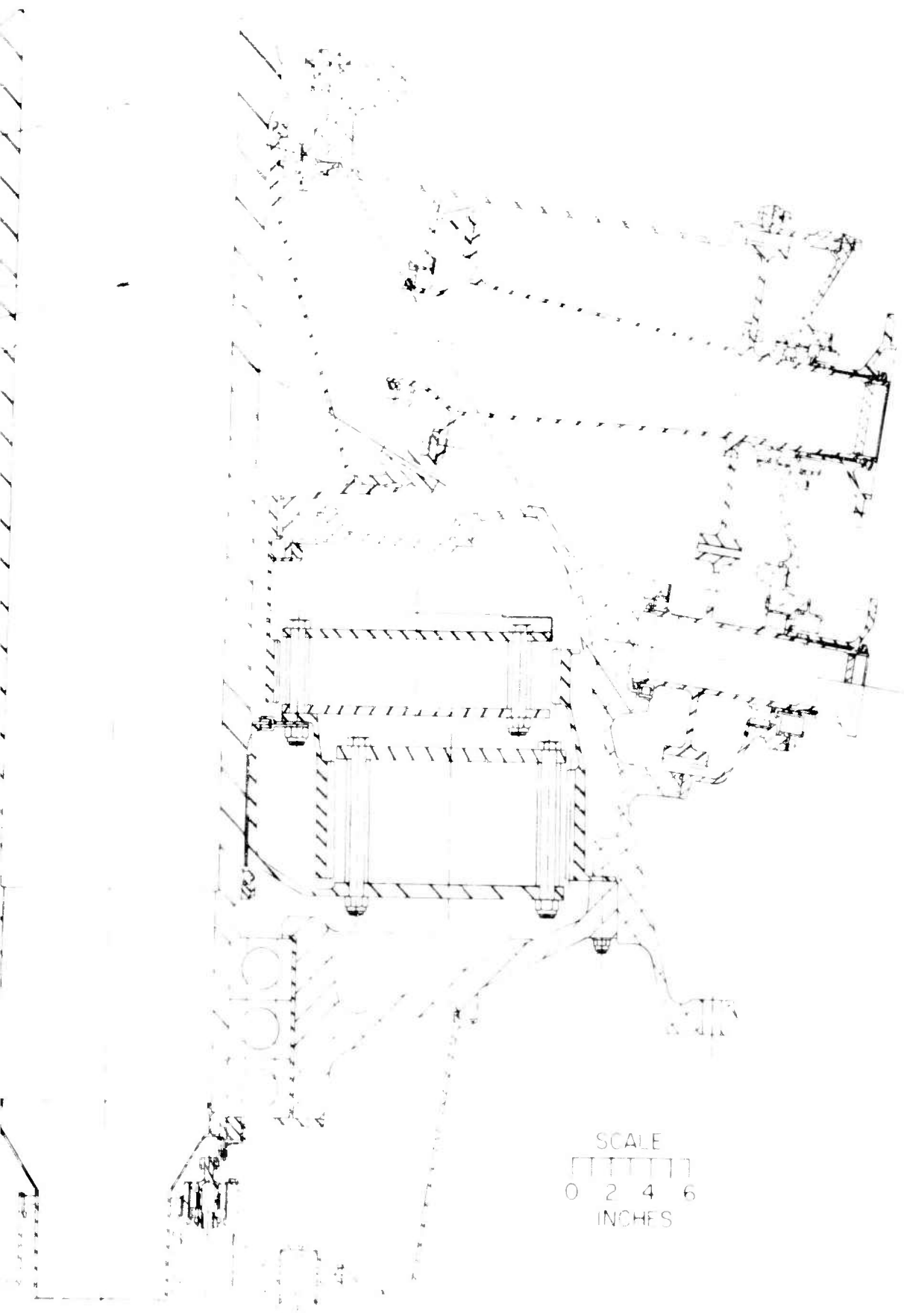
MISSION SYSTEM
(FIG 51 EXCEPT AS SHOWN)

12- TO 20- TON CRANE
MISSION SYSTEM SCHEMATIC,
VE TURBINE INSTALLATION.



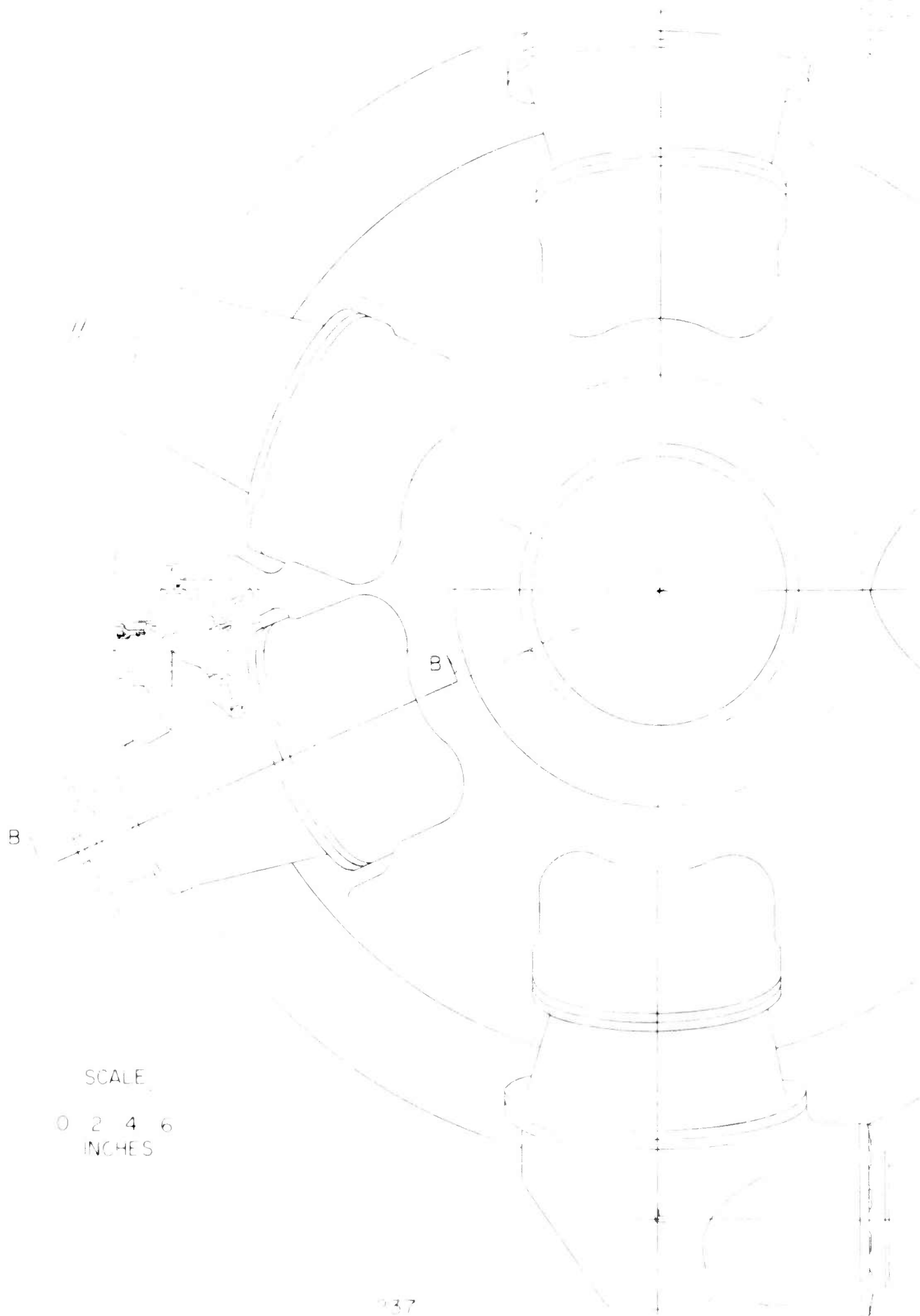
SECTION AA
(INPUT PINION ROTATED 90°)

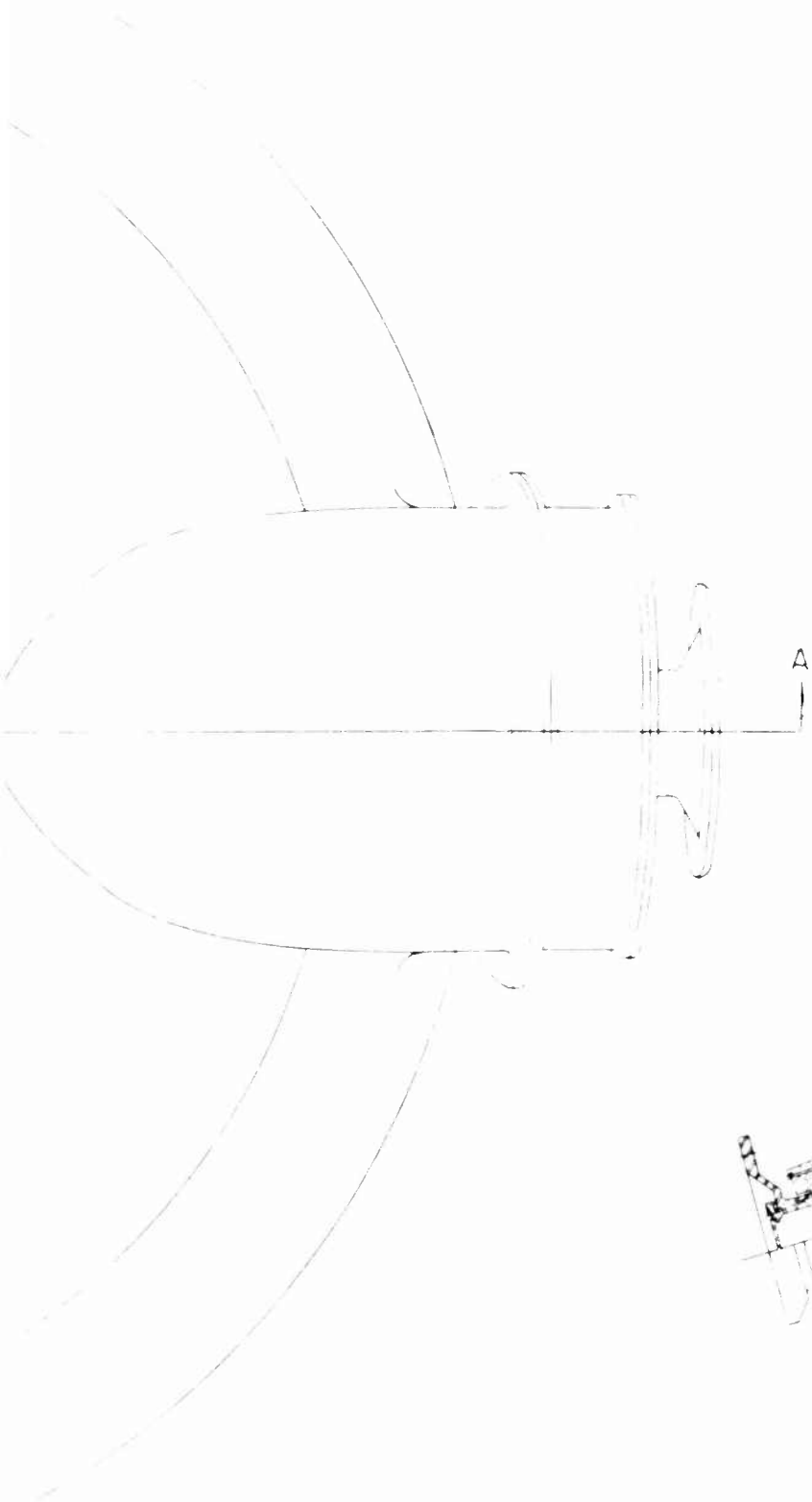
FIGURE 54 MAIN
HLP



SCALE
0 2 4 6
INCHES

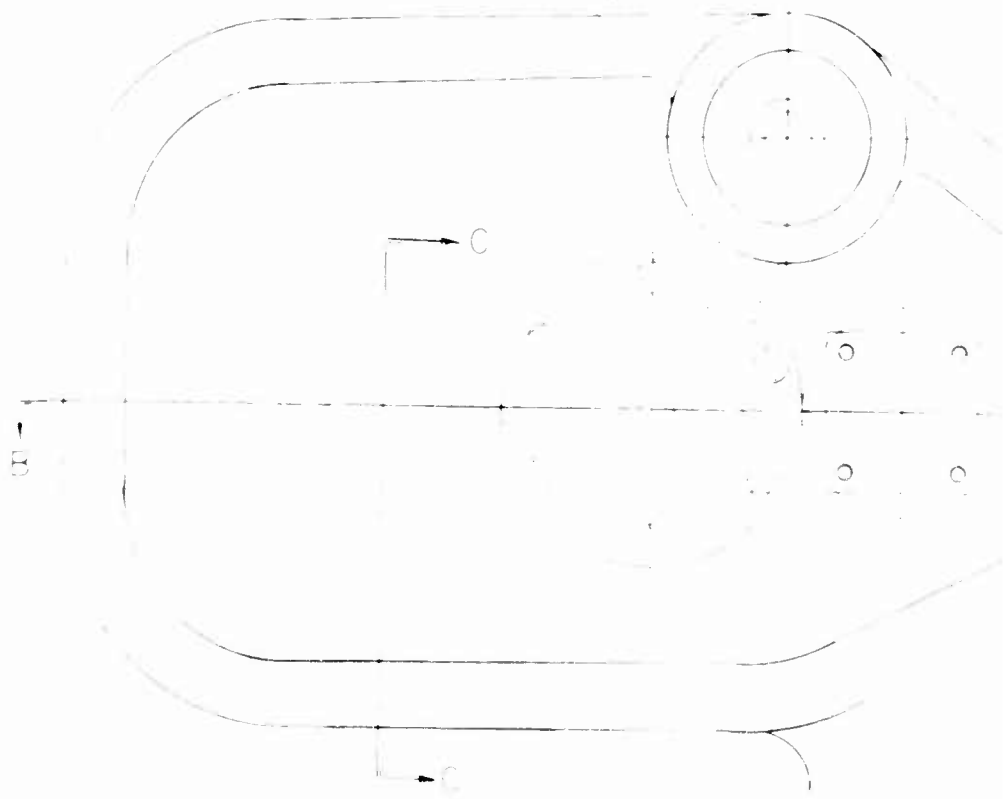
MAIN GEAR X
REL 10-20 24 10 1





SECTION B B
(INPUT ONLY)

FIGURE 54 MAIN GEARBOX
HLH-10-20 SHEET 2



A

SECTION B-B

LUBE PUMP

SECTION C-C
BOX ONLY
LEFT HAND

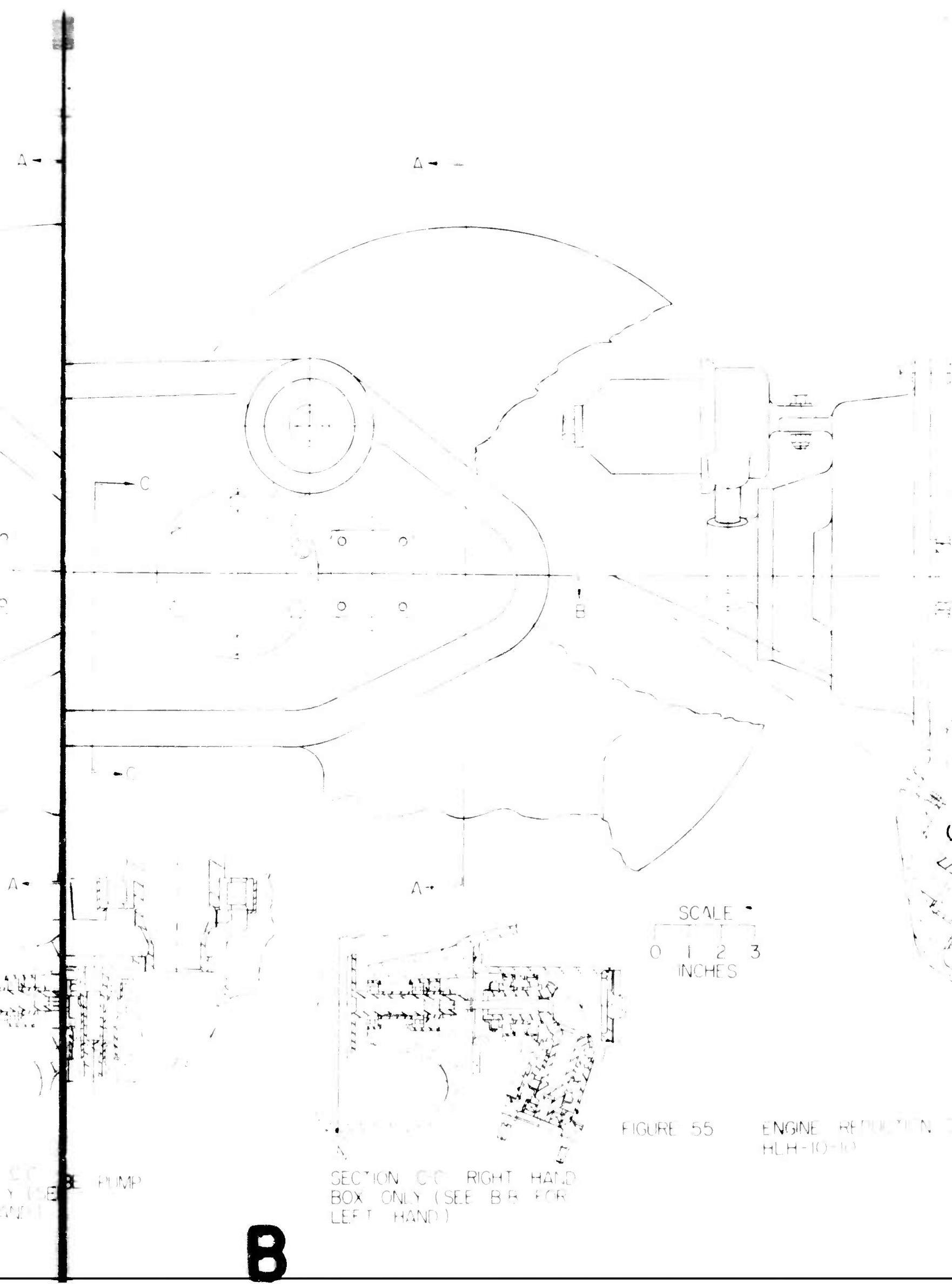
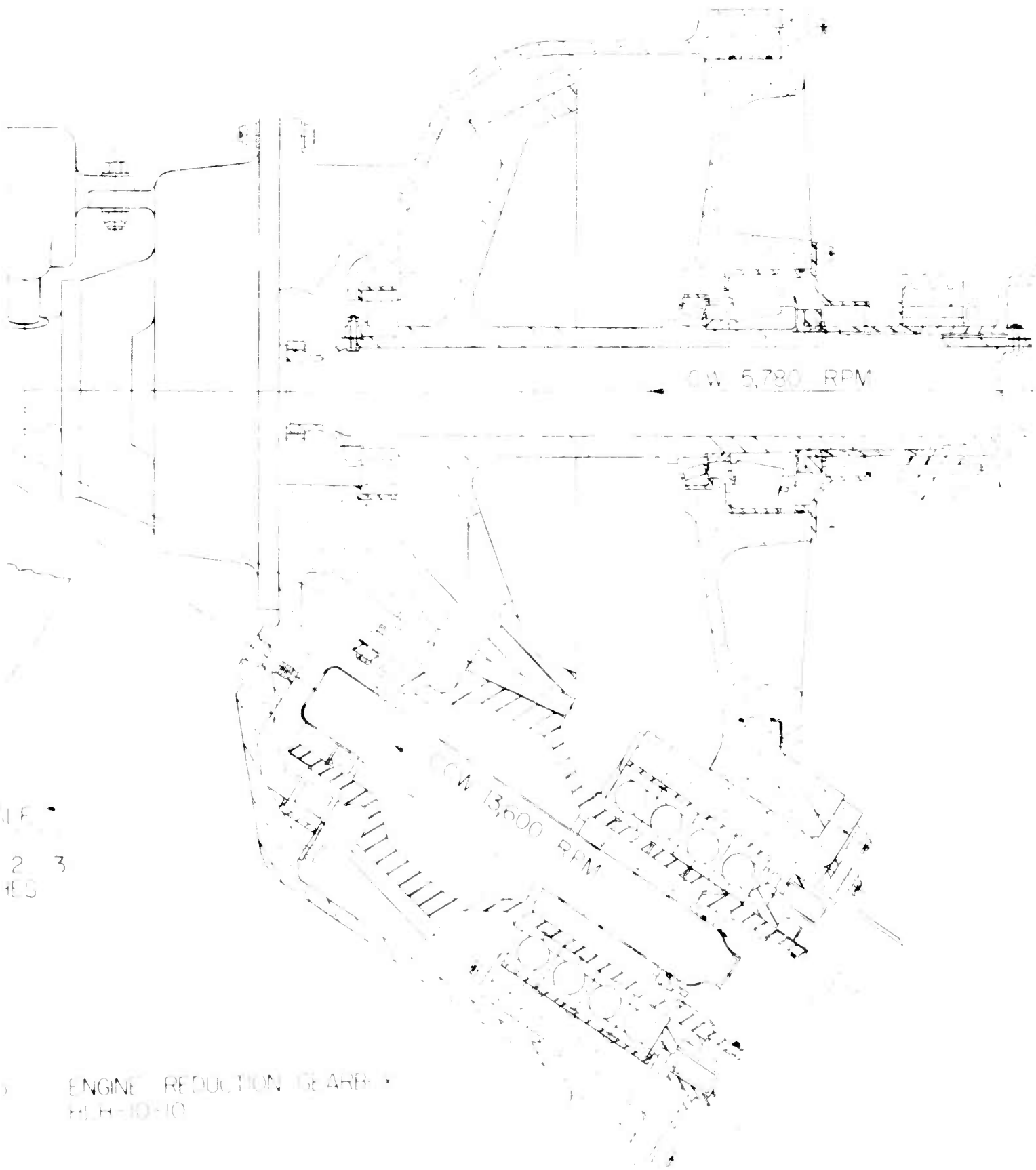


FIGURE 55

ENGINE REPRODUCTION
HLH-10-10

SECTION C-C RIGHT HAND
BOX ONLY (SEE B-B FOR
LEFT HAND)

B



C

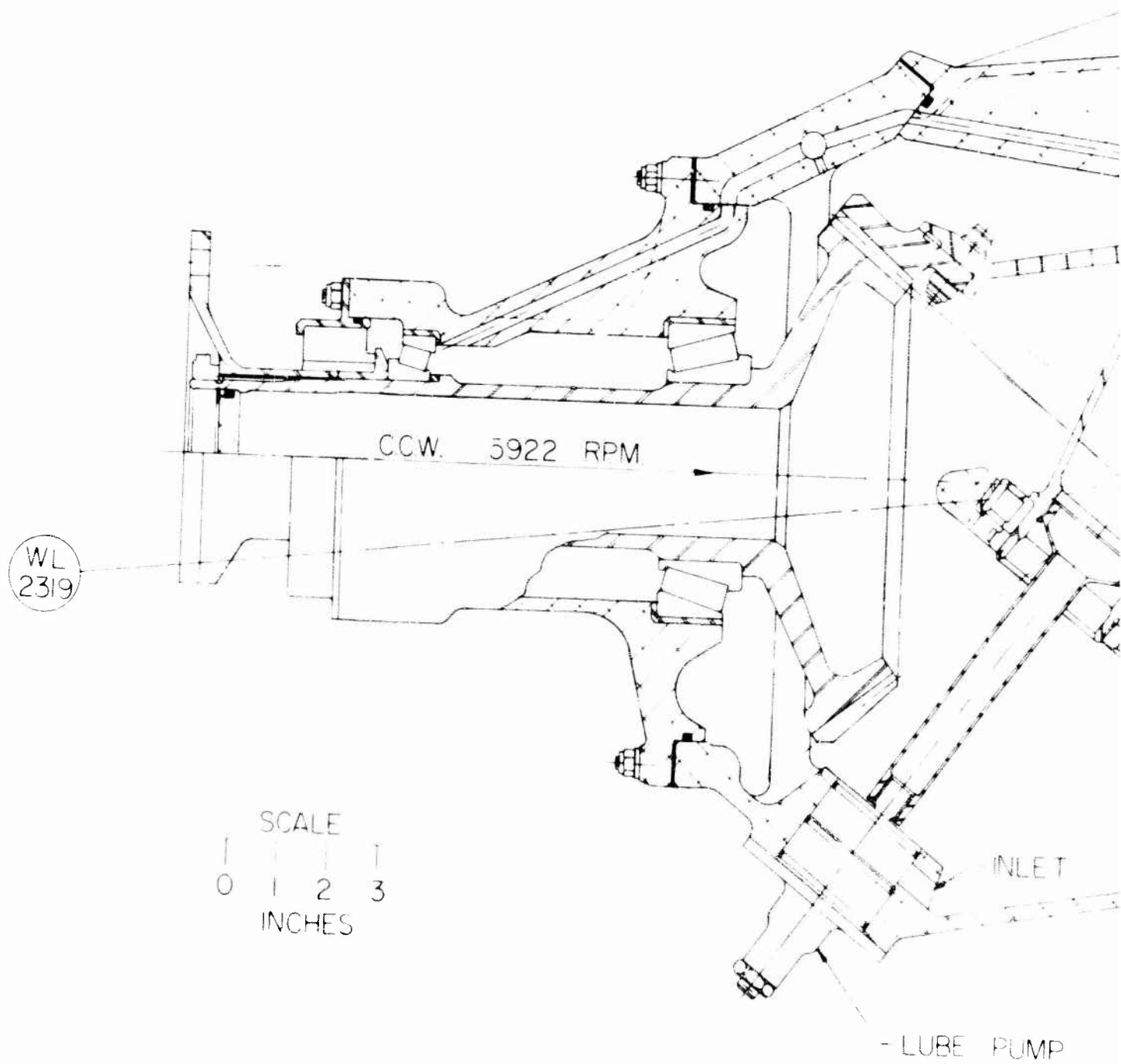


FIGURE 56 INTERMEDIATE GEARBOX
HLH-10-40

A

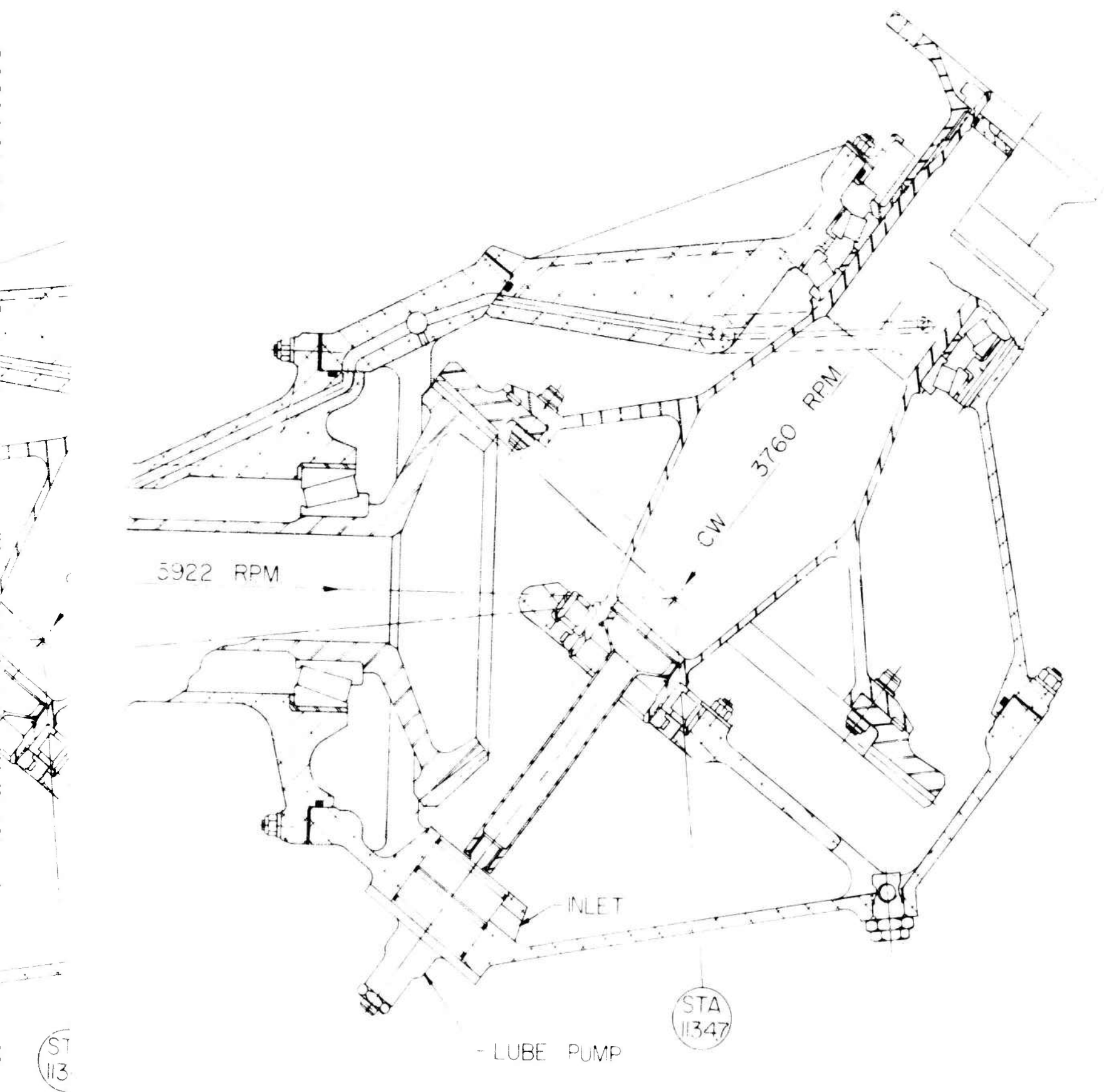
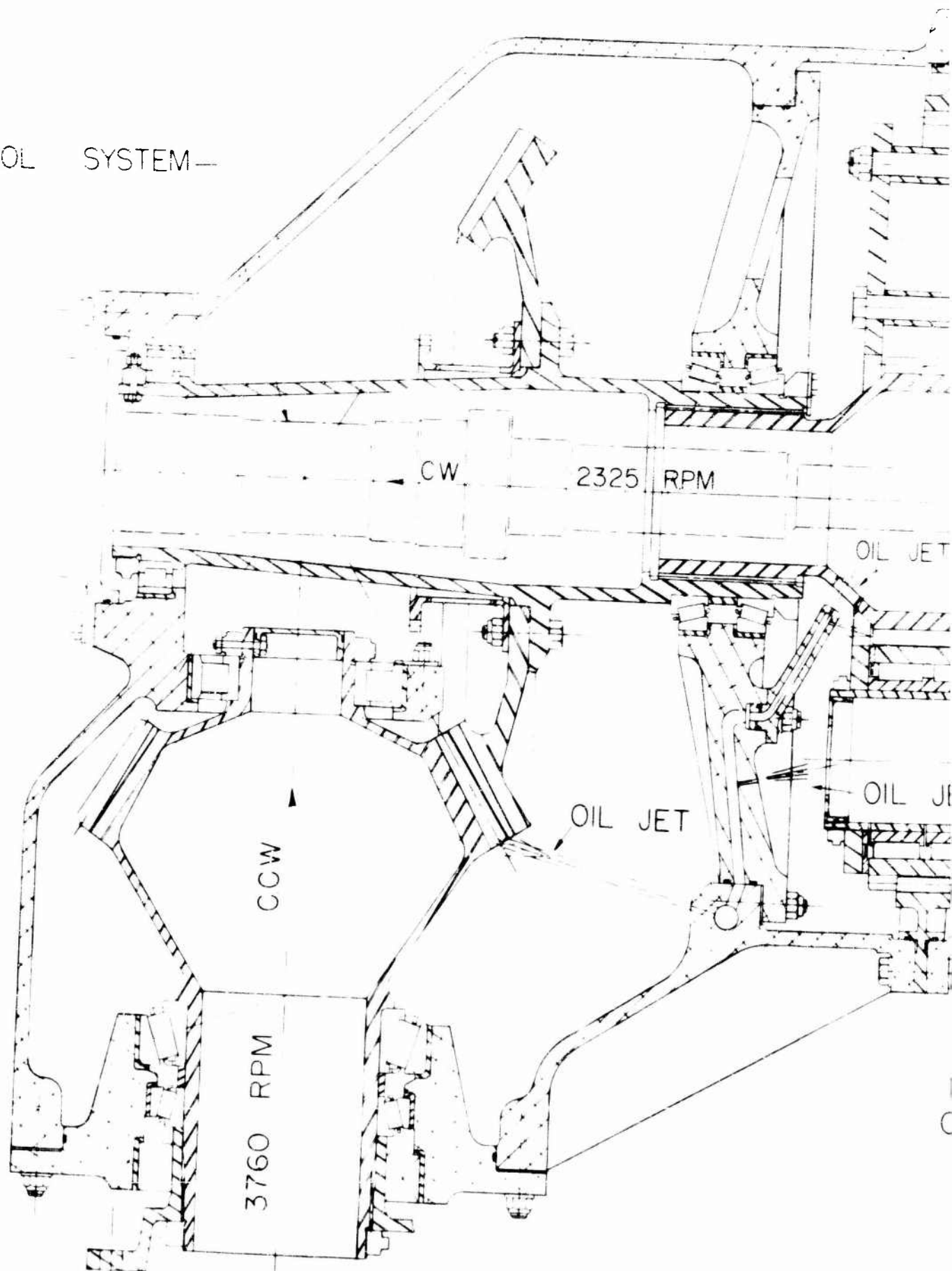


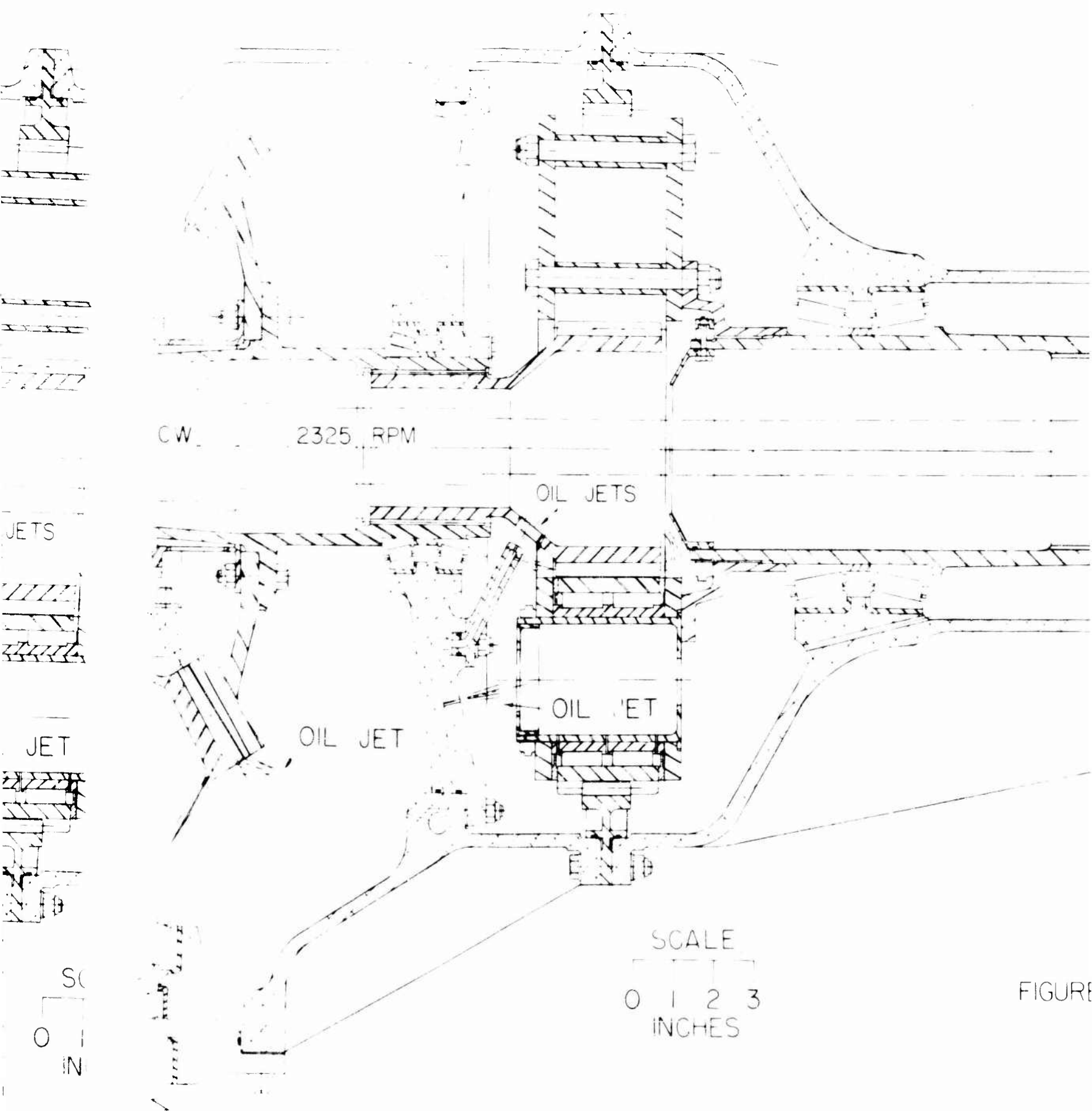
FIGURE 56 INTERMEDIATE GEAR BOX
HLH-10-40

B

CONTROL SYSTEM—



A



FIGURE

B

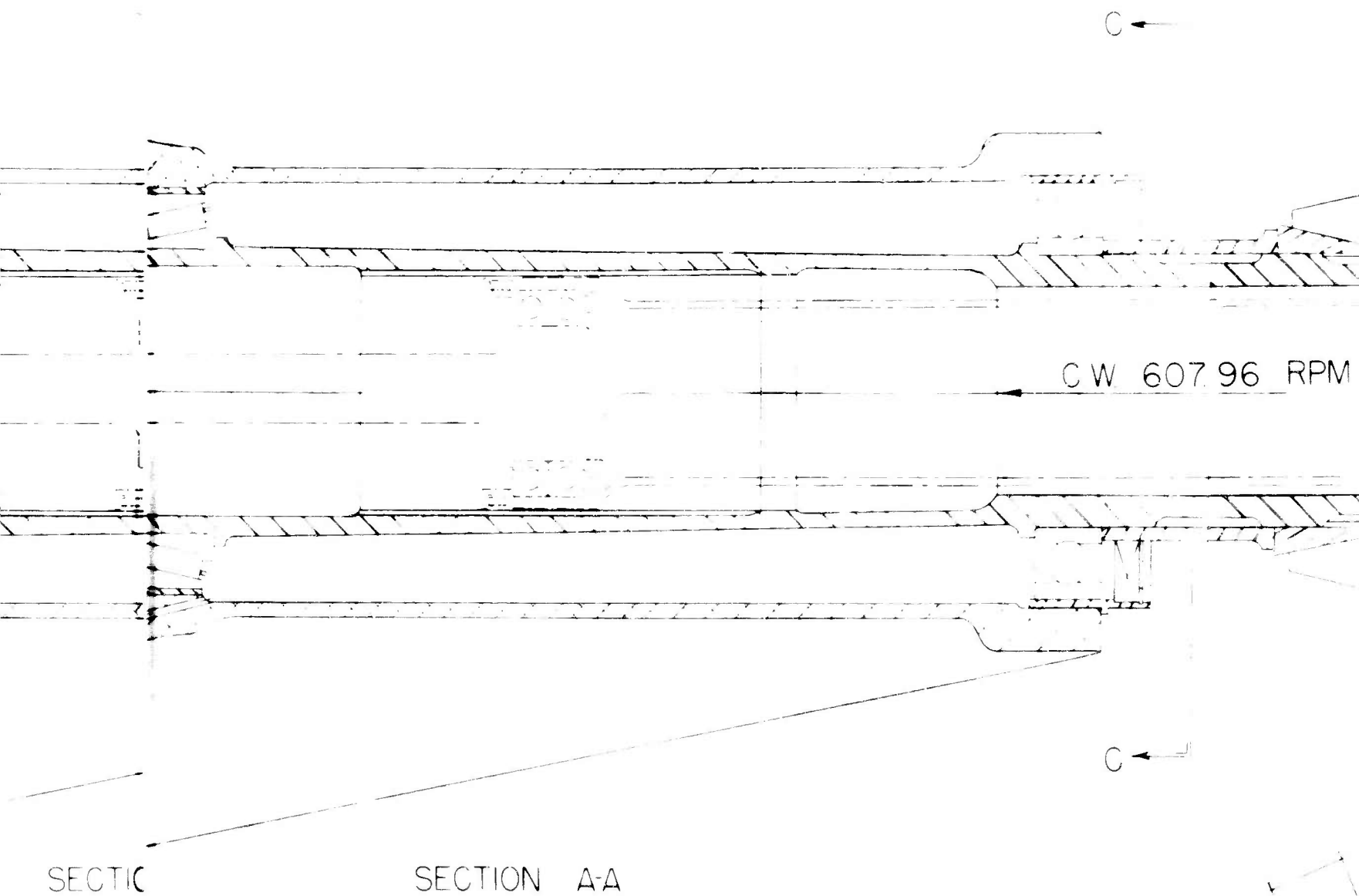
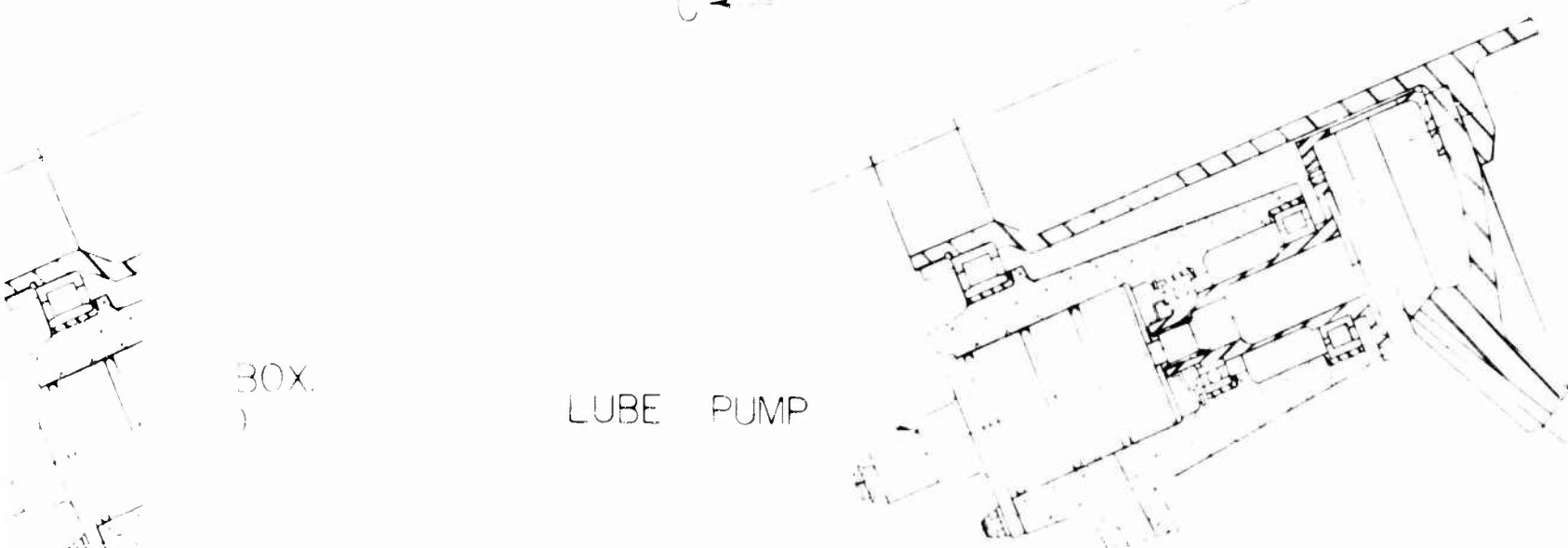
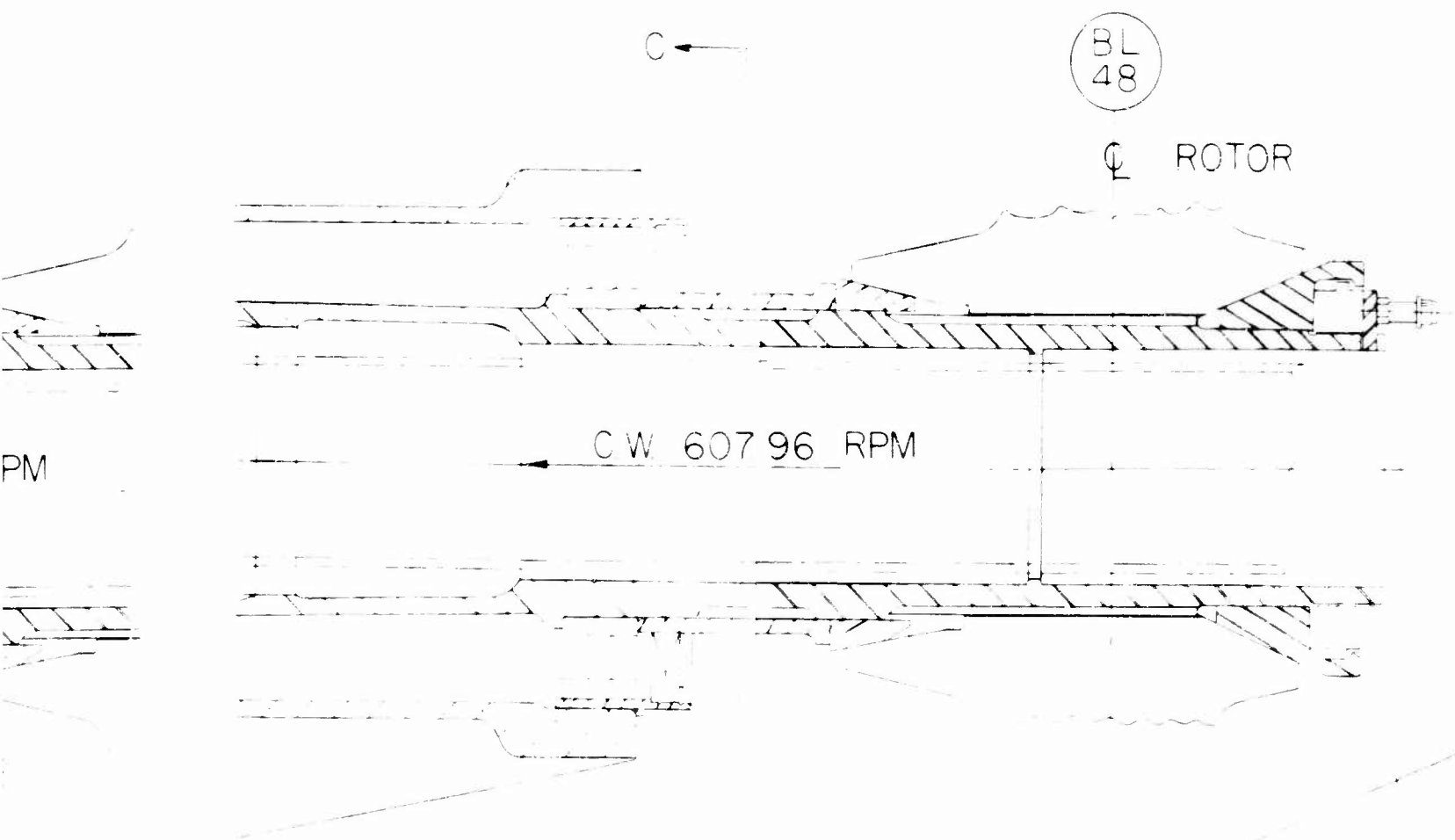


FIGURE 57

FIGURE 57 TAIL GEARBOX.
HLH-10-60

LUBE PUMP

C



SECTION B B

D

TA
(AS V

► A

WL
374

B

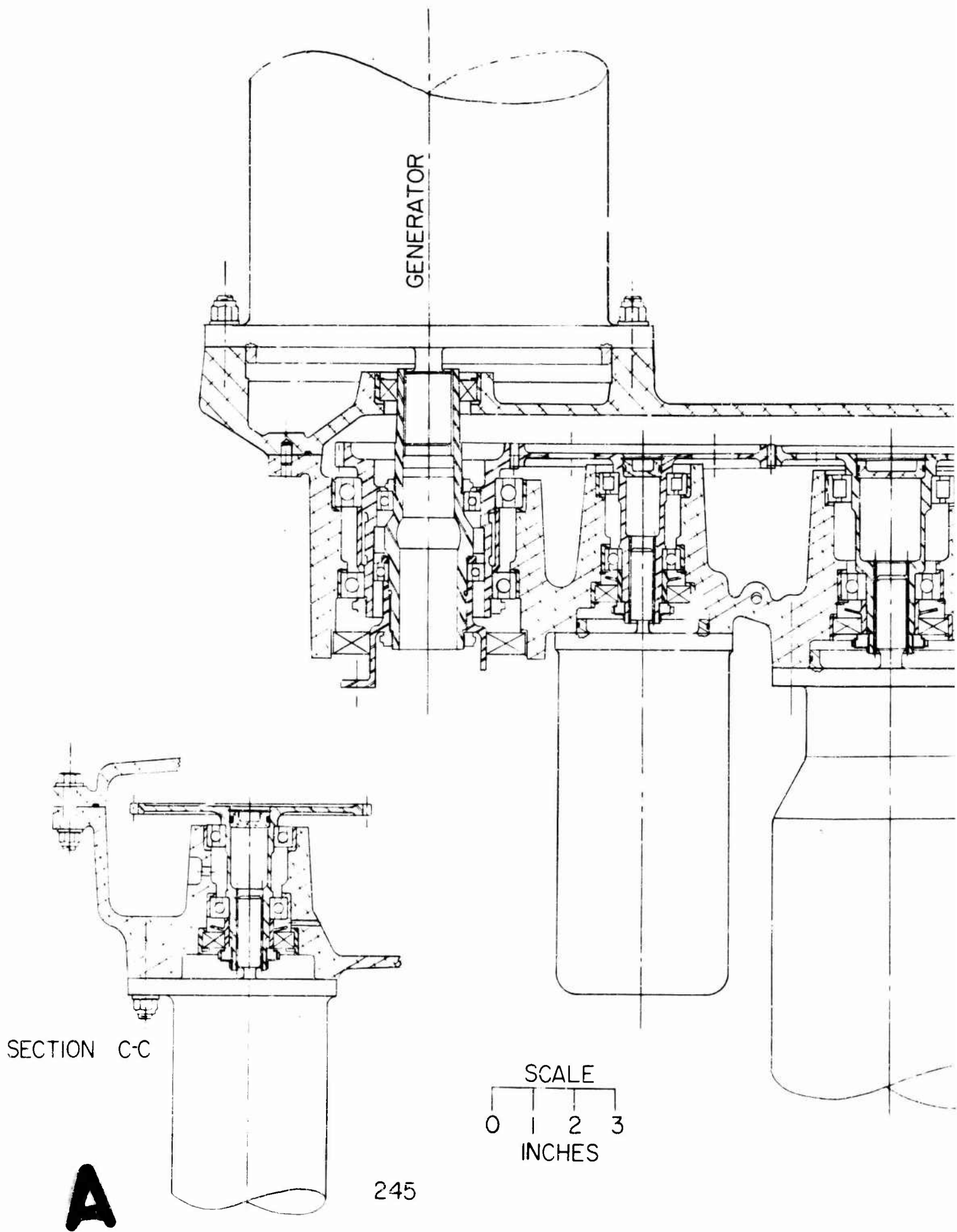
STA
1264

TAIL GE
VIEWED

TAIL GEARBOX
VIEWED FROM (C-C)

► A

E



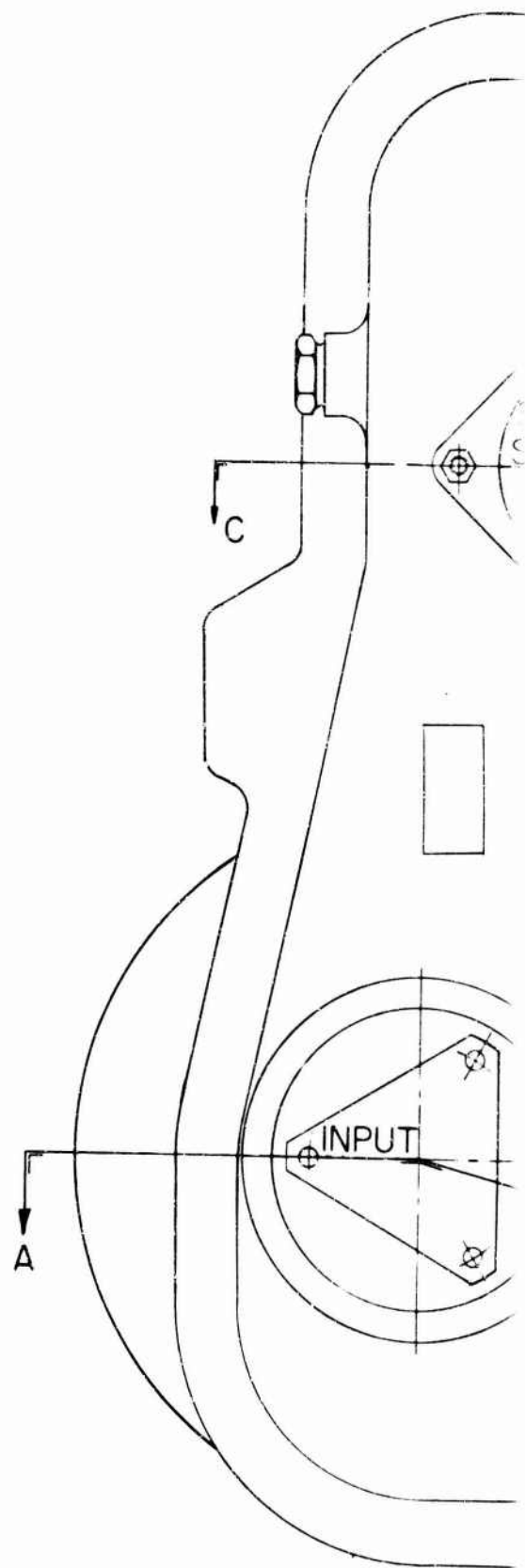
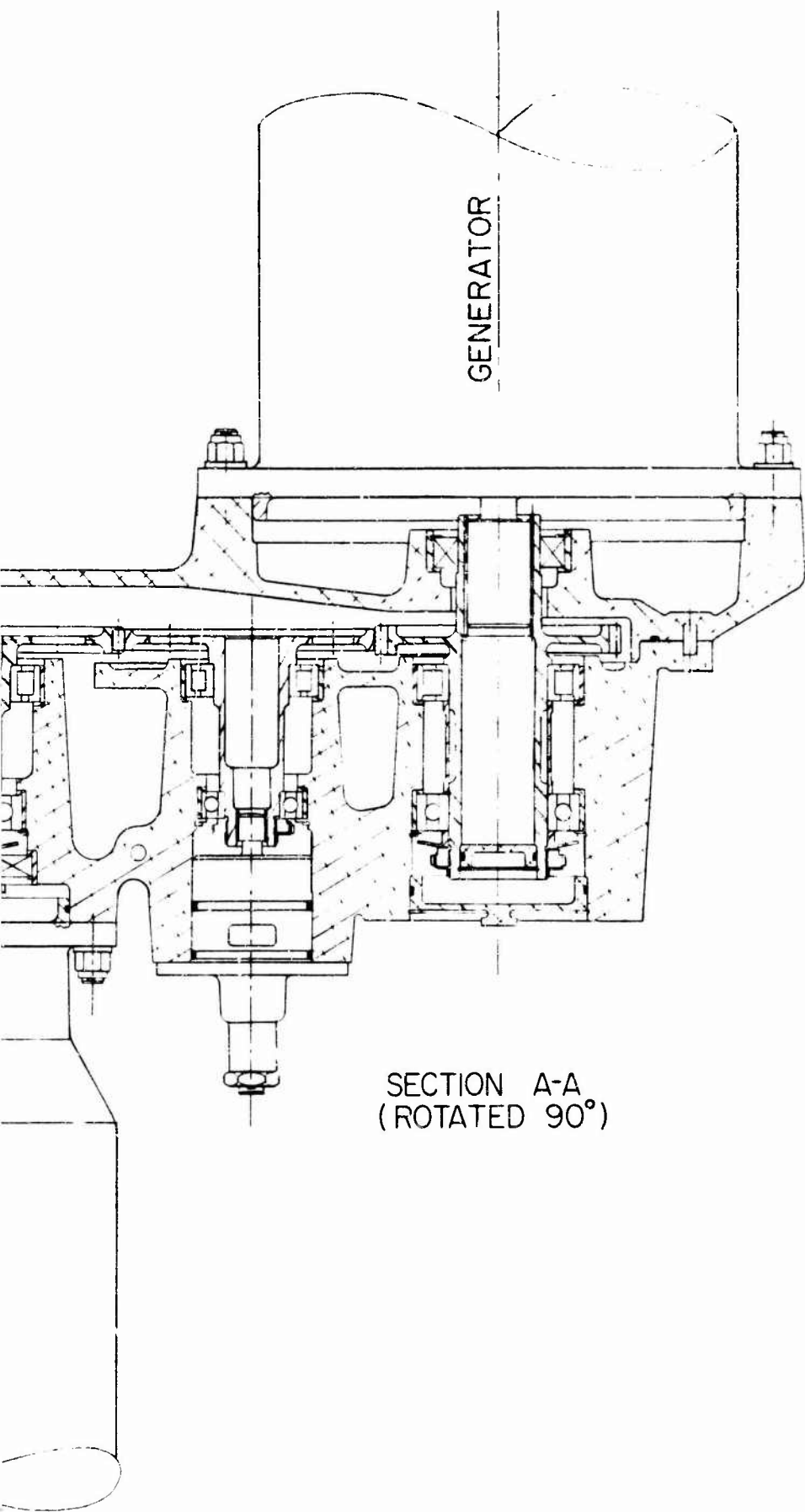
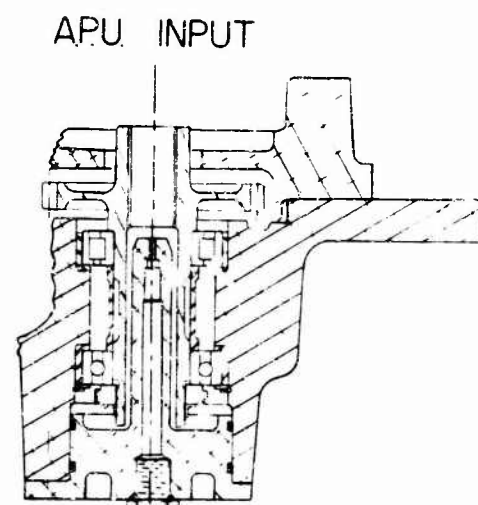
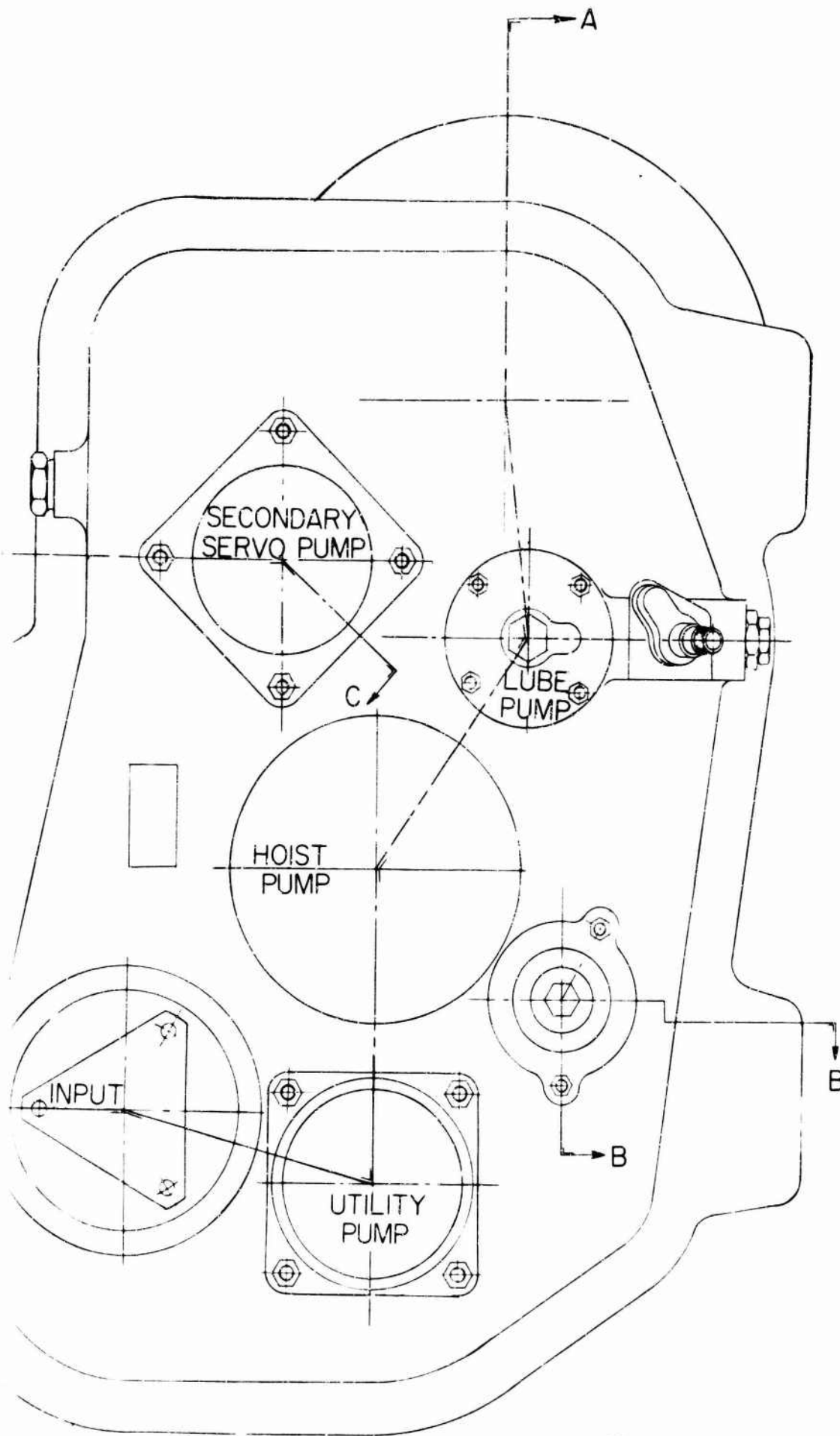


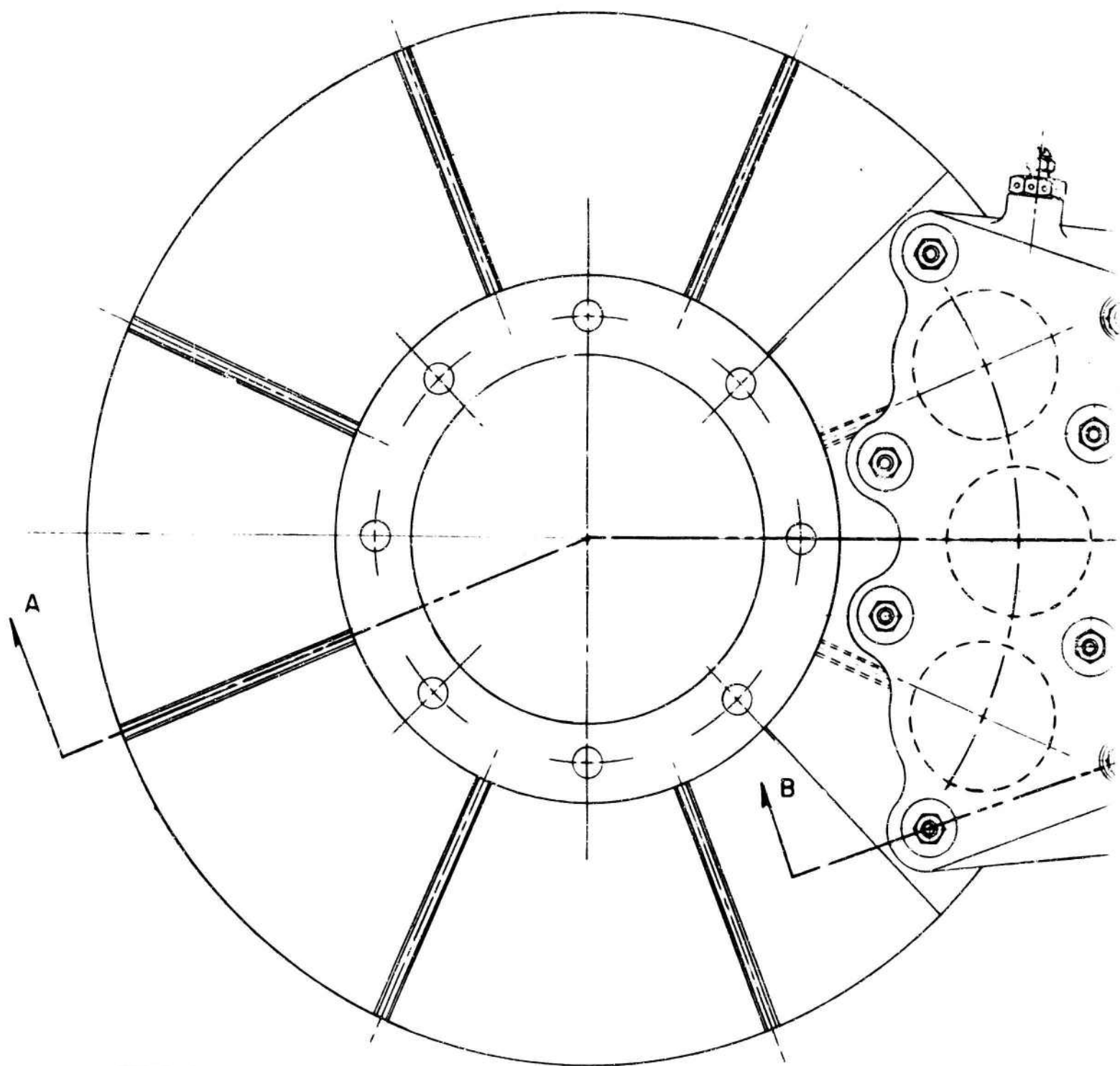
FIGURE 58 ACCESSORY GEARBOX
HLH-10-80

B



SECTION B-B

C



SCALE
0 1 2 3
INCHES

FIGURE 59. ROT.
HLH

DT
LH

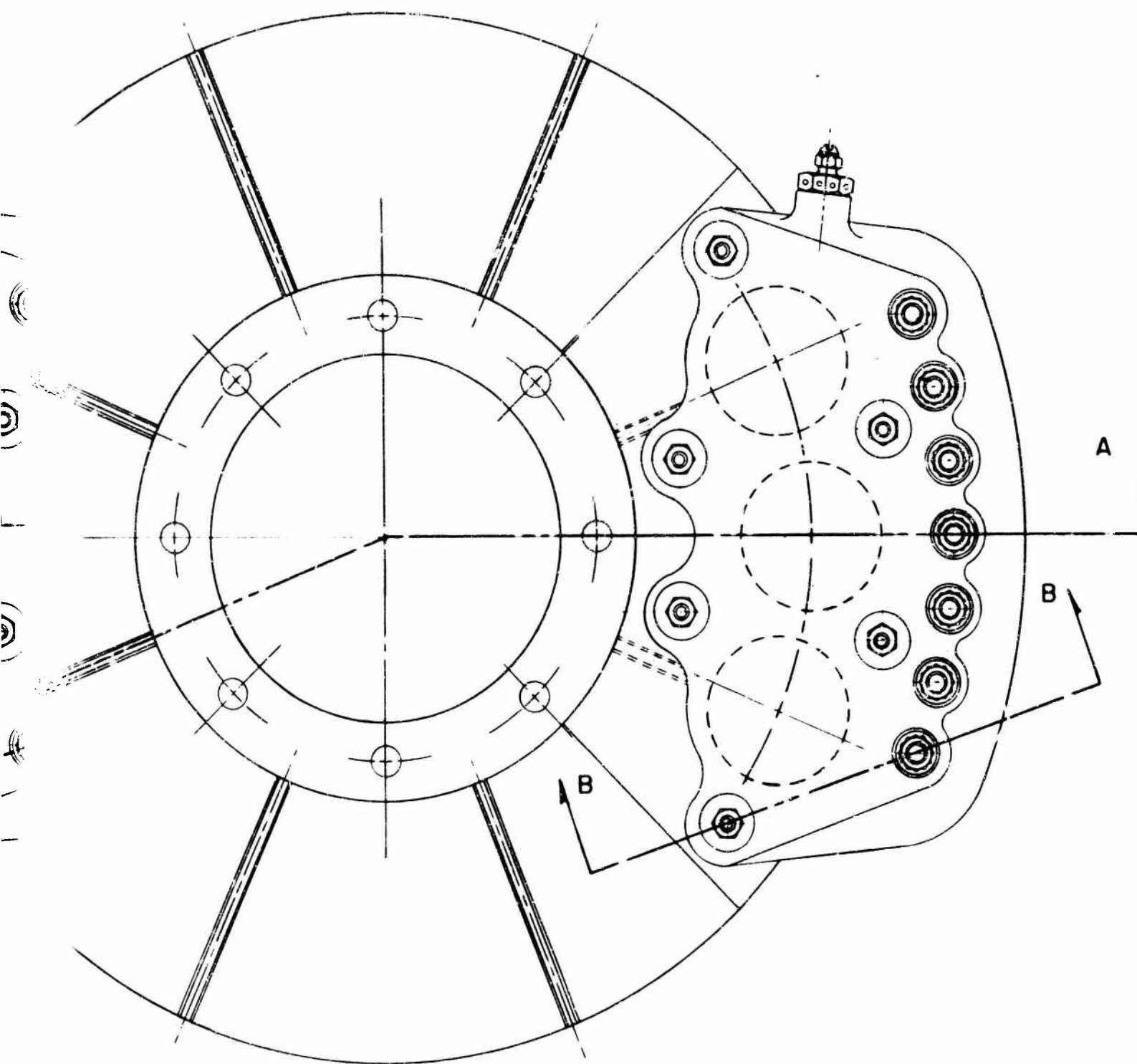
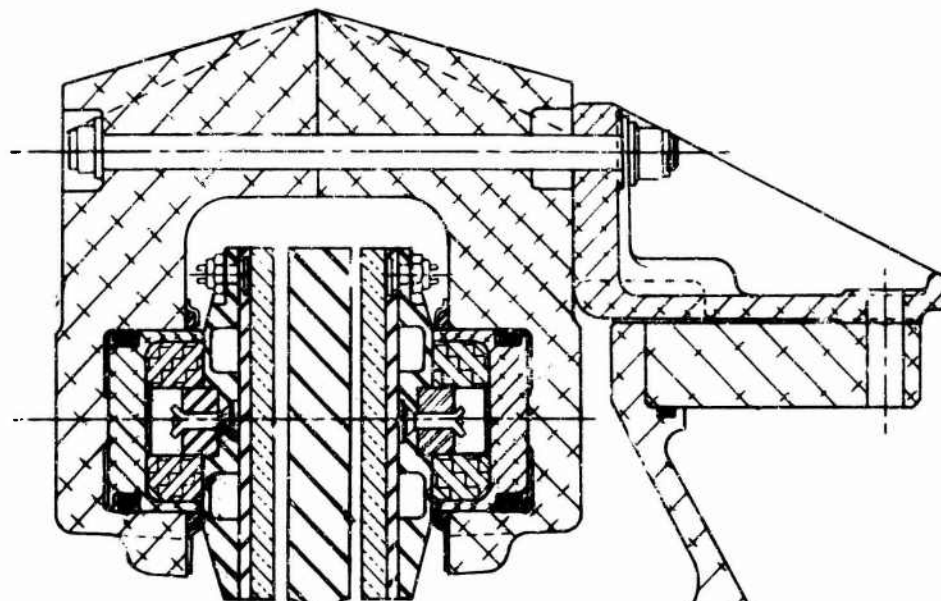
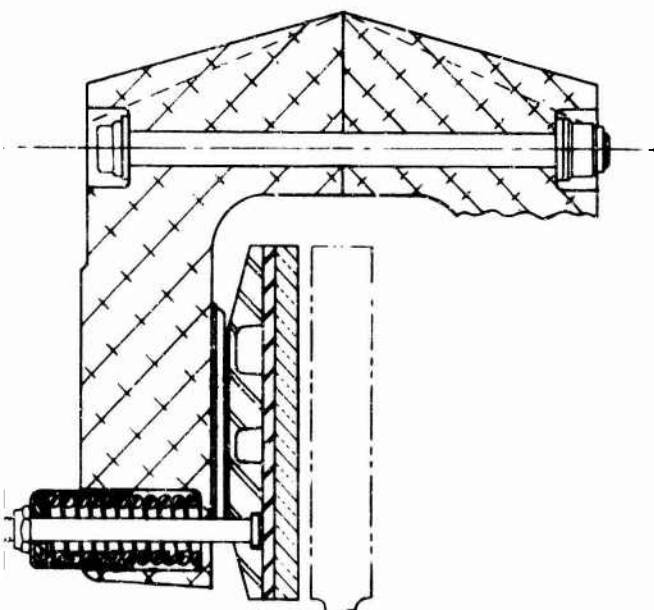


FIGURE 59. ROTOR BRAKE.
HLH-10-21

SECTION A-A
(ROTATED 90°)



SECTION B-B
(ROTATED 70°)



C

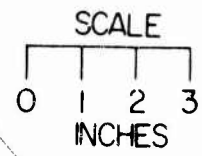
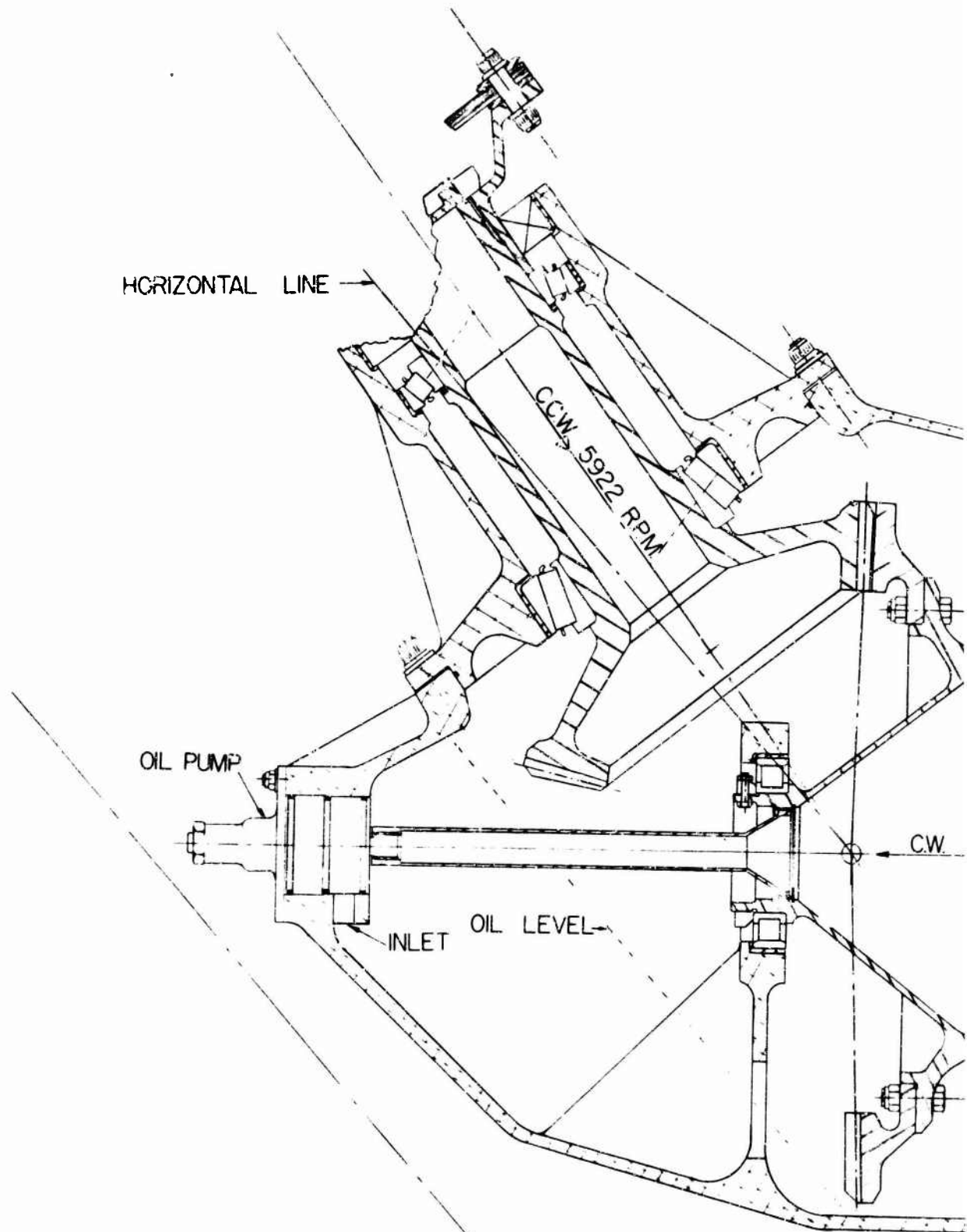
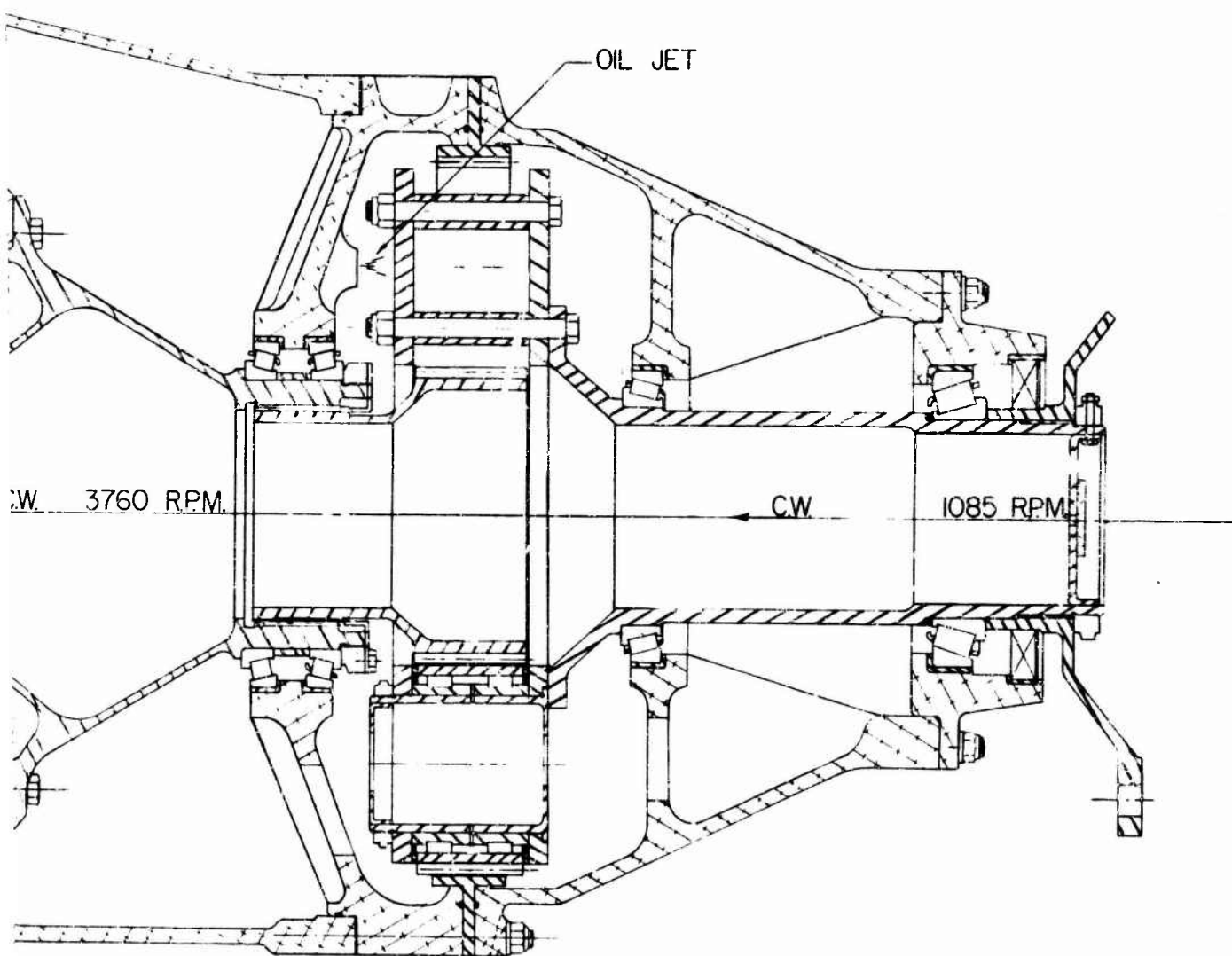


FIGURE 6



RE. 60. ALTERNATE INTERMEDIATE GEARBOX.
HLH-30-40

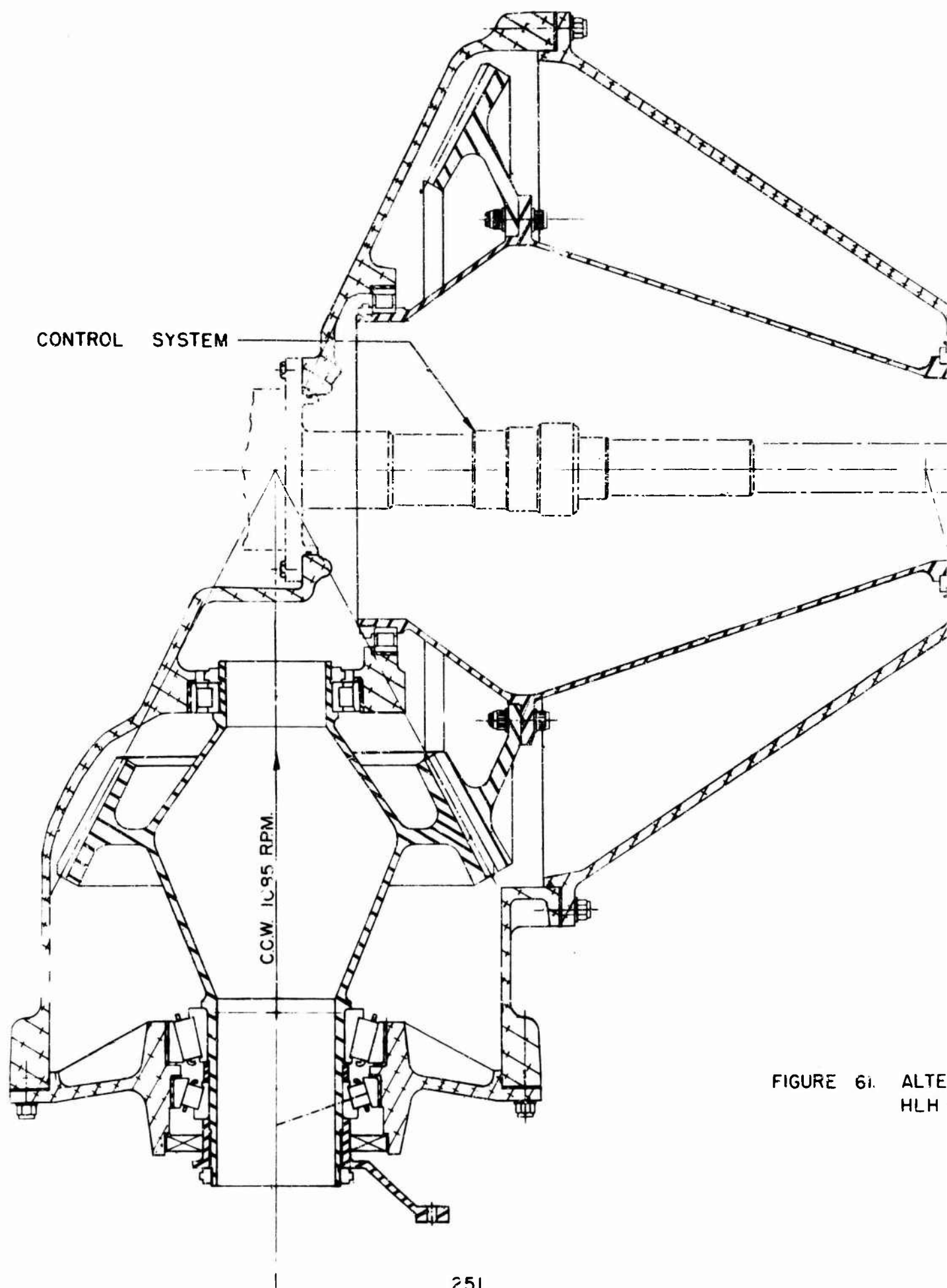
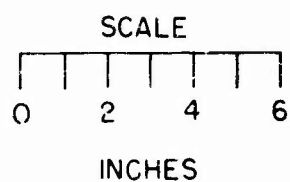
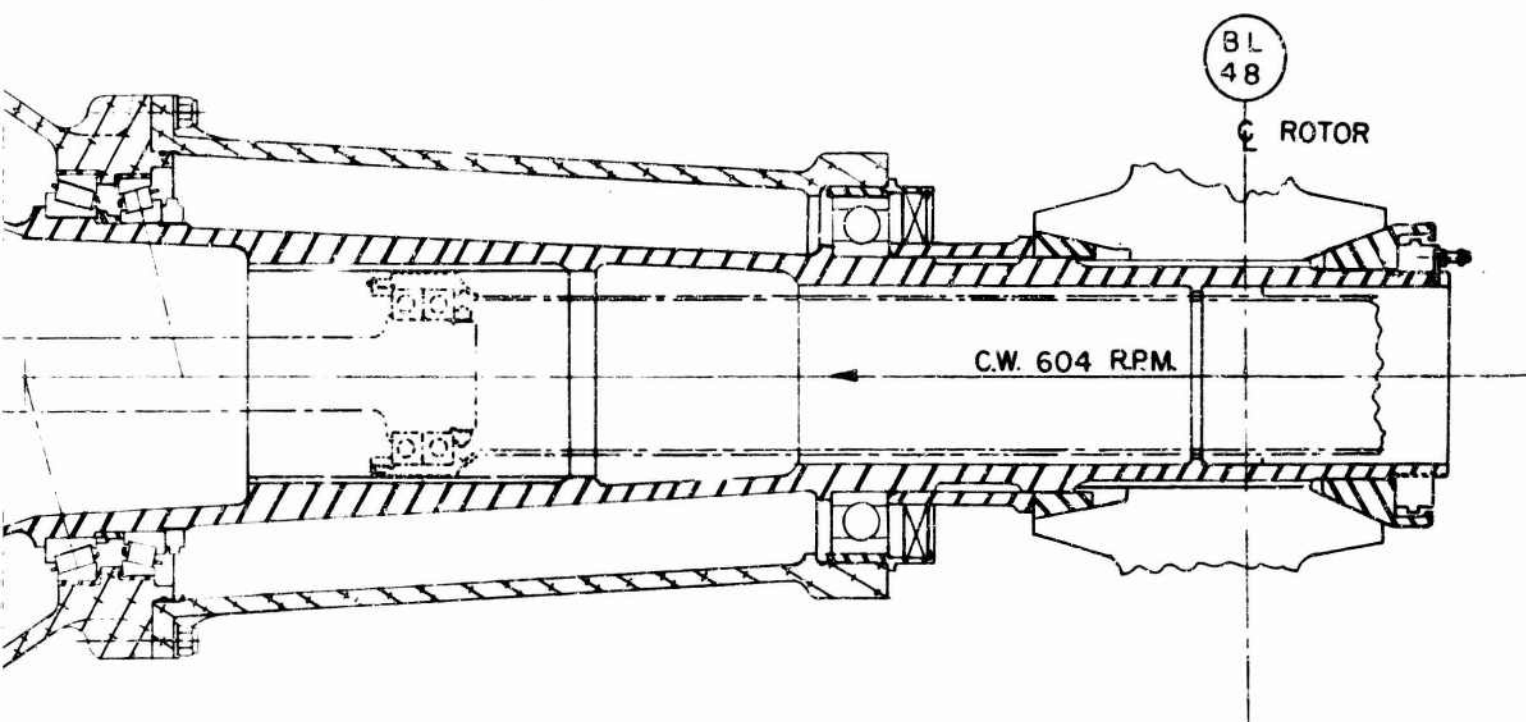
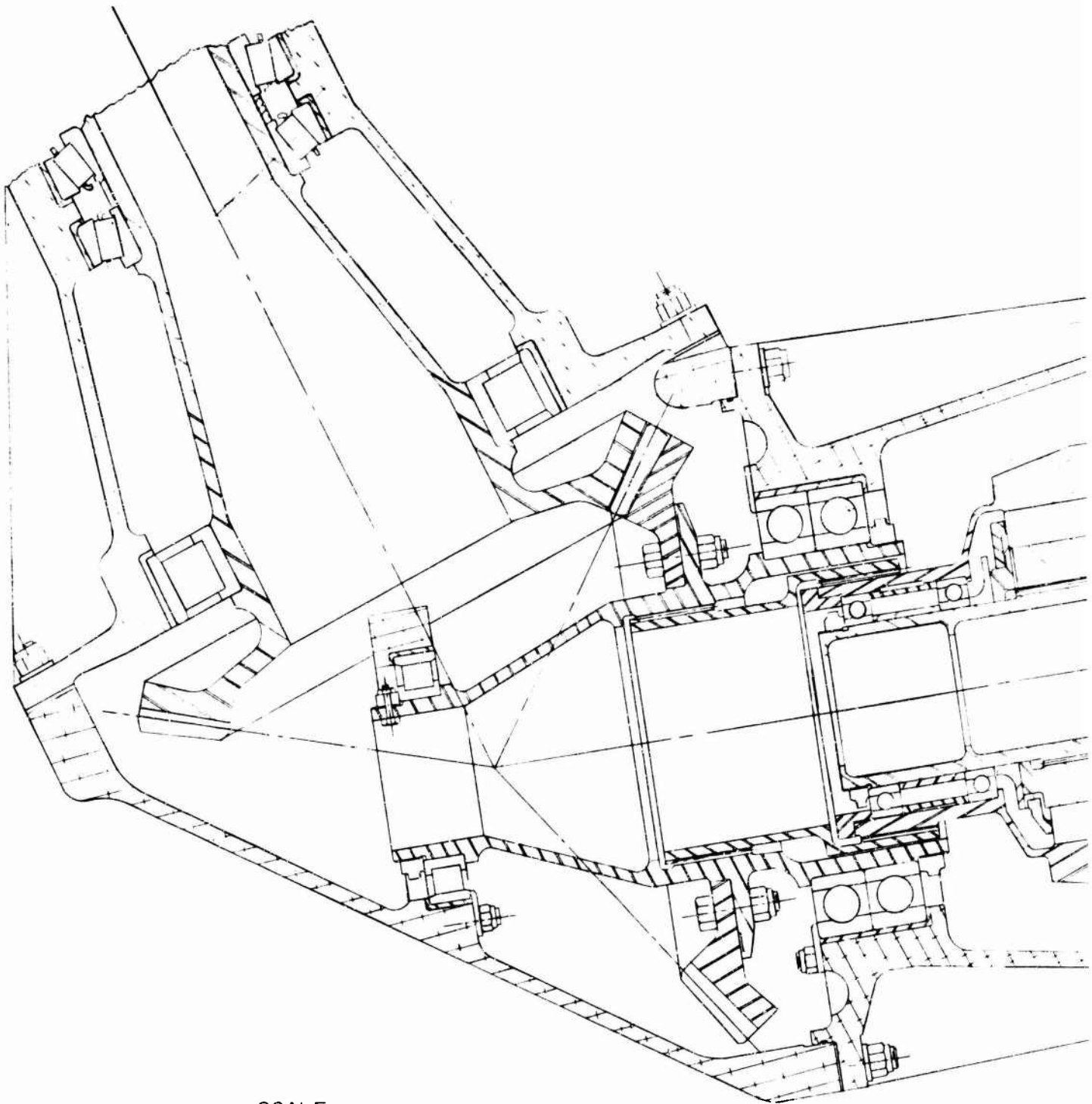


FIGURE 61. ALTE
HLH



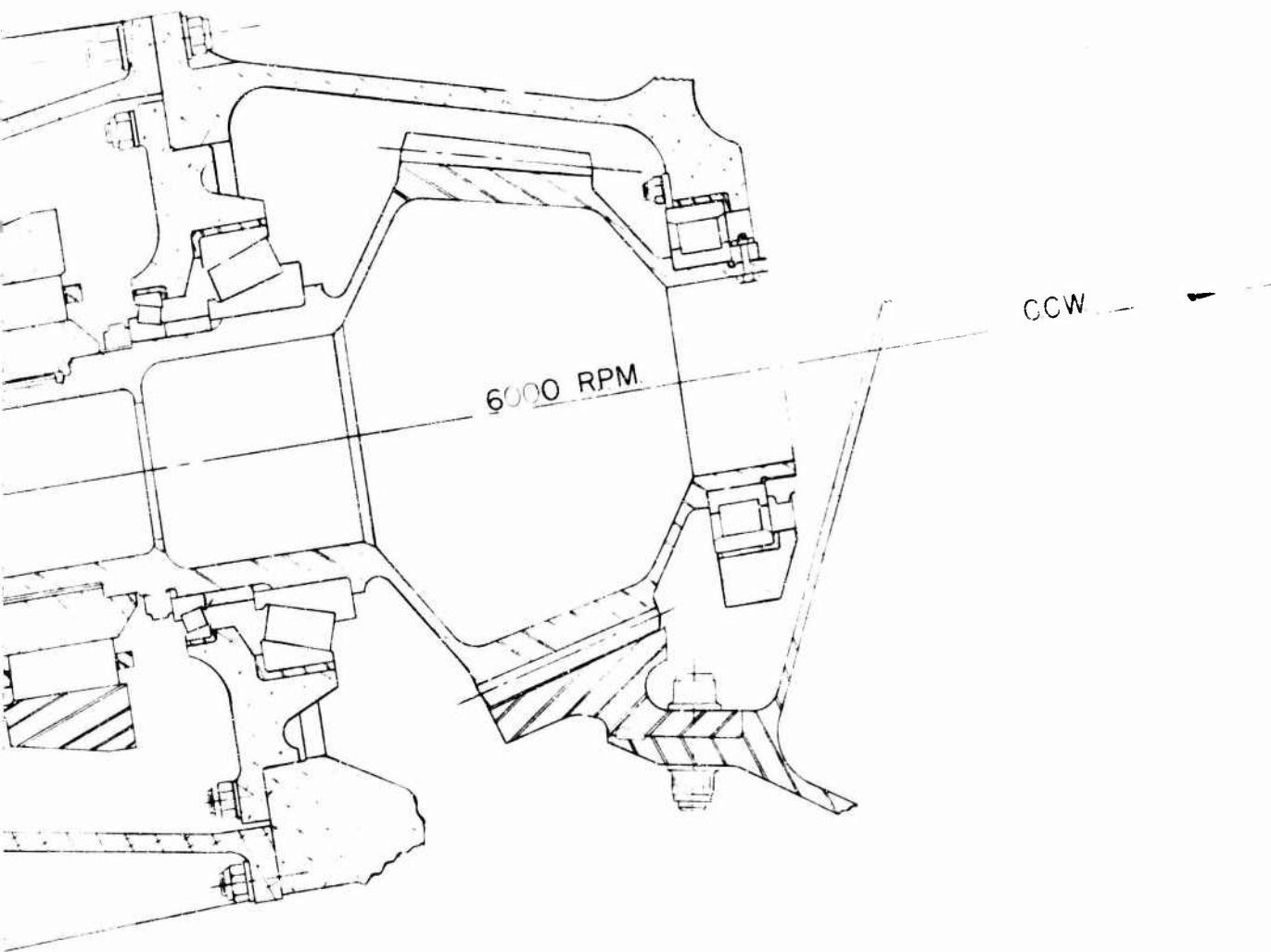
ALTERNATE TAIL GEARBOX.
ILH-30-60



SCALE
0 1 2 3
INCHES

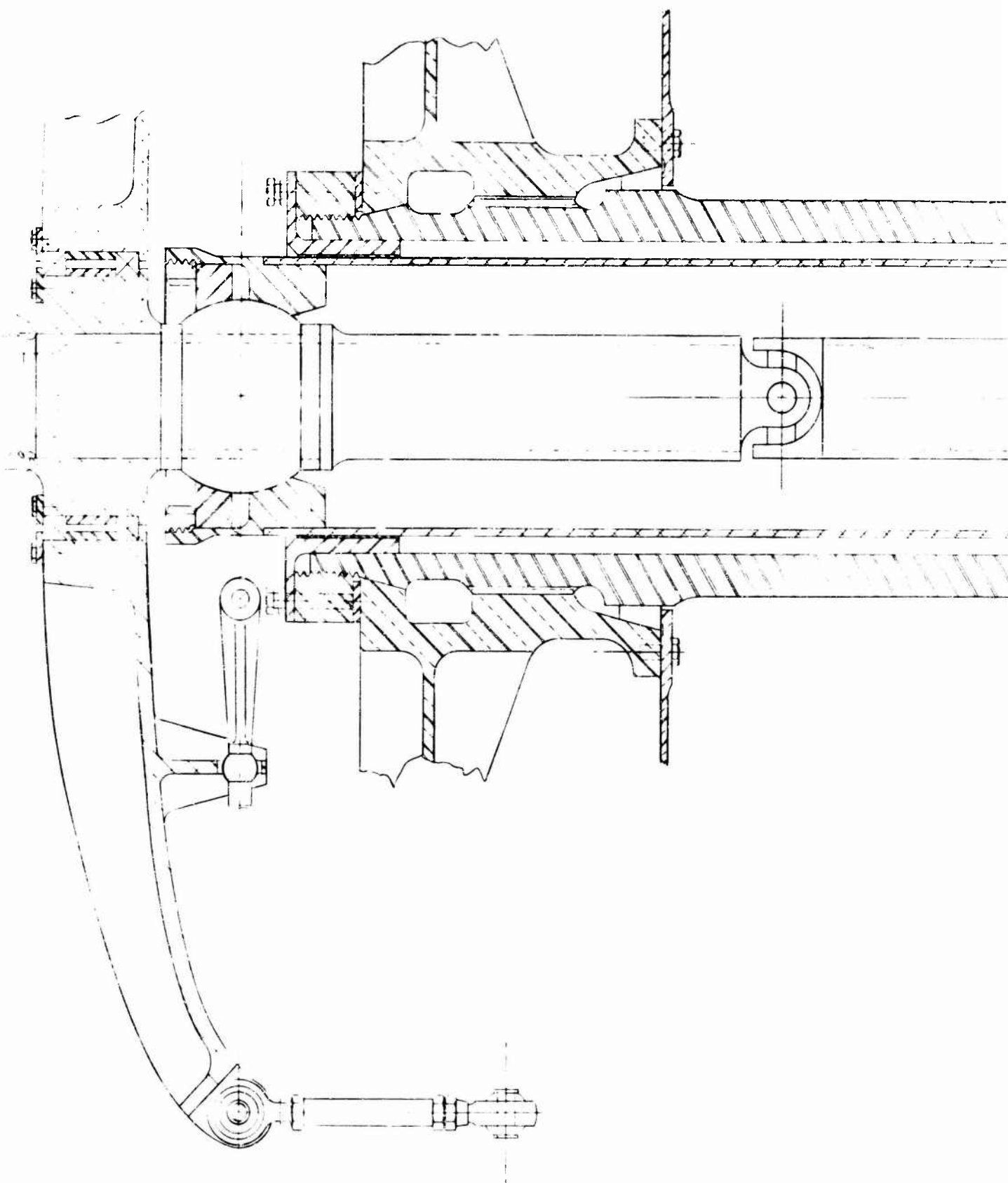
FIGURE 62.

ANGULAR INPUT DRIVE,
REAR- DRIVE ENGINES.



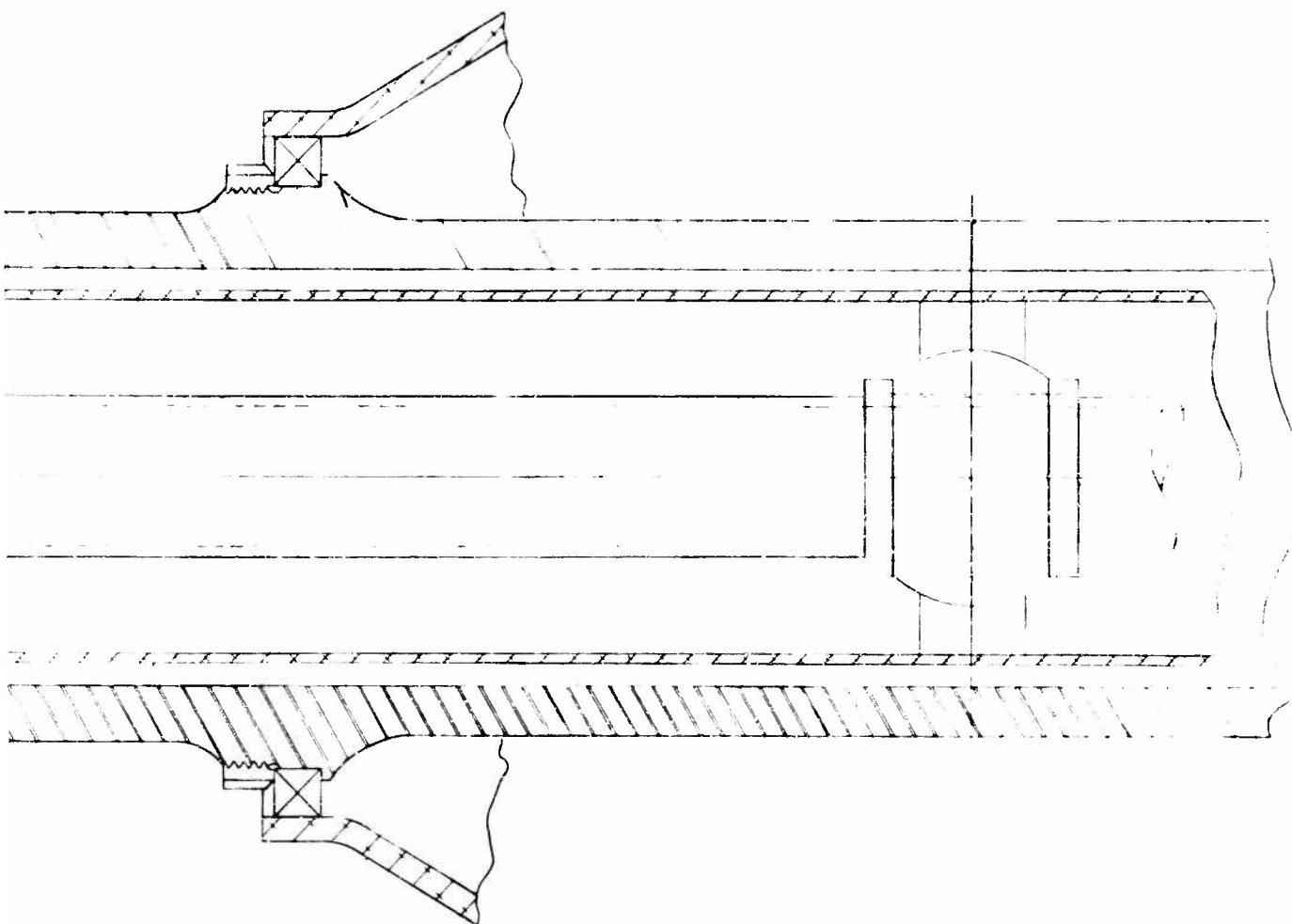
Q

VE, MAIN GEARBOX,
S. HLH-20-22

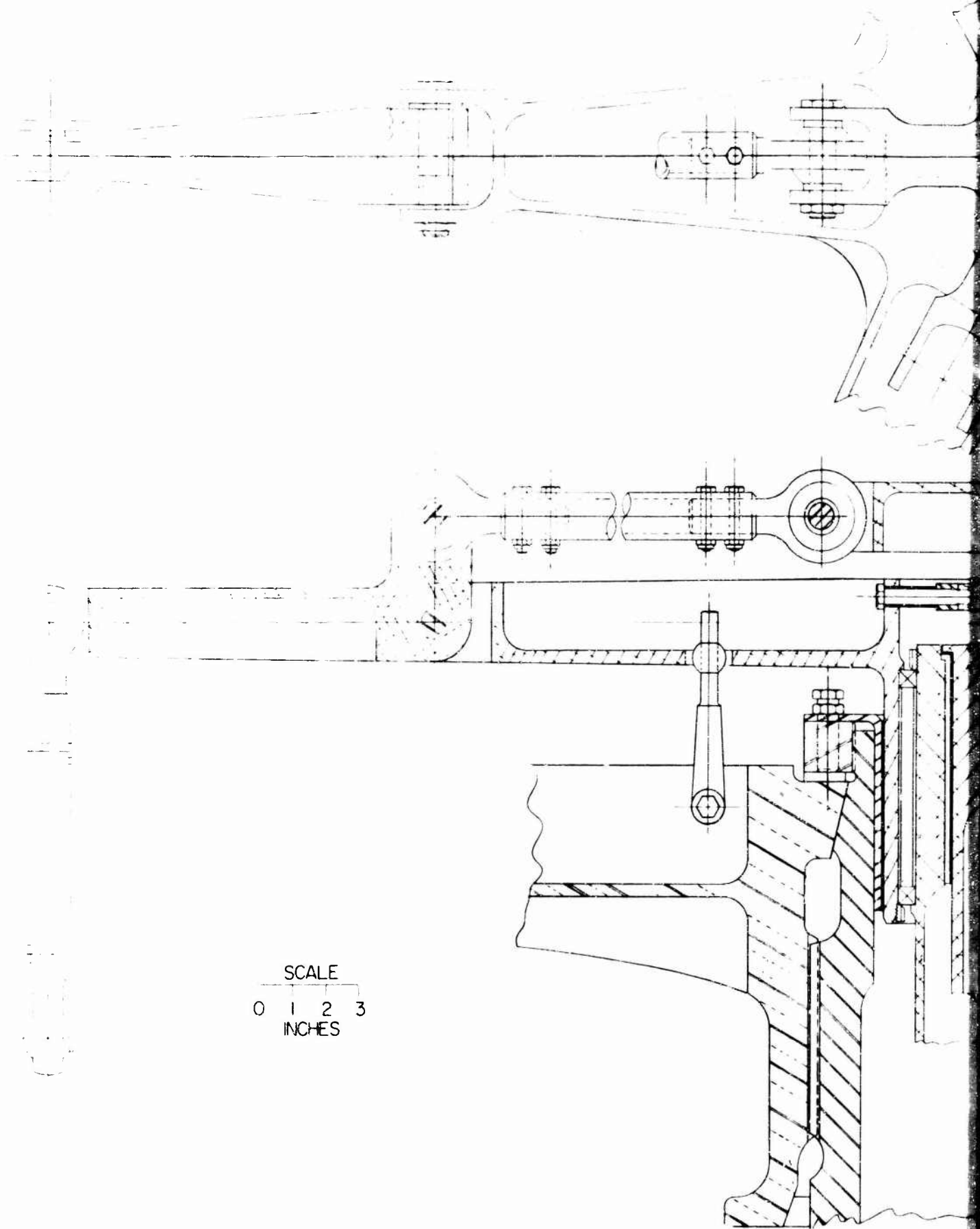


SCALE
0 2 4 6
INCHES

FIGURE 63 HAFNER
HLH - 15-



R INTERNAL CONTROL SYSTEM
15-20



SCALE
0 1 2 3
INCHES

A

FIGURE 64. DOUBLE ECCENTRIC CONTROL SYSTEM.
HLH-15-21

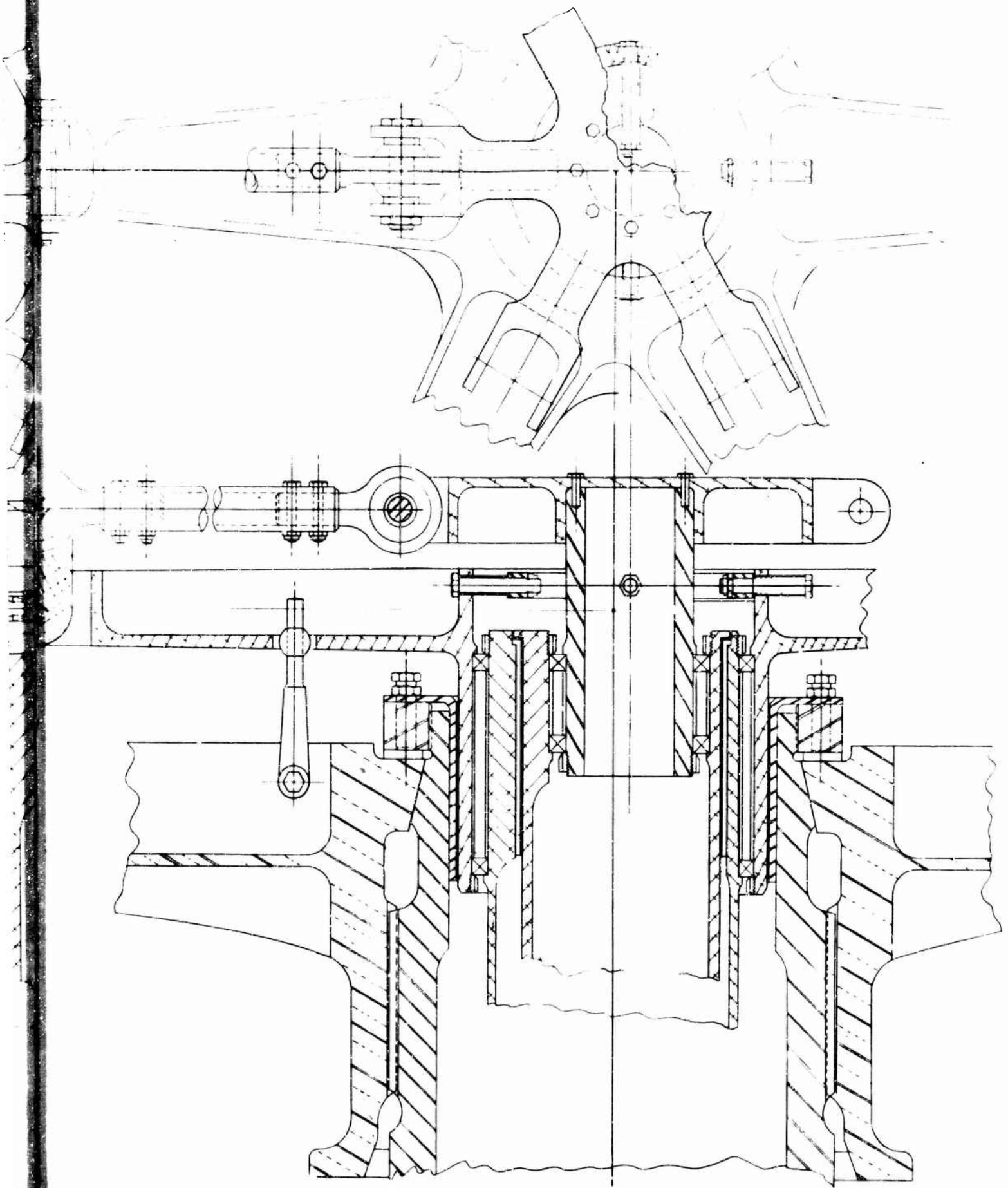


FIGURE 64. DOUBLE ECCENTRIC CONTROL SYSTEM.
HLH-15-21

B

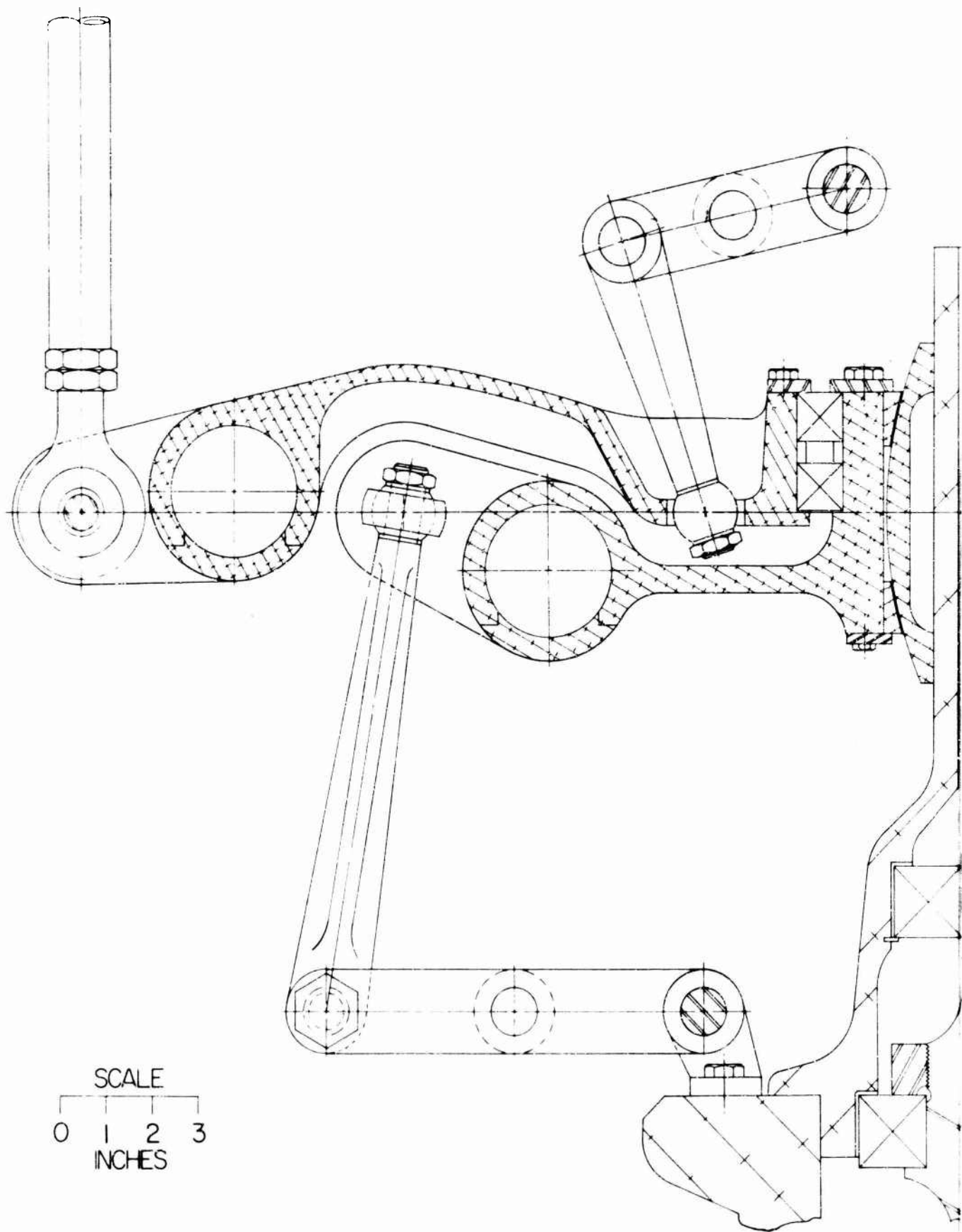
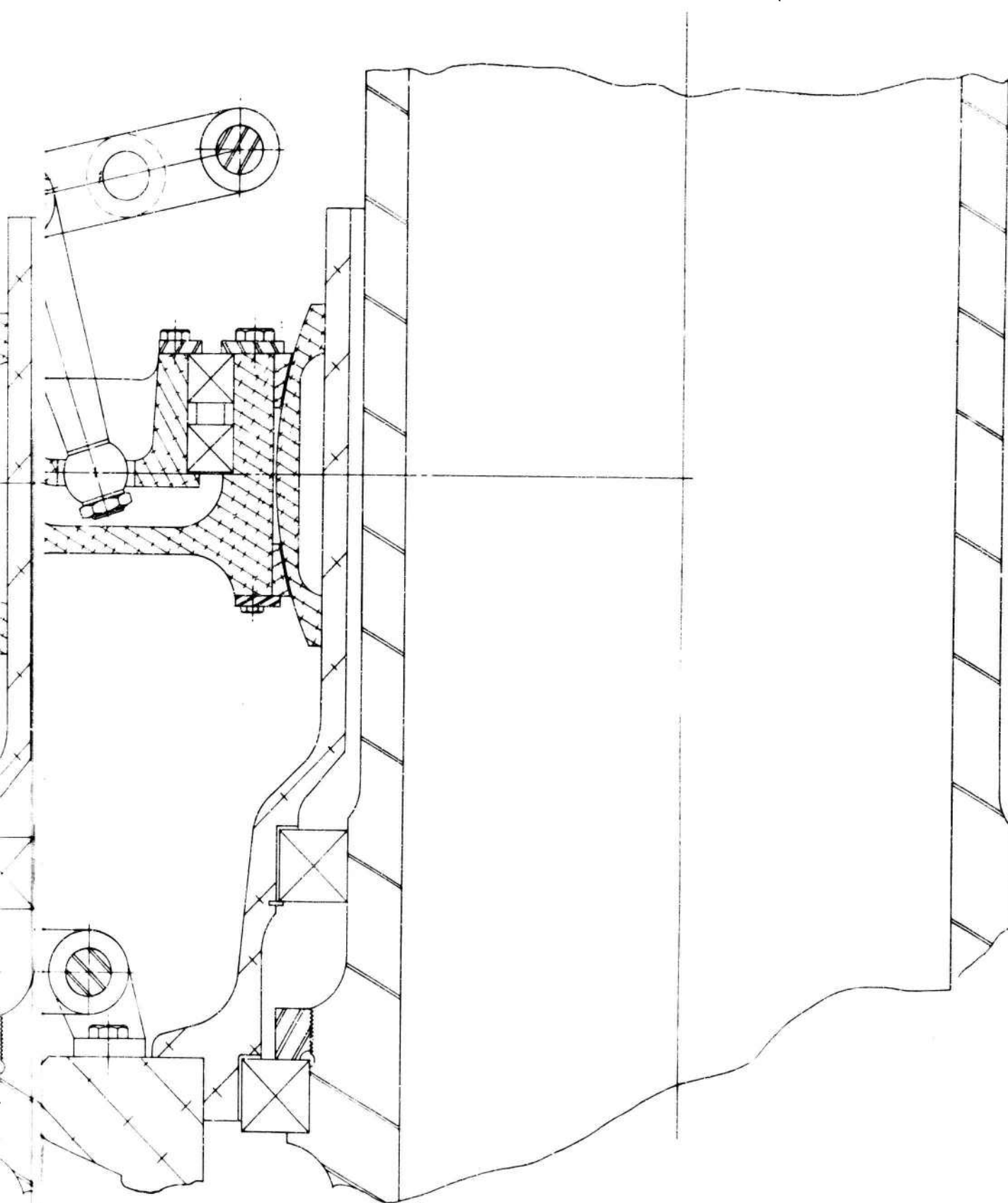


FIGURE 65. CONVENTIONAL CONTROL
HLH-15-22



RO CONVENTIONAL CONTROL SYSTEM
HLH-15-22

B

APPENDIX II

ENGINE INSTALLATION STUDIES

INTRODUCTION

The initial consideration in the design of a multiple turbine engine helicopter propulsion system is the selection and arrangement of the engines. The engines used were selected as the result of a comparison of the characteristics of available or growth engines to fulfill the primary design objectives of reliability, simplicity, accessibility, ease of maintenance, and compatibility with the transmission design. A summary of the engines considered with the pertinent weight, power, and speed data for each engine is presented in Table 30, page 262.

Engine installation arrangements have been evaluated on the basis of proper air inlet flow to counteract the effects of recirculation of engine exhaust, as well as the ingestion of foreign objects, dirt, water, or ice. An additional object of this phase was to estimate the installation losses and performance for the engine arrangements studied.

DISCUSSION

As indicated in Table 30, page 262, four different manufacturers' engines were considered in this design study. Selection of the optimum engine type, as well as the proper number of engines, was based on an analysis of mission requirements and aircraft performance. Among the factors considered in this analysis were the effects of engine power, weight, speed, and specific fuel consumption on the gear train arrangement. Additional factors influencing engine selection were reliability and maintainability, including the effect of a front or rear drive. All of the engines considered were of the free turbine type, so as to eliminate the need of using clutches (but not necessarily free wheel units).

Fuel consumption versus the need to shut down one or more engines during the ferry mission and the consideration of thrust augmentation for additional power at take off were considered.

TABLE 30
ENGINE DATA

Designation	Wt. (lb.)	SFC* (lb./HP/ Hr.)	Horsepower			RPM Output
			Mil	Norm.	6,000 ft. 95°F (Mil.)	
T64/S5A	765	.482	4,500	4,000	3,050	13,600
JFTD-12A (Growth)	1,025	.644	5,950	5,100	4,400	9,600
LTC4B-11A	640	.544	3,400***	3,000	2,640 (Max)	16,000
LTC4B-11	640	.544	3,400	3,000	2,300	16,000
548-C2	**	**	4,490	4,175	3,080	19,320
548-C2 (3.22:1 Gear Red.)	**	**	4,468	4,155	3,065	6,000

*Based on normal power

**Reference Allison Report EDR 4010

***LTC4B-11A Maximum Rating (10 minutes) = 3,750 HP, Sea Level,
Standard Day

Thrust Augmentation

The selection of a fewer number of engines utilizing water injection (thrust augmentation) for increased power was rejected due to weight and logistic and cost penalties. Additional aircraft tankage, as well as distilled water in the field, would be required.

The availability of engines with sufficient power presents a better solution without the penalties associated with water injection.

Regeneration

Regeneration has not been utilized, since the incorporation of regenerative combustion cycles to obtain improved specific fuel consumption is offset by the additional weight of the regenerators, the increased frontal area (drag) required, and the loss of hot-day takeoff power. The overall effect of regeneration for this application would be a reduction in mission performance.

Hot-Day Hover Performance

Making the logical assumption that the 1,500-nautical-mile ferry mission will be flown infrequently as compared to the transport and heavy-lift missions, then the out-of-ground-effect hover requirements of the 12-ton transport mission become a primary design factor. A detailed transport mission analysis (see page 218) indicates that approximately 11,320 HP is required for the 6,000-foot out-of-ground-effect hover on the Army hot-day (+95°F) for a gross weight of 74,000 pounds. Using the 2/3 rule for the deterioration of power for a hot-day as compared to a standard day, the hover power requirement and the mission range required dictate the selection of four engines with a standard day maximum rating of at least 4,500 horsepower. The only two engines (of Table 30) meeting this requirement at the lowest weight and specific fuel consumption are the T64/S5A and the 548-C2.

Engine Installation

While the two engine models selected in the previous paragraph produce the most favorable overall aircraft performance, all four manufacturers' engines have been considered in the study to evaluate engine-transmission arrangements. Nine such arrangements were studied and are shown in schematic form in Figures 66 through Figure 74. Evaluations of all such designs were made to estimate the installation losses and engine performance on a comparative basis. The following section of this report summarizes this comparative design analysis.

Performance Evaluation

The engine installation losses and performance estimates are based on the following considerations:

The inlet pressure distortions are within the limits imposed by the engine manufacturer.

The rear-drive engine specifications allow for the power loss associated with a 45° exhaust turn.

Power loss is the sum of the effects of inlet pressure loss, temperature effects, loss of ram, and exhaust pressure loss.

Estimated power losses due to ingestion of exhaust gases represent losses above those which may be expected in a conventional engine installation.

Losses presented in Table 32, page 266, for the engine arrangements shown in Figures 66 through 74, represent losses or gains from static no loss performance*. A summary of this data is given in Table 31.

*Note: Static no loss performance defined as engine specification performance at zero forward velocity.

TABLE 31
ENGINE INSTALLATION
PERFORMANCE SUMMARY

Figure Number	Arrangement	Losses - Percent SHP	
		Hover OGE Power Change	100 Kt. Power Change
66	Front-Drive Engine Installation, T64/S5A Turbines (Basic Transmission System)	-0.25	+1.75
67	"Fan" Engine Installation 548-C2 Rear-Drive Turbines (Alternate Transmission System)	0	+2.0

TABLE 31 Cont'd

Figure Number	Arrangement	Losses - Percent SHP	
		Hover OGE Power Change	100 Kt. Power Change
68	Four Rear-Drive Engines	0	+2.5
69	Three Engine Installation Rear-Drive Turbines Bifurcated Center Engine Exhaust	-0.08	+2.4
70	Three Rear-Drive Engines Rear Engine Inlet Facing Aft	-2.5	-1.66
71	Five Front-Drive Engines	-0.7	+0.9
72	Semi-radial Configuration Four Front-Drive Turbines	-1.25	-0.25
73	Semi-radial Configuration Four Rear-Drive Turbines	-11.25	-17.75
74	Semi-radial Configuration Four Front-Drive Turbines	-1.75	-4.5

TABLE 32
ENGINE INSTALLATION PERFORMANCE DATA

Figure Number	Item	Losses, Percent SHP*					
		Inlet Press. Loss	Temp. Effects	Exhaust Pressure Loss	Hover OGE Power Change	Ram at 100 Kt.	100 Kt. Power Change
66	Two Forward Engines	0	0	-0.5	-0.5	+2	+1.5
-	Two Rear Engines	0	0	0	0	+2	+2
-	Average Power Change	-	-	-	-0.25	-	+1.75
67	Average Power Change	0	0	0	0	+2	+2
68	Average Power Change	0	0	0	0	+2.5	+2.5
69	Two Forward Engines	0	0	0	0	+2.5	+2.5
-	Center Engine	0	0	-0.25	-0.25	+2.5	+2.25
-	Average Power Change	-	-	-	-0.08	-	+2.4
70	Two Forward Engines	0	0	-0.5	-0.5	+2.5	+2
-	Center Engine	-2	-4	-0.5	-6.5	-2.5	-9
-	Average Power Change	-	-	-	-2.5	-	-1.66
71	Four Forward Engines	0	0	-0.5	-0.5	+1.75	+1.25
-	One Rear Engine	0	-1	-0.5	-1.5	+1	-0.5
-	Average Power Change	-	-	-	-0.7	-	+0.9
72	Two Forward Engines	0	0	-1.5	-1.5	+2	+0.5
-	Two Rear Engines	0	-1	0	-1	0	-1
-	Average Power Change	-	-	-	-1.25	-	-0.25

TABLE 32 Cont'd.
ENGINE INSTALLATION PERFORMANCE DATA

Figure Number	Item	Losses, Percent SHP*					
		Inlet Press. Loss	Temp. Effects	Exhaust Pressure Loss	Hover OGE Power Change	Ram at 100 Kt.	100 Kt. Power Change
73	Two Forward Engines Hover 100 Kts.	0	-6	-5	-11	-	-
		0	0	-5	-	+2	-3
-	Two Rear Engines Hover 100 Kts.	0	-10	-1.5	-11.5	-	-
-	Average Power Change	-3.5	-25	-1.5	-	-2.5	-32.5
		-	-	-	-11.25	-	-17.75
74	Two Forward Engines Hover 100 Kts.	0	-2	-0.5	-2.5	-	-
		-3	-2	-0.5	-	-2.5	-8.0
-	Two Rear Engines	0	-1	0	-1	0	-1
-	Average Power Change	-	-	-	-1.75	-	-4.5

*Losses indicated by negative values.
Gains indicated by positive values.

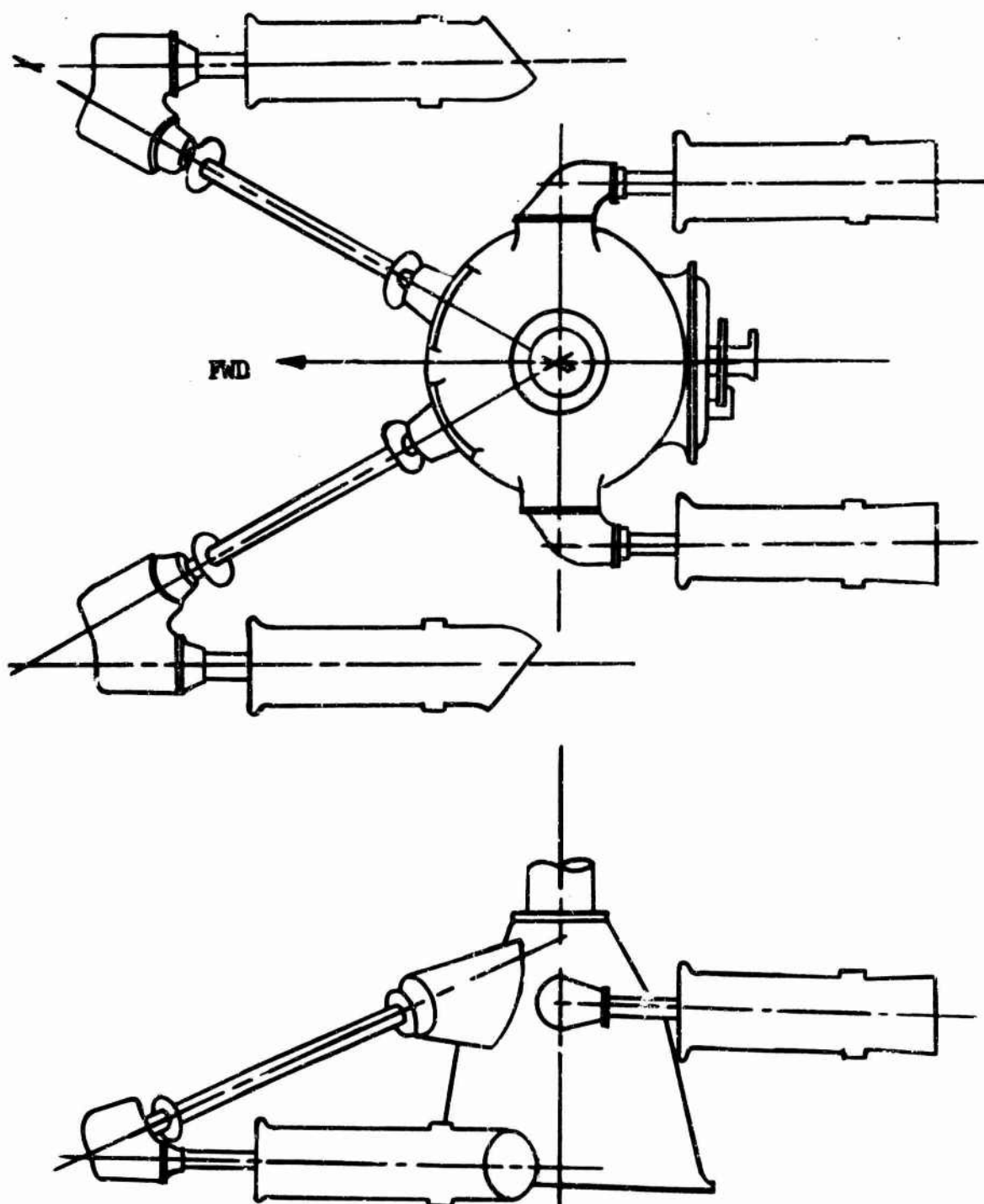


Figure 66. Front-Drive Engine Installation,
T64-S5A Turbines
(Basic Transmission System).

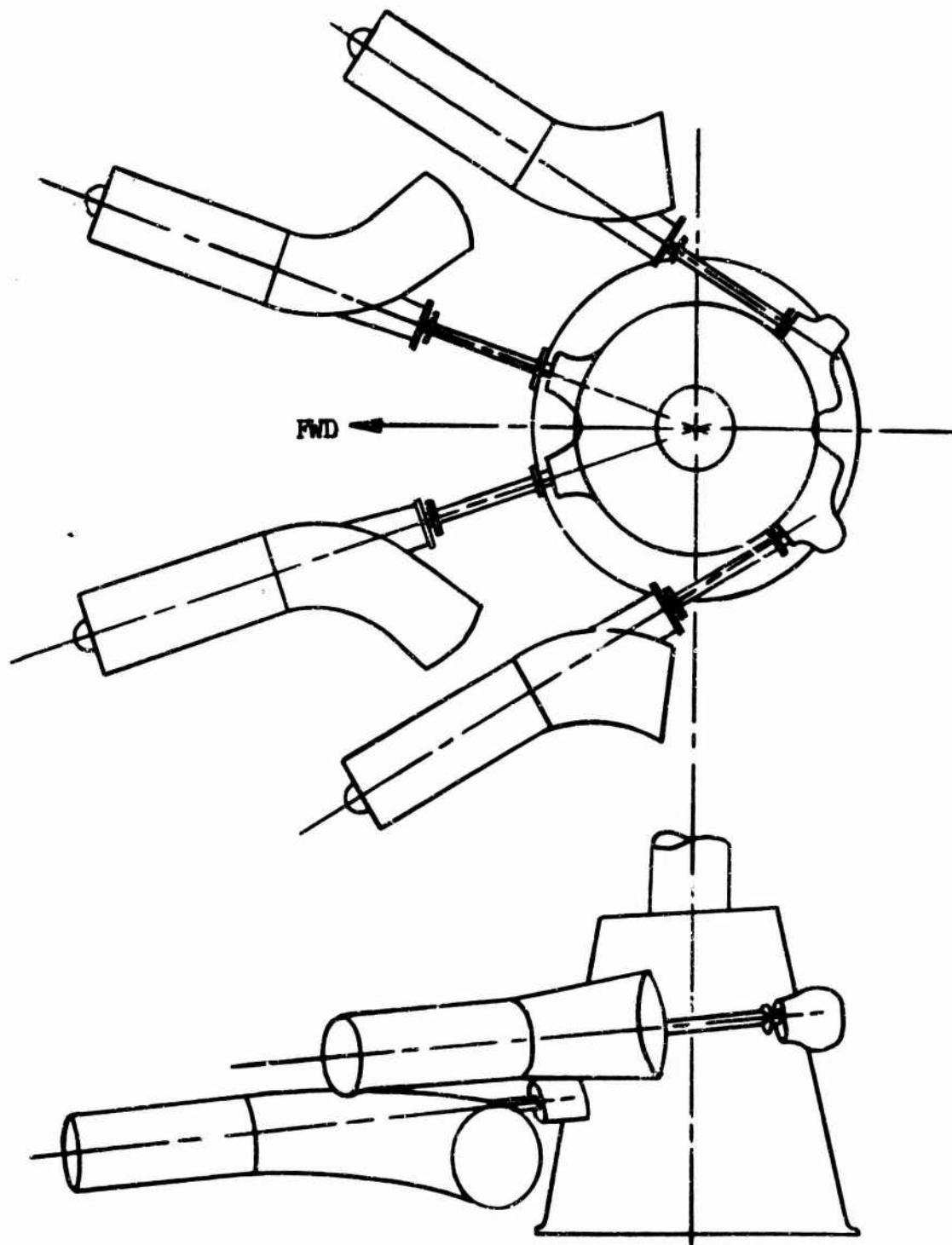


Figure 67. "Fan" Engine Installation,
548-C2 Rear-Drive Turbines
(Alternate Transmission System).

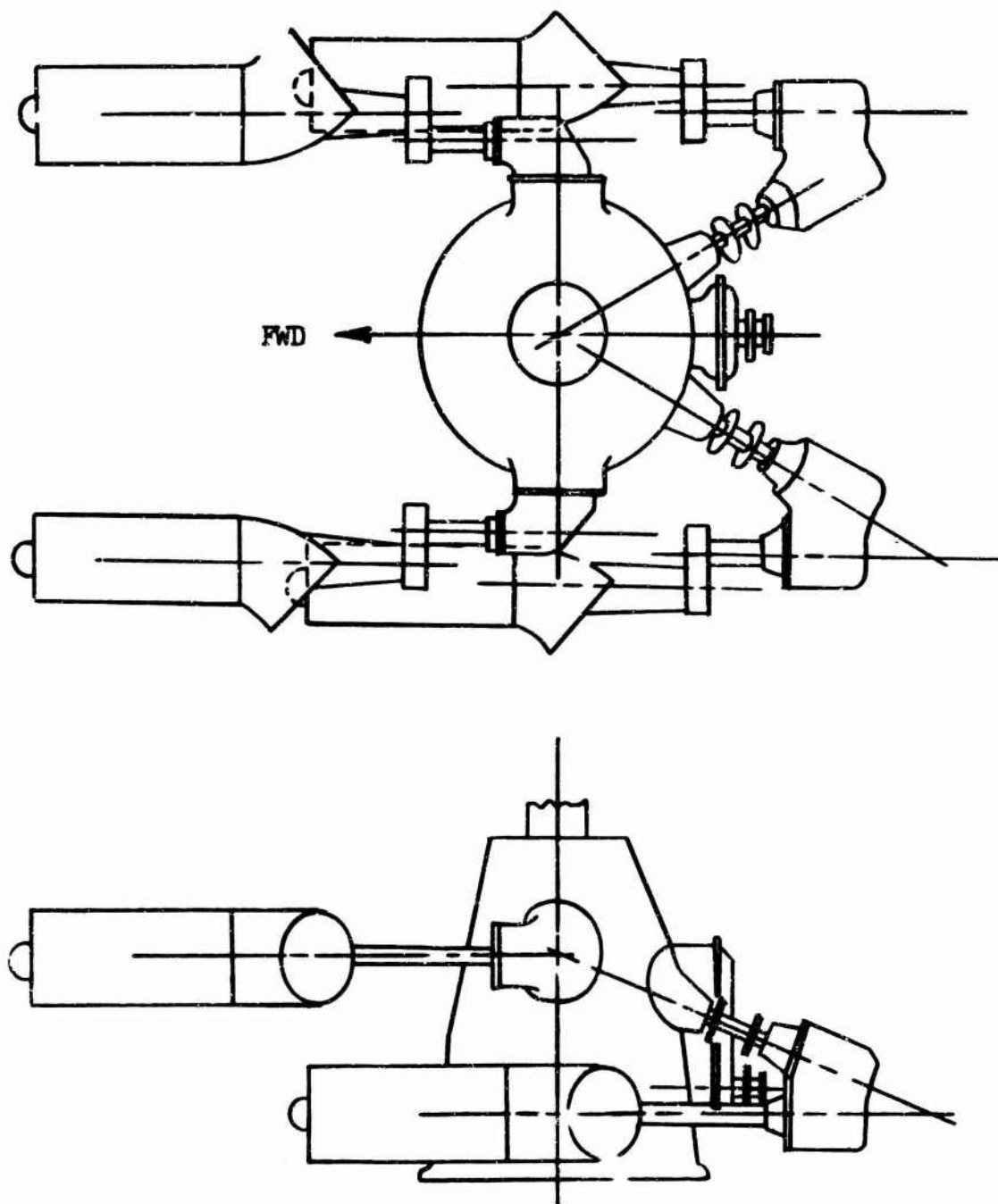


Figure 68. Four Rear-Drive Engines.

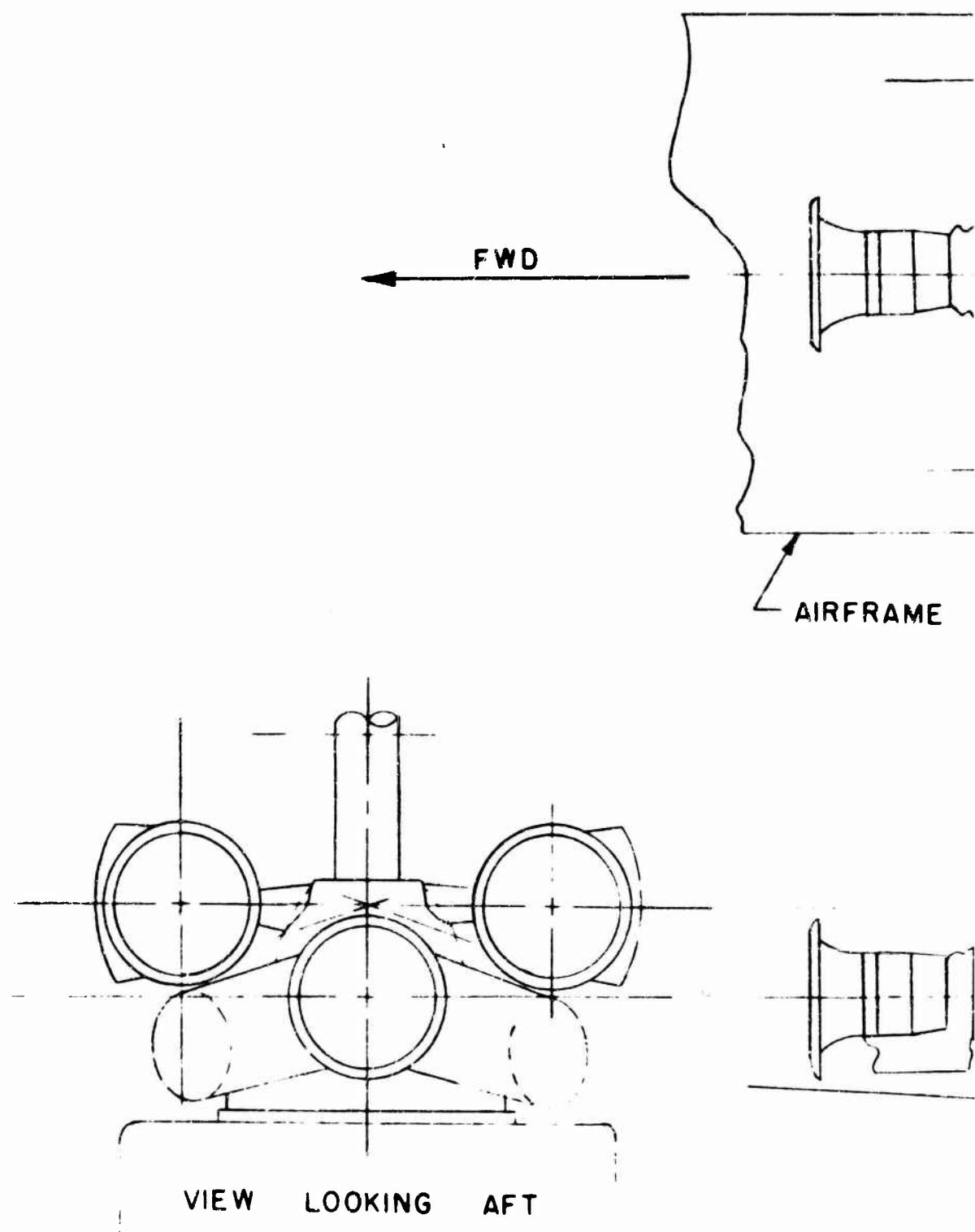
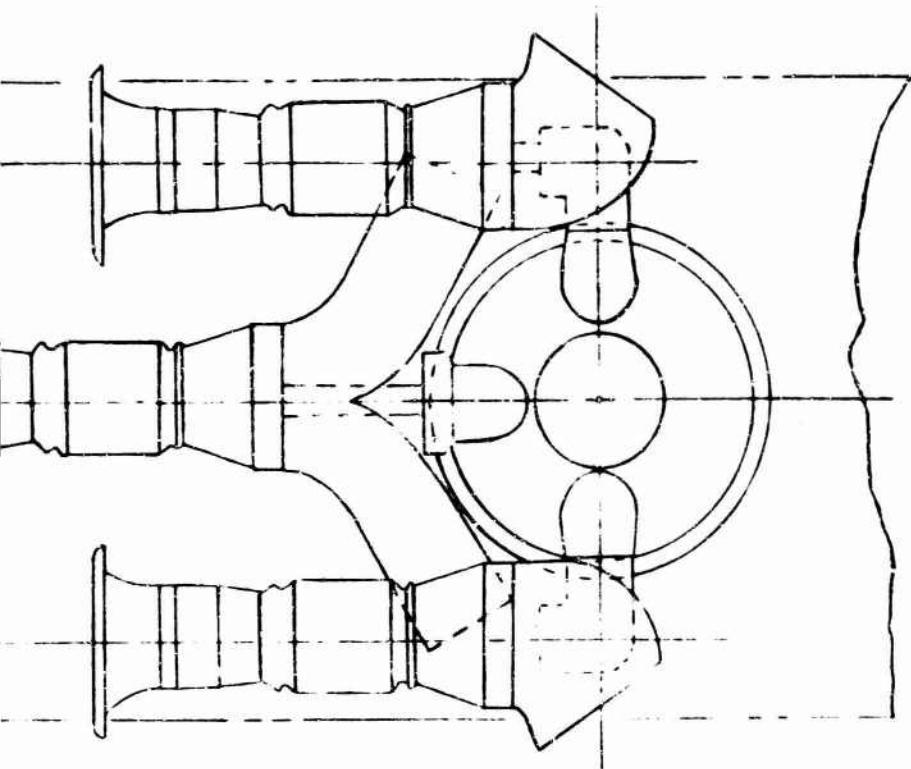
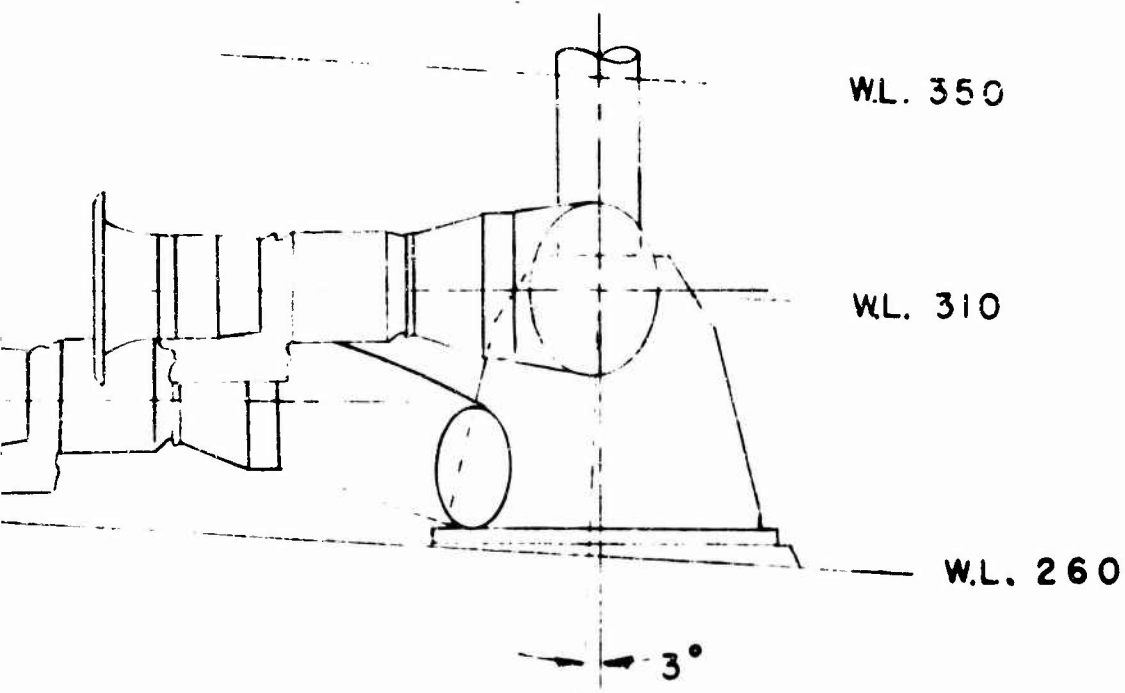


FIGURE 69. THREE-ENGINE INSTALLATION
BIFURCATED CENTER ENGINE



E OUTLINE



INSTALLATION, REAR-DRIVE TURBINES,
ENGINE EXHAUST

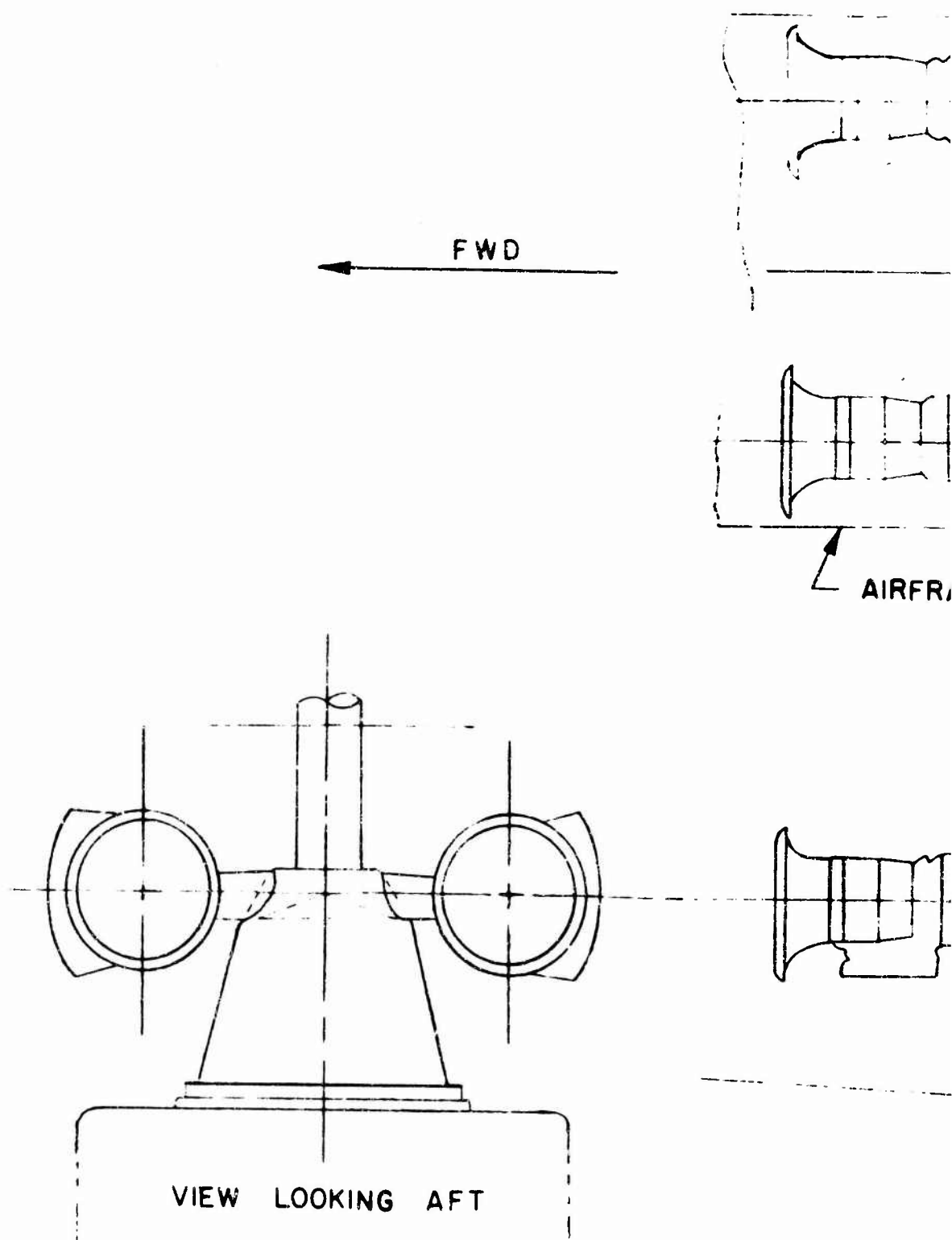
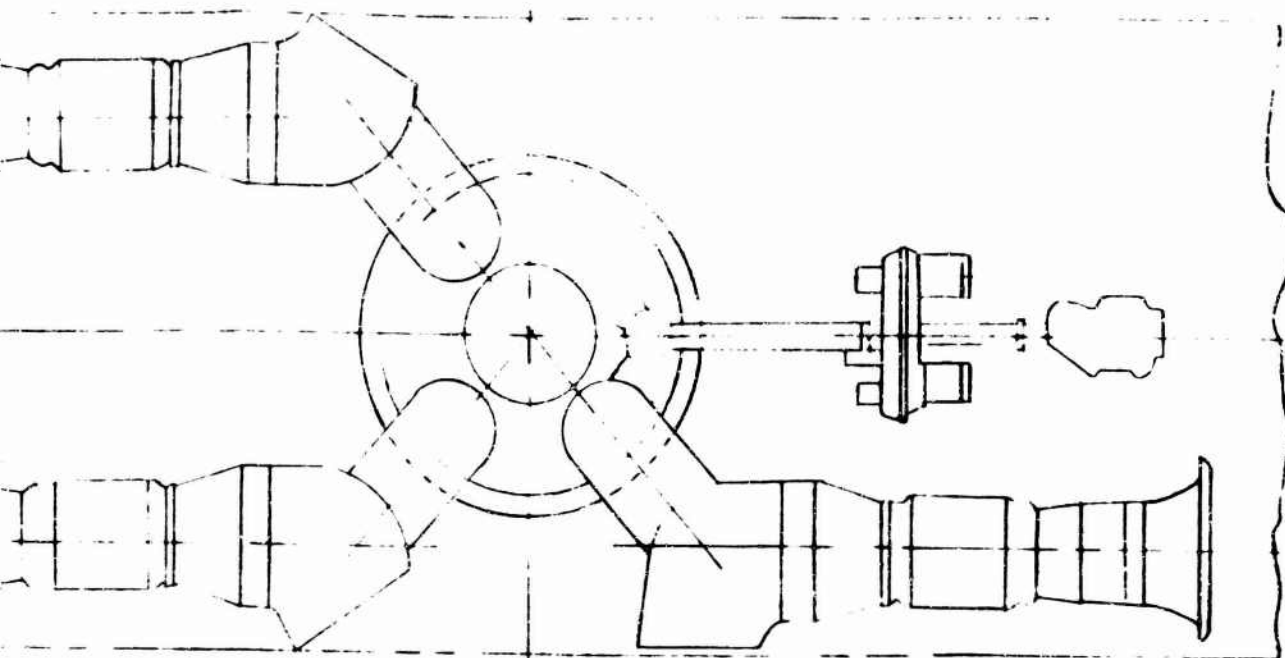
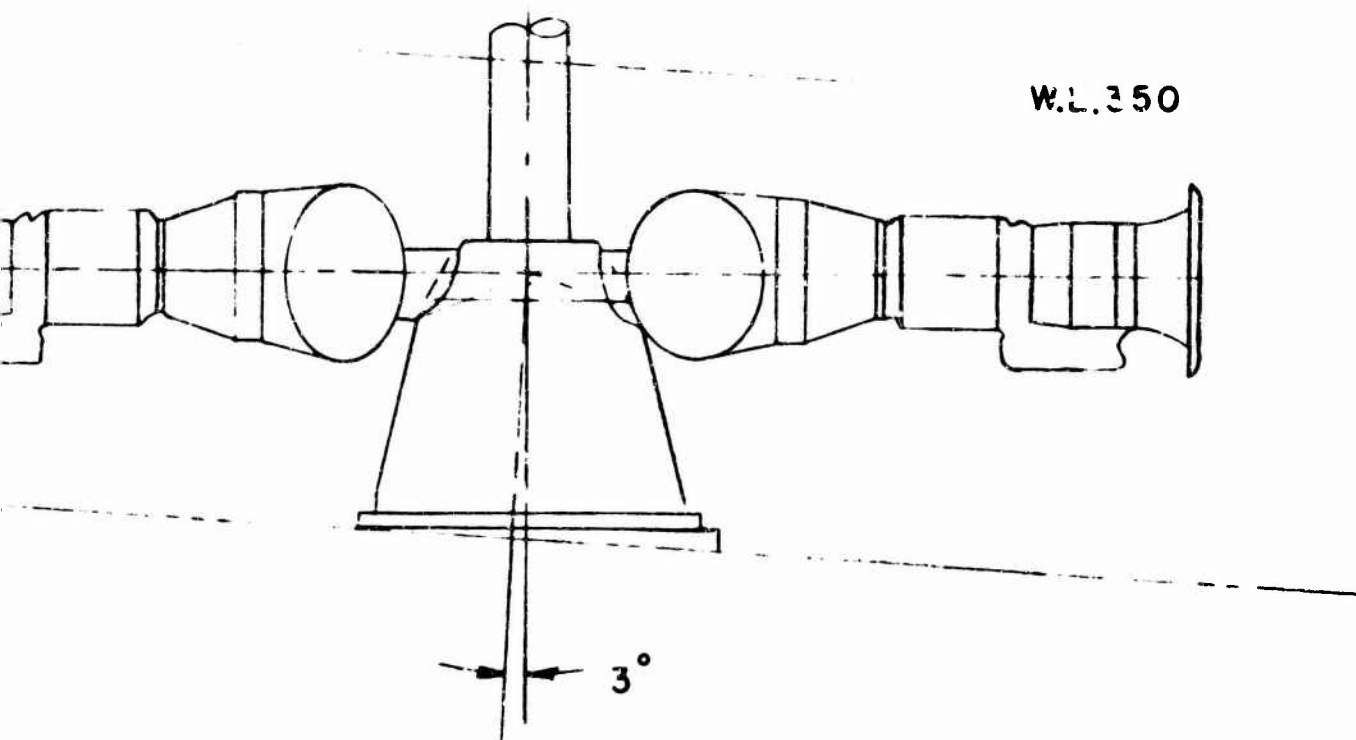


FIGURE 70. THREE R
FACING A



FRAME OUTLINE



REAR-DRIVE ENGINES, REAR ENGINE INLET
AFT

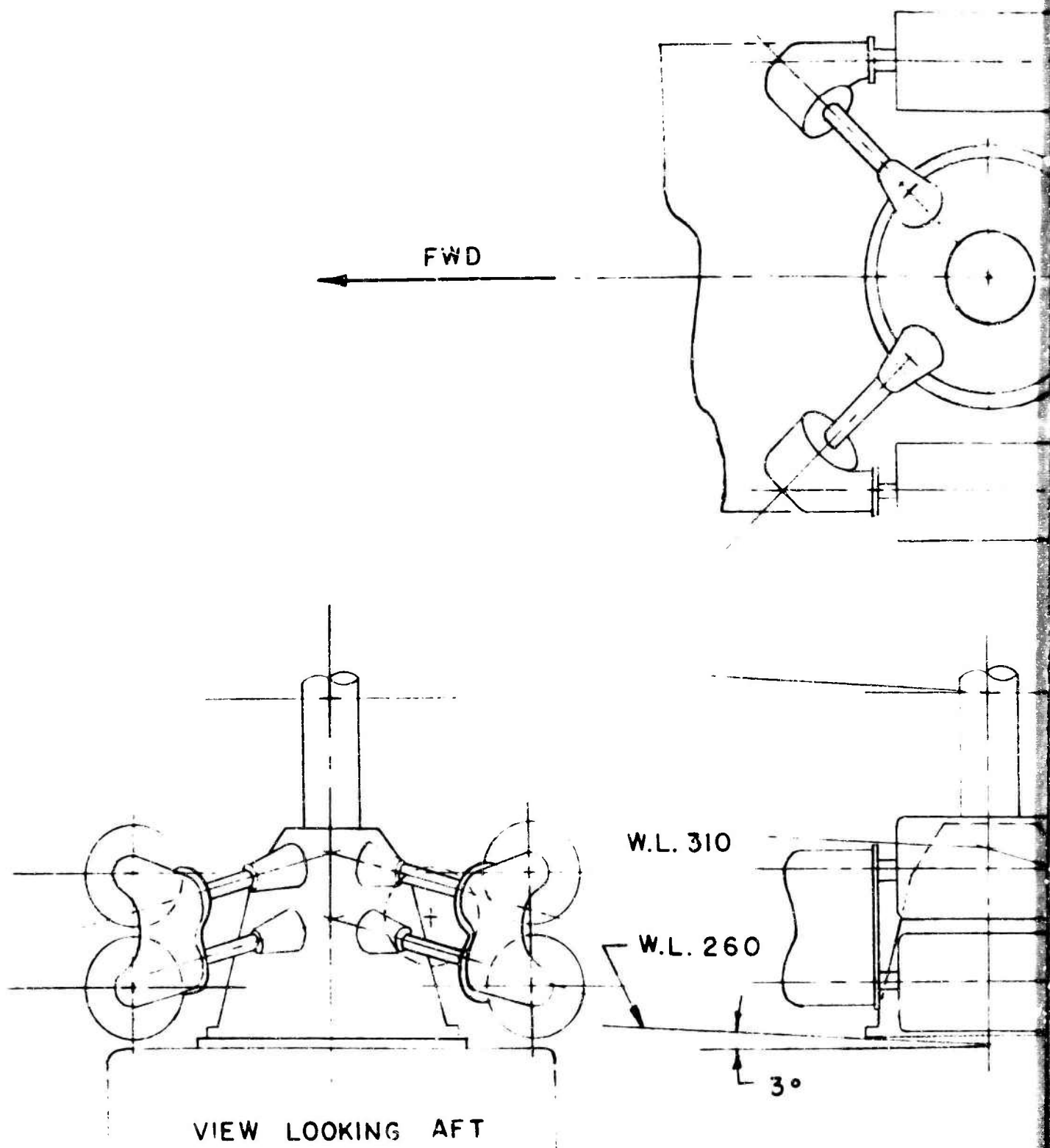
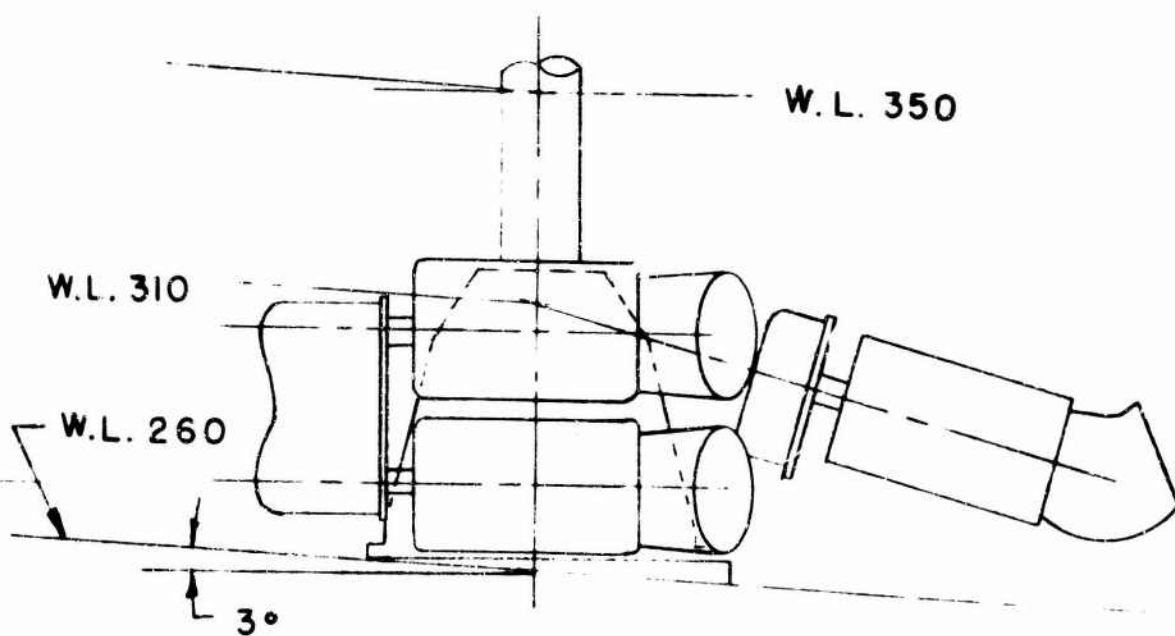
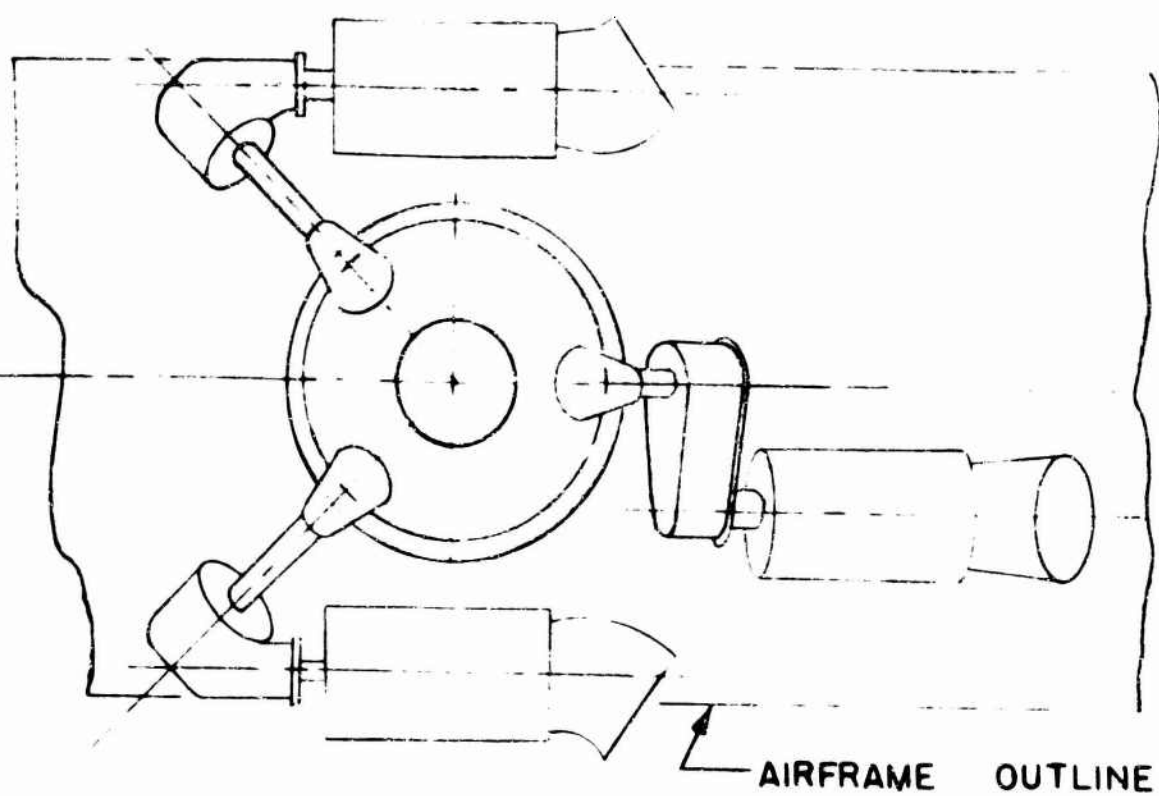


FIGURE 71. FIVE FRONT-DRIVE ENGINES.

A



FIVE FRONT-DRIVE ENGINES.

B

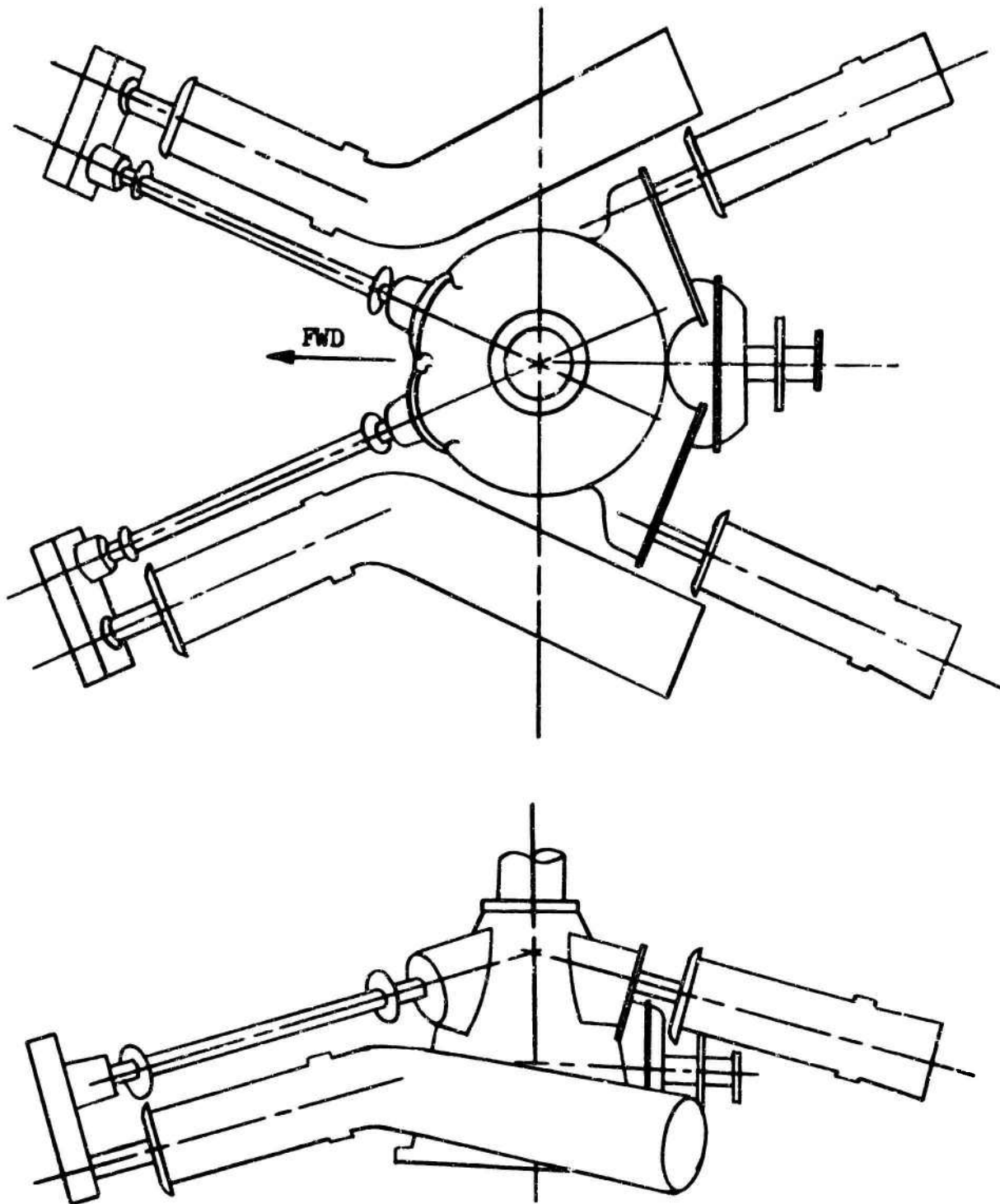


Figure 72. Semi-radial Configuration, Four Front-Drive Turbines.

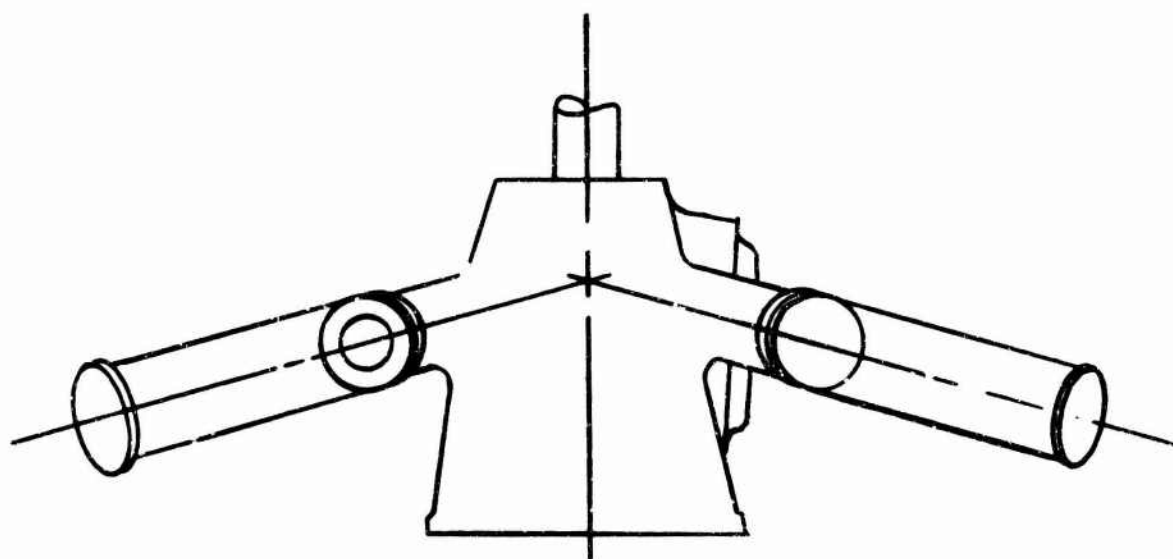
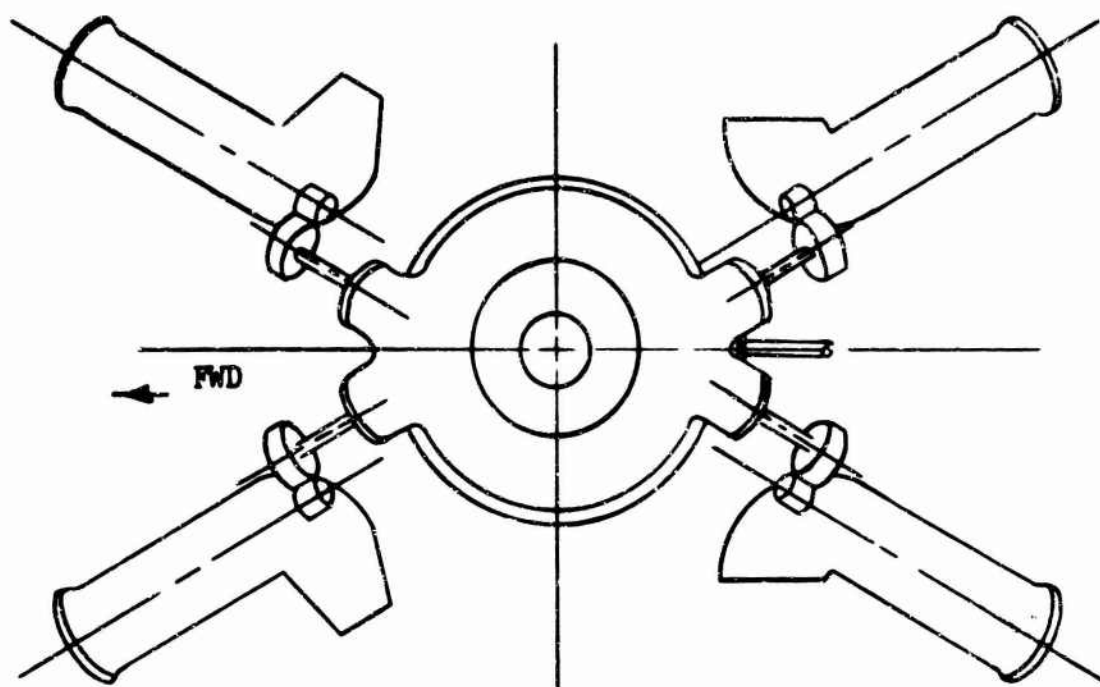


Figure 73. Semi-radial Configuration, Four Rear-Drive Turbines.

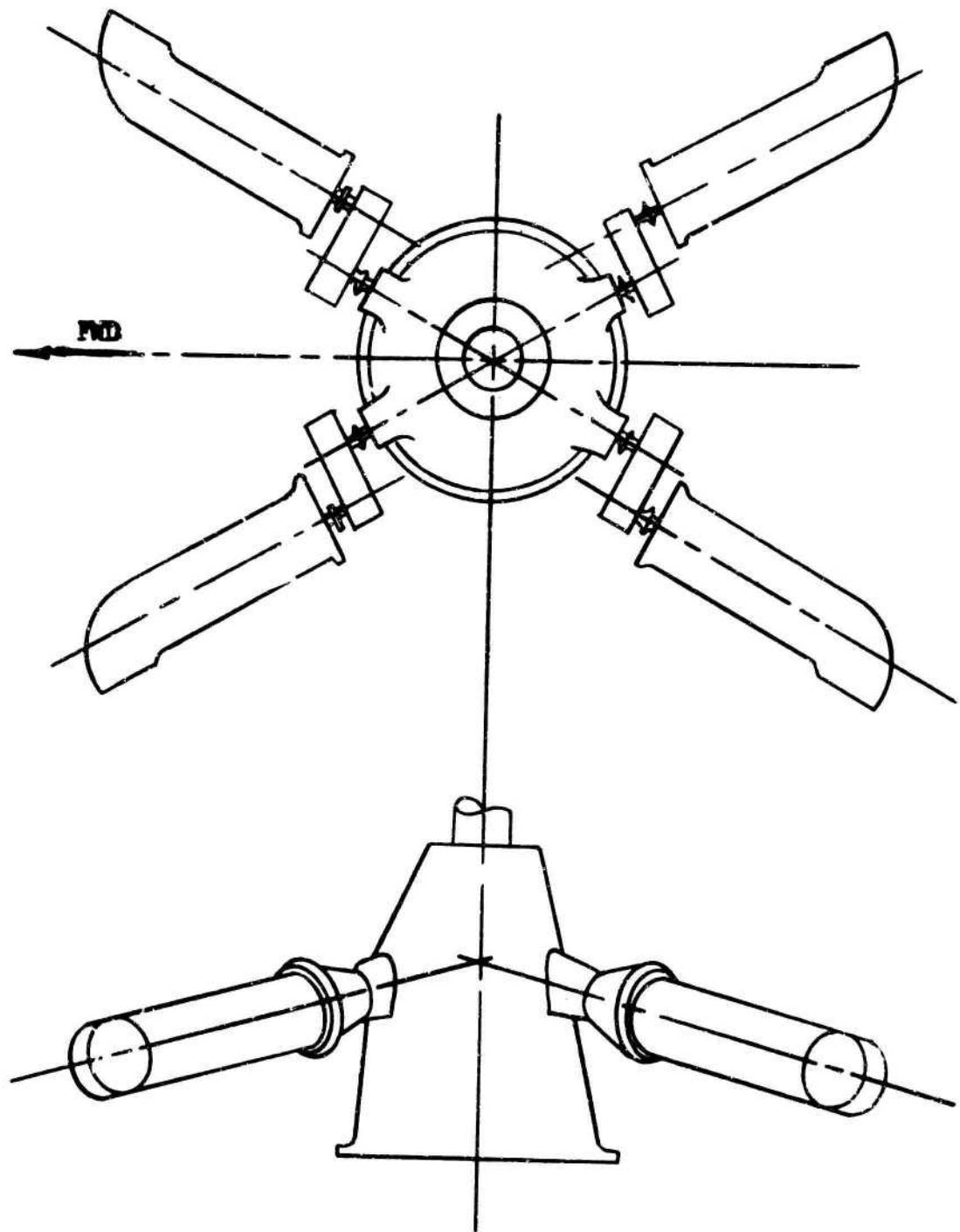


Figure 74. Semi-radial Configuration, Four Front-Drive Turbines.

APPENDIX III

SUMMARY OF GEAR DATA

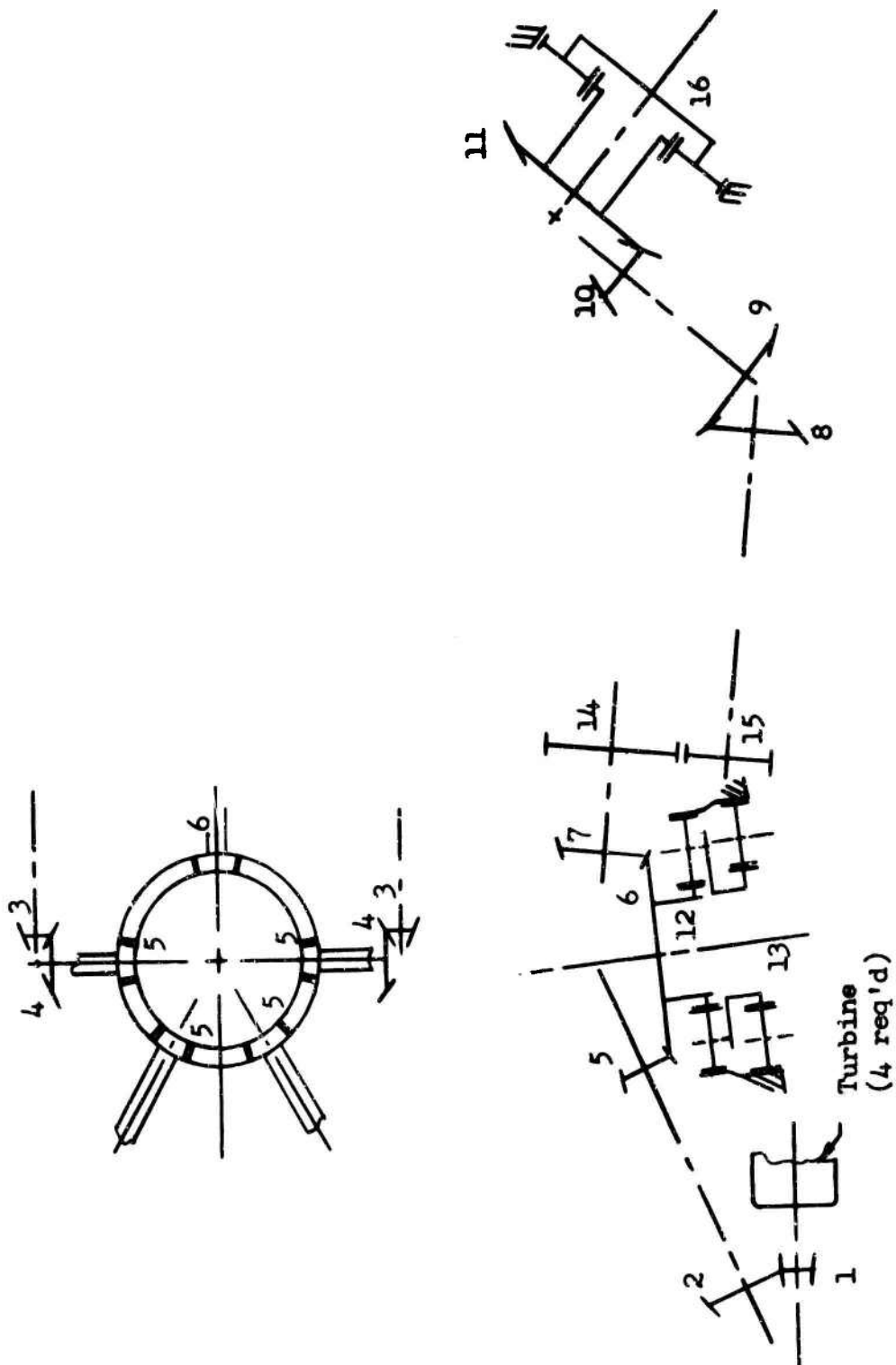


Figure '75. Gearing Schematic, Transmission System.

Gearbox	Location (Fig. 75)	Name	Diametral Pitch	Pitch Diameter (in.)	Face Width (in.)	No. of Teeth	Press. Angle	Spiral Angle	Pitch Angle	Shaft Angle
Engine Reduction	1	Pinion	5.529	6.149	2.65	34	20°	20°	8°41'	29°
	2	Gear		14.469		80			20°49'	
Main	3	Pinion	5.529	6.149	2.65	34	20°	20°	23°2'	9°
	4	Gear		14.469		80			66°58'	
	5	Pinion	4.092	9.042	3.25	37	20°	20°	13°54'	71°
	6	Gear		32.747		134			60°28'	
Inter- mediate	7	Pinion	4.092	12.952	1.75	53	20°	23°26'	20°08'	8°
	8	Pinion	4.000	10.000	2.00	40	20°	28°	29°20'	1°
	9	Gear		15.750		63			86°34'	
Tail Rotor	10	Pinion	3.676	9.249	2.632	34	20°	25°	31°43'	
	11	Gear		14.962		55			58°17'	

TABLE 33
SPIRAL BEVEL GEAR SUMMARY

Shaft Angle	on 75)	Name	Diamstral Pitch	Pitch Diameter (in.)	Face Width (in.)	No. of Teeth	Press. Angle	Spiral Angle	Pitch Angle	Shaft Angle	Hand of Spiral	D R
29		Pinion		6.149		34			8°41'		RH	
		Gear	5.529	14.469	2.65	80	20°	20°	20°49'	29°30'	LH	
9		Pinion		6.149		34			23°2'		RH	
		Gear	5.529	14.469	2.65	80	20°	20°	66°58'	90°	LH	
71		Pinion		9.042		37			13°54'		RH	
		Gear	4.092	32.747	3.25	134	20°	20°	60°28'	74°22'	LH	
8		Pinion	4.092	12.952	1.75	53	20°	23°26'	20°8'	80°36'	RH	
1		Pinion		10.000		40			29°20'		RH	
		Gear	4.000	15.750	2.00	63	20°	28°	86°34'	125°54'	LH	
		Pinion		9.249		34			31°43'		RH	
		Gear	3.676	14.962	2.632	55	20°	25°	58°17'	90°	LH	



ARY

Dir. of Rotation	Face Contact Ratio	HP	RPM	Torque (in.-lb.)	Bending Stress (psi)	Compressive Stress (psi)	Pitch Line Velocity (f.p.m.)
CCW	1.841	4,500	13,600	20,800	22,700	190,000	21,900
CW			5,780		22,700	190,000	
CCW	2.112	4,500	13,600	20,800	25,100	180,500	21,900
CW			5,780	-	25,100	180,500	
CCW	1.699	4,500	5,780	49,000	23,900	161,000	13,700
CW			1,596		23,900	161,000	
CCW	1.038	2,300	4,035	35,900	23,000	131,000	13,700
CCW	1.571	2,300	5,922	24,500	25,400	132,000	15,500
CW			3,760	-	25,400	132,000	
CCW	1.726	2,300	3,760	38,600	25,900	176,300	9,100
CW			2,324		26,900	176,300	

C

Location (Fig. 75)	Name	Diametral Pitch	Pitch Dia. (in.)	Face Width (in.)	Number of Teeth (N)	Pressure Angle
12 (First stage Planetary)	Sun	6	16.8333	3.00	101	22°30'
	Planet (6 req'd)	6	14.1667	2.90	85	22°30'
	Ring	6	45.1667	2.60	271	22°30'
13 (Second Stage Planetary)	Sun	6	22.500	5.70	135	22°30'
	Planet (3 req'd)	6	12.1667	5.60	73	22°30'
	Ring	6	46.8333	5.30	281	22°30'
14	Gear	6	15.1667	1.970	91	22°30'
15	Pinion	6	10.333	1.970	62	22°30'
16	Sun	6	5.6667	2.60	34	22°30'
	Planet (5 req'd)	6	5.1667	2.50	31	22°30'
	Ring	6	16.000	1.25	96	22°30'

TABLE 34
SPUR GEAR SUMMARY

are	Diametral Pitch	Pitch Dia. (in.)	Face Width (in.)	Number of Teeth (N)	Pressure Angle	X Factor (function of N and Pd)	K Factor (function of root radius)	Hi
	6	16.8333	3.00	101	22°30'	.2125	1.05	14,20
'd)	6	14.1667	2.90	85	22°30'	.207	1.017	
	6	45.1667	2.60	271	22°30'	.284	1.12	
	6	22.500	5.70	135	22°30'	.2143	1.05	14,20
'd)	6	12.1667	5.60	73	22°30'	.202	1.00	-
	6	46.8333	5.30	281	22°30'	.284	1.13	-
	6	15.1667	1.970	91	22°30'	.207	1.02	2,300
	6	10.333	1.970	62	22°30'	.195	1.03	2,300
	6	5.6667	2.60	34	22°30'	.1661	1.00	2,300
'd)	6	5.1667	2.50	31	22°30'	.1616	1.00	-
	6	16.000	1.25	96	22°30'	.3	1.05	-

4
SUMMARY

n	K Factor (function of root radius)	HP	RPM	Input Torque (in.-lb.)	Bending Stress (psi)	Compressive Stress (psi)	Pitch Line Velocity (f.p.m.)
	1.05	14,200	1,596	560,750	27,400	121,800	5,130
	1.017		1,381	-	28,200	121,800	-
	1.12		0	-	26,300	83,000	-
	1.05	14,200	433.3	2.065×10^6	29,700	124,600	1,725
	1.00	-	541	-	30,400	124,600	-
	1.13	-	0	-	25,900	96,000	-
	1.02	2,300	4,035	35,900	27,900	131,000	10,900
	1.03	2,300	5,922	-	25,800	131,000	10,900
	1.00	2,300	2,325	62,360	15,300	139,000	2,550
	1.00	-	1,880	-	16,400	139,000	-
	1.05	-	0	-	18,650	110,000	-

C

APPENDIX IV

COMPARATIVE RELIABILITY ANALYSIS OF HLH AND S-61

SUMMARY

The results of a comparative reliability analysis of the heavy-lift helicopter transmission system, as proposed by Sikorsky Aircraft, and an S-61 model called the Universal Tactical Vehicle (U.T.V.) designed for heavy-lift work, indicates that a 4-to-1 reduction of malfunctions per ton-mile may be expected. Also, it was concluded that the HLH has a probability of experiencing a transmission system malfunction of only approximately one-fourth that of the S-61 for a given heavy-lift task. The basic reason that these advantages may be realized is that the complexity of the transmission system is increased by a factor 1.25, whereas the payload capability is increased by a factor of 5.75.

ANALYSIS

The aircraft that the comparison was based on have the following pertinent specifications:

	<u>HLH</u>	<u>S-61 (U.T.V.)</u>
Payload (20 n.m. radius)	20 tons	3.48 tons
Vcruise out (20-ton payload)	95 knots	105 knots
Vcruise back (no payload)	130 knots	130 knots

The relative probability of failure is based on the standard 20-n.m. heavy-lift mission specified on page 4.

The relative reliability of the transmission system is determined by comparing the relative complexity of the transmission systems of the two aircraft combined with the failure rate of the components. Components included in this analysis are bearings, seals, and "O" rings whose malfunctions are conservatively estimated to comprise 80 percent of all transmission system malfunctions requiring unscheduled maintenance. Other failure modes such as chipped gear teeth, broken oil lines, etc., although when combined comprise a significant portion of all failures, are of such a varied nature that no predominant failure modes are detected and are thus very difficult to assess. The exclusion of these varied failure modes does not affect the validity of the analysis

to the extent of 20 percent, since both systems will experience these failures, and most probably in corresponding proportions, as the analysis indicates for the other 80 percent of the failures.

Bearing failure data are based on Sikorsky Aircraft's experience on the S-61 model totalling more than 5-million bearing hours. Seal and "O" ring data are taken from published data generally accepted by the industry and substantiated by Sikorsky Aircraft experience.

The results of the analysis are as follows:

	<u>S-61 Malf./10³ hr.</u>	<u>Complexity Factor</u>	<u>HLH Malf./10³ hr.</u>
Bearings	.343	1.77	.607
Seals	5.700	1.21	6.900
"O" ring	.074	1.30	.096
Totals	6.117		7.603

To determine malfunctions per ton-mile, we perform the following operation:

$$\frac{\text{Malf.}}{\text{Ton-mile}} = \frac{\text{Malf.}}{\text{hr.}} \times \frac{1}{\text{Payload}} \times \frac{1}{\text{Vcruise}}$$

For S-61

$$\frac{\text{Malf.}}{\text{Ton-mile}} = 6.117 \times 10^{-3} \times \frac{1}{3.48} \times \frac{1}{105} = .01674 \times 10^{-3}$$

For HLH

$$\frac{\text{Malf.}}{\text{Ton-mile}} = 7.60 \times 10^{-3} \times \frac{1}{20} \times \frac{1}{95} = .004 \times 10^{-3}$$

To determine the percent of reduction of malfunctions per ton-mile,

$$\% \text{ reduction} = \frac{(.017 - .004) \times 10^{-3} \times 100}{.017 \times 10^{-3}} = 76\%$$

To determine the relative probability of failure, conventional techniques are used assuming a constant failure (malfunction) rate over the useful life of the system. Previous Sikorsky reliability work documented in technical society papers has shown the validity of the

assumption for complex mechanical power transmission units. With this assumption, the probability that an item will not suffer a malfunction is given by

$$R = e^{-\lambda t}, \text{ where } \begin{array}{l} \lambda = \text{malfunction (failure) rate} \\ t = \text{time period over which the} \\ \quad \text{reliability is computed} \\ e = 2.718 \end{array}$$

and the probability that a unit will experience a malfunction is

$$Q = 1 - R = 1 - e^{-\lambda t}.$$

A good approximation of $e^{-\lambda t}$ is

$$1 - \lambda t \text{ when } \lambda t < 0.1$$

which is true for the case being considered here.

With the above information we can write the following:

$$\frac{Q_A}{Q_B} = \frac{1 - R_A}{1 - R_B} = \frac{1 - e^{-\lambda_A t_A}}{1 - e^{-\lambda_B t_B}}$$

$$\frac{Q_A}{Q_B} = \frac{1 - (1 - \lambda_A t_A)}{1 - (1 - \lambda_B t_B)}$$

$$\frac{Q_A}{Q_B} = \frac{\lambda_A t_A}{\lambda_B t_B}.$$

Let: subscript A refer to the S-61
subscript B refer to the HLH

$$\text{then } \frac{Q_A}{Q_B} = \frac{\lambda_A t_A}{1.24 \lambda_A t_B} = \frac{t_A}{1.24 t_B}$$

$$\text{or } Q_B = \frac{(1.24) t_B}{t_A} Q_A.$$

If a given task is to move 100 tons 20 nautical miles and t_A is the flight time necessary for the S-61 to do the job and t_B the flight time necessary for the HLH to do the job,

$$t_B = \frac{100 \text{ tons}}{20 \text{ tons}} \times \frac{\text{time}}{\text{round trip}}$$

$$\begin{aligned} \text{where } \frac{\text{time}}{\text{round trip}} &= 20\text{-n.m.} \times \frac{1}{95} \text{ hr.} + 0.25 \text{ hr. hovering time} \\ &+ 20\text{-n.m.} \times \frac{1}{130} \text{ hr.} \end{aligned}$$

$$t_B = 5(.21 + .25 + .15) = 3.1 \text{ hr.}$$

$$t_A = \frac{100 \text{ tons}}{3.48} \times \frac{\text{time}}{\text{round trip}}$$

$$\begin{aligned} \text{where } \frac{\text{time}}{\text{round trip}} &= 20\text{-n.m.} \times \frac{1}{105} \text{ hr.} + .25 \text{ hr. hover} + \\ &20\text{-n.m.} \times \frac{1}{130} \text{ hr.} = .19 + .25 + .15 \end{aligned}$$

$$t_A = \frac{100}{3.48} (.19 + .25 + .15) = 16.9 \text{ hr.}$$

$$Q_B = \frac{(1.24)3.1}{16.9} Q_A$$

$$Q_B = 0.23 Q_A$$

Or stated in words: the probability that the HLH will experience a malfunction (Q_B) to the transmission system is 0.23 times the probability that the S-61 will suffer a malfunction (Q_A) performing the same heavy-lift task of moving 100 tons 20 nautical miles.

This result is based on the assumption that the cargo may be loaded in such a manner as not to change the drag loads upon which the cruising speeds were calculated.

Unclassified

Security Classification

DOCUMENT CONTROL DATA - R&D		
(Security classification of title, body of abstract and indexing annotation must be entered when the overall report is classified)		
1 ORIGINATING ACTIVITY (Corporate author) Sikorsky Aircraft Division of United Aircraft Corporation Stratford, Connecticut 06497		2a REPORT SECURITY CLASSIFICATION Unclassified
		2b GROUP N/A
3 REPORT TITLE Power Transmission Studies for Shaft-Driven Heavy-Lift Helicopters		
4 DESCRIPTIVE NOTES (Type of report and inclusive dates) Final Report 30 June 1964 to 15 February 1965		
5 AUTHOR(S) (Last name, first name, initial) Burroughs, Lester R.		
6 REPORT DATE October 1965	7a TOTAL NO OF PAGES 291	7b NO OF REFS Nine
8a CONTRACT OR GRANT NO. DA 44-177-AMC-240(T)	9a ORIGINATOR'S REPORT NUMBER(S) USAAVLABS Technical Report 65-40	
b PROJECT NO. Task 1K121401D14414	9b OTHER REPORT NO(S) (Any other numbers that may be assigned this report) Sikorsky Engineering Report 50401	
10 AVAILABILITY/LIMITATION NOTICES Qualified requesters may obtain copies of this report from DDC. This report has been furnished to the Department of Commerce for sale to the public.		
11 SUPPLEMENTARY NOTES	12 SPONSORING MILITARY ACTIVITY U.S. Army Aviation Materiel Laboratories Fort Eustis, Virginia	
13 ABSTRACT <p>This report covers a 6-month design investigation of transmission system concepts capable of operation in a single-rotor heavy-lift helicopter of 75,000 to 95,000 pounds gross weight. (U)</p> <p>The study has included the selection of engines considering both front-drive and rear-drive turbine installations, as well as the design of the entire transmission system. Specific areas considered have included the study of high-speed bevel gears and bearings utilized in the initial reduction stages, high-torque lightweight planetary gearing and bearings, and the design of hypercritical shafting systems. Studies of alternate drive concepts including the harmonic drive, the roller gear drive, and redundant power path gearing systems are also included. (U)</p> <p>The results indicate that the total power transmission system weight for a single rotor HLH is approximately 8,850 pounds. This weight, which included all gearboxes, shafting, rotor brake, and lubrication systems, is approximately 7 percent less than the results of earlier studies. The mechanical efficiency of this transmission system is greater than 96.2 percent. (U)</p>		

DD FORM 1473
1 JAN 64

Unclassified

Security Classification